University of Venda

Synthesis, characterization of a sustainable Fe/Ce Doped Poly –(para-phenylenediamine) adsorbent and its potential for simultaneous removal of fluoride, arsenite and pathogens in aqueous solutions.

By

Munzhelele Elisa Pandelani

Student no: 15003264

A RESEARCH THESIS SUBMITTED TO THE DEPARTMENT OF ECOLOGY AND RESOURCE MANAGEMENT, SCHOOL OF ENVIRONMENTAL SCIENCES, UNIVERSITY OF VENDA IN PARTIAL FULFILMENT OF THE ACADEMIC REQUIREMENTS FOR THE ENVIRONMENTAL SCIENCES MASTER'S DEGREE

SUPERVISOR: PROF. GITARI W.M

CO-SUPERVISOR: Dr. AYINDE W.B

June 2021

Abstract

Water pollution due to natural and anthropogenic sources remains one of the global problems which require attention due to its long-term effect on human and the environment. Prolonged exposure to chemical and microbial contaminated water may cause both acute and chronic health hazards. The occurrence of arsenic, fluoride, and pathogen in drinking water has raised severe health issues to human beings. The health impact of consuming arsenite, fluoride, and pathogens has resulted in adverse health effects such as skin cancer, dental and skeletal fluorosis, and water-borne diseases. Thus, the present research has been conducted for their simultaneous removal from water bodies. Generally, various methods have been developed to remediate water pollution which includes membrane filtration, ion-exchange, and adsorption. Within, these developed methods adsorption methods have gained attention due to the use of various materials including natural adsorbents such as clays, agro-waste, etc, and novel conjugated polymeric composites because they are easy to operate, less expensive, and eco-friendly. The use of hydrous oxides (Fe, Ce, and Mn) of rare earth elements have been studied and have shown high affinity for fluoride, arsenite, and other toxic elements.

This study focused on the systemic synthesis of novel conjugated polymeric adsorbents by the incorporation of Fe/Ce oxides onto a phenylenediamine (pPD) polymer matrix through chemical co-polymerization route and its fluoride, arsenic and pathogen removal potentials at optimal conditions in an aqueous solution evaluation. The morphology and structural analysis of the synthesized Fe; Ce and Fe/Ce doped pPD were comparatively evaluated using the Fourier Transform Infrared (FT-IR) spectroscopy, scanning electron microscopy (SEM), energy dispersive-X-ray spectroscopy (EDS), X-ray diffraction (XRD), and transmission electron microscopy (TEM). Modified Fe/Ce was successfully incorporated onto the pPD matrix as confirmed by the different morphological characterizations. The functional groups of pPD were not altered by the incorporation of the metal oxides as shown by the FTIR results. The synthesized material has an irregular shape within an average particle size between 20 -100 nm, with a low crystalline phase pattern when compared to the amorphous plain pPD. Relatively, the optimized composite samples of 2.5 % Fe-pPD, 5 % Ce-pPD and 1:1 Fe/Ce-pPD (2.5%) showed efficient and higher fluoride and arsenic sorption as well as disinfection ability against water borne pathogens.

Moreover, the effect of contact time, adsorbent dosage, pH, initial concentration, temperature, and co-ions was assessed to determine their significance in F^- and As^{3+} removal in aqueous solution. The obtained results revealed that all the reported experimental conditions have significant effect on pollutants uptake. The kinetic data for 2.5 % Fe-pPD, 5 % Ce-pPD and 1:1 Fe/Ce-pPD composite fitted well to pseudo-second-order kinetic model for both F^- and As^{3+}. Thus, chemo-sorption is the limiting step for fluoride and arsenite uptake. However, the intra-particle diffusion plot has shown three distinctive phases for the synthesized adsorbents, thus, the adsorption process occurs with more than one sorption mechanism step. Equally, the Freundlich isotherm model better described the sorption process of the synthesized materials, hence, adsorption process was occurring on a heterogeneous surface. The fitness of the kinetics and isotherm data was validated by lower values of goodness of fit (error factors). Thermodynamically, the removal process for both pollutants when using the 2.5 % Fe-pPD and 1:1 Fe/Ce-pPD adsorbents was endothermic, whereas for 5 % Ce-pPD was exothermic and endothermic (As^{3+} (1.86, 2.11, 4.71 mg/g) and F^-(6.79, 13.29, 14.75 mg/g)). The synthesized adsorbents can be regenerated up to four cycles when using H_2O, NaOH and HCL, with H_2O being the best regenerant for both adsorbents. Further, antibacterial results showed that 2.5 % Fe-pPD, 5 % Ce-pPD and 1:1 Fe/Ce-pPD (25 % :2.5%) composite inhibited the growth of common water-borne bacterial strains. Thus, the modified composites have not only portrayed the potential ability for metal ions removal but also showed strong antimicrobial activity against water-borne pathogens.

Keywords: Water treatment, Poly-phenylenediamine, adsorption, fluoride, arsenic and pathogen removal.

Table of Contents

Abstract..... i
Table of Tables. ix
Declaration x
Acknowledgment..... x
Dedication.....xii
Acronyms and Abbreviations.....xiii
Thesis outline.....xiv
Chapter 1..... 1
1.1. Introduction 1
1.2. Problem statement. 4
1.3. Objectives 6
1.3.1. General objective..... 6
1.3.2. Specific objectives..... 6
1.4. Research questions 7
1.5. Hypothesis..... 7
1.7. Expected outcomes..... 8
Chapter 2. Literature review 17
2.1. Introduction 17
2.2. 1. Fluoride occurrence in groundwater 17
2.2.3. Fluoride removal methods..... 19
2.2.3.1. Coagulation or precipitation..... 19
2.2.3.2. Ion Exchange Process 20
2.2.3.4. Membrane process. 20
2.2.3.3. Adsorption Method..... 20
2.2.4. Future perspective of fluoride removal technologies..... 21
2.3.1. Arsenic in groundwater..... 21
2.3.2. Arsenic entry into the human body..... 22
2.3.3. Chemistry and toxicity of arsenic..... 22
2.3.4. Pathogens in ground water 23
2.4.1 Pathogen sources and entry into aquifers 24
2.4. Methods for pathogen removal. 25

2.4.2. Chlorination 25
2.4.2. UV radiation and solar disinfection 25
2.4.3. Heat pasteurization 26
2.4.4. Filtration methods 26
2.5. Use of Polymeric Composites in Water Treatment 27
2.5. Methods for Poly-phenylenediamine (pPD) preparation. 28
2.6.1. Electrochemical Polymerisations. 28
2.5.2. Photo-Oxidative Polymerization. 29
2.5.3. Enzyme-Catalyzed Oxidative Polymerization 29
2.5.4. Chemical Oxidation. 30
2.8. Use of metal, bimetallic oxides and other materials in fluoride, arsenic removal as well as microbial disinfection. 32
Chapter 3. 51
Synthesis of Fe doped poly p-Phenylenediamine composite and its potential co-adsorption of arsenite and fluoride in aqueous solution. 51
3.1. Abstract 51
3.2. introduction 52
3.3. Material and methods. 54
3.3.1. Chemicals 54
3.3.2. Composites preparation 54
3.3.2.1. Preparation of Poly-phenylenediamine (pPD). 54
3.3.2.1. Preparation of Fe Poly-phenylenediamine (Fe-pPD). 55
3.3.2.3. Adsorbent efficiency determination 55
3.3.3. Characterization 56
3.3.4. Batch experiments. 56
3.3.5. Adsorption kinetics. 57
3.3.6. Adsorption isotherms. 58
3.3.7. Goodness of fit evaluation 59
3.3.8. Antimicrobial activity test. 60
3.3.8.1. Preparation of medium agar 60
3.4. Results and Discussion 60
3.4.1 Adsorbent optimization. 60
3.4.2. Characterization. 61
3.4.2.1. FTIR results. 61
3.4.2.2. SEM-EDS results. 62
3.4.2.3. XRD results. 63

3.4.3.4. BET results 64
3.4.2.5. CHNS analysis results. 65
3.4.3. Batch experiments. 65
3.4.3.1 Effect of contact time 65
3.4.3.2. Adsorption Kinetics. 66
3.4.3.3. Effect of adsorbent dose 69
3.4.3.4. Effect of initial concentration. 70
3.4.3.5. Adsorption isotherm models 70
3.4.3.7. Effect of pH on As^{3+} and F^- sorption and point of zero charge. 75
3.4.3.9. Regeneration 77
3.4.3.10. Mechanism of As^{3+} and F^- sorption. 78
3.5 Antimicrobial potency 79
3.6. Conclusion 80
References. 81
Chapter 4 87
Synthesis and characterization of Ce doped poly(para-phenylenediamine) and its evaluation of chemical pollutants and pathogens removal in aqueous solutions. 87
4.1. Abstract. 87
4.2. Introduction. 88
4.3. Materials and methodology. 90
4.3.1. Chemicals 90
4.3.2. Composite preparation. 91
4.3.2.1. Preparation of Poly-phenylenediamine (pPD). 91
4.3.2.3 Adsorbent efficiency determination 91
4.3.3. Characterization. 92
4.3.4. Batch experiments. 93
4.3.5. Adsorption kinetics. 93
4.3.6. Adsorption isotherms. 94
4.3.7. Goodness of fit evaluation 95
4.3.4. Antimicrobial activity test. 96
4.4. Results and discussion. 96
4.4.1. Efficient adsorbent determination. 96
4.4.2. Characterization results. 98
4.4.2.1. FTIR analysis. 98
4.4.2.2. XRD analysis. 99
4.4.2.3. SEM-EDS analysis. 100

4.4.2.4 BET analysis. 101
4.4.2.5 CHNS results. 101
4.4.3. Batch experiments results. 102
4.4.3.1. Effect of contact time. 102
4.4.3.2. Kinetics model. 102
4.4.3.3. Effect of adsorbent dose. 105
4.4.3.4. Effect of Initial adsorbate concentration. 106
4.4.3.5. Isotherm models 107
Figure 27. adsorption isotherms: a) $As^{3+}$and b) F^{-}. 107
4.4.3.6. Thermodynamics. 110
4.4.3.7. Effect of pH and pH_{pzc}. 111
4.4.3.8. Effect of co-existing ions. 112
4.4.3.9. Regeneration. 113
4.4.3.10. Mechanism of As^{3+} and F^{-} sorption. 114
4.4.4. Anti-microbial potency. 115
4.5. comparison of Fe-pPD and Ce-pPD composites towards As3+ and F^{-} 116
4.5. Conclusion. 116
References. 117
Chapter 5. 125
Synthesis, characterization of a sustainable Fe/Ce Doped Poly –(para-phenylenediamine) adsorbent and its potential removal for chemical pollutants and pathogens in aqueous solutions 125
5.1. Abstract. 125
5.2. Introduction. 126
5.3. Methods and materials. 128
5.3.1. Materials. 128
5.3.2. Adsorbent preparation. 128
5.3.2.1. Preparation of Poly-phenylenediamine (pPD). 128
5.3.2.2. Fe/Ce Doped Poly-Phenylenediamine (Fe/Ce-pPD) 129
5.3.2.3 Adsorption capacity of pPD, and Fe/Ce-pPD composites 129
5.3.3. Characterizations. 130
5.3.5. Adsorption kinetics. 131
5.3.6. Adsorption isotherms. 132
5.3.7. Goodness of fit evaluation 133
5.3.4. Antimicrobial activity test. 134
5.4. Results and discussion. 134
5.4.1. Efficient adsorbent determination. 134

5.4.2. Characterization. 136
5.4.2.1. FTIR results. 136
5.4.2.2. XRD results. 137
5.4.2.3. SEM-EDS results. 138
5.4.1.4. TEM results. 139
5.4.2.5. BET analysis. 139
Chemically stability of the adsorbent. 140
5.4.2.6. IC-PMS results 140
5.4.2.7. CHNS results 141
5.4.3.1. Effect of contact time 142
5.4.3.3. Effect of adsorbent dose 145
5.4.3.4. Effect of pH 146
5.4.3.3. Effect of initial concentration of the adsorbate. 147
5.4.3.6. Adsorption isotherms 148
5.4.3.8. Thermodynamics. 151
5.4.3.9. Effect of co-existing ions. 152
5.4.3.10. Regeneration. 153
5.5. Comparison of the synthesized materials towards As^{3+} and F^- removal 155
5.6 Antimicrobial. 154
5.5. Conclusion. 155
3.4.9. References. 156
Chapter 6. 161
6.1. General conclusions. 161
6.2. Recommendation. 161

Table of figures

Figure 1: Diagram shows skeletal and dental fluorosis. 19
Figure 2: Diagram shows arsenicosis. 23
Figure 3. Microbial entry into aquifers. ..... **Error! Bookmark not defined.**
Figure 5: Chemical structures of poly-phenylenediamine 27
Figure 5. adsorbent optimization. 60
Figure 6. FTIR spectra for Fe-pPd and pPD 61
Figure 7. SEM-EDS results 63
Figure 8. XRD diffractogram 64
Figure 9. Effect of contact time. 66
Figure 10 Kinetics models. 67
Figure 11. Effect of adsorbent dose on As^{3+} and F^- sorption. 69
Figure 12. Effect of initial concentrations. 70
Figure 14. As^{3+} and F^- Langmuir and Freundlich Isotherm models plots. 71
Figure 14. Effect of pH and pH_{pzc}. 75
Figure 15. Effect of co-existing ions. 77
Figure 16. regeneration results. 78
Figure 17. Antimicrobial activity. 79
Figure 18. Adsorbents efficiency. 97
Figure 19. FTIR spectrum of bare pPD and Ce-pPD 98
Figure 20 XRD analysis for bare pPD and Ce-pPD 99
Figure 21. SEM-EDS spectral analysis 100
Figure 22. effect of contact time on arsenite and fluoride. 102
Figure 23. kinetics model for As^{3+} and F^- 103
Figure 24. Effect of adsorbent dose on As^{3+} and F^-. 105
Figure 26. effect of initial adsorbate concentration. 106
Figure 27. adsorption isotherms: a) As^{3+} and b) F^-. 107
Figure 27. effect of pH on arsenite and fluoride sorption using Ce-pPD. 111
Figure 28. effect of co-existing ions: a) As^{3+} and b) F^-. 113
Figure 29. regeneration. 113
Figure 30. antimicrobial activity. 115
Figure 32: Diagram shows the formation of Fe/Ce doped poly-phenylenediamine 129
Figure 32. Adsorbent sorption potential. 135
Figure 33. FTIR for pPD and Fe/Ce-pPD before and after application 136
Figure 34. XRD results of pPD and Fe/Ce-pPD 137
Figure 35. SEM-EDS analysis of pPD and Fe/Ce-pPD 138
Figure 37. TEM analysis of Fe/Ce-pPD. 139
Figure 38. Effect of contact time. i 142
Figure 39. Kinetics model. 143
Figure 39. Effect of adsorbent dose.. 145
Figure 40. effect of pH and point of zero charge. 146
Figure 41. Effect of initial concentration. 147
Figure 42. Adsorption isotherms models: a) As^{3+} and b) F^- 149

Figure 43. Co-existing ions..... 152
Figure 44. Regeneration results.. 153
Figure 45. antimicrobial results for bare pPD and Fe/Ce-pPD. 154

Table of Tables.

Table 1. Fe and Ce previously used adsorbents. 35
Table 2. BET analysis results. 64
Table 3. CHNS results. 65
Table 4. Table for non-linearized kinetics parameters 68
Table 5. Table for linearized k inetics models. 68
Table 6. Non-linearized Langmuir and Freundlich isotherm model. 72
Table 7. linearized D-R isotherm model 73
Table 8. Thermodynamic parameters. (Placeholder2) 74
Table 9. BET results 101
Table 10.CHNS results. 101
Table 11.Non-linearized and linearized kinetic models 104
Table 12. linearized kinetics model parameters. 104
Table 13. Langmuir and Freundlich isotherm model parameters. 108
Table 14. D-R linear isotherms parameters 109
Table 15. table showing thermodynamics parameters. 110
Table 16. comparison of Fe-pPD and Ce-pPD composites towards As and F removal 116
Table 17. BET analysis. 139
Table 18. IC-PMS results. 141
Table 19. CHNS results. 142
Table 20. Kinetics models parameters 144
Table 21. Table for adsorption model parameters. 149
Table 22. Linearized D-R calculated parameters. ..... **Error! Bookmark not defined.**
Table 23. Thermodynamic parameters. 151
Table 24. Comparison of the synthesized materials. 155

Declaration

I, **Munzhelele Elisa Pandelani** hereby declare that the dissertation for the Mater of Environmental Science in Ecology and Resources Management is submitted at the University of Venda. I clearly state that this dissertation has not been submitted to any institution before, moreover, I swear that this is my work in design as thus, all reference materials and resources have been acknowledged.

Signature: 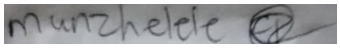 Date …17/06/2021……..

Acknowledgment

My sincere gratitude goes to my academic supervisors, **Prof. Gitari W.M**. and **Dr. Ayinde W.B.** for their guidance, facilitation, and concrete solid assistance. Your

contribution cannot be overstated for your advices that makes what looks impossible to be possible.

I am also happy, to convey my gratitude to **Service SETA** and **Sasol Inzalo** for their financial support throughout the year.

To **Munzhelele and Khorommbi`s** family, I thank you for all the role you played in my life, for your love and care you gave to me. Your love was requisite and endless.

I further thank the **EnviReN group and the Department of Ecology and Resources Management** for your facilitation, assistance, knowledge, and patience in the role you played to make my project to be a success.

Above all, I thank the **Almighty God** with whom all things are possible. It is all by his grace that all this work was possible.

Dedication

This work is dedicated to my family **(Khorommbi K, Khorommbi V.P, Muleya E.A, and Khorommbi N.T)** for standing firm by me throughout my studies and for your sacrifice, support, encouragement, and prayers.

Acronyms and Abbreviations

pPD : poly (para-phenylenediamine)

Fe-pPD : Iron doped poly (para-phenylenediamine)

Ce-pPD : Cerium doped poly (para-phenylenediamine)

Fe/Ce-pPD: Iron/ Cerium doped poly-phenylenediamine

F^- : Fluoride

As^{3+} : Arsenite

T : Transmission

Thesis outline.

The thesis is divided into six chapters, each chapter is explaining different aspects of the investigation. A summary of each chapter is given below:

Chapter 1. Introduction

A brief background of water pollution problems given was together with the different solution that was developed to attempt in reducing the challenge. An outline of the objectives, research questions, justification of the study, and the budget of the project.

Chapter 2. Literature review

An in-depth description of water pollution (arsenite, fluoride and pathogens) challenge and attempted solutions. A detailed pollutants sources, health impacts, and the available treatment technologies as well as various adsorbents that have been used in remediating the toxic metal ions and their associated problems. A brief review of polyaniline polymers specifically their properties, utilization, and various synthesis process was discussed in this chapter. The different sources, fate, impact of pathogens into the aquifers as well as the treatment methods were also elaborated.

Chapter 3. Synthesis of Fe doped poly p-Phenylenediamine composite and its potential co-adsorption for arsenite, fluoride, and pathogens in aqueous solution.

The chapter elaborates on the general problems regarding water pollution and bringing a flexible solution. The outline of this chapter is based on the synthesis of modified Fe-pPD composites and the evaluation its fluoride, and arsenite remediation as well as pathogen removal. This section further describes the synthesis process of Fe-pPD composite, morphological analysis, experimental procedures for the pollutant's removal and its obtained results.

Chapter 4. Synthesis and characterization of Ce doped poly(para-phenylenediamine) and its evaluation of fluoride, arsenite and pathogens removal in aqueous solutions

The chapter pointed out the method of synthesis, characterization of the synthesized Ce-pPD adsorbent and evaluate the potential ability towards fluoride, arsenite and microbial removal efficiency in aqueous solution. The study employs a batch

experimental procedure to determine the removal conditions as well as minimal zone of inhibition method for pathogen removal. The chapter further compares removal potency of Fe-pPD and Ce-pPD composites towards fluoride and arsenite removal.

Chapter 5. Synthesis, characterization of a sustainable Fe/Ce Doped Poly – (para-phenylenediamine) adsorbent and its potential removal for chemical pollutants and pathogens in aqueous solutions.

The chapter describes the process of synthesizing the Fe/Ce-pPD adsorbents and the adsorption process through batch experimental procedures. The obtained results were used to determine the removal performance and mechanism of the metal ions adsorption processes by the adsorbent. Also, this chapter compares the removal efficiency of the Fe-pPD, Ce-pPD and Fe/Ce-pPD composites towards metal ions

Chapter 6. Conclusions and recommendations.

The chapter presents a detailed summary of the findings and results from the discussion of the study. It further makes recommendations for more research in the improvements of the synthesized materials for effective contaminated water remediation.

Chapter 1

1.1. Introduction

Water is an important resource to sustain life, and its supply must be satisfactory (adequate, safe, and accessible) available to all (WHO, 2011). Moreover, its scarcity is one of the biggest environmental problems faced by most regions of the world (Loos et al, 2010). Worldwide, groundwater accounts for about one-third of all freshwater resources and represents around 99% of available freshwater (Lemckert, 1999; Danielopol et al, 2003). Equally, groundwater is used as a source of drinking water and the largest freshwater resource mostly in developing countries including South Africa. Several studies have emphasized groundwater quality to be better in terms of low microbial contamination and chemical composition, hence it has been used without purification. However, the introduction of microbial and chemical pollutants in groundwater due to natural and anthropogenic processes has negatively affected its quality for domestic purposes. The quality of groundwater depends on different chemical constituents and their concentrations (Brahman et al, 2013), which are mainly derived from the geology of the area. Therefore, majority of the communities must be provided with adequate knowledge and information by educating them about the danger of consuming untreated water. Furthermore, the development of sustainable technological systems to removing such pollutants must be considered for improved socio-economic impacts arising from consuming the water resources.

Contamination of groundwater is mainly due to population growth, urbanization, agricultural activities, industrialization, and natural activities such as weathering, chemical leaching, and natural hazards such as volcanos (Bhatnagar et al, 2011). The occurrence of several natural and anthropogenic chemical pollutants such as nitrates, phosphates, arsenic, fluoride, and heavy metals, as well as microbial pollutants (pathogens), may greatly affect water quality (Yadhav et al, 2015). According to World Health Organization and United Nations International Children`s Emergency Fund (WHO and UNICEF, 2019) 2.2 billion people especially in rural areas and low-income communities, do not have access to safe drinking water. The presence of these chemical and biological pollutants in groundwater can pose public health hazards.

The introduction of these pollutants is mainly due to natural systems but also includes anthropogenic as well as geological sources (Smedley, 2002 and Rfique et al, 2009).

The most significant inorganic pollutants in groundwater affecting human health globally, according to the WHO, are arsenic and fluoride (Thompson et al., 2007; WHO 2011). High levels of fluoride have been reported worldwide and in the Southern region of Africa including the Republic of South Africa (Rai et al, 2013). The introduction of fluoride elements in groundwater is mainly due to the leaching of fluoride-containing minerals such as fluorspar as well as anthropogenic activities like agriculture and industrialization due to infiltration (Izuagie et al, 2016). Intake of fluoride can be beneficial or injurious, but these depend on the concentration of constant consumption (Dhillon and Kumar, 2015). However, its excessive intake may result in detrimental health diseases such as cancer, molting teeth, brittle bones, neurological damages, etc) (Zhou et al, 2004). Due to such outcomes, the World Health Organization has set a recommended fluoride level of 1.5 m/L (WHO, 1993, 2011). Therefore, if the daily intake exceeds the recommended level it becomes toxic to human health (Thole, 2013).

Moreover, arsenic contamination of groundwater is a serious global health and environmental problem because of its toxic and carcinogenic nature. Arsenic can occur naturally in ground and surface water due to erosion and leaching from arsenic-bearing rocks and volcanic eruption (Vaclavikova et al, 2007; Adio et al, 2017). The occurrence of arsenic in groundwater has gained attention worldwide due to its negative impacts on human health (Mudzielwani et al, 2018). About 200 million people worldwide are affected by high-arsenic groundwater (Shakoor et al, 2017). The presence of arsenic in groundwater can be due to infiltration of polluted water from anthropogenic activities such as mining, industrial developments including electronics manufacturing, fertilizers, pesticides, paints, pigmenting substances, wood preservative and other economic developments (Sud et al, 2008; Yadhav et al, 2015; Zare et al, 2018). Arsenic can be found both as organic and inorganic in the environment. It rarely exists in free form in nature, it slightly occurs in combination with other elements in more than 200 different mineral forms (Asere, 2019). It has been observed that inorganic arsenic is the one which is more toxic than organic. Furthermore, inorganic arsenic is the main cause of health problems such as cardiovascular, cancer and neurological effects (Naujokas et al, 2013; Basu et al, 2014; Ye et al, 2017). Long-term exposure to arsenic may cause a disease called arsenicosis with general symptoms of red or swollen skin (Joshi and Chaudhuri, 1996;

Abdula et al, 2015; Elwakeel and Al-Bongami, 2017). As a result, the World Health Organization has set a permissible level of arsenic in drinking water to be 0.01 mg/L. The mentioned symptoms have been observed in various countries including South Africa (Mudzielwana et al, 2019).

Equally, microbiologically infested water has resulted in a lot of water-related diseases. Bacterial contamination of drinking water is major public health in the world including South Africa. Consumption of water polluted by human and animal faeces is the major cause of various water-borne diseases (diarrhea, dysentery, typhoid fever, hepatitis, and others) caused by various pathogenic bacteria, viruses, and parasites (Rai et al, 2012). Sources of faecal contamination in groundwater potentially include leakages from on-site sanitation systems such as septic tanks or sewers, underground storage tanks, disposal systems, animal manure and compost, as well as from (accidental and non-accidental) wastewater discharge or sewage sludge applied to fields in agricultural areas (Reynolds and Barrett 2003; Gerba and Smith 2005; Arnone and Walling 2007).

Contamination of groundwater sources by arsenic, fluoride and pathogenic bacteria poses a public health concern to communities who depend totally on this water supply. The World Health Organisation (WHO) has indicated that approximately 1.8 million deaths and 61.9 million disability-adjusted life-years worldwide are attributable to unsafe water, sanitation, and poor hygiene (Mpenyana-Monyatsi et al, 2012). Therefore, it is essential to remove these chemical pollutants and pathogens in water before use to reduce water-related health problems from long term consumption of such polluted water resources.

Various methods are available for the removal of fluoride, arsenic, and pathogens from water. Such techniques include ion-exchange, precipitation, membrane process, and adsorption among others (Amor et al, 2001 and Choong et al, 2007; Korotta-Gamage et al, 2017). The effectiveness of these technologies has been studied and reported (Waghmare and Arfin, 2015; Hao et al, 2018; Al-Gheethi et al, 2018). Researches have shown that adsorption technology for water purification has been far more embraced than any other technology (Izuagie et al, 2017). Various adsorbents have been used including polymeric composites such as poly-phenylenediamine isomers and other polymers doped with various elements (Mohaptra et al, 2010 and Zare et al,

2018). Nowadays, attention has been focusing on modifications of these adsorbents in order not only to enhance their adsorption capacity but also to improve their mechanical strengths and other physicochemical properties. Although these different adsorbents have yielded better results, some of them are not economically and environmentally friendly and they are mostly designed to remove one pollutant, hence this gives the motive to develop a multifunctional material. One which can efficiently and economically remove microbial pollutants pathogens, as well as co-adsorption of arsenic, and fluoride simultaneously from aqueous solutions. Therefore, the focus of this study was to synthesize an eco-friendly Fe/ Ce doped poly-phenylenediamine polymers adsorbent to enhance the removal rate of these toxic metal ions (fluoride and arsenic) and pathogens in groundwater.

1.2. Problem statement.

Water is a basic building block of life because it is the major component that maintains the quality of life. Water scarcity and water pollution are of the great problems in the world mostly in developing countries like South Africa. Recently, the World Health Organization, 2014 has reported that about 748 million people lack access to adequate and safe drinking water. The most appropriate and widely used source of drinking water for many rural communities in Sub-Saharan Africa and other developing countries like South Africa is groundwater (Masindi et al, 2013). 50-80% of global populations in rural and urban dwellers in developing countries are supplied with groundwater for domestic use (Ayoob et al, 2008; Jadhav et al, 2015).

Currently, various studies have provided evidence that naturally occurring water contains high concentrations of chemical pollutants (inorganic and organic) and pathogens. Traces of chemical pollutants such as fluoride and arsenic also with pathogens have been identified in groundwater which may result in detrimental health impacts if daily intake exceeds permissible level (Thompson et al, 2007; Cheng et al, 2012). Therefore, it is important to treat these contaminated water resources before consumption.

The World Health Organization has reported that about more than 200 million people around the world ingest water containing inorganic pollutants mainly fluoride and arsenic(Guo et al, 2013; Hongtao et al, 2018). Yadhav et al, (2015), further stated that fluoride pollution of drinking water receives much less attention than arsenic.

Arsenic is found to be frequently associated with fluoride in shallow aquifers around the world (Currell et al, 2011). Sources of fluoride and arsenic in water mostly geogenic and include several rock-forming minerals even though they are sometimes associated with anthropogenic activities such as mining and other economic developments (García and Borgnino, 2015, Ungureanu et al, 2015). Even though ingesting fluoride has some benefits stated by most studies, it is important to ingest water with fluoride less than 1.5mg/L to avoid health problems (dental and skeletal fluorosis) associated consumption of water with more than 1.5 mg/L (WHO, 1970, 2011).

Thole, (2013) reported that in some parts of Africa groundwater is contaminated with fluoride, which is high than the recommended levels by World Health Organization guidelines. The Republic of South Africa is falling within the range where fluoride levels are much high than the permissible levels in Sub-Saharan Africa. High fluoride and arsenic levels have been reported in the Republic of South Africa (Rai et al, 2013, Mudyazhezha and Kanhukamwe, 2014).

Furthermore, the occurrence of arsenic in natural waters is associated with the leaching from minerals, sediments and rocks containing arsenic (Choong et al, 2007). The existence of As in groundwater poses an even greater danger than fluoride hazards due to its excessive toxicity at a low concentration which goes unobserved especially in As(III) form (Camacho et al, 2011). Prolonged exposure to arsenic may pose severe human health impacts such as gastrointestinal problems and arsenicosis (Villaescusa and Bollinger, 2008; Sharma and Sohn, 2009).

Consumption of contaminated water resources with human and animal faeces is the major cause of various water-borne diseases (diarrhea, dysentery, typhoid fever, hepatitis, and others) caused by various pathogenic bacteria, viruses, and parasites (Craun et al, 2010; Edokpay et al, 2018). In 2000, an annual mortality rate of 2.2 million people associated with contaminated water consumption was recorded with the epidemic currently responsible for about 90% of all deaths of children under five years in developing countries (WHO/UNICEF JMP, 2010; WHO, 2000). Also, South Africa has experienced a water-borne disease epidemic in the recent past due to failing water treatment facilities in rural areas (WHO/CCU/18.02/ South Africa, 2018).

Various methods are available for the removal of fluoride, arsenic, and pathogens from water. Although, some of these methods have yield better results some are expensive to conduct and process, introduce toxic ions through leaching, produce sludge and increases water turbidity, etc. Additionally, various adsorbents have been used, which includes rare earth metal oxides (Fe, Ce, Al, Mn, etc) agricultural waste, etc. The rare earth metal oxides (Fe and Ce) have been reported as the potential sorbents due to their strong affinity towards fluoride and arsenic (Raichur and Basu et al, 2004; Chiban et al, 2012). However, the use of Fe and Ce metal oxides are commercially expensive, result in leaching problem, and their optimum adsorption pH is mostly in acidic ranges which restricts their utilization in domestic water purification (Wu et al, 2007).

The polymeric composite has acquired much attention compared to others due to its multifunction, high adsorption capacity, easy operation and environmental consideration which is mainly enhanced by the doping process. Moreover, it is advisable to choose an efficient, sustainable, and cost-effective method to have an optimum yield that will promote environmental stability (Sanghratna, 2015). As a result, this study will focus on synthesizing efficient and cost-effective Fe/Ce doped poly-phenylenediamine for highly selective of fluoride, arsenic, and the disinfection of pathogens in a water treatment system to produce potable water for household use.

1.3. Objectives

1.3.1. General objective

The overall objective is to synthesize, characterize and evaluate the co-adsorption properties of Fe/Ce doped poly-phenylenediamine composite for toxic metal ions (arsenic and fluoride) as well as pathogens removal in groundwater resources.

1.3.2. Specific objectives

1. To Synthesize Fe/Ce doped poly-phenylenediamine adsorbent.
2. To evaluate the morphological and physicochemical properties of the synthesized Fe/Ce doped poly-phenylenediamine and compare its efficiency towards the simultaneous removal of fluoride, arsenic, and pathogens from groundwater.
3. To test the adsorption performances of the adsorbent through batch experiments for fluoride and arsenic removal as well as to elucidate its

adsorption mechanisms through different isotherms and kinetic sorption processes.

4. To determine the antimicrobial property of the synthesized adsorbent on a laboratory scale.
5. To examine the applicability and economic viability of the synthesized adsorbent through regeneration and leaching capacities

1.4. Research questions

1. Can synthesized Fe/Ce doped poly-phenylenediamine polymer remove fluoride, arsenic and pathogens in groundwater?
2. What are the morphological and physicochemical properties of the synthesized Fe/Ce doped poly-phenylenediamine adsorbents?
3. Which sorption conditions affect the adsorption capacity for fluoride and arsenic?
4. Does the adsorbent display any antimicrobial property against water-borne pathogens?
5. What can be used to regenerate the adsorbent?
6. How to reduce leaching of the adsorbent?

1.5. Hypothesis

Fe/Ce doped poly-phenylenediamine polymer can remove fluoride, arsenic and pathogens simultaneously in groundwater.

1.6. Justification.

Water is one of the main important elements for life nourishment and its availability in nature is approximately three fourth of the earth`s surface. However, South Africa is observed as one of the driest countries around the world (Thole, 2013; DWA, 2000). Additionally, South Africa has a strong water dependent industry with a track record in innovation (mining, agricultural, mineral processing activities, etc.), which is one of the contributing factors to water scarcity and water pollution. Thus, groundwater is used to meet water demand. The chemical and microbial nature of groundwater determines its effectiveness for a specific need, therefore not all waters are suitable for consumption (Nagendra, 2003). The presence of high levels of chemical pollutants such as arsenic, fluoride, and pathogens in water is a serious matter of concern for

public health that requires attention (Shannon et al, 2010; WHO, 2011). The excessive occurrence of arsenic, fluoride, and pathogens in groundwater may pose severe health problems that may affect economic development. A World Health Organization (WHO) report found that almost one-tenth of the global disease burden could be prevented by improving water supply (WHO, 2008)

Safe drinking water and good hygiene are fundamental principles to protect human and environmental health, which directly attribute to achieving good health and well-being. Thus, to achieve sustainable development goal number six, water purification is required. Various methods have been used to remediate fluoride, arsenic, and pathogens occurrence in water solution. Nevertheless, they seem to have left a gap as the most developed methods are designed to remove one pollutant but not as a multifunctional system for simultaneous removal of different toxic metal ions. However, the traditional material and treatment technologies are not effective to treat complex and complicated polluted waters comprising different pollutants and pathogens. Purification using adsorption methods using polymeric composite has been assessed and has yielded better results. Therefore, the synthesis of Fe/Ce doped poly-phenylenediamine polymer is hoped to improve the fluoride and arsenic removal efficiency and at the same time inactivate the pathogens present in water.

1.7. Expected outcomes.

- Detailed physicochemical and morphological properties of the synthesized Ce/Fe doped poly-phenylenediamine polymer.
- Comprehensive technical parameters on the sorption performances of the synthesized adsorbent for fluoride and arsenic removal at a laboratory scale will be presented.
- Detailed technical parameters on water microbial filtration efficiency of the multifunctional adsorbent
- Comprehensive technical report about the applicability.

References

Abdula, K.S.M., Jayasingheb, S.S., Chandanaa, E.P.S., Jayasumanac, C.P., De Silva, M.C.S., 2015. Arsenic and human health effects: a review. Environ. Toxcol. Pharmacol. 40, 828–846.

Adio, S.O., Omar, M.H., Asif, M. and Saleh, T.A., 2017. Arsenic and selenium removal from water using biosynthesized nanoscale zero-valent iron: a factorial design analysis. *Process Safety and Environmental Protection*, *107*, pp.518-527.

Al-Gheethi, A.A., Efaq, A.N., Bala, J.D., Norli, I., Abdel-Monem, M.O. and Kadir, M.A., 2018. Removal of pathogenic bacteria from sewage-treated effluent and biosolids for agricultural purposes. *Applied Water Science*, *8*(2), p.74.

Amor, Z., Bariou, B., Mameri, N., Taky, M., Nicolas, S. and Elmidaoui, A., 2001. Fluoride removal from brackish water by electrodialysis. *Desalination*, *133*(3), pp.215-223.

Arnone, R.D. and Perdek Walling, J., 2007. Waterborne pathogens in urban watersheds. *Journal of Water and Health*, *5*(1), pp.149-162.

Asere, T.G., Stevens, C.V. and Du Laing, G., 2019. Use of (modified) natural adsorbents for arsenic remediation: A review. *Science of the total environment*, *676*, pp.706-720.

Ayoob, S., Gupta, A.K., Bhat, V.T., 2008. A conceptual overview on sustainable technologies for the defluoridation of drinking water. Crit. Rev. Environ. Sci.Technol. 38, 401e470.

Basu, A., Saha, D., Saha, R., Ghosh, T. and Saha, B., 2014. A review on sources, toxicity and remediation technologies for removing arsenic from drinking water. *Research on Chemical Intermediates*, *40*(2), pp.447-485.

Bhatnagar, A., Kumar, E. and Sillanpää, M., 2011. Fluoride removal from water by adsorption—a review. *Chemical engineering journal*, *171*(3), pp.811-840.

Brahman, K.D., Kazi, T.G., Afridi, H.I., Naseem, S., Arain, S.S. and Ullah, N., 2013. Evaluation of high levels of fluoride, arsenic species and other physicochemical

parameters in underground water of two sub districts of Tharparkar, Pakistan: a multivariate study. *Water research*, *47*(3), pp.1005-1020.

Brahman, K.D., Kazi, T.G., Afridi, H.I., Naseem, S., Arain, S.S., Wadhwa, S.K. and Shah, F., 2013. Simultaneously evaluate the toxic levels of fluoride and arsenic species in underground water of Tharparkar and possible contaminant sources: a multivariate study. *Ecotoxicology and environmental safety*, *89*, pp.95-107.

Camacho, L.M., Parra, R.R. and Deng, S., 2011. Arsenic removal from groundwater by MnO2-modified natural clinoptilolite zeolite: Effects of pH and initial feed concentration. *Journal of Hazardous materials*, *189*(1-2), pp.286-293.

Cheng, J.J., Schuster-Wallace, C.J., Watt, S., Newbold, B.K. and Mente, A., 2012. An ecological quantification of the relationships between water, sanitation and infant, child, and maternal mortality. Environmental Health, 11(1), p.4.

Chiban, M., Zerbet, M., Carja, G. and Sinan, F., 2012. Application of low-cost adsorbents for arsenic removal: A review. *Journal of Environmental Chemistry and Ecotoxicology*, *4*(5), pp.91-102.

Choong, T.S., Chuah, T.G., Robiah, Y., Koay, F.G. and Azni, I., 2007. Arsenic toxicity, health hazards and removal techniques from water: an overview. Desalination, 217(1-3), pp.139-166.

Craun, G.F., Brunkard, J.M., Yoder, J.S., Roberts, V.A., Carpenter, J., Wade, T., Calderon, R.L., Roberts, J.M., Beach, M.J. and Roy, S.L., 2010. Causes of outbreaks associated with drinking water in the United States from 1971 to 2006. *Clinical Microbiology Reviews*, *23*(3), pp.507-528.

Currell, M., Cartwright, I., Raveggi, M. and Han, D., 2011. Controls on elevated fluoride and arsenic concentrations in groundwater from the Yuncheng Basin, China. *Applied Geochemistry*, *26*(4), pp.540-552.

Danielopol, D.L., Griebler, C., Gunatilaka, A. and Notenboom, J., 2003. Present state and future prospects for groundwater ecosystems. *Environmental conservation*, pp.104-130.

Department of Water Affairs and forestry (DWAF). (2000). Policy and strategy for Groundwater quality management in South Africa. Pretoria, Republic of South Africa. https:// www.westerncape.gov.za/text/2003/groundwaterpol.pdf. Accessed July 2019.

Dhillon, A. and Kumar, D., 2015. Development of a nanoporous adsorbent for the removal of health-hazardous fluoride ions from aqueous systems. *Journal of Materials Chemistry A*, *3*(8), pp.4215-4228.

Edokpayi, J.N., Rogawski, E.T., Kahler, D.M., Hill, C.L., Reynolds, C., Nyathi, E., Smith, J.A., Odiyo, J.O., Samie, A., Bessong, P. and Dillingham, R., 2018. Challenges to sustainable safe drinking water: a case study of water quality and use across seasons in rural communities in Limpopo province, South Africa. *Water*, *10*(2), p.159.

Elwakeel, K.Z. and Al-Bogami, A.S., 2018. Influence of Mo (VI) immobilization and temperature on As (V) sorption onto magnetic separable poly p-phenylenediamine-thiourea-formaldehyde polymer. Journal of hazardous materials, 342, pp.335.

García, M.G. and Borgnino, L., 2015. Chapter 1: fluoride in the context of the environment. *Fluorine: chemistry. Analysis, Function and Effects*, pp.3-21.

Gerba, C.P. and Smith, J.E., 2005. Sources of pathogenic microorganisms and their fate during land application of wastes. *Journal of environmental quality*, *34*(1), pp.42-48.

Guo, Q. and Tian, J., 2013. Removal of fluoride and arsenate from aqueous solution by hydrocalumite via precipitation and anion exchange. *Chemical engineering journal*, *231*, pp.121-131.

Hao, J., Ji, L., Li, C., Hu, C. and Wu, K., 2018. Rapid, efficient and economic removal of organic dyes and heavy metals from wastewater by zinc-induced in-situ reduction and precipitation of graphene oxide. *Journal of the Taiwan Institute of Chemical Engineers*, *88*, pp.137-145.

Hongtao, L., Shuxia, L., Hua, Z., Yanling, Q., Daqiang, Y., Jianfu, Z. and Zhiliang, Z., 2018. Comparative study on synchronous adsorption of arsenate and fluoride in aqueous solution onto MgAlFe-LDHs with different intercalating anions. *RSC advances*, *8*(58), pp.33301-33313.

Izuagie, A.A., Gitari, W.M. and Gumbo, J.R., 2016. Synthesis and performance evaluation of Al/Fe oxide coated diatomaceous earth in groundwater defluoridation: towards fluorosis mitigation. *Journal of Environmental Science and Health, Part A*, *51*(10), pp.810-824.

Jadhav, S.V., Bringas, E., Yadav, G.D., Rathod, V.K., Ortiz, I. and Marathe, K.V., 2015. Arsenic and fluoride contaminated groundwaters: a review of current technologies for contaminants removal. *Journal of Environmental Management*, *162*, pp.306-325.

Jadhav, S.V., Bringas, E., Yadav, G.D., Rathod, V.K., Ortiz, I. and Marathe, K.V., 2015. Arsenic and fluoride contaminated groundwaters: a review of current technologies for contaminants removal. *Journal of Environmental Management*, *162*, pp.306-325.

Jadhav, S.V., Bringas, E., Yadav, G.D., Rathod, V.K., Ortiz, I. and Marathe, K.V., 2015. Arsenic and fluoride contaminated groundwaters: a review of current technologies for contaminants removal. *Journal of Environmental Management*, *162*, pp.306-325.

Joshi, A. and Chaudhuri, M., 1996. Removal of arsenic from ground water by iron oxide-coated sand. *Journal of environmental engineering*, *122*(8), pp.769-771.

Korotta-Gamage, S.M. and Sathasivan, A., 2017. A review: Potential and challenges of biologically activated carbon to remove natural organic matter in drinking water purification process. *Chemosphere*, *167*, pp.120-138.

Lemckert, C., 1999. Improving the delivery of problem/project-based learning in a traditional teaching environment. In 2nd Asia-Pacific Forum on Engineering and Technology Education, Forum Proceedings (pp. 149-152). UNESCO.

Loos, R., Locoro, G., Comero, S., Contini, S., Schwesig, D., Werres, F., Balsaa, P., Gans, O., Weiss, S., Blaha, L. and Bolchi, M., 2010. Pan-European survey on the occurrence of selected polar organic persistent pollutants in ground water. *Water research*, *44*(14), pp.4115-4126.

Masindi, V. and Gitari, W., 2013. Adsorption of oxyanions of As. *B, Cr, Mo and Se from coal fly ash leachates using*.

Mpenyana-Monyatsi, L., Mthombeni, N.H., Onyango, M.S. and Momba, M.N., 2012. Cost-effective filter materials coated with silver nanoparticles for the removal of pathogenic bacteria in groundwater. *International journal of environmental research and public health*, *9*(1), pp.244-271.

Mudyazhezha, S., Kanhukamwe, R., 2014. Environmental monitoring of the effects of conventional and artisanal gold mining on water quality in Ngwabalozi River, Southern Zimbabwe. IJEAS 4 (10), 13–18.

Mudzielwana, R., Gitari, M.W. and Ndungu, P., 2019. Enhanced As (III) and As (V) adsorption from aqueous solution by a clay based hybrid sorbent. *Frontiers in Chemistry*, *7*.

Mudzielwana, R., Gitari, M.W., Akinyemi, S.A. and Msagati, T.A., 2018. Performance of Mn 2+-modified bentonite clay for the removal of fluoride from aqueous solution. *South African Journal of Chemistry*, *71*, pp.15-23.

Nagendra Rao, C.R., 2003, December. Fluoride and environment—a review. In Proceedings of the third international conference on environment and health, Chennai, India (pp. 15-17).

Naujokas, M.F., Anderson, B., Ahsan, H., Aposhian, H.V., Graziano, J.H., Thompson, C. and Suk, W.A., 2013. The broad scope of health effects from chronic arsenic exposure: update on a worldwide public health problem. Environmental health perspectives, 121(3), pp.295-302.

Pruss-Ustun A, Bos R, Gore F, Bartram J: Safer Water, Better Health: Costs, Benefits and Sustainability of Interventions to Protect and Promote Health Geneva: WHO; 2008.

Rafiq, M., Shahid, M., Abbas, G., Shamshad, S., Khalid, S., Niazi, N.K. and Dumat, C., 2017. Comparative effect of calcium and EDTA on arsenic uptake and physiological attributes of Pisum sativum. *International journal of phytoremediation*, *19*(7), pp.662-669.

Rai SK, Onol K, Yanagida, S Ishiyama-Imura, M Kurokawa and CK Rai1. 2012.A *large-scale study of bacterial contamination of drinking water and its public health impact in Nepal*. Tokiwa University and 6Kobe Institute of Health, Kobe, Japan.

Reynolds, J.H. and Barrett, M.H., 2003. A review of the effects of sewer leakage on groundwater quality. *Water and Environment Journal*, *17*(1), pp.34-39.

Sambala, E.Z., Ngcobo, N., Machingaidze, S., Wiyeh, A.B., Mahasha, P.W., Jaca, A., Cooper, S. and Wiysonge, C.S., 2019. A global review of seasonal influenza vaccine introduction: analysis of the WHO/UNICEF Joint Reporting Form. *Expert review of vaccines*, *18*(8), pp.859-865.

Sanghratna, S. and Tanvir, A., 2015. Fluoride Removal from Water by various techniques: Review. *International journal of innovative science, engineering and technology*, *2*(9), pp.560-571.

Shakoor, M.B., Nawaz, R., Hussain, F., Raza, M., Ali, S., Rizwan, M., Oh, S.E., Ahmad, S., 2017. Human health implications, risk assessment and remediation of As-contaminated water: A critical review. Science of the Total Environment 601, 756-769.

Shannon, M.A., Bohn, P.W., Elimelech, M., Georgiadis, J.G., Marinas, B.J. and Mayes, A.M., 2010. Science and technology for water purification in the coming decades. In Nanoscience and technology: a collection of reviews from nature Journals (pp. 337-346).

Sharma, V.K., Sohn, M., 2009. Aquatic arsenic: toxicity, speciation, transformations,and remediation. Environ. Int. 35, 743e759.

Smedley, P.L. and Kinniburgh, D.G., 2002. A review of the source, behaviour and distribution of arsenic in natural waters. Applied geochemistry, 17(5), pp.517-568.

Sud, D., Mahajan, G. and Kaur, M.P., 2008. Agricultural waste material as potential adsorbent for sequestering heavy metal ions from aqueous solutions–A review. *Bioresource technology*, *99*(14), pp.6017-6027.

Thole, B., 2013. Ground water contamination with fluoride and potential fluoride removal technologies for East and Southern Africa. In Perspectives in Water Pollution. IntechOpen.

Thole, B., 2013. Ground water contamination with fluoride and potential fluoride removal technologies for East and Southern Africa. *Perspectives in Water Pollution*, pp.66-90.

Thompson, T., Fawell, J., Kunikane, S., Jackson, D., Appleyard, S., Callan, P., Bartram, J., Kingston, P., Water, S. and World Health Organization, 2007. *Chemical safety of drinking water: assessing priorities for risk management*. World Health Organization.

Ungureanu, G., Santos, S., Boaventura, R. and Botelho, C., 2015. Arsenic and antimony in water and wastewater: overview of removal techniques with special reference to latest advances in adsorption. *Journal of Environmental Management*, *151*, pp.326-342.

Villaescusa, I., Bollinger, J.C., 2008. Arsenic in drinking water: sources, occurrence and health effects (a review). Rev. Environ. Sci. Biotechnol. 7, 307e323.

Waghmare, S.S., Arfin, T., 2015. Fluoride removal from water by various techniques: review. Int. J. Innovative Sci. Eng. Technol. 2, 560–571.

WHO, 2000. *Global Water Supply and Sanitation Assessment 2000 Report*, World Health Organization, 92 4 156202 1, Geneva, Switzerland.

WHO, *Guidelines for drinking water quality, forth ed., World Health Organization*, Geneva, 2011

WHO, *Guidelines for drinking water quality, forth ed., World Health Organization*, Geneva, 2011

World Health Organization, 1993. *Guidelines for drinking-water quality*. World Health Organization.

World Health Organization, 2018. *WHO country cooperation strategy at a glance: The Gambia* (No. WHO/CCU/18.02/The Gambia). World Health Organization.

Wu, X., Zhang, Y., Dou, X. and Yang, M., 2007. Fluoride removal performance of a novel Fe–Al–Ce trimetal oxide adsorbent. Chemosphere, 69(11), pp.1758-1764.

Ye, Y., Li, P., Xu, T., Zeng, L., Cheng, D., Yang, M., Luo, J. and Lian, X., 2017. OsPT4 contributes to arsenate uptake and transport in rice. *Frontiers in Plant Science*, *8*, p.2197.

Zare, E.N., Lakouraj, M.M. and Kasirian, N., 2018. Development of effective nano-biosorbent based on poly m-phenylenediamine grafted dextrin for removal of Pb (II) and methylene blue from water. *Carbohydrate polymers*, *201*, pp.539-548.

Zhou, Y., Yu, C. and Shan, Y., 2004. Adsorption of fluoride from aqueous solution on La3+-impregnated cross-linked gelatin. *Separation and Purification Technology*, *36*(2), pp.89-94.

Chapter 2.

Literature review

2.1. Introduction

Groundwater is one of the most important sources for life which globally accounts for almost one-third of all freshwater resources and characterizes about 99% of available freshwater (Danielopol et al, 2004; Schouten, 2009, Wada, 2010). This water resource is also regarded as a precious source of drinking water (Krauss et al, 2011). The reason behind groundwater utilization is that it is naturally protected by overlaying sediments and soil layers and generally has better microbiological and biological properties (Thole, 2013; Palamuleni and Akoth, 2015). Groundwater quality is gradually challenged by human activities involving the direct and indirect introduction of chemicals (e.g. heavy metals, nutrients, nitrates fluoride, etc) and microbial (bacteria and virus) pollution due to demographic development and global climatic changes (Ellis, 2006; WHO, 2011 and 2018)

Contamination of groundwater is mainly due to natural and human activities such as agricultural, industrial, urbanization, infiltration of surface water which is chemical and microbial contaminated and leaching of organic and inorganic chemicals such as fluoride and arsenic from rocks (Sampat, 2000; Motalane and Strydom, 2004; Sorensen et al, 2015; Odiyo and Makungo, 2018). Different studies and surveys have reported that most of the boreholes used to supply water mostly in rural areas have high microbial, fluoride arsenic, heavy metals contents. The South Africa Department of Water Affairs and Forestry (DWAF) indicated that there are several boreholes across the country that contain apart from fluoride, levels of nitrate, some heavy metals, total dissolved solids, sulphates, and faecal coliforms that might pose a health risk to the human population. Hence, the co-existence of chemical and microbial pollutants in drinking water can pose severe threats to human health. Thus, water purification before any use is vital.

2.2. 1. Fluoride occurrence in groundwater

Fluoride is an electronegative element that is highly reactive. Fluoride is regarded as one of the important constituents in drinking water, even though it is required for health, it can cause detrimental health effects if it exceeds the permissible level (WHO, 1993,

Saxena and Ahmed, 2002; Raju, 2017). It is found in various rocks such as granite, granite gneisses, and pegmatite (Kim and Jeong, 2005; Blarasin et al, 2014,). Also, some studies have supported that fluoride occurrence depends on geology, geomorphology, climate, etc, (Kemambo et al, 2019). Contamination of fluoride in groundwater mainly occurs naturally through the dissolution of fluoride-containing minerals (Saxena and Ahmed, 2003; Blarasin et al, 2016; Li et al, 2019).

During rainfall seasons, fluoride element is released into groundwater and soil through weathering of primary minerals in rocks such as calcite (CaF), therefore leaching of fluoride-containing minerals yield fluoride solution (Adimalla and Venkatayogi, 2017). Besides natural occurrence, fluoride occurrence may be due to human activities such as agriculture, industrialization, etc (Jabal et al, 2014; Belete et al, 2015; Onipe, 2018). As a result of extensive utilization of material that contains fluoride e.g. fertilizers, fluoride is eventually leached to groundwater through infiltration during rainfall periods or irrigation.

2.2.2. Health implications of fluoride concentrations (its chemistry).

Fluoride is one of the pollutants that challenges living life forms, especially people. Fluoride enters the aqueous environment by weathering of fluoride-rich minerals and through anthropogenic actions, for example, industrial drains (Bhatnagar et al, 2011). Fluoride is widely distributed in the geological environment and is generally released into the groundwater by slow dissolution of fluorine-containing rocks (Abe et al, 2004). Fluoride is vital in little amount for mineralization of bone and assurance against dental caries, its excessive intake may result in decay of teeth and bone embrittlement bone which is called fluorosis (Waghmare and Arfin, 2015) as shown in Figure 1.On the contrary, excess intake of fluoride leads to various diseases such as osteoporosis, arthritis, brittle bones, cancer, infertility, brain damage, Alzheimer`s syndrome, and thyroid disorder (Harrison, 2005; Jha et al, 2011). Various studies have shown that excessive intake of water with fluoride exceeding 1.5mg/l may cause human health problems, hence, the significance of its removal.

Figure 1: Diagram shows skeletal and dental fluorosis (Luke et al,2001; Avocefohoun et al, 2017; Kumar and Sharma, 2017).

2.2.3. Fluoride removal methods

Fluoride removal techniques include coagulation, precipitation, membrane separation processes, ion exchange and adsorption techniques (Waghmare and Arfin, 2015 and Sanghratna et al, 2015). These methods have been assessed and each has its positive and negative outcomes (Yadav et al, 2009).

2.2.3.1. Coagulation or precipitation

The most useful precipitates for defluoridation of water are Lime and alum (Sanghratna et al, 2015 Yadav and Khandegar, 2020;) The method of precipitation involve adding aluminum salts, lime, and bleaching powder to fluoride-contaminated water or prepared fluoride solution, allowed to mix, then followed by flocculation, sedimentation, filtration, and disinfection (Renuka and Pushpanjali, 2013). This method is rarely applied in fluoride removal because it is of high cost, and the chemicals that are used can produce toxic sludge of aluminum fluoride, treated water can have an unpleasant taste (Singh et al, 2014; Yadav et al., 2019).

2.2.3.2. Ion Exchange Process

The ion-exchange process is a method in which contaminated water flows over a bed of ion material to remove an unwanted ion such as fluoride, arsenic, lead, and other ionic species (Yadav et al, 2017). This process involves two cation exchanges, which are positively and negatively charged ions. There are different anion exchangers, which include grounded charcoal, which has been previously used to remove fluoride using an ion-exchange process. Equally, synthesized resin (Singh et al., 1999), zeolites (Maurice et al, 2004), inorganic metallic oxides, greensand and zeolites are commonly used cations for fluoride removal (Mukherjee et al, 2017). This method has a high capacity to remove fluoride (95%); however, the ion exchangers or resins are expensive making it economically impossible, and the regeneration process yields a large quantity of waste (Jadav et al, 2015).

2.2.3.4. Membrane process.

This technique involves the use of a semi-permissible membrane to act as a barrier for pollutants such as pesticides, microbial, organic, and inorganic pollutants, etc. (Velazquez-Jimenez et al, 2015; Sangeetha et al, 2015). The membrane technique involves various processes, which include reverse osmosis, nanofiltration, dialysis, and electrodialysis. These methods of fluoride removal have been assessed and have a high capacity of fluoride removal, although it has such advantage, it cannot be used as it removes all ions, moreover, it is expensive as it requires re-mineralization process and operating cost.

2.2.3.3. Adsorption Method

Adsorption is a process in which solid holds liquid or gas molecules. The adsorption method involves the use of various materials as adsorbents for contaminant removal from aqueous solution. The adsorption technique has attracted many scientists since it involves the use of various materials for water treatment (Thole, 2013). Due to its removal efficiency, cost-effectiveness, ease of the process, and environmental stability, adsorption has become dominant for research techniques used in the treatment of polluted water (Mustafa et al, 2016). Although, different methods are being used for fluoride removal, the adsorption technique has attracted many scientists and engineers towards the successful, development of various adsorbents (Mondal et al, 2013). The materials used include activated alumina, carbon and charcoal, silica gel, calcite, activated sawdust, magnesia, serpentine, tricalcium

phosphate, activated soil sorbents and other synthetic ion-exchange resin (Bulusu and Pathak, 1980; Wang and Reardon, 2000; Raichur and Basu, 2001; Shrivastava and Vani, 2009).

Generally, various adsorbents have been assessed under various experimental conditions for water treatment (Yu et al., 2002). When preparing such adsorbent, it is important to optimize conditions such as pH, the dose of the adsorbent, temperature, fluoride concentration (initial level and after adding the adsorbent), and others to assess its adsorption capacity at those conditions (Rathinam et al, 2018). Several processes can be used to prepare the adsorbent which includes co-precipitation, hydrothermal, micelle (Chumming, 2016), solvothermal process (Gitari et al., 2017), chemical polymerization, electro-chemical, enzyme-catalyzed oxidative polymerization (Li et al, 2002; Obijole et al 2019).

2.2.4. Future perspective of fluoride removal technologies

Traditional technologies for defluoridation of drinking water that have been reviewed by various studies seem to be effective, although most of them have shown some negative outcomes (Yadav et al, 2018). Most of these technologies are not cost-effective (operational and upkeep costs) and indirectly cause environmental pollution e.g generation of toxic sludge due to the reaction process involved in the treatment (Sanghratna et al, 2015). Therefore, the mission for an appropriate fluoride removal method that is cost-effective and eco-friendly is very important.

2.3.1. Arsenic in groundwater

Many pollutants have been identified to be harmful to the environment and human health. Among these pollutants, arsenic is regarded as one of the most toxic heavy metal ions. It can occur naturally in the air, water, soils, etc. Erosion of rocks and minerals containing arsenic and volcanic activities are also considered to be natural sources of arsenic in the environment (Vaclavikova et al, 2008; Ungureanu et al, 2015). However, there are some anthropogenic activities which include painting, pesticides and insecticides application, fertilizers applications from agricultural fields, leather tanning and other related manufacturing and commercial activities that also influence arsenic occurrence into groundwater through the infiltration of water mostly during rainfall seasons, water discharges (industries and mines) and also irrigation processes (Lacasa et al, 2011; Le Pape et al, 2017; Elwakeel et al, 2016). Various

factors such as adsorption-desorption, precipitation-dissolution, oxidation-reduction, ion-exchange, the grain size of sediments, organic content, biological activity, and aquifer characteristics influence the occurrence of arsenic in groundwater (Ungureanu et al, 2015). Kim et al, (2012) and Ma et al (2012) further stated that the major mechanism that influences arsenic occurrence in groundwater is desorption from iron oxides or hydroxides from natural rocks and their reductive dissolution. A study was done by Mohan and Pittman 2007 revealed that unusually large concentrations of arsenic are existing in potential soluble forms.

2.3.2. Arsenic entry into the human body

A human can be exposed to arsenic in various ways which include airborne particulate matter, foods, and water consumption (Ungureanu et al, 2015). It is mostly stated that arsenic entry into the human body is due to excessive intake of polluted water (Bissena, 2003).

2.3.3. Chemistry and toxicity of arsenic

Arsenic is a metalloid inorganic compound. It occurs in two forms, which are arsenite (As(lll)) and arsenate (As(v)). The inorganic compounds that contain arsenic include hydrides, halides, oxides, acids, and sulphides (Krink-Othmer, 1992; Smedley and Kinniburgh, 2002). Besides, arsenite is more likely to occur in ground water because it is mainly prevalent in an anaerobic area, while arsenate is mainly prevalent in aerobic conditions (Smedley and Kinniburgh, 2002). Kundu and Gupta, 2005 further described that pH and redox are potential factors that influence arsenic occurrence in the environment. Arsenite usually occurs in less acidic environments, while arsenate predominant in high acidic (Bednar et al, 2002).

Also, it has been stated that the toxicity of arsenic is determined by its oxidation state, thus it can change its state depending on the abiotic and biotic factors of water (Hughes et al, 2011). It has also been proved that As^{3+} is more toxic than As^{5+} (Stylbo et al, 2000; Dopp et al, 2010). The toxicity of arsenic is directly associated with mobility in water and body liquids (Ungureanu et al, 2015). It has also been stated that arsenite is more mobile, soluble, and toxic than arsenate. The occurrence of arsenic in drinking water can pose threat to human health. Thus, the World Heathy Organisation has set a threshold of 0.1mg/L.

Figure 2: Diagram shows arsenicosis. (physics.harvard.edu/~wilson/arsenic/remediation/arsenic_project_remediation_technology.htm).

Prolonged exposure to arsenic may result in a chronic illness called arsenicosis (WHO, 2004) as shown in Fig. 2. Long-term exposure to arsenic during pregnancy may cause changes in fetal development and abortion (Smith et al, 2006).

2.3.4. Pathogens in ground water

One of the major public health risks globally is waterborne microbes (Bain et al, 2014). The occurrence of a pathogen in drinking water can lead to a variety of diseases such as fevers, dysenteries, cholera, diarrhea, etc which can further cause death both in children and adults (Lima et al, 2000; Behrman et al, 2004; Sorensen et al, 2015). Lack of safe drinking water and insufficient sanitation is the primary cause of the water borne disease (W.H.O/UNICEF, 2014). Equally, about 325 million people in sub-Saharan Africa lack access to safe drinking water, and only 30% of the population have access to adequate sanitation.

Introduction of a pathogen in groundwater is mainly due to human activities such as poor waste disposal, agricultural activities (e.g. animal droppings), discharge of wastewater from industries and municipality sewage into the water source and other untreated environments (Toze, 2004; Feichtmayer et al, 2017; Fout et al, 2017).

Pathogens enter groundwaters through the infiltration of polluted water from rivers, irrigation, stormwater runoffs, etc (Foster and Chilton, 2004; Schwarzenbach et al, 2010). Krauss and Griebler, (2011) further suggested that the entrance of pathogens may depend on environmental conditions and matrix characteristics (soil and sediment porosity and aquifer fractures). In addition, regions with thin soil layers and fractured aquifers are vulnerable to contamination, hence thick soil layers reduce or protect against pathogen entry (Rogasky, 2007; Nasser et al, 2002).

2.4.1 Pathogen sources and entry into aquifers

Due to high population growth and excessive land use, ground waters are increasingly contaminated with pathogens, which may pose threat to human health (Brink et al, 2007). Sources of microbes in groundwater include wastewater discharge from households and industries, sewage sludge use in agricultural farms, animal manure

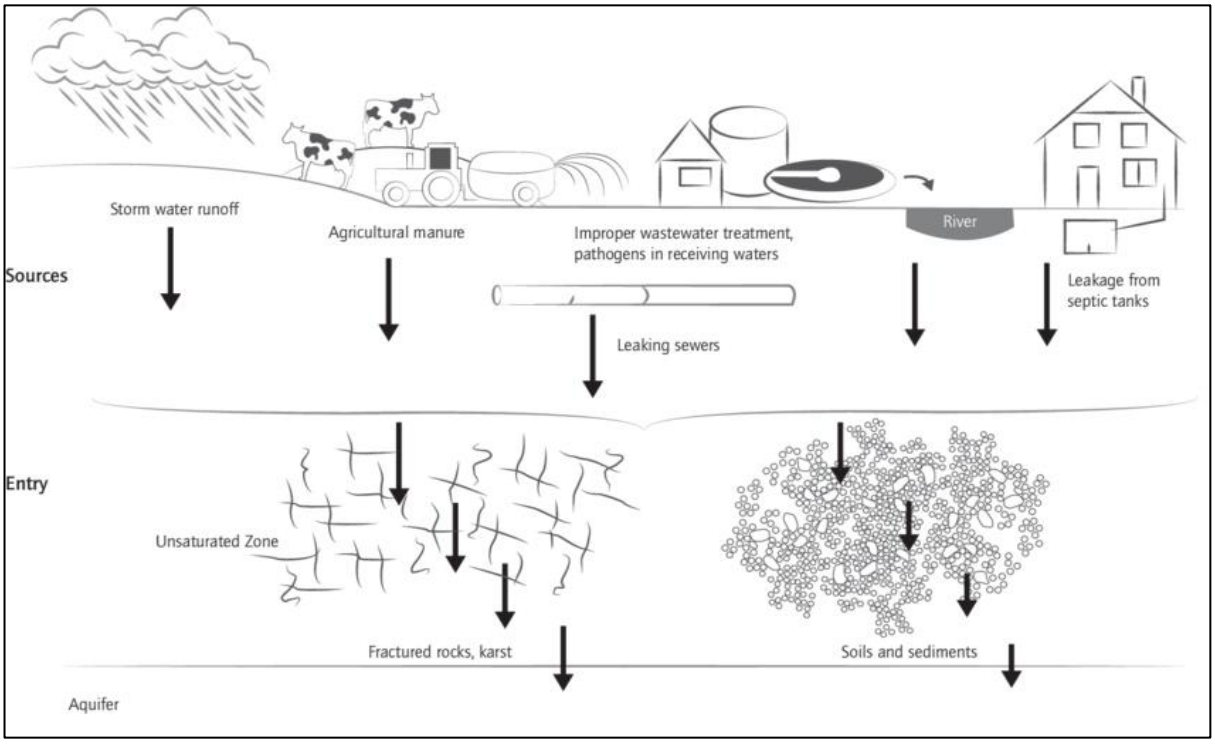

Figure 3. Microbial entry into aquifers (Kruass and Griebler, 2011).

Transportation of pathogens into groundwater mainly depends on the hydrogeology and climatic conditions of the environment (Bruce and Jon, 2000). Infiltration of polluted water from the surface is associated with floods, hence waterborne outbreaks mainly occur during floods and heavy rainfall events (King et al, 2016). Stormwater act as a transport agent of pathogens from the sources mainly livestock manure and

compost and wild animal dropping into difference surface water sources, thus increasing the concentration of microbes into rivers and other surface water sources. Infiltration of wastewater from a different source and rainfall water increases the proportion of microbes into groundwater (Besmer et al, 2016). As wastewater percolates into the ground with pathogens, the concentration of pathogens is initially decreased by soil and sediments through filtration. If percolation occurs continuously the number of pathogens in these soil and sediment layers rise, hence pathogens accumulate in the aquifer (Jurado et al, 2019). Different factors influence pathogen occurrence in groundwater. This involves pH, temperature, and dissolved oxygen (Regan et al, 2017).

Proper wastewater, waste disposal (planned landfill site) and wastewater transportation to the treatment sites are required to reduce the risk of health problems due to pathogens (UNESCO, 1999). Also, different disinfection methods have been used to remove pathogens in drinking water (Al-Rekabi et al, 2007). Methods include chlorination, UV irradiation, filtration technology, solar disinfection, and heat pasteurization (Bruce et al, 2000; Gomez et al, 2006, Peng et al, 2009; Al-Gheethiet al, 2018)

2.4. Methods for pathogen removal.

2.4.2. Chlorination

The most used disinfection method in developing countries is chlorination because it is readily present and regarded as a cheaper method when comparing it to oxidizing techniques (Al-Gheethiet al, 2018). Some studies have shown that chlorination could remove pathogens such as bacteria (e.g *E. coli*) (Tree et al, 2003). Although this method can remove pathogens in contaminated water, the presence of bacteria in treated sewage has been observed after chlorination (Al-Gheethiet al, 2018), therefore it is not effective enough to remove pathogens in water (Dungeni et al, 2010). Moreover, chlorination has a disadvantage of increasing/ causing turbidity, and discharge of free and combined chlorine which is regarded as a hazardous pollutant to the environment (Pehlivanoglu-Mantas et al, 2006).

2.4.2. UV radiation and solar disinfection

Ultraviolet radiation has been reported to have the ability to remove pathogens from water (Keller et al, 2003). It is regarded as one of the physical methods of water

disinfection method that is used to destroy the genetic components of bacteria (Shannon et al, 2008). Kollu and Ormeci, (2012) stated that the efficiency of UV methods depends on the concentration of the present microbes, the intensity of the UV radiation, and the time of the treatment. Also, some studies have suggested that UV can be used as an additional method or require to be used with other methods to be more effective (Dungeni et al, 2010).

Recently, solar disinfection methods have been used to remove microorganisms in water (Meierhofer and Wegelin; 2002; Sobsey et al, 2008; Gomez-Couso et al, 2009 and Al-Gheethiet al, 2018). Gomez-Couso et al, (2009), further stated that it is mostly used because it is readily available and it cheaper than adsorption methods. Although, it is low-cost, has no residual protection against recontamination, and it has no impact on removing chemical pollutants (Laurent, 2005).

2.4.3. Heat pasteurization

The fact that heating water can be used to reduce or remove pathogens has been known for decades, especially when the temperature of boiling water is at optimum (Himathongkham and Riemann, 1999; Al-Gheethiet al, 2018). Studies have shown that retention time and temperature are very important factors for the reduction of the pathogen when using this method (Alcalde et al, 2003). Although, this method is been used because it is easy to operate and cheap it cannot be used for chemical removal.

2.4.4. Filtration methods

Filtration systems have high efficiency in microbial removal (Sobsey et al, 2008). Despite its high efficiency, the treated water cannot be considered as microbial free since the treatment process results in the introduction of the pathogens due filter saturation after prolonged use (Gomez et al, 2006). Furthermore, membrane filtration technologies are expensive as it needs to be constructed and maintained (Neis and Blume 2002; Al-Gheethiet al, 2018). Various filtration structures have been manufactured depending on the low cost of the raw materials that are being used to produce a filter such as sour dust from carpentry industries and sand (Mohamed et al, 2016). However, the system has displayed high efficiency in the removal of turbidity, particulates, and organic matter, but its use for microbial reduction still needs more examination (Al-Gheethiet al, 2018).

2.5. Use of Polymeric Composites in Water Treatment

Various studies have shown that the aromatic diamine polymers have attracted great attention due to their multifunctionality, low cost and stability (Huang et al., 2000; Li et al, 2009; Yu et al, 2013). It has been stated these polymers are active absorbers and has attracted great attention because of their strong redox reversibility, chelation ability, adjustable conductivity, good electroactivity, photosensitive and magnetic activity, and associated with various environmental applications (Li et al., 2002; Baker et al, 2008; Yu et al, 2013). The composites that have been derived from a variety of monomers recently have become popular because of their effective infinite possibilities of monomer and composition, including different functional groups which allow them to be doped with other materials (e.g metal oxides) (Mezhuev et al, 2017). Mikitaev et al, (2014) gave an example of such polymers, which is poly-phenylenediamine (Fig. 3) with a wide range of application which includes water purification, protecting metals from corrosion, catalysis, electrorheology, sensors, energy-conversion devices, electrochromism and noble-metal recovery, and unique cations potential. Poly-phenylenediamine can remove various pollutants in water such as heavy metals (Huang, 2006), copper (Abdelwahab et al, 2015), phosphates (Mdlalose et al, 2017) and other pollutants.

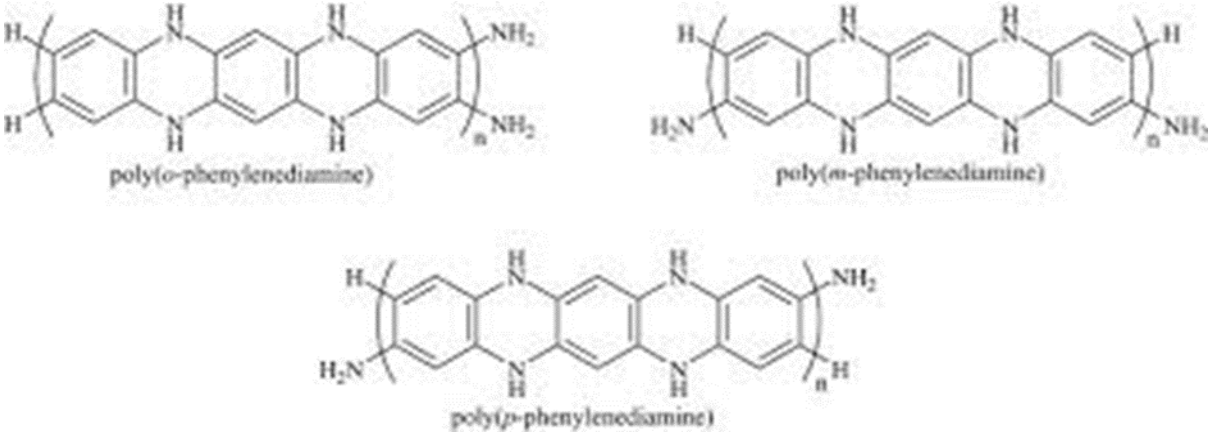

Figure 4: Chemical structures of poly-phenylenediamine (Mdlalose et al, 2017)

Furthermore, isomers of phenylenediamine polymer (poly-m-phenylenediamine, poly-o-phenylenediamine, and poly-para-phenylenediamine) have been used separately for water purification (Mdlalose et al, 2017). It has been discovered that the polymerization of these isomers depends on the monomer structure and solution polymerization medium (Huang et al, 2006). Polymers of poly-phenylenediamines are

manufactured as powders, colloidal dispersions, thin films, or composites, depending on reaction conditions and the process used to produce the polymers (Stejskal, 2014).

2.5. Methods for Poly-phenylenediamine (pPD) preparation.

Various methods have been used for synthesizing pPD which includes electrochemical, photo-oxidative polymerization, enzyme-catalyzed oxidative polymerization and chemical polymerization (Li et al, 2002; Chao et al, 2006 and Mdlalose et al, 2017).

2.6.1. Electrochemical Polymerisations.

Phenylenediamines can be polymerized using electrochemical polymerization by using cyclic voltammetry, constant potential, and constant current (Li et al., 2002 and Mdlalose et al, 2017). The polymerization process is obtained by the presence of electrical current through a solution of the monomer, solvent, and electrolyte mixture (Mdlalose et al, 2017). Various electrolytes have been used in this process which includes organic solvent-soluble and ion-dissociating organic (Li et al, 2002). Previous research has described that electrochemical polymerization exhibit several advantages which are the choice of monomer, diversity, and facility of polymerization, variety of macromolecular structure, the variability of electroactivity, multifunctionality, and potentially wide applicability (Li et al, 2002). This method of polymerization yields thin films that are deposited at the electrode surface (Li et al 2002 and Mdlalose et al, 2017). The properties of the attained film are co-ordinated by the varying electrolyte, concentration, and temperature or the current used for the polymerization process (Maksymiuk, 2006).

Li et al (2000), further describes the procedure that is followed in this method when synthesizing polymers of diamines, where pPD is carried out in a single- or dual compartment cell employed by three-electrode configuration comprising of working, counter, and reference electrodes in an electrochemical bath consisting of monomer and supporting electrolytes, which are both dissolved in a suitable solvent. After dissolving a monomer and electrolyte an appropriate power is supplied, cyclic voltammetry, electrical current potentiostatically or galvanostatically, is applied through the solution in the cell and finally, a thin film is obtained (Wang et al, 2001).

2.5.2. Photo-Oxidative Polymerization.

Some progress has been done in photo-oxidative polymerization of diamine polymers in the previous years, yet it seems like few studies have been done in this process when comparing it with chemical and electrochemical oxidations (Li et al, 2002). However, photo-oxidative polymerization has been also used to synthesize conducting polymers such as polyaniline {PAN} (Li et al, 2002). When polymerizing using this method, it is significant to optimize some conditions such as organic solvent, pH value, additive, and water content in the polymerization systems because if not optimized, these conditions could affect the synthesis process (Li et al, 2002). Uemura et al, (1999) and Li et al, (2002) described some of the procedures that have been followed when synthesizing PAN as stated below.

The N-phenyl-pPD and aniline mixture solution for the photopolymerization can be first prepared by a special technique because N-phenylpPD shows poor solubility in HCl aqueous solution. N-phenyl-pPD (1mM) could not be solubilized in 2 M HCl. The homogeneous solution containing 1 M Mn-phenyl-pPD, 300 mM AN, 60 mM tris(2.2′bipyridyl) ruthenium complex, and methyl viologen ion was illuminated under oxygen bubbling with visible light with a wavelength of 42600 cm and a power of 89.5 mW/cm^2 from the glass substrate side with a 500 W xenon lamp (Uemura et al, 1999) After illumination, the PAN formed was precipitated by adding NaOH aqueous solution, filtered, and dried under reduced pressure (Li et al, 2002).

2.5.3. Enzyme-Catalyzed Oxidative Polymerization

Recently, polymerizations of aromatic diamines using enzyme-catalyzed oxidation have been assessed, and it was concluded that it is chemically and environmentally friendly (Alva et al, 1997). In the nineteenth-century Li et al, (2002) proposed that this method is expected to have an excessive potential for producing polymers with new structures and properties of poly-phenylenediamines. The catalyst that was often used in the polymerization of polymers of diamines was horseradish peroxidative and a reversed micellar system was also used to enzyme-catalyzed polymerization of phenylenediamines (Li et al, 200; Ichinohe et al, 1998).

Li et al, (2002), explained the procedures of enzyme-catalyzed oxidation as follows: Firstly, prepare a solution of the solution of poly-phenylenediamine, horseradish peroxidative in a mixture of 1, 4-dioxane, phosphate, and 4-(2-hydroxyethyl)-1-

piperazineethanesulfonic acid buffer. Initiate the reaction by adding the same amount of oxidant (H_2O) solution three times at an interval of 30 min and the mixture was magnetically stirred for 24 hours at 30 ^oC. The polymerization reaction is also carried out utilizing reversed micelles using sodium di-ethylhexyl sulfosuccinate as a surfactant and isooctane as a solvent. The reversed micellar solution was obtained by dissolving di-ethylhexyl sulfosuccinate and pure water in isooctane, then polyphenylenediamine and 4-(2-hydroxyethyl)-1-piper-azineethanesulfonic buffer solutions were added to the micellar solution, and finally, the mixture was magnetically stirred at 30 °C overnight. The polymeric material is obtained by using HRP as the catalyst in a mixture of 1,4-dioxane and phosphate buffers. Furthermore, it is proposed that polymerization in this method depends on reaction time, solvent composition, monomer and its concentration, and the oxidant amount. In addition, when comparing chemically oxidative polymerization, the enzyme-catalyzed oxidative polymerization can provide aromatic diamine polymers with different macromolecular structures (Li et al, 2002). Although this method has such an advantage, it cannot be used for industrial applications because the materials that are used are more expensive (Mart, 2006).

2.5.4. Chemical Oxidation.

Among the various technologies that can be used to produce poly-phenylenediamines; chemical oxidation has been mostly used to synthesis these polymers because of its simplest procedures (Chao et al, 2006; Mdlalose et al, 2017). Mdlalose et al, (2017) and Orlov et al, (2006), described that the polymerization process is assumed to occur by allowing cation interaction followed by poly recombination of cation intermediates during oxidation. According to cation interaction, the primary diamine undertakes polymerization through N-C dimerization (head-to-tail addition) of the monomer due to nitrogen atom causing steric prevention (Mdlalose et al, 2017). Chemical oxidation occurs by introducing a poly-phenylenediamine monomer in a hydrochloric acid solution as it is the most-used polymerization medium (Li et al, 2002 and Pham et al. 2011). Furthermore, the solution is mixed with an oxidant which includes sodium, potassium, ammonium persulfate, ammonium peroxydisulfate, and others (Li et al, 2002, Trchova et al, 2014, Abdelwahab et al., 2015, and Mdlalose et al., 2017). When adding this oxidant, there is a change of colour, this shows that polymerization is taking place, the solution is left for 24 hours then filtered to collect the polymer residue and washed with deionized water and the polymer is dried (Li et al, 2014; Mdlalose et al,

2017). Furthermore, they are several conditions that have a great effect on polymerization reactions during the synthesis which include a monomer, solvent composition, oxidant, temperature, and time (Li et al, 2002). Poly-phenylenediamines powders produced from chemical oxidation can be used alone, and they have a functional property that allows them to be able to attach with other materials (Trchova et al, 2014). Hence, this property makes it easy to be doped with other chemicals especially metal oxides.

2.6. Principles of doping process of metal oxides into pPD matrix

The word doping is widely utilized in the field of conductive polymers. It has originated from semiconductor physics and explained the process in which the polymers are transformed into organic nature. Literature has stated that the new doped polymer is chemically different from its origin (do Nascimento et al, 2010). However, it has been stated that there are two different types of doping process namely red-ox and acid-base one (Haung et al,1986). Various studies have shown that the acid-base cannot be only achieved using H^+ acids (Bronsted) but can also be achieved using a variety of acid groups. The most used acids are the inorganic acid groups such as HCl, H_2SO_4 and H_3PO_4 (Sharma and Manchanda, 1982). However, HCl is the most used inorganic acid due to its non-oxidizing and volatile properties that make it easily removed or washed. Polymers of aniline (PANI) doped with inorganic acids are neither soluble nor fusible. The transformation of PANI into soluble or processible can be achieved using doping with acids or integrating soluble elemental groups to the aromatic rings of the polymer (Kulszewicz-Bajer, 2000).

Additionally, the process of doping has induced processability of aniline polymers which was achieved through PANI protonation. Hence, it is the reason for PANI transformation and exploration for various utilization and the researcher's attention attraction (Bieńkowski, 2006). Processability occurs due to the presence of a huge volume of anions which enables the separation of polymer chain by destroying the interchain interactions, making it more soluble (Łużny et al, 2002). Formally, two stages can be differentiated in PANI protonation. The first stage occurs when the imine groups of PANI are protonated by an acid, simultaneously anions that neutralize the positive charges on the chain are inserted into the polymer structure (Genoud et al,

2000). The formed di-cationic spinless species with quinoid type order of bonds can be conserved as a bipolar (Monahar et al, 1989).

PANI structures have a pair of nitrogen atoms with a lone electron pair. Thus, polymers of polyaniline can be considered as Lewis base (Genoud et al, 2000). Equally, to the process of protonation, one particle of dopant is bonded to a nitrogen atom, but different from protonation, both types of nitrogen sites are complex (Kulszewicz-Bajer,2000). In this process, the development of a covalent or mixed ionic-covalent bond was hypothesized.

2.7. Protonation of polyaniline with Lewis acid

As stated before, PANI can not only be doped with red-ox reactions but with acid-base reactions (acid(dopant) and base(polymer)) as other conjugative polymers. Thus, the simple polyaniline properties are determined especially from the practical point of view. However, PANI protonation was achieved by doping induced processability. The existence of a huge anion separates the polymer chains, weakens interchain interactions and purifies the polymer soluble (Bienkowski, 2006). These explanations can be extended to most bulky protonic polyaniline dopants**.**

Additionally, the structures of PANI isomers doped with Lewis acid can differ significantly from those of protonated polyaniline. Consequently, the structures of Lewis acid doped polyaniline exhibit significant chemical and spectroscopic different properties. Examples of Lewis acids used for PANI doping were metal halides such as $SnCl_4$, $AlCl_3$, and $FeCl_3$ (Kulszewicz-Bajer et al, 1999).

2.8. Use of metal, bimetallic oxides, and other materials in fluoride, arsenic removal as well as microbial disinfection.

Contamination of different water sources is a global challenge that requires immediate interventions. Various technologies have been used for pollutants removal such as fluoride, arsenic, and pathogen in aqueous solution. Furthermore, removal methods include ion-exchange, coagulation, membrane filtration, and adsorption (Gregor, 2001 and Zhang et al, 2003). Among these methods, adsorption techniques have been embraced as a better option for fluoride, arsenite, and pathogens removal because it is easy to operate, cost-effective, and it promotes environmentally stability.

Moreover, different salts, doped polymers, and agricultural waste have been used for fluoride and arsenic removal as well as microbial disinfection which includes iron oxides, cerium salts, aluminium, and others (Jiang et al 2001, Zhang et al, 2003, Modlalose et al, 2018). The use of these materials has been assessed by World Health Organization and has yield better results, but they are of high cost, time-consuming and it has been stated that some produce sludge when utilizing (WHO, 2001). Hence, this affects their use.

Additionally, it has been stated that the hydrous oxides of rare earth elements have a high affinity towards fluoride and arsenic removal (Zhang et al, 2003, 2010 and Wu et al, 2002 and 2005). The synthesized composites have high adsorption potential due to their high cation exchange capacity and high surface area. Recently, the hydrous Ce(IV) oxide was the most effective for removing fluoride without significant dissolution even at pH 2 but the problem for the use of Ce compounds is of high cost and leaching at high pH (Zhang et al, 2005).

Conversely, iron oxides have been reported to be effective for fluoride and arsenic removal (Reed et al, 2000, Wu et al, 2007) due to their affinity toward inorganic pollutants and their consequent selectivity of the adsorption process (Cornell and Schwertmann, 1996). Zhang et al, (2005), further described that iron hydroxides have indicated low adsorption capacities, slow adsorption process, and narrow optimum pH ranges (4, 5) which compromises their applicability.

Although hydrous oxides of rare earth elements have been proposed as a new sorption medium for removing aqueous hazardous anions such as arsenic, fluoride, and phosphate, they have a problem of the high cost to synthesize and process and some pose a problem of leaching (Hideaki, eta al, 1997). The fluoride and arsenic removal effectiveness of Fe, Mg, Ce, or Mn oxides individually or in combination with other metal oxides from water has been widely reported (Wu et al, 2007; Wang et al, 2015) as shown in Table 1. Mixing metal oxides such as Fe, Ce, Zr, La, Ti, Al, Mg, etc, with each other or with agricultural waste (e.g., sour dust) and polymers has attracted researcher`s attention. The reason being that these materials they act as a supporting agent which can reduce leaching problem as well as the expenses of using bulk rare earth metal oxides. Also, this could be an emerging way to enhance the surface area of the adsorbent. Thus, increasing adsorption efficiency of the resulting material.

However, the antimicrobial action of the rare earth elements such as Ag, Mg, etc., has been done but there is limited data for such. Hence, efforts are being tailored to the importance of evaluating whether the number of metals in a sorbent has a consistent determinant of enhanced toxic metal ions adsorption as well as microbial disinfection.

As the literature revealed , it is imported to develop a low-cost composite material that will promote environmental stability. Also, the developed material must also work as a conventional method of water treatment, which can simultaneously remove multiple contaminants. Thus , reducing the cost. Hence, the aim of this study is to simultaneously remove various water contaminants from aqueous solution. This could be supported by the material that were developed due to their different functional groups, which after modification will aid to an enhanced surface area with more available active sites to bind with inorganic pollutants.

1 Table 1. Fe and Ce based previously used adsorbents for fluoride and arsenite removal from aqueous solutions.

	F^-	As^{3+}	
Adsorbents	Adsorption parameters	Adsorption parameters	Ref
Mg-Al-Ce	3,33 hrs, 200 g, pH 7, 50-120 mg/L, 24.89 mg/g	-	Chi et al,2017
Ce-Fe bimetal	24 hrs, 0.5 g, pH 7, 10-30 mg/L, 60.71 mg/g	-	Zhang et al, 2017.
Fe/Ce bimetal oxide	-	24 hrs, 0.2g, pH 8, 1-150 mg/L, 281.34 mg/g	Wen et al, 2020
Ce-AlOOH	2 hrs, 50 g,1-10 mg/L, pH 3, 62.8 mg/g	-	Tao et al, 2020
CTS-Ce composite	12 hrs, desired, 5-100 mg/L, pH 4, 153 mg/g	-	Zhu et al, 2017
A-ZVI-ferric chloride	-	200 mins, 2.5 g, pH 6.7, 2-10 mg/L, 3.79 mg/g	Jain and Agarwal, 2017
Fe3O4	3.3 hrs, 0.05 g, 1-10 mg/L, pH 6.5, 1.78mg/g	3.3 hrs, 0.05 g,1-10 mg/L, pH 6.5, 0.91 mg/g	Prathna et al, 2017
Fe-Ti-Mn composite oxide	-	10 hrs, none ,1-35 mg/L, pH 4.5, 24.2 mg/g	Zhang et al, 2019
Fe3O4@TiO2 sheets	-	1hr, 0.025g, 1-60 mg/L, pH 4, 30.96 mg/g	Deng et al, 2019
Fe3O4@Mg–Al–O	2.30 hrs, 0.5 g, 250 mg/L, pH 4, 170 mg/g	-	Ma et al, 2019

2.9. References

Abdelwahab N.A; AL-Ashkar E.A; El-Gihaffai M.A.A. 2015. Preparation and characterization of eco-friendly poly (p-phenylenediamine) and its composite with chitosan for removal of copper ions from aqueous solutions. Polymers and Pigments Department, National Research Centre, Egypt.

Abe, S. Iwasaki, T. Tokimoto, N. Kawasaki, T. Nakamura, S. Tanada, Adsorption of fluoride ions onto carbonaceous materials, J. Colloid Interface Sci. 275 (2004) 35–39.

Adimalla, N. and Venkatayogi, S.J.E.E.S., 2017. Mechanism of fluoride enrichment in groundwater of hard rock aquifers in Medak, Telangana State, South India. *Environmental Earth Sciences*, *76*(1), p.45.

Alcalde, L., Oron, G., Gillerman, L., Salgot, M. and Manor, Y., 2003. Removal of fecal coliforms, somatic coliphages and F-specific bacteriophages in a stabilization pond and reservoir system in arid regions. Water Science and Technology: Water Supply, 3(4), pp.177-184.

Al-Gheethi, A.A., Efaq, A.N., Bala, J.D., Norli, I., Abdel-Monem, M.O. and Kadir, M.A., 2018. Removal of pathogenic bacteria from sewage-treated effluent and biosolids for agricultural purposes. *Applied Water Science*, *8*(2), p.74.

Al-Rekabi, W.S., Qiang, H. and Qiang, W.W., 2007. Review on sequencing batch reactors. Pakistan Journal of nutrition, 6(1), pp.11-19.

Alva, K.S., Kumar, J., Marx, K.A. and Tripathy, S.K., 1997. Enzymatic synthesis and characterization of a novel water-soluble polyaniline: poly (2, 5-diaminobenzenesulfonate). Macromolecules, 30(14), pp.4024-4029.

Avocefohoun, A.S., Gbaguidi, B.A., Sina, H., Biaou, O., Houssou, C.S. and Baba-Moussa, L., 2017. Fluoride in water intake and prevalence of dental fluorosis stains among children in Central Benin. *International Journal of Medical Research & Health Sciences*, *6*(12), pp.71-77.

Baker, C.O., Shedd, B., Innis, P.C., Whitten, P.G., Spinks, G.M., Wallace, G.G. and Kaner, R.B., 2008. Monolithic actuators from flash-welded polyaniline nanofibers. Advanced Materials, 20(1), pp.155-158.

Bednar, A.J., Garbarino, J.R., Ranville, J.F. and Wildeman, T.R., 2002. Preserving the distribution of inorganic arsenic species in groundwater and acid mine drainage samples. *Environmental Science & Technology*, *36*(10), pp.2213-2218.

Behrman, Richard E., Kliegman, RobertM.,Jenson,HalB. 2004. NelsonTextbook of Pediatrics, 17thed. Saunders, Philadelphia, Pennsylvania.

Belete, A., Beccaluva, L., Bianchini, G., Colombani, N., Fazzini, M., Marchina, C., Natali, C. and Rango, T., 2015. Water–rock interaction and lake hydrochemistry in the Main Ethiopian Rift. In *Landscapes and Landforms of Ethiopia* (pp. 307-321).

Besmer, M.D., Epting, J., Page, R.M., Sigrist, J.A., Huggenberger, P. and Hammes, F., 2016. Online flow cytometry reveals microbial dynamics influenced by concurrent natural and operational events in groundwater used for drinking water treatment. *Scientific reports*, *6*, p.38462.

Bhatnagar, A., Kumar, E. and Sillanpää, M., 2011. Fluoride removal from water by adsorption—a review. *Chemical engineering journal*, *171*(3), pp.811-840.

Bieńkowski, K., 2006. *Polyaniline and its derivatives doped with Lewis acids-synthesis and spectroscopic properties* (Doctoral dissertation, Chair Of Polymer Chemistry And Technology).

Bissen, M. and Frimmel, F.H., 2003. Arsenic—a review. Part I: occurrence, toxicity, speciation, mobility. *Acta hydrochimica et hydrobiologica*, *31*(1), pp.9-18.

Blarasin, M., Cabrera, A. and Matteoda, E., 2014. Groundwater from the province of Córdoba. *I'll take it. National University of Rio Cuarto. Argentina*.

Blarasin, M., Quinodóz, F.B., Cabrera, A., Matteoda, E., Alincastro, N. and Albo, J.G., 2016. Weekly and monthly groundwater recharge estimation in a rural piedmont environment using the water table fluctuation method. *International Journal of Environmental & Agriculture Research*, *2*(5), pp.104-113.

Bradshaw, J.K., Snyder, B.J., Oladeinde, A., Spidle, D., Berrang, M.E., Meinersmann, R.J., Oakley, B., Sidle, R.C., Sullivan, K. and Molina, M., 2016. Characterizing relationships among fecal indicator bacteria, microbial source tracking markers, and associated waterborne pathogen occurrence in stream water and sediments in a mixed land use watershed. *Water research*, *101*, pp.498-509.

Brink, A., Moolman, J., Da Silva, M.C. and Botha, M., 2007. Antimicrobial susceptibility profile of selected bacteraemic pathogens from private institutions in South Africa. *South African Medical Journal*, *97*(4), pp.273-279.

Bruce A.M and Jon C.M. 2000. Current knowledge on groundwater microbial pathogens and their control. US Environmental Protection Agency, California, USA, Hydrogeology Journal (2000) 8:29±40

Bulusu KR and Pathak BN.1980. Discussion on water defluoridation with activated alumina. Journal of Environmental Engineering Division 1980; 106 (2) 466–469.

Chandrashekara, M. and Yadav, A., 2017. Water desalination system using solar heat: a review. Renewable and Sustainable Energy Reviews, 67, pp.1308-1330.

Chao, D., Lu, X., Chen, J., Zhao, X., Wang, L., Zhang, W. and Wei, Y., 2006. New method of synthesis of electroactive polyamide with amine-capped aniline pentamer in the main chain. Journal of Polymer Science Part A: Polymer Chemistry, 44(1), pp.477-482.

Danielopol, D.L., Gibert, J., Griebler, C., Gunatilaka, A., HAHN, H.J., Messana, G., Notenboom, J. and Sket, B., 2004. Incorporating ecological perspectives in European groundwater management policy. *Environmental Conservation*, *31*(3), pp.185-189.

do Nascimento, G.M., Sestrem, R.H. and Temperini, M.L., 2010. Structural characterization of poly-para-phenylenediamine–montmorillonite clay nanocomposites. *Synthetic metals*, *160*(23-24), pp.2397-2403.

Dopp, E., Von Recklinghausen, U., Diaz-Bone, R., Hirner, A.V. and Rettenmeier, A.W., 2010. Cellular uptake, subcellular distribution and toxicity of arsenic compounds in methylating and non-methylating cells. *Environmental Research*, *110*(5), pp.435-442.

Dungeni, M., van Der Merwe, R.R. and Momba, M., 2010. Abundance of pathogenic bacteria and viral indicators in chlorinated effluents produced by four wastewater treatment plants in the Gauteng Province, South Africa. *Water SA*, *36*(5).

Ellis, J.B., 2006. Pharmaceutical and personal care products (PPCPs) in urban receiving waters. Environ. Pollut. 144 (1), 184e189.

Elwakeel, K.Z. and Al-Bogami, A.S., 2018. Influence of Mo (VI) immobilization and temperature on As (V) sorption onto magnetic separable poly p-phenylenediamine-thiourea-formaldehyde polymer. Journal of hazardous materials, 342, pp.335

Feichtmayer, J., Deng, L. and Griebler, C., 2017. Antagonistic microbial interactions: contributions and potential applications for controlling pathogens in the aquatic systems. *Frontiers in microbiology*, *8*, p.2192.

Foster, S.S.D. and Chilton, P.J., 2004. Downstream of downtown: urban wastewater as groundwater recharge. Hydrogeology Journal, 12(1), pp.115-120.

Fout, G.S., Borchardt, M.A., Kieke, B.A. and Karim, M.R., 2017. Human virus and microbial indicator occurrence in public-supply groundwater systems: meta-analysis of 12 international studies. Hydrogeology journal, 25(4), pp.903-919.

Genoud, F., Kulszewicz-Bajer, I., Bedel, A., Oddou, J.L., Jeandey, C. and Pron, A., 2000. Lewis acid doped polyaniline. Part II: Spectroscopic studies of emeraldine base and emeraldine hydrochloride complexation with FeCl3. *Chemistry of materials*, *12*(3), pp.744-749.

Genoud, F., Kulszewicz-Bajer, I., Bedel, A., Oddou, J.L., Jeandey, C. and Pron, A., 2000. Lewis acid doped polyaniline. Part II: Spectroscopic studies of emeraldine base and emeraldine hydrochloride complexation with FeCl3. *Chemistry of materials*, *12*(3), pp.744-749.

Gerba, C.P. and Smith, J.E., 2005. Sources of pathogenic microorganisms and their fate during land application of wastes. *Journal of environmental quality*, *34*(1), pp.42-48.

Gitari M.W, Izuage A.A, Gumbo J.R. 2017. *Synthesis, characterisation and batch assessment of groundwater fluoride removal capacity of Mg/Ce/Mn oxide-modified diatomaceous earth.* Department of Ecology and Resources Management, University of Venda, South, Africa

Godfrey, S., Timo, F. and Smith, M., 2006. Microbiological risk assessment and management of shallow groundwater sources in Lichinga, Mozambique. *Water and Environment Journal*, *20*(3), pp.194-202.

Goel, V., Islam, M.S., Yunus, M., Ali, M.T., Khan, A.F., Alam, N., Faruque, A.S.G., Bell, G., Sobsey, M. and Emch, M., 2019. Deep tubewell microbial water quality and access in arsenic mitigation programs in rural Bangladesh. *Science of The Total Environment*, *659*, pp.1577-1584.

Gomez M, Rua A, Garralon G, Plaza F, Hontoria E, Gomez MA 2006 Urban wastewater disinfection by filtration technologies. Desalination 190(1–3):16–28.

Gomez-Couso H, Fontan-Sainz M, Sichel C, Fernandez-Ibanez P, Ares-Mazas E (2009) Efficacy of the solar water disinfection method in turbid waters experimentally contaminated with Cryptosporidium parvum oocysts under real field conditions. Trop Med Int Health 14(6):620–627

Harrison, P.T., 2005. Fluoride in water: a UK perspective. *Journal of fluorine chemistry*, *126*(11-12), pp.1448-1456.

Himathongkham S, Riemann H (1999) Destruction of S. typhimurium, E. coli O157:H7 and L. monocytogenes in chicken manure by drying and/or gassing with ammonia. FEMS Microbiol Lett 171(2):179–182

Huang, M.R., Peng, Q.Y. and Li, X.G., 2006. Rapid and effective adsorption of lead ions on fine poly (phenylenediamine) microparticles. Chemistry-A European Journal, 12(16), pp.4341-4350.

Huang, S.J. and Roby, M.S., 1986. Biodegradable Polymers Poly (amide-urethanes). *Journal of Bioactive and Compatible Polymers*, *1*(1), pp.61-71.

Huang, W.S., 1986. BD Humphrey and AG MacDiarmid. *J. Chem. Soc. Faraday Trans. I*, *82*(2385), p.117.

Hughes, M.F., Beck, B.D., Chen, Y., Lewis, A.S. and Thomas, D.J., 2011. Arsenic exposure and toxicology: a historical perspective. *Toxicological Sciences*, *123*(2), pp.305-332.

Ichinohe, D., Saitoh, N. and Kise, H., 1998. Oxidative polymerization of phenylenediamines in reversed micelles. Macromolecular Chemistry and Physics, 199(6), pp.1241-1245. Indian J. Environ. Toxicol. 117–32.

Izumi, C.M., Constantino, V.R., Ferreira, A.M.C. and Temperini, M.L., 2006. Spectroscopic characterization of polyaniline doped with transition metal salts. *Synthetic metals*, *156*(9-10), pp.654-663.

Jabal, M.S.A., Abustan, I., Rozaimy, M.R. and Al-Najar, H., 2014. Fluoride enrichment in groundwater of semi-arid urban area: Khan Younis City, southern Gaza Strip (Palestine). *Journal of African Earth Sciences*, *100*, pp.259-266.

Jha, S.K., Mishra, V.K., Sharma, D.K. and Damodaran, T., 2011. Fluoride in the environment and its metabolism in humans. In *Reviews of Environmental Contamination and Toxicology Volume 211* (pp. 121-142). Springer, New York, NY.

Jurado, A., Bofill-Mas, S., Vázquez-Suñé, E., Pujades, E., Girones, R. and Rusiñol, M., 2019. Occurrence of pathogens in the river–groundwater interface in a losing river stretch (Besòs River Delta, Spain). *Science of The Total Environment*, *696*, p.134028.

Keller R, Passamani F, Vaz L, Cassini ST, Goncalves RF (2003) Inactivation of Salmonella spp. from secondary and tertiary effluents by UV irradiation. Water Sci Technol 47(3):147–150

Kim, K. and Jeong, G.Y., 2005. Factors influencing natural occurrence of fluoride-rich groundwaters: a case study in the southeastern part of the Korean Peninsula. *Chemosphere*, *58*(10), pp.1399-1408.

Kim, S.H., Kim, K., Ko, K.S., Kim, Y, Lee, K.S., 2012. Co-contamination of arsenic and fluoride in the groundwater of unconsolidated aquifers under reducing environments. *Chemosphere*, *87*(8), pp.851-856.

Kimambo, V., Bhattacharya, P., Mtalo, F., Mtamba, J. and Ahmad, A., 2019. Fluoride occurrence in groundwater systems at global scale and status of defluoridation–state of the art. *Groundwater for Sustainable Development*, *9*, p.100223.

King, D.N., Donohue, M.J., Vesper, S.J., Villegas, E.N., Ware, M.W., Vogel, M.E., Furlong, E.F., Kolpin, D.W., Glassmeyer, S.T. and Pfaller, S., 2016. Microbial pathogens in source and treated waters from drinking water treatment plants in the United States and implications for human health. *Science of the Total Environment*, *562*, pp.987-995.

Kirschner, D.E. and Linderman, J.J., 2009. Mathematical and computational approaches can complement experimental studies of host–pathogen interactions. *Cellular microbiology*, *11*(4), pp.531-539.

Kollu K, Ormeci B (2012) Effect of particles and bio-flocculation on ultraviolet disinfection of E. coli. Water Res 46(3):750–760

Krauss, S., Griebler, C. and Deutsche Akademie der Technikwissenschaften, 2011. Pathogenic microorganisms and viruses in groundwater. Acatech.

Kulszewicz-Bajer, I., Proń, A., Abramowicz, J., Jeandey, C., Oddou, J.L. and Sobczak, J.W., 1999. Lewis acid doped polyaniline: preparation and spectroscopic characterization. *Chemistry of materials*, *11*(3), pp.552-556.

Kulszewicz-Bajer, I., Zagorska, M. and Rozalska, I., 2001. Polyaniline doped with esters of 5-sulfo-i-phthalic acid and its blends with nonconducting polymers. *Synthetic metals*, *119*(1-3), pp.69-70.

Kumar, S. and Sharma, S.K., 2017. Groundwater quality of Hisar city of Haryana state, India—status of fluoride content. *Int J Chem Sci*, *15*(4), pp.1-10.

Kumar, S. and Sharma, S.K., 2017. Groundwater quality of Hisar city of Haryana state, India—status of fluoride content. *Int J Chem Sci*, *15*(4), pp.1-10.

Lacasa, E., Canizares, P., Saez, C., Fernández, F.J. and Rodrigo, M.A., 2011. Electrochemical phosphates removal using iron and aluminium electrodes. Chemical Engineering Journal, 172(1), pp.137-143.

Laurent, P., 2005. Household drinking water systems and their impact on people with weakened immunity. MSF-Holland, Public Health Department, February.

Le Pape, P., Battaglia-Brunet, F., Parmentier, M., Joulian, C., Gassaud, C., Fernandez-Rojo, L., Guigner, J.M., Ikogou, M., Stetten, L., Olivi, L. and Casiot, C., 2017. Complete removal of arsenic and zinc from a heavily contaminated acid mine drainage via an indigenous SRB consortium. *Journal of hazardous materials*, *321*, pp.764-772.

LI X G; MA X L; SUN J and Huang M R. 2009. Powerful reactive sorption of silver (I) and mercury (II) onto poly (o-phenylenediamine) microparticles [J]. Langmuir, 25: 16751684.

Li, P., He, X., Li, Y. and Xiang, G., 2019. Occurrence and health implication of fluoride in groundwater of loess aquifer in the Chinese loess plateau: a case study of Tongchuan, Northwest China. *Exposure and Health*, *11*(2), pp.95-107.

Li, X., Zhang, B., Li, W., Lei, X., Fan, X., Tian, L., Zhang, H. and Zhang, Q., 2014. Preparation and characterization of bovine serum albumin surface-imprinted thermosensitive magnetic polymer microsphere and its application for protein recognition. *Biosensors and Bioelectronics*, *51*, pp.261-267.

Li, X.G., Huang, M.R., Duan, W. and Yang, Y.L., 2002. Novel multifunctional polymers from aromatic diamines by oxidative polymerizations. Chemical Reviews, 102(9), pp.2925-3030.

Li, X.G., Huang, M.R., Duan, W. and Yang, Y.L., 2002. Novel multifunctional polymers from aromatic diamines by oxidative polymerizations. Chemical Reviews, 102(9), pp.2925-3030.

Lima, A. A. M. et al. Persistent diarrhea signals a critical period of increased diarrhea burdens and nutritional shortfalls: a prospective cohort study among children in northeastern brazil. J. Infect. Dis. 181, 1643–1651 (2000).

Łużny, W., Śniechowski, M. and Laska, J., 2002. Structural properties of emeraldine base and the role of water contents: X-ray diffraction and computer modelling study. *Synthetic metals*, *126*(1), pp.27-35.

Ma, L., Wang, L., Jia, Y. and Yang, Z., 2016. Arsenic speciation in locally grown rice grains from Hunan Province, China: spatial distribution and potential health risk. *Science of the Total Environment*, *557*, pp.438-444.

Maksymiuk, K., 2006. *Chemical reactivity of polypyrrole and its relevance to polypyrrole based electrochemical sensors*. Electroanalysis, 18(16), pp.1537–1551.

Mart, H., 2006. Oxidative polycondensation reaction. *Designed monomers and polymers*, *9*(6), pp.551-588.

Mdlalose, L., Balogun, M., Setshedi, K., Tukulula, M., Chimuka, L. and Chetty, A., 2017. Synthesis, characterization and optimization of poly (p-phenylenediamine)-based organoclay composite for Cr (VI) remediation. *Applied Clay Science*, *139*, pp.72-80.

Mezhuev, Y.O., Korshak, Y.V. and Shtilman, M.I., 2017. Oxidative polymerization of aromatic amines: kinetic features and possible mechanisms. *Russian Chemical Reviews*, *86*(12), p.1271.

Mikitaev, A.K., BEDANOKOV, A. and Mikitaev, M.A., 2014. Polymeric Nanocomposites: Structure, Manufacture, And Properties. *Engineering of Polymers and Chemical Complexity, Volume II: New Approaches, Limitations and Control*, p.1.

Mohamed, R.M.S.R., Al-Gheethi, A.A., Miau, J.A. and Kassim, A.H.M., 2016. Multi-component Filters for Domestic Graywater Treatment in Village Houses. Journal-American Water Works Association, 108(7), pp.E405-E415.

Mohan, D. and Pittman Jr, C.U., 2007. Arsenic removal from water/wastewater using adsorbents—a critical review. *Journal of hazardous materials*, *142*(1-2), pp.1-53.

Mondal, N.K., Bhaumik, R., Roy, P., Das, B. and Datta, J.K., 2013. Investigation on fixed bed column performance of fluoride adsorption by sugarcane charcoal. *Journal of environmental biology*, *34*(6), p.1059.

Mukherjee, S., Yadav, V., Mondal, M., Banerjee, S. and Halder, G., 2017. Characterization of a fluoride-resistant bacterium Acinetobacter sp. RH5 towards assessment of its water defluoridation capability. *Applied Water Science*, *7*(4), pp.1923-1930.

Mustafa, G., Wyns, K., Buekenhoudt, A. and Meynen, V., 2016. Antifouling grafting of ceramic membranes validated in a variety of challenging wastewaters. *Water research*, *104*, pp.242-253.

Nasser, A.M., Glozman, R. and Nitzan, Y., 2002. Contribution of microbial activity to virus reduction in saturated soil. Water Research, 36(10), pp.2589-2595.

Neis U, Blume 2002.Ultrasonic disinfection of wastewater effluents for high-quality reuse. IWA Regional Symposium on Water Recycling in Mediterranean Region, Iraklio, Greece, 26.-29.0

Obijole, O.A., Gitari, M.W., Ndungu, P.G. and Samie, A., 2019. Mechanochemically Activated Aluminosilicate Clay Soils and their Application for Defluoridation and Pathogen Removal from Groundwater. *International Journal of Environmental Research and Public Health*, *16*(4), p.654.

Odiyo, J.O. and Makungo, R., 2018. Chemical and microbial quality of groundwater in Siloam village, implications to human health and sources of contamination. *International journal of environmental research and public health*, *15*(2), p.317.

Onipe, T.A., 2018. *Geogenic fluoride source in groundwater: A case study of Siloam Village, Limpopo Province, South Africa* (Doctoral dissertation).

Orlov, A.V., Ozkan, S.Z. and Karpacheva, G.P., 2006. Oxidative polymerization of diphenylamine: A mechanistic study. Polymer Science Series B, 48(1), pp.11-17.

Othmer, K., 1992. Encyclopedia of Chemical Technology (halaman 659).

Palamuleni, L. and Akoth, M., 2015. Physico-chemical and microbial analysis of selected borehole water in Mahikeng, South Africa. *International journal of environmental research and public health*, *12*(8), pp.8619-8630.

Pang, L., Nowostawska, U., Ryan, J.N., Williamson, W.M., Walshe, G. and Hunter, K.A., 2009. Modifying the surface charge of pathogen-sized microspheres for studying pathogen transport in groundwater. *Journal of Environmental Quality*, *38*(6), pp.2210-2217.

Pehlivanoglu-Mantas E, Elisabeth L, Hawley R, Deeb A, Sedlak DL (2006) Formation of nitrosodimethylamine (NDMA) during chlorine disinfection of wastewater effluents prior to use in irrigation systems. Water Res 40(2):341–347

Raichur A.M and Basu M.J. 2001. Adsorption of fluoride onto mixed rare earth oxides. Separation and Purification Technology, Bangladed; 24, 121–12Mustafa, H. B and Hassan A; Youssef F. 2016. Poly o-phenylenediamineMgAl@CaFe204 nanohybrid for effective removing of lead (II), chromium (III) and anionic azo dye, School of Chemistry, University College of Science, University of Tehran, Tehran, Iran, P 687-699

Raju, N.J., 2017. Prevalence of fluorosis in the fluoride enriched groundwater in semi-arid parts of eastern India: Geochemistry and health implications. *Quaternary International*, *443*, pp.265-278.

Rathinam, K., Singh, S.P., Arnusch, C.J. and Kasher, R., 2018. An environmentally friendly chitosan-lysozyme biocomposite for the effective removal of dyes and heavy metals from aqueous solutions. *Carbohydrate polymers*, *199*, pp.506-515.

Regan, S., Hynds, P. and Flynn, R., 2017. An overview of dissolved organic carbon in groundwater and implications for drinking water safety. *Hydrogeology Journal*, *25*(4), pp.959-967.

Renuka, P., Pushpanjali, K. and Sangeetha, R., 2013. Review on “Influence of host genes on dental caries”. *J Dent Med Sci*, *4*(3), pp.86-92.

Reynolds, I.H., and Barrett, M.H. (2003): A review of the effects of sewer leakage on groundwater quality. Water and Environment Journal 17: 34-39.

Rogasky, J., 2007. Occurrence and survival of zoonotic bacterial pathogens and indicator organisms in groundwater and sandy soil following field application of hog manure.

Sampat, P., 2000. *Deep trouble: The hidden threat of groundwater pollution*. Worldwatch Inst.

Sangeetha, S., Kalaignan, G.P. and Anthuvan, J.T., 2015. Pulse electrodeposition of self-lubricating Ni–W/PTFE nanocomposite coatings on mild steel surface. *Applied Surface Science*, *359*, pp.412-419.

Sanghratna, S. and Tanvir, A., 2015. Fluoride Removal from Water by various techniques: Review. *International journal of innovative science, engineering and technology*, *2*(9), pp.560-571.

Saxena, V. and Ahmed, S., 2003. Inferring the chemical parameters for the dissolution of fluoride in groundwater. *Environmental Geology*, *43*(6), pp.731-736.

Saxena, V. and Ahmed, S., 2003. Inferring the chemical parameters for the dissolution of fluoride in groundwater. *Environmental Geology*, *43*(6), pp.731-736.

Schouten, M., 2009. *Strategy and performance of water supply and sanitation providers: UNESCO-IHE PhD Thesis*. CRC Press.

Schouten, M., 2009. *Strategy and performance of water supply and sanitation providers: UNESCO-IHE PhD Thesis*. CRC Press.

Schwarzenbach, R.P., Egli, T., Hofstetter, T.B., Von Gunten, U. and Wehrli, B., 2010. Global water pollution and human health. Annual Review of Environment and Resources, 35, pp.109-136.

Shannon, M.A., Bohn, P.W., Elimelech, M., Georgiadis, J.G., Marinas, B.J. and Mayes, A.M., 2010. Science and technology for water purification in the coming decades. In Nanoscience and technology: a collection of reviews from nature Journals (pp. 337-346).

Sharma, L.R. and Manchanda, A.K., 1982. G. Singh and RS Verma. *Electrochim. Acta*, *27*, p.223.

Shrivastava KB and Vani A.2009. Comparative Study of Defluoridation Technologies in India. Asian Journal of Experimental Science; 23 (1) 269-274

Singh, G., Kumari, B., Sinam, G., Kumar, N. and Mallick, S., 2018. Fluoride distribution and contamination in the water, soil and plants continuum and its remedial technologies, an Indian perspective–a review. *Environmental Pollution*, *239*, pp.95-108.

Smedley, P.L. and Kinniburgh, D.G., 2002. A review of the source, behaviour and distribution of arsenic in natural waters. Applied geochemistry, 17(5), pp.517-568.

Sorensen, I.M. and McBean, E.A., 2015. Beyond appropriate technology: Social considerations for the sustainable use of arsenic–iron removal plants in rural Bangladesh. *Technology in Society*, *41*, pp.1-9.

Sorensen, I.M. and McBean, E.A., 2015. Beyond appropriate technology: Social considerations for the sustainable use of arsenic–iron removal plants in rural Bangladesh. *Technology in Society*, *41*, pp.1-9.

Sorensen, J.P.R., Lapworth, D.J., Nkhuwa, D.C.W., Stuart, M.E., Gooddy, D.C., Bell, R.A., Chirwa, M., Kabika, J., Liemisa, M., Chibesa, M. and Pedley, S., 2015. Emerging contaminants in urban groundwater sources in Africa. *Water Research*, *72*, pp.51-63.

Stejskal J .2014. *Polymers of phenylenediamines*, Institute of Macromolecular Chemistry, Academy of Sciences of the Czech Republic.

Stejskal, J., 2015. *Polymers of phenylenediamines*. Progress in Polymer Science, 41, pp.1-31

Styblo, M., Del Razo, L.M., Vega, L., Germolec, D.R., LeCluyse, E.L., Hamilton, G.A., Reed, W., Wang, C., Cullen, W.R. and Thomas, D.J., 2000. Comparative toxicity of trivalent and pentavalent inorganic and methylated arsenicals in rat and human cells. *Archives of toxicology*, *74*(6), pp.289-299.

Thole, B., 2013. Ground water contamination with fluoride and potential fluoride removal technologies for East and Southern Africa. *Perspectives in Water Pollution*, pp.66-90.

Toze, R.S.G., 2004. Literature Review on the Fate of Viruses and Other Pathogens and Health Risks in Non-Potable Reuse of Storm Water and Recalimed Water.

Trchová, M., Morávková, Z., Bláha, M. and Stejskal, J., 2014. Raman spectroscopy of polyaniline and oligoaniline thin films. Electrochimica Acta, 122, pp.28-38.

Tree, J.A., Adams, M.R. and Lees, D.N., 2003. Chlorination of indicator bacteria and viruses in primary sewage effluent. Appl. Environ. Microbiol., 69(4), pp.2038-2043.

Uemura, S., Teshima, K., Tokuda, S., Kobayashi, N. and Hirohashi, R., 1999. Photopolymerized Conducting Potyaniline Micropattern and Its Application. Synthetic metals, 101(1-3), pp.701-702.

Ungureanu, G., Santos, S., Boaventura, R. and Botelho, C., 2015. Arsenic and antimony in water and wastewater: overview of removal techniques with special reference to latest advances in adsorption. Journal of environmental management, 151, pp.326-342.

Vaclavikova, M., Gallios, G.P., Hredzak, S. and Jakabsky, S., 2008. Removal of arsenic from water streams: an overview of available techniques. *Clean Technologies and Environmental Policy*, *10*(1), pp.89-95.

Velazquez-Jimenez, L.H., Vences-Alvarez, E., Flores-Arciniega, J.L., Flores-Zuñiga, H. and Rangel-Mendez, J.R., 2015. Water defluoridation with special emphasis on adsorbents-containing metal oxides and/or hydroxides: a review. *Separation and Purification Technology*, *150*, pp.292-307.

Wada, Y., Van Beek, L.P., Van Kempen, C.M., Reckman, J.W., Vasak, S. and Bierkens, M.F., 2010. Global depletion of groundwater resources. *Geophysical research letters*, *37*(20).

Waghmare, S.S. and Arfin, T., 2015. Fluoride removal from water by various techniques. *Int. J. Innov. Sci. Eng. Technol*, *2*, pp.560-571.

Wang Y, Reardon EJ. 2001. *Activation and regeneration of a soil sorbent for defluoridation of drinking water.* Applied Geochemistry; 16, 531–539

Wang Y, Reardon EJ. 2001. *Activation and regeneration of a soil sorbent for defluoridation of drinking water.* Applied Geochemistry; 16, 531–539

WHO/UNICEF JMP (Joint Monitoring Programme for Water Supply and Sanitation). 2010. JMP Rapid Assessment on Drinking-water Quality pilot report 2010. 8-10.

WHO/UNICEF, 2014. Progress on Drinking-water and Sanitation e 2014 Update.World Health Organization, 1, 1.

World Health Organization, 1993. *Guidelines for drinking-water quality*. World Health Organization.

World Health Organization, 2018. WHO country cooperation strategy at a glance: South Africa.

Yadav, A. and Khandegar, V., 2020. Removal Comparison and Cost Evaluation of 2, 6-Dichlorophenol. *Journal of Hazardous, Toxic, and Radioactive Waste*, *24*(4), p.04020033.

Yadav, K.K., Gupta, N., Kumar, V., Khan, S.A. and Kumar, A., 2018. A review of emerging adsorbents and current demand for defluoridation of water: bright future in water sustainability. *Environment international*, *111*, pp.80-108.

Yadav, K.K., Kumar, V., Gupta, N., Kumar, S., Rezania, S. and Singh, N., 2019. Human health risk assessment: study of a population exposed to fluoride through groundwater of Agra city, India. *Regulatory Toxicology and Pharmacology*, *106*, pp.68-80.

Yadav, S.K., Mahapatra, S.S., Cho, J.W., Park, H.C. and Lee, J.Y., 2009. Enhanced mechanical and dielectric properties of poly (vinylidene fluoride)/polyurethane/multi-walled carbon nanotube nanocomposites. *Fibers and Polymers*, *10*(6), pp.756-760.

Yu Z, Min Y, Xia H. 2002. *Arsenic (V) removal with a Ce (IV)-doped iron oxide adsorbent. De*partment of Environmental Science and Engineering, Tsinghua University

Yu Z, Min Y, Xia H. 2002. *Arsenic (V) removal with a Ce (IV)-doped iron oxide adsorbent. De*partment of Environmental Science and Engineering, Tsinghua University

Yu, J.C., Yu, J., Ho, W., Jiang, Z. and Zhang, L., 2002. Effects of F-doping on the photocatalytic activity and microstructures of nanocrystalline TiO2 powders. Chemistry of materials, 14(9), pp.3808-3816.

Chapter 3.

Synthesis of Fe doped poly p-Phenylenediamine composite and its potential co-adsorption of arsenite and fluoride in aqueous solution.

E.P Munzhelele*, M.W Gitari, W.B Ayinde

Environmental Remediation and Nanoscience (EnviReN), Department of Ecology and Resource Management, School of Environmental Sciences. University of Venda, Private Bag X5050, Thohoyandou, 0950, Limpopo Province, South Africa.

3.1. Abstract

Water is regarded as an important natural resource to sustain life and its purification is an important criterion that determines its quality and usefulness. In this study, the incorporation of Fe^{3+} oxide onto a phenylenediamine (pPD) polymer matrix through a chemical co-polymerization route was prepared and its arsenite and fluoride removal potentials at optimal conditions from aqueous solution were evaluated. The morphology and structural analysis of the synthesized Fe doped pPD (Fe-pPD) were comparatively evaluated using the FT-IR, SEM, EDS, and XRD techniques. Fe^{+3} was successfully incorporated onto pPD matrix as confirmed by the different morphological characterizations. The functional groups of pPD were not altered by the incorporation of the Fe^{+3} by the FTIR results. The synthesized composite displayed a clustering of an irregular fragmental particle at an average particle size between 2-50 nm, with a crystalline phase pattern when compared to the amorphous raw pPD. The synthesized adsorbents were evaluated for potential defluoridation and arsenite sorption applicability. Batch experiments were carried out to determine optimum conditions, process, and the mechanism that attributes to both As^{3+} and F^{-} sorption using 2.5 % Fe-pPD composite. Comparatively, the obtained results revealed that different sorption parameters of the adsorbent have a significant effect on adsorbate removal . The rate of adsorption of F^{-} and As^{3+} onto 2.5 % Fe-pPD composite best followed the pseudo-second-order kinetic model. However, the intra-particle diffusion plot has shown three distinctive phases, which shows that the adsorption process occurred with more than one sorption process step. Furthermore, the experimental data for both As^{3+} and F^{-} onto the 2.5 % Fe-pPD composite better fit the Freundlich

isotherm model at different operating temperatures. Overall, the synthesized composite exhibited a strong affinity towards fluoride uptake (96.6 %) than arsenite uptake (71.14 %) with a maximum capacity of 6.79 (F^-) and 1.86 mg/g (As^{3+}). Thermodynamically, the removal process of both pollutants by the 2.5 % Fe-pPD was endothermic. Also, the synthesized adsorbent shows some level of antimicrobial activity against common water-borne bacterial. Therefore, the developed 2.5 % Fe doped pPD composite has the potential ability for inorganic metal species pollutants remediation and bacterial disinfection in community-level water purification processes.

Keywords: Water pollution, arsenic and fluoride remediation, antibacterial disinfection; poly para-phenylenediamine composite, adsorption experiments

3.2. Introduction

The most important component of all forms of living organisms on earth is water. Water scarcity has been observed frequently in many parts of the world including Africa (WHO/UNICEF JMP, 2010; 2019). Contamination of water resources by multiple pollutants has been known as the most consequential and severe problem worldwide due to natural and anthropogenic activities. Chronic co-existence of pollutants such as fluoride, nitrates, arsenic and other heavy metal ions, as well as harmful bacteria, by these activities in drinking water sources, has resulted in many complicated life-threatening health effects (Fu et al, 2014; Jadhav et al, 2015). Arsenic and fluoride have been identified as the most inorganic pollutants in groundwater resources due to water-rock interaction, groundwater recharge, and anthropogenic activities, thus endangering public health (Thompson et al. 2007; Sarkar and Paul, 2016).

Ravenscoft, (2007) reported that natural arsenic pollution of ground and surface water resources affected several millions of people in at least 70 countries of the world. The most predominant valence state of arsenic is the less toxic arsenates (As^{5+}) and the more toxic arsenite (As^{3+}), which are found in contaminated water resources (Sharmar and Sohn, 2009). Comparatively, As^{3+} predominantly form in the reducing environment between pH 4-10 existed as being neutrally charged, whereas As^{5+} species exist as negatively charged (Jadhav et al, 2015). Chronic contamination of arsenic in drinking water affects various types of biological properties including cancer, cardiovascular diseases, skin thickening, and neurological diseases, gastrointestinal problems and

arsenicosis found in the human and aquatic ecosystem (Vallaescusa and Bollinge, 2008; WHO, 2011; Sarkar and Paul, 2016; Huang et al, 2019).

Furthermore, fluoride (F^-) is considered the most significant pollutant in groundwater affecting human health adversely across the globe (Mumtaz et al. 2016). It has been stated that a very small amount of fluoride is beneficial for the human body (improves dental health), nevertheless its excessive intake can cause molting teeth, neurological damages, as well as dental and skeletal fluorosis (Miretzky and Cirelli, 2011; Dhillon and Kumar, 2015). Fluorosis is an irreversible skeletal disorder with no medical treatment. Comparatively, arsenic exposure in water resources constitutes more danger than fluoride because of its acute toxicity at low concentration Camacho et al, 2011; Singh et al, 2015). Hence, the World Health Organization (W.H.O), set a provisional guideline for arsenic and fluoride concentration in drinking water at 10 µg/L and 1.5 mg/L respectively (WHO, 2000; 2017). Therefore, the detrimental effects associated with the different fates and transport ways of both As^{3+} and F^- when ingested has deemed it necessary to remove these toxicants from contaminated water.

Many developing countries are affected by fluoride, arsenite and microbially polluted water with no affordable purification technologies to enhance drinking water quality. The reduction of these pollutants in water has been tested, established, and reviewed by different techniques and materials (Hichour et al, 2000, Amor et al, 2001; Mohapatra et al, 2009; Jadhav et al, 2015; Sarkar and Paul, 2016). Studies have shown that adsorption technology amongst other techniques has proven to be efficient in remediating these toxic pollutants (García and Borgnino, 2015; Izuagie et al, 2017).

Recently, researchers have channeled the use of innovative low scale sorbent materials suitable for rural areas in the co-adsorption of As^{3+} and F^- from portable water. Metal oxides like iron oxide and iron-based sorbents have been used because of their high affinity towards these hazardous inorganic species and pathogen disinfection (Dhillon and Kumar, 2015; Alvarez-Cruz and Garrido-Hoyos, 2019). However, their applicability has been compromised by the introduction of secondary pollution, where maximum adsorption was at high pH. It is important to note that the removal of these mentioned pollutants must be effective and must not result in other environmental and health implications.

Equally, when selecting a treatment method, it is advisable to choose the best alternative that will have an optimum yield and must be environmentally friendly. The introduction of polymers as an adsorbent in water treatments have been on the rise due to their varied functional groups and structural frameworks. Poly-phenylenediamine of the polyaniline family has been used to assess its adsorption applications for various pollutants ranging from anionic to heavy metals ions (Zhang et al, 2012; Yu et al, 2013; Stejskal, 2015). Furthermore, the excellent antibacterial properties of these metal oxides and polymeric materials to the water purification technologies have been reported (Ramos et al, 2019). The development of metal-metal oxides/polymer to improve and enhance adsorption capacities for efficient water treatment has been an increasing trend lately. Hence, extensive research is required for the development and implementation of a low-cost, multifunctional, eco-friendly, sustainable, and hybrid technology with high sorption capacity. In this study, we focus on synthesizing a non-toxic Fe doped poly-phenylenediamine composite and its potential arsenite and fluoride sorption capacity in groundwater. The adsorption properties of the synthesized sorbent were examined through various experimental conditions, its adsorption kinetics, and isotherms, as well as thermodynamics, were also studied and reported.

3.3. Material and methods.

3.3.1. Chemicals

Poly (p-phenylenediamine), Ammonium persulfate ($(NH4)_2S_2O_8$), Iron (III) chloride heptahydrate ($FeCl_3.5H_2O$), sodium fluoride (NaF) and sodium hydroxide (NaOH), NaCl, KCl, HCl, and $NaAsO_3$ were purchased from Rochelle chemicals, South Africa. All reagents were of analytical grade and used without any purifications. The working solutions of different As^{3+} and F^- concentrations were prepared in deionized water from Millipore water (18.2 MΩ/cm).

3.3.2. Composites preparation

3.3.2.1. Preparation of Poly-phenylenediamine (pPD).

Poly-pPD was synthesized by a modified method (Pham et al., 2011; Mdlalose et al., 2017). Briefly, 0.015 M pPD (1.62 g, M) was dissolved in HCl (50 mL, 0.1 M) and stirred for 3 h on an ice bath. Next, the pPD polymerization was initiated by a dropwise addition of the freshly prepared oxidant solution of ammonium persulfate (3.42 g) in HCl (25 mL, 0.1 M) for 30 min. The resulting mixture was stirred for 24 hours at room

temperature to ensure complete polymerization of the pPD monomer. The pH of each poly (p-phenylenediamine) solution was adjusted to 9 with the addition of 2 M NaOH and shaken at 250 rpm for 30 min. The reaction was quenched by adding acetone and the resulting crude product was washed with de-ionized water and dried under vacuum at 60 °C for 24 hrs.

3.3.2.1. Preparation of Fe Poly-phenylenediamine (Fe-pPD).

pPD (1.62 g, 0.015 M) was dissolved in HCl (50 mL, 0.1 M) and stirred for 3 hours on an ice bath. 0.25 M FeCl3.5 H_2O solution with the various percentages by weight (2.5%, 5%, and 10%) was prepared in 20 mL deionized water before the doping process. Each of these salt solutions was added and mixed separately with the pPD solutions by ultrasonication for 25 min. Next, the Fe-pPD solution was initiated by a dropwise addition of the freshly prepared oxidant solution of ammonium persulfate (3.42 g) in HCl (25 mL, 0.1 M) for 30 min. The solution was under stirring for 24hours to allow the formation of Fe-pPD at room temperatures at 400 rpm. The pH of each Fe-pPD was adjusted to 9 with the addition of 2 M NaOH to precipitate the metal hydroxides and shaken at 250 rpm for 30 min. The product was collected by filtration and washed with deionized water, then dried in a vacuum oven at 60 ^oC 24hrs.

3.3.2.3. Adsorbent efficiency determination

A mass of 0.4 g of each modified species was contacted with 50 mL of 10 mg/L fluoride and 5 mg/L of As^{3+} solution at 250 rpm for 30 min. The equilibrium pH of each mixture was measured to evaluate the pH status of untreated and treated water. After the equilibrium pH measurement, the mixtures were centrifuged, and the supernatants analyzed for residual fluoride using a fluoride ion-selective electrode (9609 BNWP Orion, USA) coupled to an ISE/pH/EC electrode (Thermo SCIENTIFIC-ORION VERSA STAR Advanced Electrochemistry meter fluoride ion-selective electrode) calibrated with four fluoride standards containing TISAB III at the volume ratio of 1:10 as in the case of the samples. While, As^{3+} measurements in the supernatants were determined using Metrohm 850 professional ion chromatography (Switzerland).

T*he percentage of fluoride removal will be calculated by using the following formula*

$$\% \text{ of fluoride removal} = \frac{Co - Ce}{Co} * 100 \qquad (1)$$

C_o is the initial fluoride concentration in mg/L, C_e equilibrium concentration in mg/L

The adsorption equilibrium capacity of the adsorbent will be calculated using

$$q_e = \frac{Co-Ce}{m} * v \quad (2)$$

qe is the equilibrium capacity of the adsorbent, m is mass of the adsorbent in g and v is the volume of fluoride in mg/l.

3.3.3. Characterization

The morphological and physicochemical properties of the synthesized adsorbent were evaluated using the Scanning Electron Microscope (SEM) (SEM with an FEI Nova NanoSEM 230 with the field emission gun equipped with an Oxford Xmax SDD detector operating at an accelerating voltage of 20Kv for the EDS detector (Oxford X-Max with INCA software). An infra-red spectrum of the adsorbent was obtained using ALPHA Fourier Transform Infra-red spectrum equipped with ATR-Diamond (Bruker, Germany). Bruker-D8 Powder Diffractometer with a theta-theta goniometer X-ray diffraction (XRD) technique was employed to examine the crystalline phase's identification. CHNS analysis was done using the Thermo Flash 2000 series CHNS/O organic Elemental analyzer. F^- and pH measurements of the fluoride in the supernatants were determined using a fluoride ion-selective electrode (9609 BNWP Orion, USA) coupled to an ISE/pH/EC electrode (Thermo SCIENTIFIC-ORION VERSA STAR Advanced Electrochemistry meter fluoride ion-selective electrode) calibrated with four fluoride standards containing TISAB III at the volume ratio of 1:10. As^{3+} measurements in the supernatants were determined using Metrohm 850 professional ion chromatography (Switzerland).

3.3.4. Batch experiments.

Stock solutions containing 1000 mg/L As^{3+} and F^- were prepared by dissolving 0.1733 g of $NaAsO_3$ and 2.210 g NaF, respectively in a 1000 mL volumetric flask using Milli-Q water (18.2 MΩ/cm). The working solutions were prepared through appropriate dilutions from the stock solution. To evaluate the effect of contact time and adsorption kinetics, the contact time was varied from 0.5 to 120 min. Adsorbent dosage of 0.4 g/50 mL and adsorbate concentration of 5 and 10 mg/L of F^- and As^{3+} concentration respectively was maintained. After agitation, mixtures were centrifuged at 250 rpm for 20 min. The optimum adsorbent dosage was evaluated by varying adsorbent dosage from 0.1-0.4 g/50 mL. To evaluate the adsorbate concentration and adsorption

isotherms, initial concentration of F^- and As^{3+} were varied from 5 to 100 mg/L at a temperature of 298, 323, and 343 K.

The obtained data were used to determine the adsorption thermodynamics. The effects of parameters like pH (from 2-12) and co-existing ions (F, Cl, NO_3^- , CO_3^{2-}, SO_4^{2-}) were also evaluated. The initial pH was adjusted using 0.01 M NaOH and 0.01 M HCl. All experiments were conducted in triplicate and the mean values were reported. The pH_{pzc} was evaluated using the solid addition method as described by Gitari et al, (2017). Eqs. 1 and 2 were used to determine the percentage removal and adsorption capacity respectively.

3.3.5. Adsorption kinetic models.

The As^{3+} and F^- adsorption kinetics were studied at an initial concentration of 5 and 10 mg/L respectively. The experimental data were analysed using the non-linear equation of pseudo-first-order and pseudo-second-order models as well as intraparticle diffusion (Eqs. 3, 4, and 5) (Lagergren, 1898; Ho and McKay 1998 and Sharma et al, 1990):

$$qt = qe(1 - e^{-kit}) \quad (3)$$

$$qt = \frac{qe^2\, k_2 t}{1 + k_2\, q_e t} \quad (4)$$

$$qt = k_t t^{0.5} + ci \quad (5)$$

q_e and q_t (both in mg/g) are the amount adsorbed per unit mass at a time, t (in min). K_1 (min^{-1}) and K_2 ($g.mg^{-1}min$) are first and second-order rate constant respectively. Ki (mg /g min^{-1}) is the intra particle diffusion rate constant and is determined from the slope of $t^{0.5}$ vs qt, and C_i is the constant attained from the intercept and reflects the thickness of the boundary layer. The greater the intercept, the bigger the boundary layer effect (Mudzielwana et al, 2018).

The Elovich linear equation (Eq. 6) has general application to chemisorption kinetics.

$$qt = \beta \ln(\partial\beta) + \beta lnt \quad (6)$$

The equation was used to validate that chemisorption is the limiting step for fluoride and arsenic uptake. It is often valid for systems in which the adsorbing surface is heterogeneous. qt is the quantity of adsorbate adsorbed at time t (mg/g), α is a

constant related to chemisorption rate and β is a constant which depicts the extent of surface coverage. The two constants (α and β) can be calculated from the intercept and slope of the plot from the equation.

3.3.6. Adsorption isotherm models.

The adsorption isotherms were modeled using the theoretical Langmuir and empirical Freundlich isotherms (Weber and Chakravorti, 1974, Bolster and Homberger, 2007). The Langmuir isotherm model assumes monolayer interaction between the adsorbate molecules attached to the surface of the adsorbent during equilibrium. The non-linearized data are shown in Eq 7.

$$qe = \frac{q_m K_L C_e}{1+K_L C_e} \quad (7)$$

Where: C_e is the equilibrium concentration (mg/L); Q_e is the adsorption capacity (mg/g); Q_m is the theoretical maximum adsorption capacity (mg/g) and k_L is the Langmuir constant related to the enthalpy of adsorption (L/mg).

Equally, Langmuir isotherm can be expressed in terms of a dimensionless constant separation factor or equilibrium parameter R_L (Eq. 8). (when R_L=1 irreversible, 0<R_L<1 favourable, R_L=1 linear and R_L>1 unfavourable).

$$R_L = \frac{1}{1 + k_L C_i} \quad (8)$$

Freundlich isotherm model assumes that there is a mutual interaction between the adsorbate molecules adsorbing onto the multilayer or heterogeneous surface of the adsorbent. The non-linear equation of Freundlich (Eq. 9) is expressed as:

$$qe = K_f Ce^{\frac{1}{n}} \quad (9)$$

K_f is the Freundlich constant related to adsorption capacity and 1/n is the adsorption intensity. When 0 < 1/n < 1, the adsorption is favourable; when 1/n=1, the adsorption is irreversible; and when 1/n > 1, the adsorption is unfavourable.

The Dubinin Radushkevich (D-R) model (Eq. 10) was also employed using the experimental data. D-R is a more general model in which assumption is not based on homogenous surface or constant adsorption potential, it gives insight into the sorbent porosity as well as the adsorption energy. The value of adsorption energy further

provides information as to whether the adsorption process is physical or chemical in nature (Dubinin, 1947).

$$lnqe = lnqo - \beta e^2 \quad (10)$$

where qe is the amount of ions adsorbed per unit weight of adsorbent (mg/g), qo is the maximum adsorption capacity, β is the activity coefficient useful in obtaining the Ɛ (Eq (11)) is the Polanyi potential and mean sorption energy E (kJ/mol) (Eq (12))

$$\varepsilon = RT\ In\left(1 + \frac{1}{Ce}\right) \quad (11)$$

$$\mathrm{E} = \sqrt{\frac{1}{2\beta}} \quad (12)$$

where R is the gas constant (J/mol K) and T is the temperature (K). qo and β (mol2 /kJ2) can respectively calculated from the intercept and the slope of the plot of lnqe vs $Ɛ^2$.

3.3.7. Goodness of fit evaluation

The fitness between the experimental data and the simulated data were determined by the coefficient of determination (R^2) (Eq. (13), root mean square error (RMSE) (Eq. (14), and the sum of the squared errors (SSE) (Eq. (15)).

$$R^2 = 1 - \frac{\Sigma(q_{e,exp} - q_{e,calc})2}{\Sigma(q_{e,exp} - q_{e,mean})2} \quad (13)$$

$$RMSE = \sqrt{\frac{1}{n-1}\sum_{i=1}^{n}\left(q_{e,exp} - q_{e,calc}\right)^2}_{\mathrm{i}} \quad (14)$$

$$SSE = \sum_{i=1}^{n}\left(q_{e,calc} - q_{e,exp}\right)^2 \quad (15)$$

where qe, calc is the theoretical concentration of adsorbate on the adsorbent, which has been calculated from one of the isotherm models. qe, i, means is the experimentally measured adsorbed solid-phase concentration.

3.3.8. Antimicrobial activity test.

3.3.8.1. Preparation of medium agar

Bacterial resistance and efficacy of the synthesized pPD and Fe-pPD were determined from the observed zone of inhibition (mm) using the standard Agar-Well disc diffusion method (Kirby Bauer disk diffusion test). Medium 1 agar plates were divided into half; 1-5 mL pipette tips were used to punch a small circle to add the adsorbent. 50 µl of the bacterial strains (*E. coli*; ATCC 25922 IN; *S. Aureus*; ATCC 259231 Tm and *K. Pneumoniae*; ATCC 700603) was inoculated into the sterile medium 1 agar. Then, 50 µl of 1 mL/0.01 g of the sorbent was deposited into the punched circles. Then incubated for 24 hrs at 37 °C. The minimal zone of inhibition was observed and measured.

3.4. Results and Discussion

3.4.1 Adsorbent optimization.

Fig 5. shows the adsorption capacities of the concerned pollutant ions (F^- and As^{3+}) by varying the weight percentages of the synthesized materials. The experiment was carried out with an initial concentration of 10 mg/L and 5 mg/L for F^- and AS^{+3} respectively, and a dosage of 0.4 g at room temperature at an agitation speed of 250 rpm for 30 minutes. The respective sorption experiment was carried out by observing the effects of percentage variation (v/v %) of Fe-pPD (2.5 %, 5 %, and 10 %) compared with bare pPD.

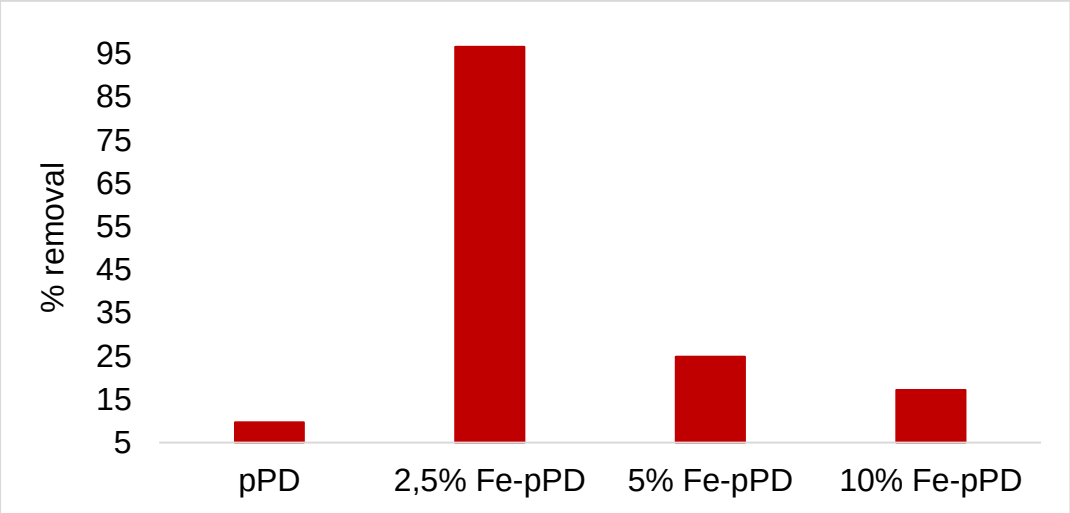

Figure 5. Variation of % removal of F^- and As^{3+} as a function of Fe doped in pPD (Initial concentration of F^- and As^{3+}: 10 mg/L and 5 mg/L, dose 0.4 g, volume of the solution: 50 mL at 298 K).

Fig. 5 portrayed the raw pPD polymer having the lowest pollutants removal potential, where only 10% of the initial concentration was removed. However, when doped pPD with Fe, the percentage removal of the composite improved considerably. An increase in the adsorption capacity occurred because the iron-based sorbents have high binding infinity towards inorganic pollutants (As and F) (Sun et al, 2016). Also, the introduction new functional groups could possibly help to improve the adsorption efficiency of the modified composite (Fe-pPD). The modification of the pPD through introduction of $FeCl_3$ has influenced the formation of an emeraldine (changed colour) hydrochloride Fe doped poly-(para-phenylenediamine) (R-$FeCl_3$) (Bienkowski, 2006). Thus, the proposed mechanism for As^{3+} and F^- removal might be through ligand exchange (Qiao et al, 2014), where the metal ions are attached to Fe replacing chloride ion. Thus, the introduction of Fe^{3+} into the pPD network has improved the surface area and ionic state by increasing the active binding sites and solubility, which had enhanced the adsorption efficiency of the Fe-pPD. Consequently, an improvement in surface area was further validated by the BET analysis, confirming high availability of active binding site. From the data, 2. 5% was chosen as better adsorbent and further used for arsenic, and fluoride removal. The interaction of the Fe^{3+} modified polymeric composite was a consistent determinant in the enhancement of the As^{3+} and F^- uptake.

3.4.2. Characterization.

3.4.2.1. FTIR results.

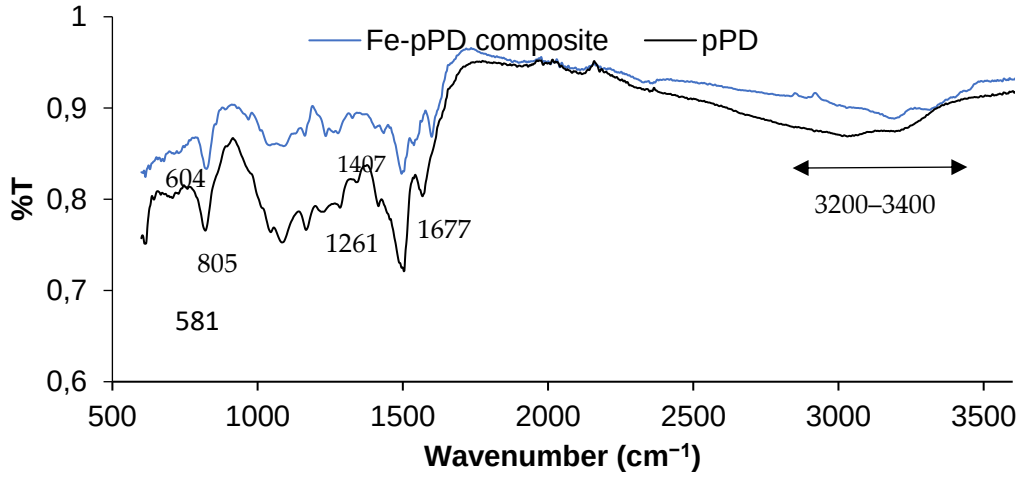

Figure 6. FTIR spectra for 2.5% Fe-pPd and pPD

Fig 6 portrays FTIR spectra of the 2.5 % Fe-pPD. The FTIR spectra of the 2.5 % Fe-pPD composite were carried out to determine the functional groups and any transition within the composite spectrum due to the incorporation of Fe metal oxide. Fig. 6 shows the FTIR spectra of pPD and 2.5 % Fe-pPD composite with their respective peaks. The pPD spectrum shows a typical broad band between 3200-3400 cm^{-1} attributed to the presence of stretching vibration of N–H group and hydroxyl group (-OH) stretching from physically adsorbed H−O−H bonded to the surface (Haldorai et al, 2009; Pham et al, 2011). The appearances of strong peaks at 1677 cm^{-1} and 1504 cm^{-1} relate to the C=C and C=N stretching vibrations of the phenazine ring (Archana and Jaya, 2014). The C–N–C stretching vibrations of benzenoid and quinoid imine units are recognized by the peaks at 1407 cm^{-1} and 1261 cm^{-1} with and the characteristic of C–H out-of-plane bending vibrations of benzene bases in the phenazine skeletons are the bands at 805 cm^{-1} and 581 cm^{-1} respectively (Hao et al, 2009).

3.4.2.2. SEM-EDS results.

Fig. 7 displays the SEM-EDS micrographs of raw pPD and the 2.5 % Fe-pPD composite. Generally, the surface morphology of these polymer-based metal-oxide composites is depended on the type of polymers of the phenylenediamines as well as the oxidant used during the synthesis (Stejskal, 2015). The morphology of the bare pPD (Fig. 7 (a)) was found to be a globular arrangement, while structurally the 2.5 % Fe-pPD (Fig. 7(b)), depicts a well-ordered aggregation due to interaction and incorporation of Fe surfactant across polymer matrix of pPD. Both materials were measured possessing average particle size ranges between 2-20 µm. The successful incorporations of the metal oxide within the polymer backbone in 2.5 % Fe-pPD as compared to the raw pPD polymer framework were confirmed by the various elemental compositions present in the EDS mapping analysis (Fig. 7 (c-d)). The presence of Fe element in 2.5 % Fe-pPD composite together with other elements exhibited in pPD as shown in the EDS spectra supported the formation of 2.5 % Fe-pPD composite. Additionally, Fig. 7(e) portrayed the potential ability of Fe-pPD composite in the simultaneous removal of As^{3+} and F^{-}; which was validated by the presence of As and F in the EDS spectrum.

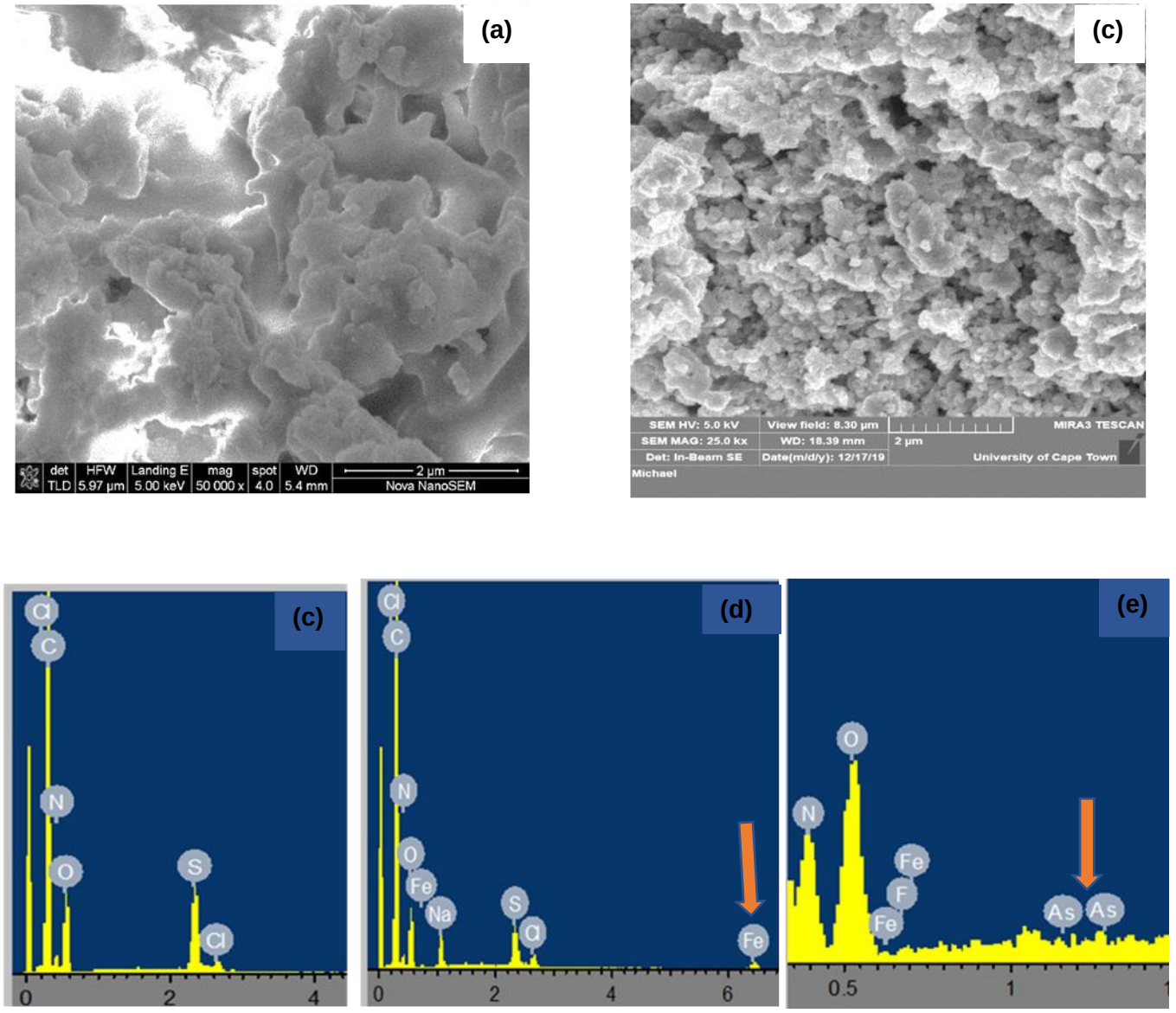

Figure 7. SEM-EDS results: (a) and (b) SEM images of raw pPD and 2.5 % Fe-pPD, (c) and (d) respective EDS spectra of raw pPD and 2.5% Fe-pPD, and (e) EDS spectra of 2.5 % Fe-pPD after application.

3.4.2.3. XRD results.

The Structural phases of the raw pPD and 2.5 % Fe doped pPD composite are shown in Fig. 8. The X-ray diffractogram of bare pPD shows a large, broad diffraction peak around 25º, signifying the amorphous nature of pPD synthesized by the oxidative polymerization process. A similar phase of the raw pPD was reported by Li et al, (2001). The transformation from the amorphous state exhibited by the raw pPD network to the crystalline form of 2.5 % Fe doped pPD composite was confirmed by the emergence of four distinct new peaks observed (2θ = 28.9º, 33.65º, 48.5º, and

57.9º). The diffraction peaks patterns of Fe oxides indexed at 33.65° and 58.65°, which were the characteristic peaks of two-line ferrihydrite (ICDD database).

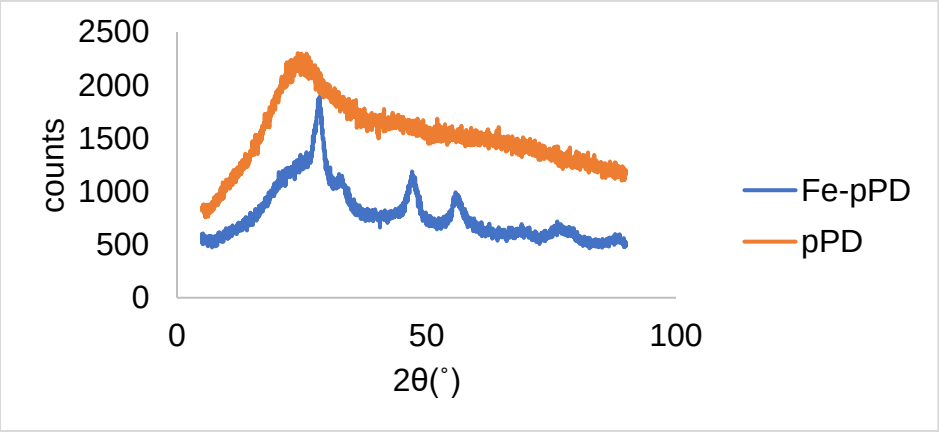

Figure 8. XRD diffractogram of 2.5 % Fe-pPD and pPD

3.4.3.4. BET results

Table 2. is displaying the BET results of raw pPD and 2.5 % Fe-pPD. The BET analysis of the raw pPD and 2.5 % Fe-pPD was done to evaluate the change in surface area and to determine the porous nature of the material. The results from the BJH pore size distribution portrayed an improvement in surface area, pore diameter and volume from the pPD to the 2.5 % Fe-pPD composite (Table 2). The increase in the surface area might be due to the decrease in particle sizes pPD (60.99 nm) > 2.5 % Fe-pPD (31.62 nm), thus, aiding in an increase in adsorption capacity. Additionally, the resulting pore diameters affirm the mesoporosity of the composite

Table 2. BET analysis results of pPD and 2.5% Fe-pPD.

	raw pPD	2.5 % Fe-pPD
BET surface area (m2/g)	8.68	18.41
Pore volume (cm3/g)	0.02	0.07
Pore diameter (nm)	7.79	15.12
Average particle size (nm)	60.99	31.62

3.4.2.5. CHNS analysis results.

Table 3 shows the CHNS composition in the 2.5 % Fe-pPD composite before and after application. As shown, the percentage of CHN increases after the metal ions sorption, whereas S content was below the detection limit The increase in CHN contents after application might be because the polymers polyaniline results in chain growth due to condensation polymerization, thus increasing the percentage of CHN (Bienkowski, 2006). However, the S content in the composite before the application may be due to the use of ammonium persulphate as an oxidant during the polymerization processes. It is known that ammonium persulphate tends to easily dissolve in water; thus, the reduction in S percentage after application.

Table 3. CHNS results of 2.5 % Fe-pPD before and after fluoride and arsenite adsorption from aqueous solution.

CHNS	N [%]	C [%]	H [%]	S [%]
Before application	14.9	52.96	4.315	2.54
After application	23.1	62.4	4.367	BDL

3.4.3. Batch experiments.

3.4.3.1 Effect of contact time

Fig 9. shows the significant effect of contact time on the uptake of As^{3+} and F^- in aqueous solution by the synthesized 2.5 % Fe-pPD composite studied between 0.5–120 min. In both sorption processes of As^{3+} and F^-, the percentage removal increases exponentially with contact time in the first 40 minutes and subsequently slows down to indicate that it has reached equilibrium point. The obtained results showed that the maximum percentage removal for As^{3+} and F^- was recorded at 99 (60 min) and 81 % (120 min) respectively. The initial increase of As^{3+} and F^- sorption was due to the presence of active sorption sites on the surface of the 2.5 % Fe-pPD. Hence, the low uptake of the pollutant ions might be attributed to unavailability of active sites due to saturation of the adsorbent. The optimal time of 60 mins and 40 mins were further used for subsequent batch experiments.

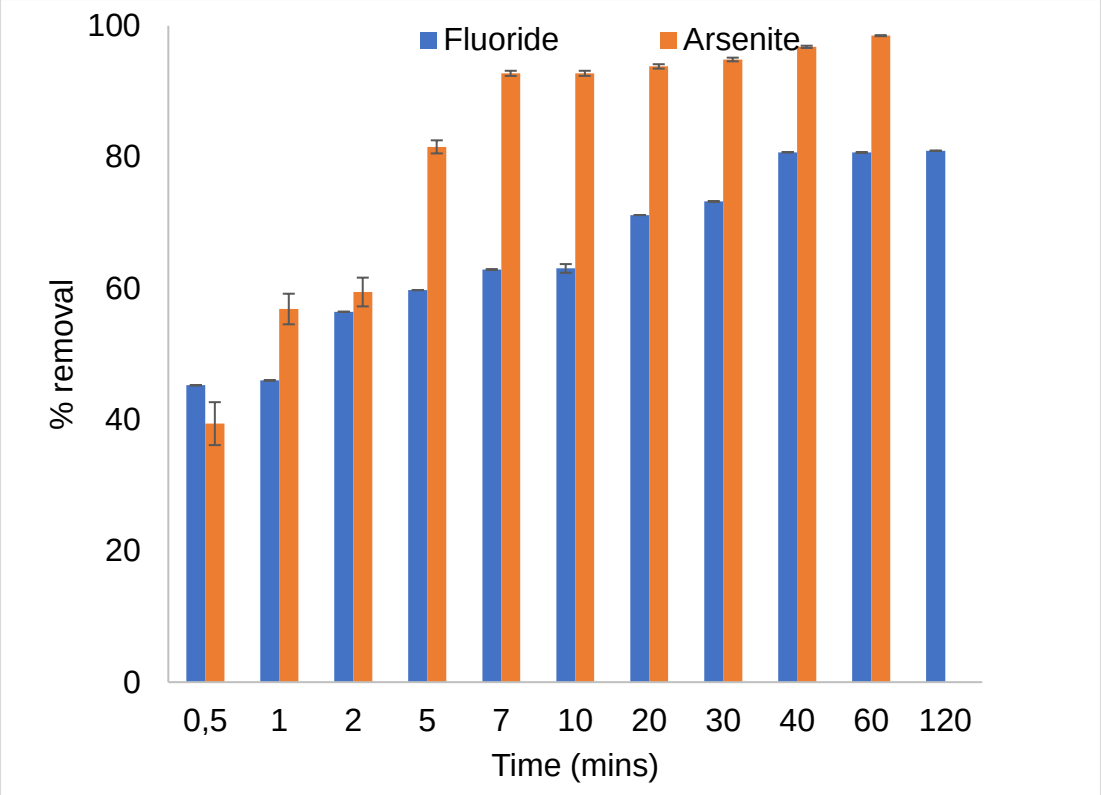

Figure 9. Effect of contact time on F^- and As^{3+} removal using 2.5 % Fe-pPD. (Initial F^- and As^{3+} concentration: 5 mg/L and 10 mg/L, adsorbent dose: 0.4 g, solution volume: 50 mL, shaking speed: 250 rpm and temperature: 297 K).

3.4.3.2. Adsorption Kinetics.

Fig 10 and table 4 and 5 presents the obtained kinetic data models of fluoride and arsenite removal from aqueous solution. The estimated parameters for the reaction and diffusion-based kinetic model data for both F^- and As^{3+} are presented in Table 4. The rate of adsorption of F^- and As^{3+} onto Fe-pPD composite best followed the pseudo-second-order kinetic model, with R^2 for As^{3+} (1) > R^2 for F^- (0.923). Thus, chemisorption is the limiting step for fluoride and arsenite removal. From the statistical point of view the reduced chi-square (χ^2) and root mean square error (RMSE) pseudo-first-order model presented low values for both F^- and As^{3+}. Thus, implying favourability and suggesting the uptake mechanisms of both pollutants by the 2.5 % Fe-pPD composite is associated with the chemisorption process. Moderately, the obtained correlation coefficient (R^2) of the linearized Elovich (shown in Table 4) greater than that of both the pseudo-first-order and pseudo-second-order. Thus, implying favourability of chemisorption of the solid-liquid adsorption process.

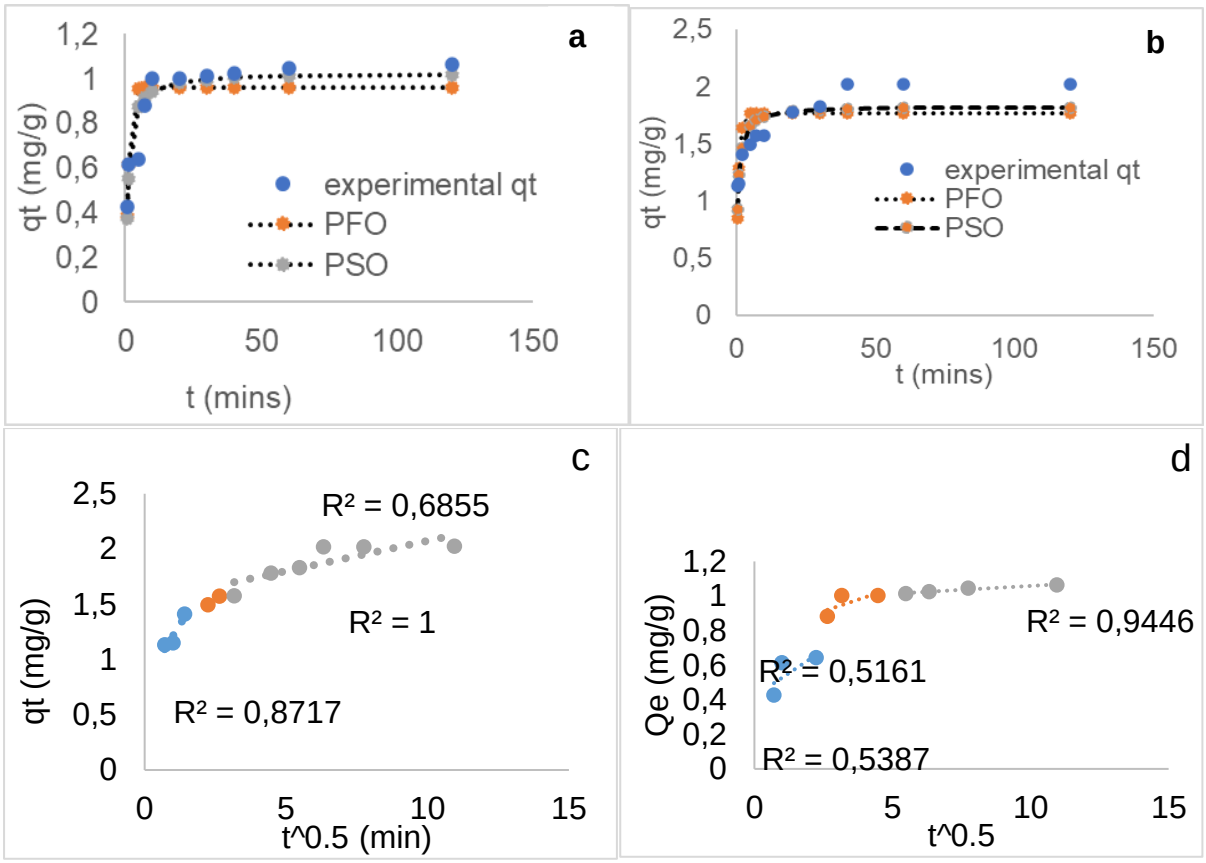

Figure 10. Kinetics models of F^- and As^{3+} removal by 2.5 % Fe-pPD composite: Pseudo-first and pseudo-second-order plots of (a) As^{3+} and (b) F^-; The intraparticle diffusion plots of(c) As^{3+} and (d) F^-.

Generally, the overall mass transfer mechanism in solid-liquid phase adsorption is normally represented by the external mass transfer, intraparticle diffusion and adsorption on the active sites consecutively. Fig 10(c-d). show the intra-particle diffusion simulated plots of both As^{3+} and F^- uptake by 2.5 % Fe-pPD composite. For an adsorption process to be controlled by this model, the plot (q_t against $t^{0.5}$) should give a straight line passing through the origin.

However, in this work, the intra-particle plot attained from the adsorption data (Fig. 10 (c-d)) shows that the adsorption phenomena take place in more than one step. This was consistent with the results for both the As^{3+} and F^- adsorption processes, indicating the uptakes of both pollutants were not controlled by only intra-particle diffusion. As shown on the plot, three defined phases, which deviate from the origin occurred for both As^{3+} and F^- uptake by the 2.5 % Fe-pPD composite.

Table 4. Table for non-linearized kinetics parameters of F^- and As^{3+} removal by 2.5% 2.5 % Fe-pPD.

Parameters	Pseudo-first order		Pseudo-second order	
	F^-	As^{3+}	F^-	As^{3+}
K_1	1.31	1.03	1.13	1.14
Q_e	1.77	0.96	1.83	1.03
R^2	0.54	0.71	0.76	0.85
χ^2	0.03	0.21	0.01	0.15
RMSE	0.02	0.12	0.008	0.09

These phases show the systematic mechanisms of both the As^{3+} and F^- species in solution occurring through the boundary layer diffusion, intraparticle pore diffusion as

Table 5. Table for linearized kinetic models of F^- and As^{3+} removal by 2.5% Fe-pPD.

Elovich			Intra-particle diffusion					
			phase1		phase 2		phase 3	
	F^-	As^{3+}		F^-	As^{3+}	F^-	As^{3+}	F^-	As^{3+}
β	0.18	0.12	C_i	0.42	1.53	0.78	1.07	0.98	0.8
α	$4.08*10^3$	$1.05*10^3$	R^2	0.53	0.69	0.52	1	0.94	0.87
R^2	0.96	0.86	K_1	0.1	0.05	0.05	0.19	0.01	0.41

well as on the active sites across the external surface 2.5 % Fe-pPD composite. The rate for phase 1, phase 2 and phase 3 suggests that the adsorption process was very rapid on the layer and dominates the intraparticle diffusion for F^-, whereas on As^{3+} it was the attachment of As^{3+} on the internal surface of the adsorbent due to the

difference in the rate of mass transfer in the initial and final phase of adsorption based on the respective coefficient of determination values (Table 5). The positive value of C_i indicates that intra-particle diffusion is the main mechanism for adsorption and external diffusion occurred to some extent.

3.4.3.3. Effect of adsorbent dose

The response of the adsorbent dose on As^{3+} and F^- ions removal is presented in Fig 11. The adsorbent dose was varied from 0.05-0.4 g. The attained data portrayed an increase in As^{3+} and F^- removal with increasing adsorbent dose. The gradually increase in removal ability with a rapid increase of adsorbent load is due to an increase in surface area, where more active sites were available for adsorption of As^{3+} and F^- ions. Thus, 2.5 % Fe-pPD, can effectively remove As^{3+} and F^- ions as the dose increases. Equally, the less As^{3+} and F^- sorption by 2.5 % Fe-pPD at low adsorbent is due saturation of the active sites on the surface area of the adsorbent. Thus, implying significancy of the adsorbent dose towards As^{3+} and F^- uptake. Therefore, the maximum uptake recorded, and the optimum dosage was 0.25 g and 0.2 g /50 mL for As^{3+} and F^- respectively. These optimal doses were used for subsequent batch adsorption experiment.

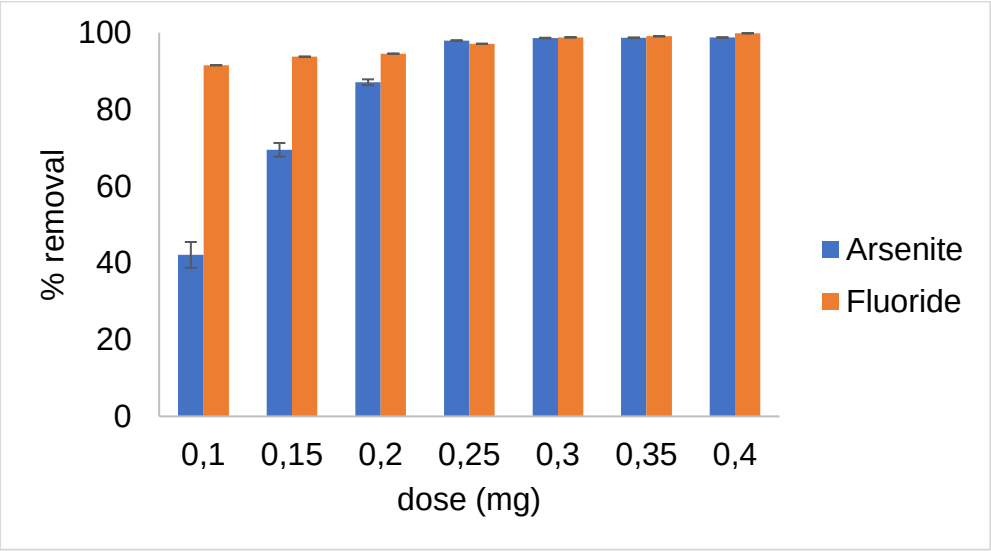

Figure 11. Effect of adsorbent dose on As^{3+} and F^- sorption by 2.5 % Fe-pPD. (Initial F^- and As^{3+} concentration: 5 mg/L and 10 mg/L, adsorbent solution volume: 50 mL, contact time: 40 mins, shaking speed: 250 rpm and temperature: 297 K).

3.4.3.4. Effect of initial concentration.

The effect of initial adsorbate concentration on adsorption efficiency of 2.5 % Fe-pPD composite was evaluated between 5–100 mg/L at different operating temperature. As shown from the obtained data (Fig 12), the percentage removal of both As^{3+} and F^- by the 2.5 % Fe-pPD composite decreased with an increase in the initial concentration. The decrease in removal efficiency by both As^{3+} and F^- species with increasing initial concentration may be due to the increasing number of these species in the solution. Thus, saturation of the binding adsorption sites on the 2.5 % Fe-pPD adsorbent surface area. This trend was consistent throughout the different operating temperatures and can be attributed to decrease in the mass transfer movement, which allow better binding interaction between both As^{3+} and F^- ions and 2.5 % Fe-pPD composite.

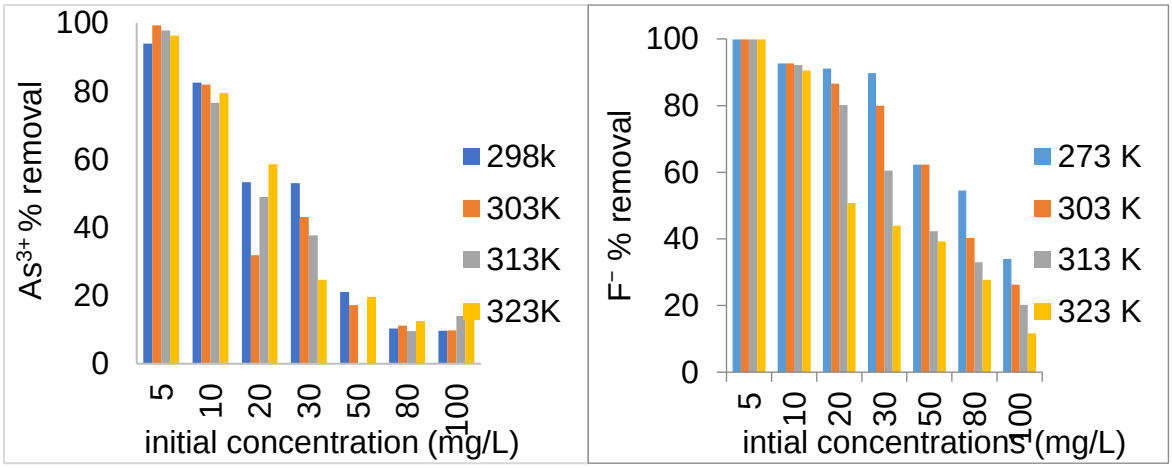

Figure 12. Effect of initial concentrations on F and As removal using 2.5 % Fe-pPD composite. (Initial F^- and As^{3+} concentration: 5 mg/L and 10 mg/L, adsorbent dose: 0.25 g and 0.2 g, solution volume: 50 mL, contact time: 24 hrs, shaking speed: 250 rpm and temperature: 298K-323 K).

3.4.3.5. Adsorption isotherm models

The non-linearized plots and the respective parameters of both the Langmuir and Freundlich models for As^{3+} and F^- sorption onto 2.5 % Fe-pPD at different temperatures are summarized in Fig 13 and Table 5. Evidently from the coefficient of determination values (R^2), adjusted correlation coefficient values(adjusted R^2), R ch-squared (χ^2)values and the residual sum of squares (RSS) (Table 6), the adsorption process of both As^{3+} and F^- by Fe-pPD followed the Freundlich isotherm model with higher affinity for F^- than As^{3+} based on the maximum adsorption capacity (Q_m).

Thus, indicating the heterogeneity adsorption phenomenon at the sorbate-sorbent interphase. The maximum adsorption capacities increase for As^{3+} and decreased for F^- uptakes as the temperature increases. Thus, suggesting that adsorption infinity is high at high temperature for As^{3+}, whereas for F^- it is favourable at low operating temperature. Moreover, the n values within the range of 1 and 10 validate the favourability of the sorption processes.

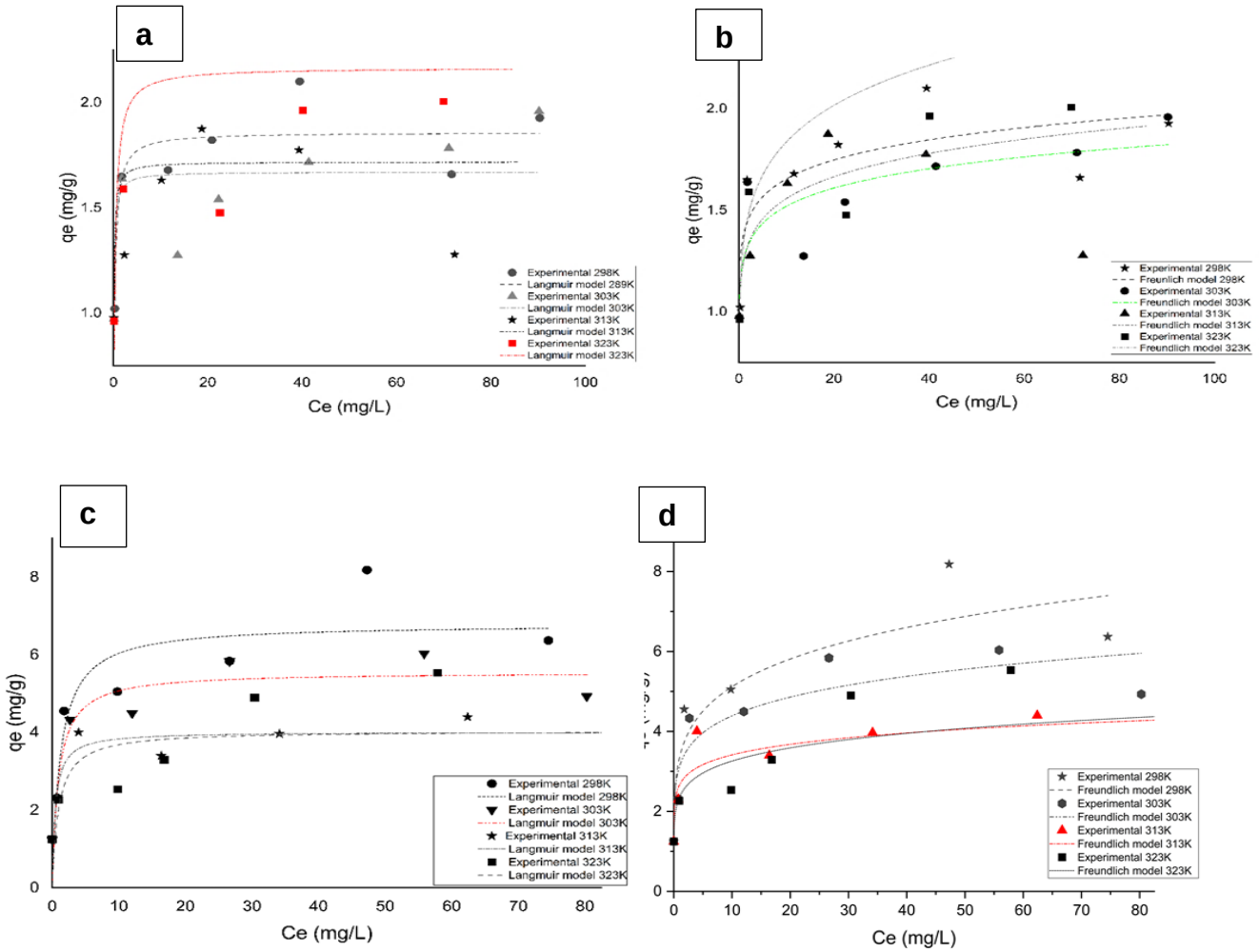

Figure 13. (a) and (b) As^{3+} for Langmuir and Freundlich Isotherm models plots, and (c) and (d) F^- for Langmuir and Freundlich Isotherm models plots removal using 2.5 % Fe-pPD composite.

Table 6. Non-linearized Langmuir and Freundlich isotherm model of F^- and As^{3+} adsorption by 2.5 % Fe-pPD.

	Langmuir			Freundlich		
Temperature	Parameters	F^-	As^{3+}	Parameters	F^-	As^{3+}
298 K	Q_m	6.79	1.86	K_f	3.36	1.38
	K_L	0.80	4.05	n	5.46	12.6
	R^2	0.83	0.82	R^2	0.87	0.65
	Adj.R^2	0.80	0.78	Adj.R^2	0.84	0.58
	R_L	0.11	0.05	χ^2	0.89	0.049
	χ^2	1.15	0.03	RSS	4.46	0.24
	RSS	5.76	0.13			
303 K	Q_m	5.55	1.67	K_f	3.13	1.26
	K_L	1.053	10.32	n	6.83	12.08
	R^2	0.85	0.60	R^2	0.85	0.67
	Adj.R^2	0.82	0.52	Adj.R^2	0.82	0.61
	R_L	0.09	0.02	χ^2	0.57	0.04
	χ^2	0.56	0.05	RSS	2.85	0.22
	RSS	2.81	0.76			
313 K	Q_m	4.02	1.72	K_f	2.67	1.25
	K_L	2.08	10.66	n	9.32	10.42
	R^2	0.7224	0.39	R^2	0.82	0.51
	Adj.R^2	067	0.27	Adj.R^2	0.78	0.42
	R_L	0.05	0.02	χ^2	0.28	0.12
	χ^2	0.42	0.15	RSS	1.38	0.61
	RSS	2.11	0.76			
323 K	Q_m	4.04	2.17	K_f	2.37	1.35
	K_L	1.03	3.28	n	7.19	7.41
	R^2	0.43	0.44	R^2	0.56	0.54
	Adj.R^2	0.32	0.33	Adj.R^2	0.49	0.45
	R_L	0.09	0.057	χ^2	1.18	0.26
	χ^2	1.54	0.32	RSS	5.91	1.31
	RSS	7.72	1.578			

Additionally, the D-R model was also plotted to determine the effect of the porous nature of the composite as well as the mean free energy of the sorption process. Table 7 displayed the various D-R model parameters of 2.5 % Fe-pPD composite sorption of As^{3+} and F^-. It was observed that the Q_{max} value of F^- decrease

Table 7. Linearized D-R isotherm model F^- and As^{3+} of removal by 2.5 % Fe-pPD composite.

D-R model		F^-	$As^{3\cdot}$
298 K	R^2	0.67	0.88
	β	$9*10^{-9}$	$4*10^{-9}$
	E	7.45	3.54
	Q_{max}		1.82
303 K	R^2	0.72	0.68
	β	9*10-9	$2*10^{-9}$
	E	7.45	5
	Q_{max}	4.5	1.64
313 K	R^2	0.8	0.48
	β	$6*10^{-9}$	$1*10^{-9}$
	E	9.13	7.07
	Q_{max}	3.6	1.66
323 K	R^2	0.58	0.58
	β	$6*10^{-9}$	$3*10^{-9}$
	E	9.13	4.08
	Q_{max}	3.4	2.03

with increasing temperature confirming that adsorption infinity is high at low temperature. Whereas, As^{3+} data revealed that adsorption infinity is high at high temperatures as shown in table 6. The obtained Polanyi potential (E) value is < 8 kg/mol, thus, the adsorption process occurred through physical nature.

3.4.3.6. Thermodynamics

Thermodynamic parameters such as enthalpy changes (ΔH°(kJ/mol^{-1})), entropy changes (ΔS°(kJ/mol^{-1})) and Gibbs free energy changes (ΔG° (kJ/mol^{-1})) were used to determine the spontaneity, type of reaction and the degree of randomness during the uptakes of both $As^{3+}$and F^- by the 2.5 % Fe-pPD. The parameters from the plot of 1/T vs ln K_C were calculated using the following equations:

$$lnK = \frac{\Delta H^*}{R} + \frac{\Delta S^\circ}{R} \quad (16)$$

$$\Delta G = \Delta H^\circ - T\Delta S^\circ \quad (17)$$

Where K is the equilibrium constant, R is the gas constant (8.134kJ mol^{-1} K^{-1}) and T is the solution temperature (K)

Table 8. Thermodynamic parameters of F^- and As^{3+} adsorption by 2.5 % Fe-pPD composite.

Parameters	F^-	As^{3+}
ΔH° (kJ/mol^{-1})	1.3	0.57
ΔS° (kJ/mol^{-1})	0.01	0.03
	ΔG° (kJ/mol^{-1})	
298 K	-9.19	-0.41
303 K	-9.35	-0.44
313 K	-9.68	-0.50
323 K	-10.01	-0.55

Table 8. shows the obtained relative thermodynamic values for the As^{3+} and F^- adsorption process. From the tabulated parameters, ΔG° values were calculated to be negative for F^- and positive for As^{3+} sorption processes. Thus, this indicates feasibility and spontaneity for both As^{3+} and F^- uptake by the 2.5 % Fe-pPD. In both removal processes, the ΔG° values decreased with an increasing temperature, which indicates

the favourability of the sorbate-sorbent mechanisms. Thermodynamically, the removal process for both $As^{3+}$and F^- by the 2.5 % Fe-pPD was endothermic with an increase in the degree of randomness as validated by the positive values of ΔH° and ΔS° respectively.

3.4.3.7. Effect of pH on As^{3+} and F^- sorption and point of zero charge.

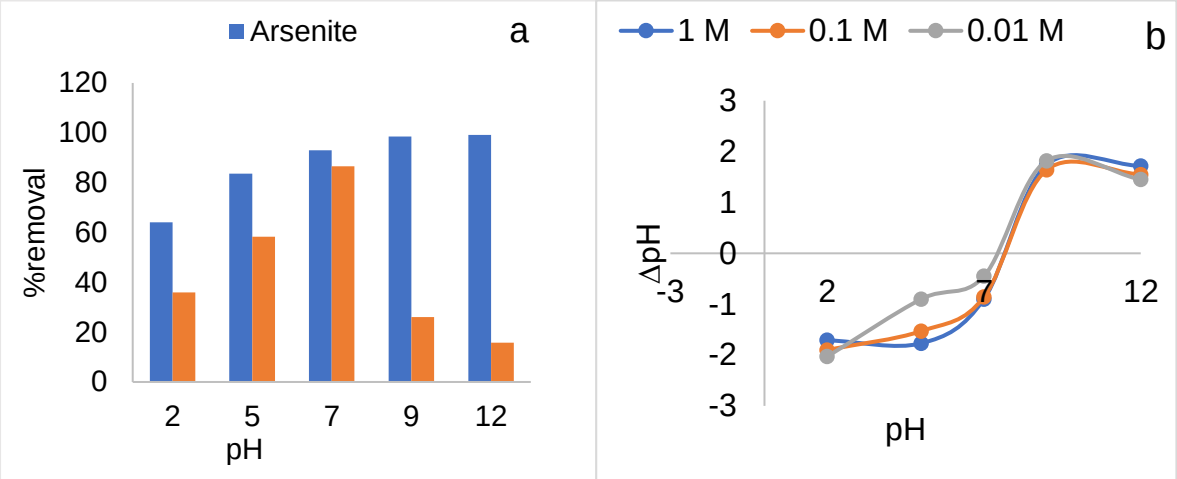

Figure 14: (a) and (b) Effect of pH on F^- and As^{3+} removal by 2.5 % Fe-pPD and pH_{pzc}. (Initial As^{3+} and F^- concentration: 5 mg/L and 10 mg/L, adsorbent dose: 0.25 g and 0.2 g, solution volume: 50 mL, contact time: 40 mins, shaking speed: 250 rpm and temperature: 297K).

Fig 14. is showing obtained results of the point of zero charge and effect of pH on As^{3+} and F^- removal uptake from aqueous solution. The effects of pH and ionization abilities of the composite on As^{3+} and F^- species sorption was evaluated by varying the pH of the solution between 2-12. Based on the results obtained from the above Fig, As^{3+} and F^- uptake highly depends on the solution pH. The point of zero charge of Fe-pPD was examined and the attained result is shown in Fig 14(b). The pH at the point of zero charge is defined as the pH at which the net charge of the surface is equal to zero. However, the importance of this phenomenon is that the surface will be positively charged at solution pH values less than pH_{pzc}, whereas negatively charged when solution pH is greater than the pH_{pzc}. From the obtained results, the pH_{pzc} is 7.

As revealed on the plot (Fig. 14(a)), it was observed that As^{3+} uptakes by the 2.5% Fe-pPd composite increase with increasing the solution pH. From the obtained results, the optimal As^{3+} removal pH was reported to be 9. Recently, it has been reported that As^{3+} is an oxy ion that speciates at different pH under reducing and oxidizing

conditions. The literature has demonstrated that As^{3+} speciation demonstrates that at pH below 9, the dominant species is neutrally charged H_3AsO_3 while at pH beyond 9 it exists $H_2AsO_3^-$ (Mudzielwani et al , 2019, Smedley and Kinniburgh, 2002) However, at extreme acidic pH As^{3+} species occurs as HAs_3^- (Eq. 18 and 19) which also illustrate behaviour in acidic and alkaline conditions . Thus, at pH below and above the point of zero charge, the adsorption might be attributed to electrostatic attraction and ion exchange.

$$\equiv MOH + H_3As_3 \leftrightarrow \equiv MH_2As_3 + H_2O \quad (18)$$

$$\equiv MOH + H_2As_3^- \leftrightarrow \equiv MHAs_3^- + H_2O \quad (19)$$

Additionally, it was detected that F^- removal by the 2.5 % Fe-pPD increases in less acidic to neutral pH and decreases as the pH increase to alkalinity. An optimal F^- removal pH was reported to be 7, where about 85.51% removal was observed. An initial increase in F^- removal is due to between the adsorbate and adsorbent surface charges as validated by the pH_{pzc}. However, as detected from the pH_{pzc} phenomenon (7), reduction in F^- uptake is due to repulsion force between the adsorbent surface charge and the F^- ions and competition between and F^- ions. Eq. 20 and 21 is the hypothesized fluoride mechanism.

$$\equiv MOH + H^+ + F^- \leftrightarrow \equiv MF + H_2O \quad (20)$$

$$\equiv M(OH)2 + 2F^- \leftrightarrow \equiv MF_2 + 2OH^- \quad (21)$$

3.4.3.8. Effect of co-existing ions.

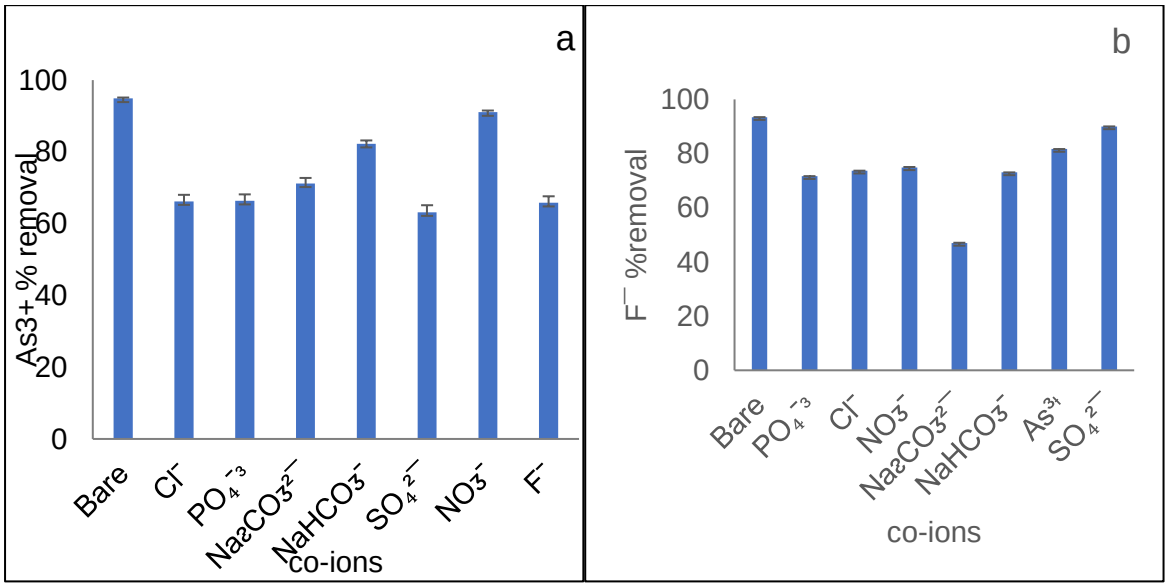

Figure 15: effect of co-existing ions on (a) As^{3+} and (b) F^- removal by 2.5 % Fe-pPD (Initial F^- and As^{3+} concentration: 5 mg/L and 10 mg/L, adsorbent dose: 0.25 g and 0.2 g, solution volume: 50 mL, contact time: 24 hrs, shaking speed: 250 rpm and temperature: 297 K)

Fig 15. Show effect of co-existing ions towards As^{3+} and F^- uptake from aqueous solution. The presence of co-existing ions such as phosphates, sulphate, chlorine, fluoride, arsenite, carbonates nitrates, etc in water, might pose greater or minimum effect upon As^{3+} and F^- ions uptake by the composite in aqueous solution. Fig. 15 clearly shows that co-existing ions have a significant effect on both fluoride and arsenite uptake, which was validated by reduction in percentage removal . Hence, reduction in pollutants ion removal is due to the capacity of the competing ion with As^{3+} and F^- ions for the present binding active adsorbent surface sites (Ayinde et al, 2018). Additionally, the co-occurrence of existing ions reduces interaction mobility of the adsorbate ions with active sites, thus, causing high coulombic repulsion forces. As shown in Fig 15(a), the results revealed that SO_4^{2-}, F^-, $PO_4^-$and Cl^- pose a great effect on As^{3+} removal whereas, CO_3^{2-} and NO_3^- pose minimal effect. Additionally, the obtained F^- results revealed greater CO_3^{2-} effect, where as SO_4^{2-}, As^{3+}, $PO_4^-$and Cl^- pose minimal as shown in Fig 15 (b). Equally, the effect order can be summarized in the following way: arsenite: $SO_4^{2-} > F^- > PO_4^- > Cl^- > CO_3^{2-} > HCO_2^- > NO_3^-$ and fluoride: $CO_3^{2-} > PO_4^- > HCO_2^- > Cl^- > NO_3^- > As^{3+} > SO_4^{2-}$

3.4.3.9. Regeneration

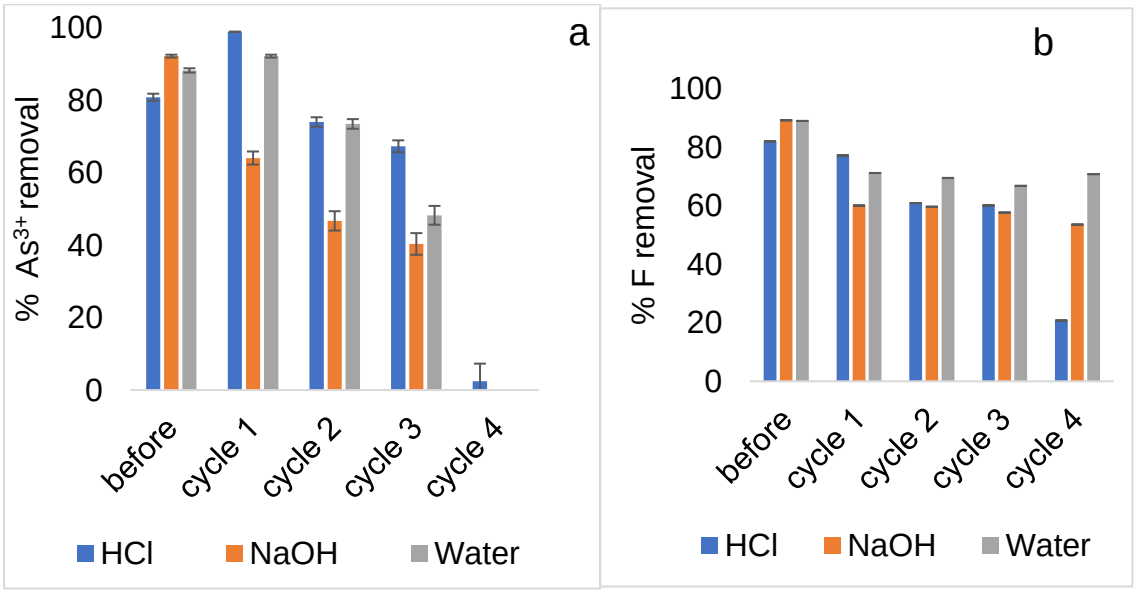

Figure 16: Are regeneration results of (a) As^{3+} and (b) F^- by 2.5% Fe-pPD composite (Initial F^- and As^{3+} concentration: 5 mg/L and 10 mg/L, adsorbent dose: 0.25 g and 0.2 g, solution volume: 50 mL, contact time: 40 mins, shaking speed: 250 rpm and temperature: 297 K).

Fig 16 shows regeneration results of the 2.5 % Fe-pPD. The reusability and economic viability of the adsorbent were evaluated through the regeneration experiment. The efficiencies of the adsorbent in the removal of As^{3+} and F^- ions in an aqueous solution were studied up to four regeneration cycles. As^{3+} and F^- percent removal as a function of the regeneration cycle using 0.01 M NaOH, 0.01 M HCl and H_2O were used as regenerants. From the obtained results in Fig 11 (a-b), the As^{3+} and F^- sorption potential of the regenerated material reduced with increasing regeneration cycles when using HCl, NaOH, and H_2O regenerants. The reduction in As^{3+} and F^- uptake might be due to a reduction in adsorbent dose probably because the polymeric composite was loss during washing process (Mdlalose et al, 2017) as well as the dissolution of Fe in the regenerants.

3.4.3.10. Mechanism of As^{3+} and F^- sorption.

Based on the experimental results, different mechanisms are involved in fluoride and arsenite removal by 2.5 % Fe-pPD composite. However, the kinetics models, isotherm models, thermodynamics, effect of pH as well as point of zero charges were examined to determine the pollutants removal mechanisms. Eq 18-22 expressed that As^{3+} and F^- uptake is also attributed by electrostatic attraction and ion exchange between the adsorbate and adsorbent ions as validated by the results of point of zero charge and effect of solution pH. Also, the kinetics data revealed that the removal process includes physio-sorption and chemo-sorption interface based on kinetic plots and calculated parameters. The obtained intra-particle diffusion kinetic plots and Freundlich isotherm model further supports that 2.5 % Fe-pPD material is multilayer which was further validated by the BET results. Thus, several process or mechanism such as physio-sorption and chemical internal attachment of solid/liquid interface could have a role in As^{3+} and F^- uptake.

3.5 Antimicrobial potency

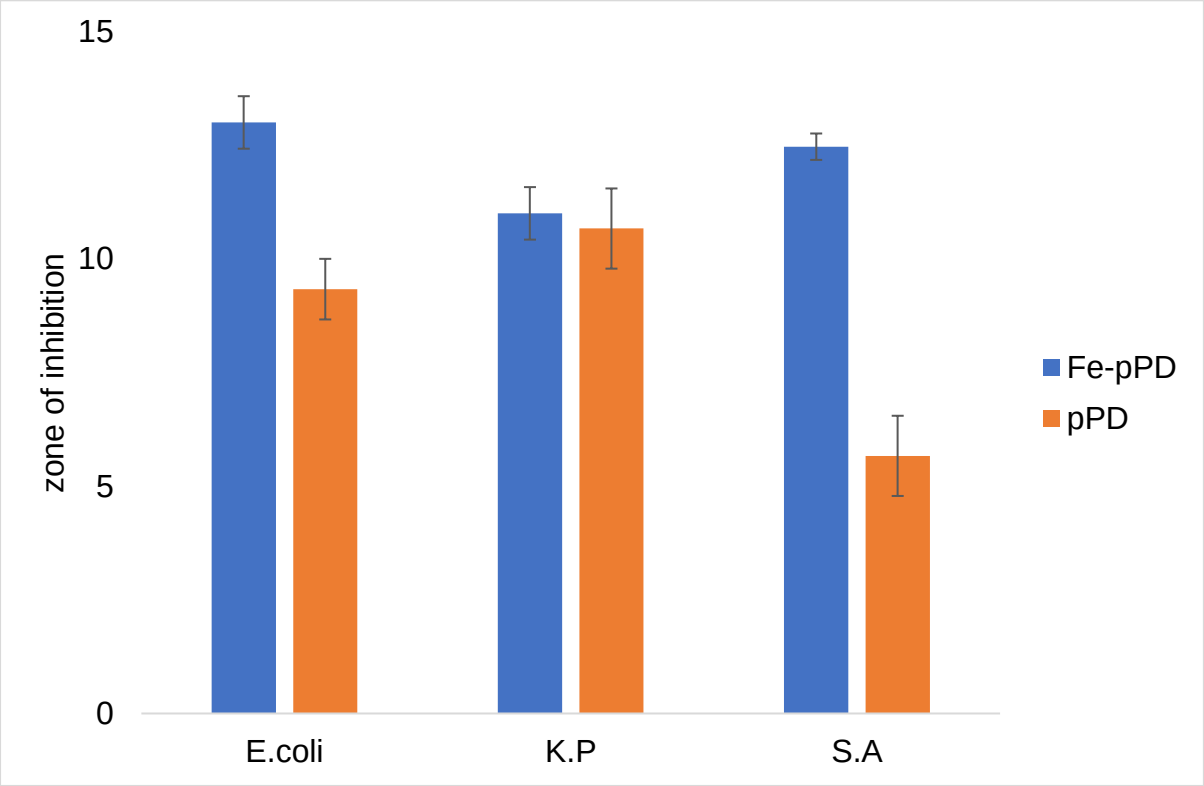

Figure 17. Antimicrobial activity of 2.5 % Fe-pPD and pPD.

The antimicrobial activities of raw pPD and 2.5 % Fe-pPD composites against *Escherichia coli, Klebsiella pneumonia and staphylococcus aureus* are displayed in Fig 17. Comparatively, raw pPD has inhibited portrayed low zon of inhibition (9,10, and 6mm), whereas the modified 2.5 % Fe-pPD composite portrayed high zone of inhibition (13, 11 and12.5 mm). Thus, the modified composite has more susceptibility towards the concerned pathogens compare to bare pPD. The antimicrobial property of the synthesized adsorbent might be due to the existence of a complex and well arrenged Fe^{i3} doped pPD compositec material which generates reactive oxidative species to assist cellular distraction and cell death (Dhillon et al, 2015). Furthermore, different functional groups especially the amines within the Fe-pPD composite are also responsible for the denaturation of cell membrane proteins that ultimately lead to the breakdown of the cellular structure of the bacterial (Chauhan et al, 2014). Additionally, the interaction between the negatively charged substances of the microbial cell surface and the positively charged surface of the adsorbent (expressed by the pHpzc) might exhibits cell wall lysis (Inbaraj et al, 2012). Hence, the composites have high

antimicrobial action towards gram-negative bacteria compared to gram-positive ones as confirmed by the attained results.

3.6. Conclusion

The Fe doped poly-phenylenediamine was successfully synthesized using chemical co-oxidative polymerization. Fe was successfully incorporated onto pPD matrix as validated by the different morphological characterization. The synthesized 2.5 % Fe-pPD composite was evaluated for As^{3+} and F^- uptake in an aqueous solution. However, the study discovered the proposed adsorbent has the potential to remove As^{3+} and F^- effectively. The attained batch experiment data has shown that the assessed parameters such as contact time, adsorbent dose, pH, etc have a significant effect on As^{3+} and F^- adsorption. The rate of adsorption of F^- and As^{3+}onto 2.5 % Fe-pPD composite followed the pseudo-second-order kinetic model, thus, the uptake mechanisms of both pollutants by the 2.5 % Fe-pPD composite is due to the chemisorption process. However, in this study, the intra-particle plot obtained from the adsorption data show that the adsorption phenomena occur in more than one step. This was the same for both F^- and As^{3+} adsorption processes results, indicating the uptakes of both pollutants were not controlled by only intra-particle diffusion. These phases show the systematic mechanisms of both the As^{3+} and F^- species in solution occurring through the boundary layer diffusion, intraparticle pore diffusion as well as on the active sites across the external surface Fe-pPD composite. Comparatively, the adsorption of both As^{3+} and F^- by 2.5 % Fe-pPD displayed that the sorption process followed the Freundlich isotherm model with higher affinity for F^- than As^{3+} based on the obtained n values, R^2, AdJ.R^2, reduced chi-squares and residual sum of squares values. Thus, the adsorption phenomenon occurred on a homogeneous layer meaning the synthesized sorbent is multi-layer. Also, thermodynamically, the removal process for both $As^{3+}$and F^- by the 2.5 % Fe-pPD was endothermic with an increase in the degree of randomness as validated by the positive values of ΔH^O and ΔS^O respectively. The synthesized 2.5 % Fe-pPD composite successfully portrayed effective antimicrobial action towards waterborne pathogens. Also, the synthesized composite serves a multiple purpose for both arsenite, fluoride as well as pathogen removal. Thus, reducing the expenses of using multiple sorbents to remediate water pollution.

References.

Amini, M., Younesi, H., Bahramifar, N., Lorestani, A.A.Z., Ghorbani, F., Daneshi, A. and Sharifzadeh, M., 2008. *Application of response surface methodology for optimization of lead biosorption in an aqueous solution by Aspergillus niger.* Journal of hazardous materials, 154(1-3), pp.694-702.

Amor, Z., Bariou, B., Mameri, N., Taky, M., Nicolas, S., Elmidaoui, A.2001. *Fluoride removal from brackish water by electrodialysis.* Desalination 133, 215–223.

Archana, S. and Jaya Shanthi, R., 2014. *Dielectric relaxation, AC conductivity and photoluminescence properties of poly (p-phenylenediamine)/TiO2nanocomposites.* International Journal of Advanced Research, 2(10), pp.778-790.

Ayinde, W.B., Gitari, W.M., Munkombwe, M. and Amidou, S., 2018. Green synthesis of Ag/MgO nanoparticle modified nanohydroxyapatite and its potential for defluoridation and pathogen removal in groundwater. *Physics and Chemistry of the Earth, Parts A/B/C*, *107*, pp.25-37.

Ayoob, S., Gupta, A.K. and Bhat, V.T., 2008. A conceptual overview on sustainable technologies for the defluoridation of drinking water. *Critical reviews in environmental science and technology*, *38*(6), pp.401-470.

Bernard T. 2013. *Ground Water Contamination with Fluoride and Potential Fluoride removal Technologies for East and Southern Africa.* (http//dx.doi.org/10: 5772/54985

Bhatnagar, A., Kumar, E. and Sillanpää, M., 2011. *Fluoride removal from water by adsorption—a review.* Chemical Engineering Journal, 171(3), pp.811-840.

Bolster, C.H., Hornberger, G.M., 2007. *On the use of Linearized Langmuir equation*.

Camacho, L.M., Parra, R.R. and Deng, S., 2011. Arsenic removal from groundwater by MnO2-modified natural clinoptilolite zeolite: Effects of pH and initial feed concentration. *Journal of Hazardous materials*, *189*(1-2), pp.286-293.

Chauhan, D., Dwivedi, J. and Sankararamakrishnan, N., 2014. Facile synthesis of smart biopolymeric nanofibers towards toxic ion removal and disinfection control. *RSC advances*, *4*(97), pp.54694-54702.

Dhillon, A. and Kumar, D., 2015*. Development of a nanoporous adsorbent for the removal of health-hazardous fluoride ions from aqueous systems.* Journal of Materials Chemistry A, 3(8), pp.4215-4228.

García, M.G., Borgnino, L., 2015. *Fluoride in the context of the environment. In: Preedy, V.R. (Ed.), Fluorine: Chemistry, Analysis, Function and Effects*. The Royal Society of Chemistry, UK, pp. 3–21.

Gitari W.M; Ngulube, T; Masindi, V; and Gumbo, J.R., 2017. *Defluoridation of groundwater using Fe3+-modified bentonite clay:* Optimization of adsorption conditions, Desalin. Water Treat. 1–13, 10.1080/ 19443994.2013.855669.

Gitari, M.W; Izuage A.A and Gumbo J.R. 2017. *Synthesis, characterisation and batch assessment of groundwater fluoride removal capacity of Mg/Ce/Mn oxide-modified diatomaceous earth.* Department of Ecology and Resources Management, University of Venda, South, Africa

Haldorai, Y., Lyoo, W.S. and Shim, J.J., 2009. *Poly (aniline-co-pphenylenediamine)/MWCNT nanocomposites via in situ microemulsion: synthesis and characterization.* Colloid and Polymer Science, 287(11), p.1273

Hao, Q., Sun, B., Yang, X., Lu, L. and Wang, X., 2009. *Synthesis and characterization of poly (o-phenylenediamine) hollow multi-angular microrods by interfacial method.* Materials Letters, 63(2), pp.334-336

Hichour, M., Persin, F. and Sandeaux, J., 2000. Prediction study of the structural, elastic, electronic and optical properties of the antiperovskite. *Separation and Purification Technology*, *18*(1), pp.1-11.

Ho, Y.S. and McKay, G., 1998. Sorption of dye from aqueous solution by peat. *Chemical engineering journal*, *70*(2), pp.115-124.

Ho, Y.S., 2006. Second-order-kinetic model for the sorption of cadmium onto tree fern: a comparison of linear and non-linear methods. Water Res. 40, 119–125.

Inbaraj, B.S., Tsai, T.Y. and Chen, B.H., 2012. Synthesis, characterization and antibacterial activity of superparamagnetic nanoparticles modified with glycol chitosan. *Science and Technology of Advanced Materials*.

Izuagie, A.A., Gitari, W.M. and Gumbo, J.R., 2017. Effects of calcination temperature and solution pH on the defluoridation potential of Al/Fe oxide-modified diatomaceous earth: metal leaching and sorbent reuse. *Water Science and Technology: Water Supply*, *17*(3), pp.688-697.

Jadhav, S.V., Bringas, E., Yadav, G.D., Rathod, V.K., Ortiz, I. and Marathe, K.V., 2015. Arsenic and fluoride contaminated groundwaters: a review of current technologies for contaminants removal. *Journal of Environmental Management*, *162*, pp.306-325.

Kamble, S.P., Jagtap, S., Labhsetwar, N.K ., Thakare, D., Godfrey, S., Devotta, S. and Rayalu, S.S., 2007. Defluoridation of drinking water using chitin, chitosan and lanthanum-modified chitosan. *Chemical Engineering Journal*, *129*(1-3), pp.173-180.

Lagergren, S., 1898. About the theory of so-called adsorption of soluble substances.

Langmuir, I., 1918. The adsorption of gases *adsorbers*. AIChE J. 20 (2), 228e238.

LI X G; MA X L; SUN J and Huang M R. 2009. *Powerful reactive sorption of silver (I) and mercury (II) onto poly (o-phenylenediamine) microparticles* [J]. Langmuir, 25: 16751684.

Li XG, Huang MR, Duan W, Yang YL. 2002. *Novel multifunctional polymers from aromatic diamines by oxidative polymerizations.* Chemical Reviews, 102(9), pp.2925–3030.

Li, X.G., Huang, M.R., Chen, R.F., Jin, Y. and Yang, Y.L., 2001. *Preparation and characterization of poly (p phenylenediamine co xylidine).* Journal of applied polymer science, 81(13), pp.3107-3116

Liu, G., Zheng, L., Duzgoren-Aydin, N.S., Gao, L., Liu, J. and Peng, Z., 2007. *Health effects of arsenic, fluorine, and selenium from indoor burning of Chinese coal*. In Reviews of environmental contamination and toxicology (pp. 89-106). Springer, New York, NY.

Madsen, H.O., Krenk, S. and Lind, N.C., 2006. *Methods of structural safety*. Courier Corporation.

Mahapatra M, Anand S, Mishra B.K, Giles D.E, Singh P. 2009. *Review of fluoride removal from drinking water.* Institute of Minerals and Materials Technology, Orissa, India

Maheshwari, R.C., 2006. *Fluoride in drinking water and its removal.* Journal of Hazardous materials, 137(1), pp.456-463.

Masindi, V., Gitari, M.W., Tutu, H. and De Beer, M., 2015. Passive remediation of acid mine drainage using cryptocrystalline magnesite: A batch experimental and geochemical modelling approach. *Water SA*, *41*(5), pp.677-682.

Mdlalose, L., Balogun, M., Setshedi, K., Tukulula, M., Chimuka, L. and Chetty, A., 2017. *Synthesis, characterization, and optimization of poly (p-phenylenediamine) based organoclay composite for Cr (VI) remediation.* Applied Clay Science, 139, pp.72-80.

Miretzky, P. and Cirelli, A.F., 2011. Fluoride removal from water by chitosan derivatives and composites: a review. *Journal of Fluorine Chemistry*, *132*(4), pp.231-240.

Mudzielwana, R., Gitari, W.M. and Ndungu, P., 2019. Evaluation of the adsorptive properties of locally available alumino-silicate clay in As (III) and As (V) remediation from groundwater. *Physics and Chemistry of the Earth, Parts A/B/C*, *112*, pp.28-35.

Mudzielwana, R., Gitari, M.W., Akinyemi, S.A. and Msagati, T.A., 2018. Performance of Mn 2+-modified bentonite clay for the removal of fluoride from aqueous solution. *South African Journal of Chemistry*, *71*(1), pp.15-23.

Pham, T.A., Kawai, S. and Murata, K., 2011. Visualization of the synergistic effect of lithium acetate and single-stranded carrier DNA on Saccharomyces cerevisiae transformation. *Current genetics*, *57*(4), pp.233-239.

Qiao, J., Cui, Z., Sun, Y., Hu, Q. and Guan, X., 2014. Simultaneous removal of arsenate and fluoride from water by Al-Fe (hydr) oxides. *Frontiers of Environmental Science & Engineering*, *8*(2), pp.169-179.

Ravenscroft, P., 2007. Predicting the global extent of arsenic pollution of groundwater and its potential impact on human health. *Report for UNICEF, New York*.

removal of Ni(II) from aqueous solutions. Water Air Soil Pollut. 49 (1), 69e79.

Ramos AR, Tapia AKG, Piñol CMN et al (2019) Morphological, electrical and antimicrobial properties of polyaniline-coated paper prepared via a two-pot layer-by-layer technique. Mater Chem Phys. https ://doi.org/10.1016/j.match emphy s.2019.12197 2

Sharma, V.K. and Sohn, M., 2009. Aquatic arsenic: toxicity, speciation, transformations, and remediation. *Environment international*, *35*(4), pp.743-759.

Sharma, Y.C., Gupta, G.S., Prasad, G., Rupainwar, D.C., 1990. *Use of wollastonite in the* Soil Sci. Soc. Am. J. 71 (6), 1796e1806.

Smedley, P.L. and Kinniburgh, D.G., 2002. A review of the source, behaviour and distribution of arsenic in natural waters. *Applied geochemistry*, *17*(5), pp.517-568.

Stejskal, J., 2015. *Polymers of phenylenediamines.* Progress in Polymer Science, 41, pp.1-31

Thompson, R.I., Eisenstein, D., Fan, X., Rieke, M. and Kennicutt, R.C., 2007. *Evidence for az< 8 origin of the source-subtracted near-infrared background*. The Astrophysical Journal, 666(2), p.658.

Villaescusa, I. and Bollinger, J.C., 2008. Arsenic in drinking water: sources, occurrence, and health effects (a review). *Reviews in Environmental Science and Bio/Technology*, *7*(4), pp.307-323.

Wang, L., Guo, S. and Dong, S., 2008. *Facile synthesis of poly (o-phenylenediamine) microfibrils using cupric sulfate as the oxidant.* Materials Letters, 62(17-18), pp.32403242.

Weber, T.W., Chakravorti, R.K., 1974. *Pore and solid diffusion models for fixed-bed*

Weber, W.J. and Morris, J.C., 1964. Equilibria and capacities for adsorption on carbon. *Journal of the Sanitary Engineering Division*, *90*(3), pp.79-108.

WHO, 2000. *Global Water Supply and Sanitation Assessment 2000 Report*, World Health Organization, 92 4 156202 1, Geneva, Switzerland

WHO, *Guidelines for drinking water quality, forth ed*., World Health Organization, Geneva, 2011.

WHO/UNICEF JMP (Joint Monitoring Programme for Water Supply and Sanitation). 2010. *JMP Rapid Assessment on Drinking-water Quality* pilot report 2010. 8-10.

WHO/UNICEF *Joint Water Supply and Sanitation Monitoring Programme, 2014. Progress on drinking water and sanitation.* World Health Organization.

World Health Organization, 2016. *Report on the technical consultation on poliomyelitis eradication in Pakistan, Islamabad, Pakistan, 28–29 June 2016 (No. WHO-EM/POL/429/E).* World Health Organization. Regional Office for the Easte of nanocrystalline TiO2 powders. Chemistry of materials, 14(9), pp.3808-3816.

Chapter 4

Synthesis and characterization of Ce doped poly(para-phenylenediamine) and its evaluation of chemical pollutants and pathogens removal in aqueous solutions.

E.P Munzhelele*, M.W Gitari, W.B Ayinde

Environmental Remediation and Nanoscience (EnviReN), Department of Ecology and Resource Management, School of Environmental Sciences. University of Venda, Private Bag X5050, Thohoyandou, 0950, Limpopo Province, South Africa.

4.1. Abstract.

Water pollution is one of the global challenges that is faced by most developing continents like Africa. The introduction of a huge volume of chemical and microbial pollutants due to natural and anthropogenic activities has greatly affected water quality. Consumption of water contaminated with fluoride (F^-), arsenite (As^{3+}), and pathogens can lead to complicated health issues. Thus, inversely affecting environmental dynamics and economical functions, leading to water scarcity as well as causing public health problems. This study focused on the synthesis of cerium doped poly(-para-phenylenediamine) (Ce-pPD) using chemical co-oxidative polymerization and the evaluation of its potential ability in remediating F^- and As^{3+} at optimal conditions in aqueous solution as well as its antimicrobial activity.

The chemical modification of Ce on pPD matrix was assessed using FTIR, SEM-EDS, BET, CHNS, and XRD. The obtained morphological analysis successfully validates the incorporation of Ce metal oxide across the pPD matrix. The FTIR results confirmed that the functional groups of pPD were not altered due to Ce metal oxide integration. The SEM spectral image of the 5 % Ce-pPD composite shown a well-arranged combination with a crystalline phase compared to bare pPD composite, with a slight improvement on the BET surface area (9.86m^2/g). The synthesized composite was evaluated for potential F^- and As^{3+} removal efficiency. It was discovered that 5 % Ce-pPD composite has the potential ability to remove about 95% and 86 % of F^- (13.29 mg/g) and As^{3+} (2.11 mg/g) respectively. Batch experiments were carried out to determine the optimal conditions and their significance towards F^- and As^{3+} sorption using 5 % Ce-pPD. The attained results revealed that the assessed conditions have a significant effect on these pollutants uptake in an aqueous solution.

The obtained kinetics data for the adsorption process was better described by the pseudo-second-order kinetic model. The intra-particle diffusion plot showed that intra-particle is not the only limiting step through the distinctive phases. The adsorption isotherm model for both F^- and As^{3+} followed the Freundlich isotherm model. The synthesized composite has the potential ability for microbial disinfection and is proven to be economically viable and feasible as multifunctional materials in the remediating polluted water.

Keywords: Inorganic pollutants, pathogens, cerium, composite, sorption experiments, antimicrobial, and regeneration.

4.2. Introduction.

The introduction of bulk pollutants into water sources by humans and natural activities has greatly affected water quality. Thus, inversely affecting environmental dynamics and economical functions, leading to water scarcity as well as causing public health problems (Thines et al, 2016). Contamination of water by arsenite, fluoride, lead, nitrates, and pathogens have been reported worldwide as a potential risk to the human population. The main sources of chemical and microbial pollutants in water systems involve the uncontrolled release of industrial, mining wastes, sewage, herbicides, agricultural waste, insecticides, erosion as well as infiltration of polluted water into aquifers. Simultaneous occurrence and chronic poisonings through continuous intake of water contaminated by pathogens, fluoride, and arsenite is an emergent widespread disease in Africa (Potgieter et al, 2006; Ma et al, 2012; Walters et al, 2012; Nephalama and Muzerengi, 2016). Since most developing nations depend on groundwater as the main source of water for domestic use, thus, giving a motivation for groundwater assessment and purification before utilization.

The introduction of microbes in water sources has been reported and affected millions of people worldwide especially in developing countries like Africa. The most contributing factor for pathogen occurrence in water sources is poor sewage disposal and poor sanitation distribution across the globe. Moreover, about 1.1 billion people have no access to clean water, and 2.4 billion have no basic sanitation (WHO, 2014). Due to poor water quality, sanitation and hygiene, about 1.7 million deaths caused by infectious water-borne diseases such as diarrhoea and nine of the tenth of deaths happen in children, with a significant, majority of deaths in developing countries are

being reported annually (Ashbolt, 2004). Hence, this greatly affects human healthy and economic development. Hence, it calls for researchers' attention to arise-up with emerging technologies that may help to resolve microbial pollution without excessive damage to the environment.

Fluoride occurrence in drinking water due to natural and anthropogenic activities has been known as one of the global challenges, affecting human health. Elevated fluoride concentrations in water sources have been reported in most Southern African nations (Taghipour et al, 2016; Abiye et al, 2018). An estimate of more than 200 million people globally is ingesting water with high fluoride levels that surpass the WHO standard of 1.5 mg/L (W.H.O. 2004; 2011; 2017). The concentration and the duration of continuous intake of water containing fluoride determine the impact of fluoride uptake for it to be beneficial or detrimental to the human body. Nevertheless, excessive intake of water containing fluoride might result in adverse health effects which include bone diseases and mottling of teeth, risk of suffering from fluorosis (Tor, 2006; Edmunds and Smedley, 2005; Rango et al, 2014).

Equally, arsenic is one of the abundant elements on the earth`s crust. Among different arsenic compounds, arsenite (As^{3+}) is the most toxic pollutants in the global environment even at low concentrations. The primary source of arsenic is natural activities such as interactions between groundwater and aquifer sediments and hard rock minerals, particularly pyrite (Maity et al, 2012). Furthermore, secondary producers are human activities that expose rocks and minerals containing arsenic due to various economic developments including mining, agriculture, etc (Bhowmik et al, 2015; Jones et al, 2015). Arsenite occurrence in groundwater that exceeds the World Health Organization limit of 0.1 mg/L has greatly affected human heath due to excessive intake of arsenite polluted water (WHO,1981). Hence, an increased in arsenite concentration in drinking water sources has gained global attention as a threat to public health (Nriagu et al, 2007). Human poisoning and death from arsenic have occurred because of excessive intake of water contaminated with arsenic in different parts of the world (Jiang, 2001, Berg et a, 2001). General symptoms of chronic exposure are skin and lung cancer, while prolonged exposure to arsenite may result in a disease called arsenicosis.

Due to an increase in water contamination, different methods have been developed to remedy this global issue. The methods used include ion-exchange, adsorption, precipitation, and membrane (Mo et al, 2003, Chouhan and Flora, 2010, Shannon et al, 2010). Among these techniques, adsorption has been by far embraced compared to others, because it is cheap, easy to operate, considered to be eco-friendly, promote environmental stability, and produces less sludge (Vrutangkumar et al, 2015). Different adsorbents have been developed to remediate water pollution, this includes metal oxides (Fe, Ce, Mn, etc.), clay, agricultural wastes, charcoal, activated carbon, ashes, conjugated polymers, and bio-sorbents (Zhang et al, 2002; Mark et al, 2008; Mohaptra et al, 2009; Lacasa et al, 2012; Ma et al, 2015; Fito et al, 2017).

In the past years, the use of metal oxides such as Fe, Ce, Mn, etc have been assessed and yield better results on water purification (Wu et al, 2007, Wang et al, 2015). However, the use of Ce and Fe for arsenite, fluoride removal has a disadvantage of leaching and less ability for simultaneously pollutants removal. Moreover, the use of doped polymeric composite has gained much attention due to high pollutant removal capabilities abetted to high surface area and reusability (Amier and Brandt,2017). Hence, doping polymeric materials with metal oxides aided in improving the surface area, pore size, pore-volume, and pore diameter which enhance its adsorption capacity. Thus, this study focused on synthesizing an effective adsorbent with potency to remove these concerned pollutants simultaneously. As a result, this study focused on synthesizing Ce doped poly (para-phenylenediamine) using the chemical oxidative method and its uptake potency for fluoride and arsenic as well as disinfecting potency.

4.3. Materials and methodology.

4.3.1. Chemicals

Poly (p-phenylenediamine), Ammonium persulfate ($(NH4)_2S_2O_8$), cerium (IIII) chloride heptahydrate ($CeCl_4.5H_2O$), sodium fluoride (NaF) and sodium hydroxide (NaOH), NaCl, KCl, HCl, and $NaAsO_3$ were purchased from Rochelle chemicals, South Africa. All reagents were of analytical grade and used without any purifications. The working solutions of different As^{3+} and F^- concentrations were prepared in deionized water from Millipore water (18.2 MΩ/cm).

4.3.2. Composite preparation.

4.3.2.1. Preparation of Poly-phenylenediamine (pPD).

Poly-pPD was synthesized by a modified method (Pham et al., 2011; Mdlalose et al., 2017). Briefly, pPD (1.62 g, 0.015 mol) was dissolved in HCl (50 mL, 0.1 M) and stirred for 3 hours on an ice bath. Next, the pPD polymerization was initiated by a dropwise addition of the freshly prepared oxidant solution of ammonium persulfate (3.42 g) in HCl (25 mL, 0.1 M) for 30 min. The resulting mixture was stirred for 24hours at room temperature to ensure complete polymerization of the pPD monomer. The pH of each poly (p-phenylenediamine) was adjusted to 9 with the addition of 2 M NaOH and shaken at 250 rpm for 30 min. The reaction was quenched by adding acetone and the resulting crude product was washed with de-ionized water and dried under vacuum at 60 °C for 24 hours.

4.3.2.2. Ce Doped Poly-Phenylenediamine (Ce-pPD)

The para-Phenylelediamine (pPD) (1.62 g, 0.015 mol) was dissolved in HCl (50 mL, 0.1 M) and stirred for 3 hours on an ice bath. 0.25 M $Ce_4Cl_3.5H_2O$ solution was prepared in a 250 mL volumetric flux, where various percentage of the stock solution (2.5%, 5%, and 10%) was prepared in 20 mL deionized water before the doping process. Each of these salt solutions was added and mixed separately with the pPD solutions by ultrasonication for 25 min. Next, each of the Ce-pPD solution was initiated by a dropwise addition of the freshly prepared oxidant solution of ammonium persulfate (3.42 g) in HCl (25 mL, 0.1 M) for 30 min. The solution was under stirring for 24 hours to allow the formation of Ce-pPD at room temperatures at 400 rpm. The pH of each Ce-pPD was adjusted to 9 with the addition of 2 M NaOH to precipitate the metal hydroxide and shaken at 250 rpm for 30 min. The product was collected by filtration and washed with deionized water, then dried in a vacuum oven at 60 ^{o}C 24hours.

4.3.2.3 Adsorbent efficiency determination

A mass of 0.4 g of pPD and Ce-pPD modified species was contacted with 50 mL of 10 mg/L fluoride solution at 250 rpm for 30 min using a shaker. The equilibrium pH of each mixture was measured to evaluate the pH status of untreated and treated water. After the equilibrium pH measurement, the mixture was centrifuged, and the supernatants analyzed for residual fluoride using a fluoride ion-selective electrode

(9609 BNWP Orion, USA) coupled to an ISE/pH/EC electrode (Thermo SCIENTIFIC-ORION VERSA STAR Advanced Electrochemistry meter fluoride ion-selective electrode) calibrated with four fluoride standards containing TISAB III at the volume ratio of 1:10 as in the case of the samples.

T*he percentage of fluoride removal was calculated by using the following formula*

$$\% \text{ of fluoride removal} = \frac{Co - Ce}{Co} * 100 \quad (1)$$

C_o is the initial fluoride concentration in mg/L, C_e equilibrium concentration in mg/L

The adsorption equilibrium capacity of the adsorbent was calculated using

$$q_e = \frac{Co - Ce}{m} * v \quad (2)$$

qe is the equilibrium capacity of the adsorbent, m is the mass of the adsorbent in g and v is the volume of fluoride in mg/L.

4.3.3. Characterization.

The morphological and physicochemical properties of the synthesized adsorbent were evaluated using the Scanning Electron Microscope (SEM) (SEM with an FEI Nova NanoSEM 230 with the field emission gun equipped with an Oxford Xmax SDD detector operating at an accelerating voltage of 20Kv for the EDS detector (Oxford X-Max with INCA software).The infra-red spectrum of the adsorbent was obtained using the ALPHA Fourier Transform Infra-red spectrum equipped with ATR-Diamond (Bruker, Germany). Bruker-D8 Powder Diffractometer with a theta-theta goniometer X-ray diffraction (XRD) technique was employed to examine the crystalline phase's identification. CHNS analysis was done using the Thermo Flash 2000 series CHNS/O organic Elemental analyser. F^- and pH measurements of the fluoride in the supernatants were determined using a fluoride ion-selective electrode (9609 BNWP Orion, USA) coupled to an ISE/pH/EC electrode (Thermo SCIENTIFIC-ORION VERSA STAR Advanced Electrochemistry meter fluoride ion-selective electrode) calibrated with four fluoride standards containing TISAB III at the volume ratio of 1:10. Furthermore, the As^{3+} measurements in the supernatants were determined using Metrohm 850 professional ion chromatography (Switzerland).

4.3.4. Batch experiments.

Stock solutions containing 1000 mg/L As^{3+} and F^- were prepared by dissolving 0.1733 g of $NaAsO_3$ and 2.21 g NaF, respectively in a 1000 mL volumetric flask using Milli-Q water (18.2 MΩ/cm). The working solutions were prepared through appropriate dilutions from the stock solution. To evaluate the effect of contact time and adsorption kinetics, the contact time was varied from 0.5 to 120 min. Adsorbent dosage of 0.4 g/50 mL and adsorbate concentration of 5 and 10 mg/L of F^- and As^{3+} concentration respectively was maintained. After agitation, mixtures were centrifuged at 250 rpm for 20 min. The optimum adsorbent dosage was evaluated by varying adsorbent dosage from 0.1-0.4 g/50 mL. To evaluate the adsorbate concentration and adsorption isotherms, initial concentration of F^- and As^{3+} were varied from 5 to 100 mg/L at a temperature of 298, 323 and 343 K.

The obtained from effect of initial concentration and adsorption isotherms was used to calculate adsorption thermodynamics data. The effect of co-existing anions (Cl^-, NO_3^-, CO_3^{2-}, SO_4^{2-}) on F^- and As^{3+} uptake efficiency of the Fe-pPD was evaluated with the same concentrations of the pollutant anion concentration using the obtained optimal initial concentration, contact time and adsorbent doseThe initial of pH solution was adjusted using 0.01 M NaOH and 0.01 M HCl. All experiments were conducted in triplicate and the mean values were reported. The pHpzc was evaluated using the solid addition method as described by Gitari et al, (2017).

4.3.5. Adsorption kinetics.

The As^{3+} and F^- adsorption kinetics were studied at an initial concentration of 5 and 10mg/L respectively. The experimental data were analyzed using the non-linear equation of pseudo-first-order and pseudo-second-order models as well as intraparticle diffusion (Eqs. 3, 4, and 5) (Lagergren, 1898; Ho and McKay 1998 and Sharma et al, 1990):

$$qt = qe(1 - e^{-kit}) \quad (3)$$

$$qt = \frac{qe^2\, k_2 t}{1 * k_2\, q_e t} \quad (4)$$

$$qt = k_t t^{0.5} + ci \quad (5)$$

q_e and q_t (both in mg/g) are the amounts adsorbed per unit mass at a time, t (in min). K_1 (min^{-1}) and K_2 ($g.mg^{-1}min$) are first and second-order rate constant respectively These values at different temperatures were calculated from the plots of q_t versus t for $F^-$and As^{3+} ions. Ki (mg /g min^{-1}) is the intra particle diffusion rate constant and is determined from the slope of $t^{0.5}$ vs qt and C_i is the constant attained from the intercept and reflects the thickness of the boundary layer. The greater the intercept, the bigger the boundary layer effect (Mudzielwana et al, 2018).

Also, the Elovich linear equation (Eq. 6) has general application to chemisorption kinetics.

$$qt = \beta \ln(\partial\beta) + \beta lnt \quad (6)$$

The equation was used to validate that chemisorption is the limiting step for fluoride and arsenic uptake. It is often valid for systems in which the adsorbing surface is heterogeneous. qt is the quantity of adsorbate adsorbed at time t (mg/g), α is a constant related to chemisorption rate and β is a constant which depicts the extent of surface coverage. The two constants (α and β) can be calculated from the intercept and slope of the plot from the equation.

4.3.6. Adsorption isotherms.

The adsorption isotherms were modeled using the theoretical Langmuir, Freundlich, and Dubinin Radushkevich (D-R) isotherms (Weber and Chakravorti, 1974, Bolster and Homberger, 2007). The Langmuir isotherm model assumes monolayer interaction between the adsorbate molecules attached to the surface of the adsorbent during equilibrium. Freundlich isotherm model assumes that there is a mutual interaction between the adsorbate molecules adsorbing onto the multilayer or heterogeneous surface of the adsorbent. The non-linear forms of Langmuir and Freundlich equations are expressed as (Eq. 7and 8):

$$qe = \frac{q_m K_L C_e}{1+K_L C_e} \quad (7)$$

$$qe = K_f Ce^{\frac{1}{n}} \quad (8)$$

Where: C_e is the equilibrium concentration (mg/L); Q_e is the adsorption capacity (mg/g); Q_m is the theoretical maximum adsorption capacity (mg/g) and k_L is the Langmuir constant related to the enthalpy of adsorption (L/mg). K_f is the Freundlich

constant related to adsorption capacity and 1/n is the adsorption intensity. When 0 < 1/n < 1, the adsorption is favourable; when 1/n=1, the adsorption is irreversible; and when 1/n > 1, the adsorption is unfavourable.

Equally, Langmuir isotherm can be expressed in terms of a dimensionless constant separation factor or equilibrium parameter R_L (Eq. 9). (when R_L=1 irreversible, 0<R_L<1 favourable, R_L=1 linear and R_L>1 unfavourable).

$$R_L = \frac{1}{1 + k_L C_i} \quad (9)$$

The Dubinin Radushkevich (D-R) model (Eq. 10) was also employed using the experimental data. D-R is a more general model in which assumption is not based on homogenous surface or constant adsorption potential, it gives insight into the sorbent porosity as well as the adsorption energy. The value of adsorption energy further provides information as to whether the adsorption process is physical or chemical in nature (Dubinin, 1947).

$$lnqe = lnqo - \beta e^2 \quad (10)$$

where qe is the amount of ions adsorbed per unit weight of adsorbent (mg/g), qo is the maximum adsorption capacity, β is the activity coefficient useful in obtaining the mean sorption energy E (kJ/mol) and Ɛ is the Polanyi potential. Ɛ and E are expressed by Eq (11 and 12)

$$£ = RT\left(1 + \frac{1}{Ce}\right) \quad (11)$$

$$\mathrm{E} = \sqrt{\frac{1}{2\beta}} \quad (12)$$

where R is the gas constant (J/mol K) and T is the temperature (K). qo and β (mol2 /kJ2) can be calculated respectively from the intercept and the slope of the plot of lnqe vs $Ɛ^2$.

4.3.7. Goodness of fit evaluation

The fitness between the experimental data and the simulated data was determined by the coefficient of determination (R^2) (Eq. (13)), root mean square error (RMSE) (Eq. (14)), and the sum of the squared errors (SSE) (Eq. (15)).

$$R^2 = 1 - \frac{\Sigma(q_{e,exp} - q_{e,calc})2}{\Sigma(q_{e,exp} - q_{e,mean})2} \quad (13)$$

$$RMSE = \sqrt{\frac{1}{n-1}\sum_{i=1}^{n}\left(q_{e,exp} - q_{e,calc}\right)^2}_{\text{i}} \quad (14)$$

$$SSE = \sum_{i=1}^{n}\left(q_{e,calc} - q_{e,exp}\right)^2 \quad (15)$$

where qe, calc is the theoretical concentration of adsorbate on the adsorbent, which has been calculated from one of the isotherm models. qe, i, means is the experimentally measured adsorbed solid-phase concentration.

4.3.4. Antimicrobial activity test.

Bacterial resistance and efficacy of the synthesized pPD and Ce-pPD composites were determined from the observed zone of inhibition (mm) using the standard Agar-Well disc diffusion method (Kirby Bauer disk diffusion test). Medium 1 agar plates were divided into half; a small circle to add the adsorbent was punch using the bottom of the 1-5 mL pipette. 50µl of the bacterial strains (*E. coli*; ATCC 25922 IN; *S. Aureus*; ATCC 259231 Tm and *K. Pneumoniae*; ATCC 700603) was inoculated into the sterile medium 1 agar. Then, 50 µl of 1 mL/0,01 mg of the sorbent was deposited into the punched circles. Then incubated for 24hrs at 37 $^{\circ}$C. The minimal zone of inhibition was observed and measured.

4.4. Results and discussion.

4.4.1. Adsorbent Optimization.

Fig 18. portrays the adsorption capacity of pollutants ions (F^- and As^{3+}) by varying the percentage weight of the synthesized composite with an initial concentration of (F^- and As^{3+}) at 10 mg/L and 5 mg/L respectively. The material dosage of 0.4 g was agitated with 50 mL of the initial pollutant ions concentrations for 30 minutes at 250 rpm at room temperature. The sorption potential of the adsorbent was evaluated by observing the effect of percentage volume variation (v/v %) of pPD and Ce-pPD (2.5 %, 5 %, and 10 %) respectively for F^- and As^{3+} uptake.

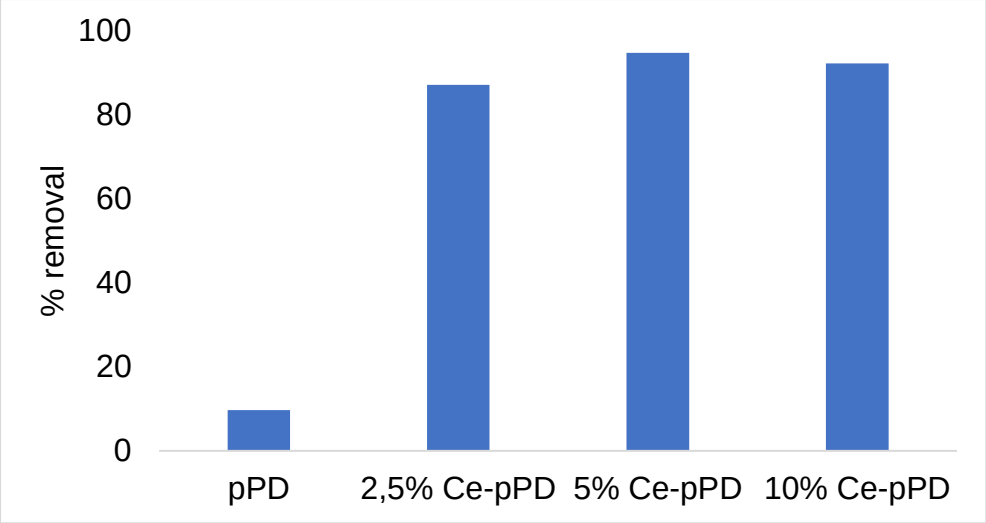

Figure 18. Percentage removal F^- and As^{3+} removal using raw pPD and Ce modified pPD adsorbents. (Initial concentration: 10 mg/L and 5 mg/L, adsorbent dose: 0.4 g, contact time: 30 mins and temperature: 297 K).

The obtained data revealed that raw pPD has lowest removal efficiency compared to doped Ce-pPD. Thus, doped polymeric composite has improved surface area aiding to high adsorption efficacy. An improvement in removal efficiency of Ce-pD might be due to the strong binding infinity on Ce based adsorbents (He et al, 2020). Also, doping pPD with Ce metal ion might have resulted into a crystal structure with protonated and unprotonated functional groups (Bienkowski, 2006). Furthermore, each of the R-Ce molecule is surrounded by four chlorine ligands forming the defects of lattice in the hybrid adsorbent, hence, the proposed mechanisms involved for metal ions include ion exchange and electrostatic attraction. Thus, chemical modification of pPD by doping process might have enhanced the Ce-pPD solubility and ionic state. Also, the introduction of Ce metal oxide on the pPD matrix attributed to an increase in active adsorption sites on the surface of the adsorbent. Comparatively, 5 % Ce-pPD has high fluoride removal efficiency compared to all adsorbents, thus, it was further used for subsequent optimization experiments.

4.4.2. Characterization results.

4.4.2.1. FTIR analysis.

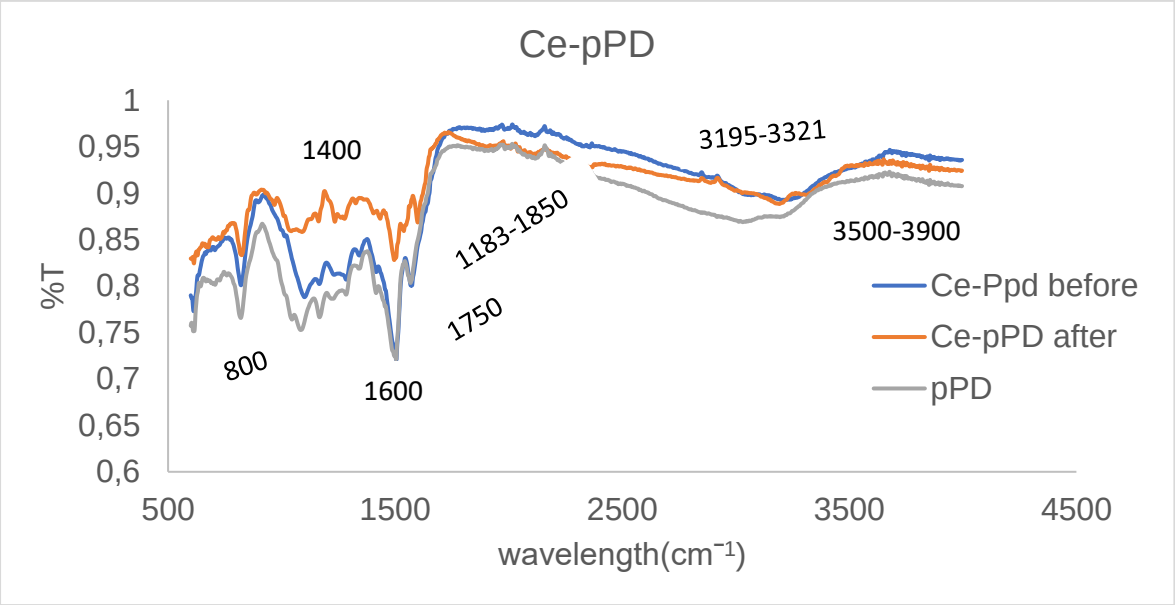

Figure 19. FTIR spectrum of raw pPD and 5 % Ce-pPD (Before and after adsorption application).

Fig 19. shows the FTIR spectrum of raw pPD and 5 % Ce doped pPD (before and after adsorption application). The obtained FTIR analysis revealed that incorporation of 5 % Ce on pPD network did not destroy the functional groups within the original pPD matrix, while a shift in transmittance peaks (800- 1500cm^{-1} and 1750-3900cm^{-1}) shows that the pPD matrix adsorbed Ce metal ion as well as the adsorbates species after 5 % Ce-pPD application. The broad absorption peaks stretching from 3321-3195cm^{-1} originated from the N-H and N-H2 asymmetric stretching which showed that there are many imino and amino groups (Sun et al, 2017). The two solid peaks at 1600cm^{-1} and1496cm^{-1} are linked to the C=N and C=C stretching vibrations in phenazine (Magdziarz et al, 2015). The C-N stretching units were observed at 1183 - 1850cm^{-1} and the stretching peak from 3500-3900^{-1} were due to the OH groups (Rajagopalan et al, 2017). Thus, the successful synthesis of 5 % Ce-pPD was validated by the FTIR spectrum which corresponds with the literature (Pham et al, 2011).

4.4.2.2. XRD analysis.

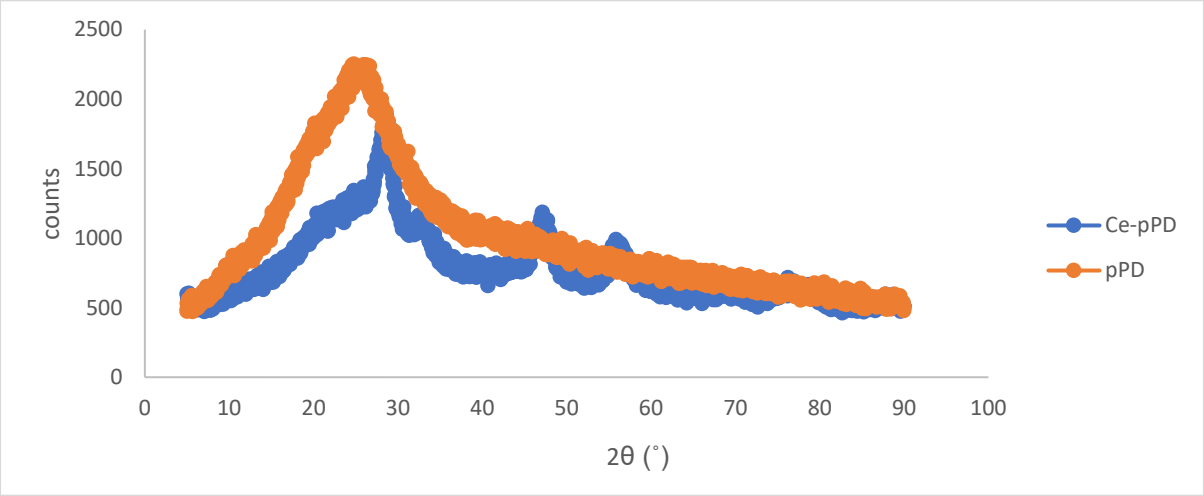

Figure 20. XRD analysis for raw pPD and 5 % Ce-pPD.

The XRD obtained results have revealed that the introduction of Ce metal across the pPD network helped to transform the amorphous structure of raw pPD into a crystalline phase as shown in Fig 20. This was validated through the shifting of the centred peak fom 2θ (25˚) to 35˚. Hence this might be attributed to the integration of Ce metal oxide with pPD network (Dahaghin, et al, 2020). In addition, the development of new peaks was observed in the 5 % Ce-pPD spectrum 2θ (35-40˚, 45-50˚, 55-60˚, 70-75˚, and 75-83˚). Thus, doping of Ce metal oxide onto the polymer matrix successfully increased the crystallinity of the bare pPD.

4.4.2.3. SEM-EDS analysis.

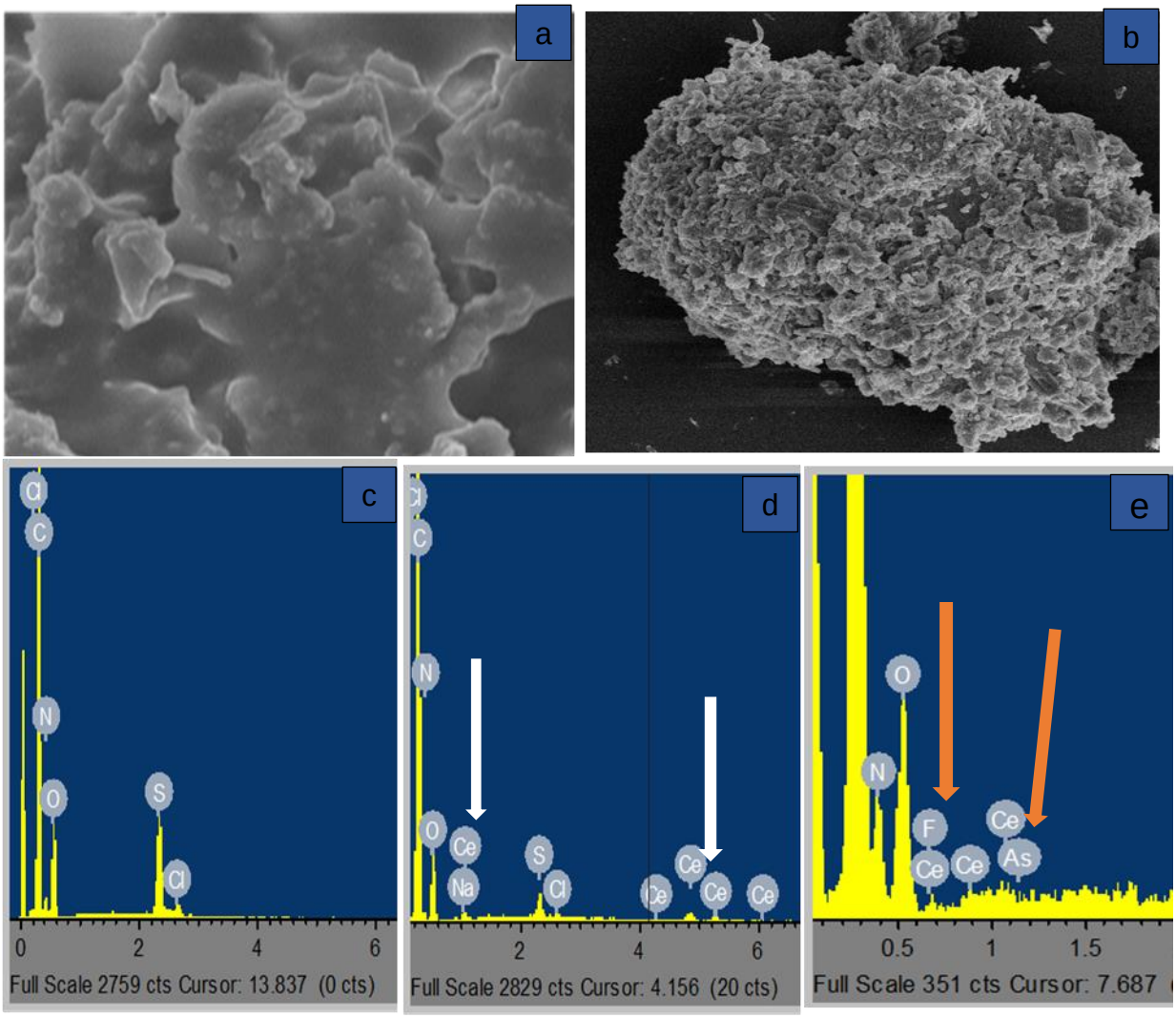

Figure 21: (a) and (b) The respective SEM-EDS spectral analysis of raw pPD and 5% Ce-pPD; (c) and (d) the respective EDS spectra of raw pPD and 5 % Ce-pPD; and (e) EDS spectra of 5 % Ce doped pPD after application.

Fig 21. portrayed SEM-EDS images of raw pPD and 5 % Ce-pPD. The morphological and elemental composition of pPD and 5 % Ce-pPD (before and after application) of the adsorbent was analyzed by SEM-EDS. Fig 21 (a). Shows an ambiguous aggregation morphology of the raw pPD, while 5 % Ce-pPD displayed a well-organized layered combination due to the incorporation of Ce metal oxide on pPD network as presented in Fig 21 (a-b). The EDS spectrum in Fig 21 (c-d) indicates the presence of the Ce element on the pPD network. Additionally, the adsorption potency of the proposed adsorbent on fluoride and arsenite was confirmed by the EDS spectrum

shown in Fig 21(g), which shows the presence of As and F elements on the spectrum. Thus, 5 % Ce-pPD composite has the potential for As^{3+} and F^- uptake.

4.4.2.4 BET analysis.

Table 9. BET results pPD and 5 % Ce-pPD composites.

	pPD	5 % Ce-pPD
BET surface area (m^2/g)	8.68	9.86
Pore volume (cm^3/g)	0.02	0.03
Pore diameter (nm)	7.79	10.25
Average particle size (nm)	69.99	60.69

The surface properties of the raw pPD and 5 % Ce-pPD composite are shown in Table 9. The results showed an increase in surface area after doping with the Ce metal oxide. Comparatively, the pore volume and pore diameter have increased, while the average particle size has decreased. Thus, validating an improvement in surface area of the Ce doped polymeric composite while enhancing the adsorption capacity. An increase (7.79-10.25 nm) in pore diameter confirms the mesoporosity of the 5 % Ce-pPD composite.

4.4.2.5 CHNS results.

Table 10.CHNS results of 5 % Ce-pPD before and after As^{3+} and F^- removal.

CHNS	N [%]	C [%]	H [%]	S [%]
Before application	14.7	49.69	4.101	2.806
After application	22.4	60.33	5.085	1.796

Table 10. presents the CHNS results of 5 % Ce-pPD before and after application. The attained CHNS results of 5 % Ce-pPD composite revealed that the percentage of CHN increases after application, whereas S content has decreased as shown in Table 10. An increase in carbon, hydrogen, and nitrogen (CHN) contents after application might be due to condensation polymerization of the polymers polyaniline with adsorbate resulting in the chain growth, thus increasing the percentage of CHN (Sadeghi et al, 2018). Nevertheless, the present S content in the composite before the application is due to the use of ammonium persulphate as an oxidant. It is known that ammonium persulphate tends to easily dissolve in water; thus, the reason behind the decrease in S percentage after application.

4.4.3. Batch experiments results.

4.4.3.1. Effect of contact time.

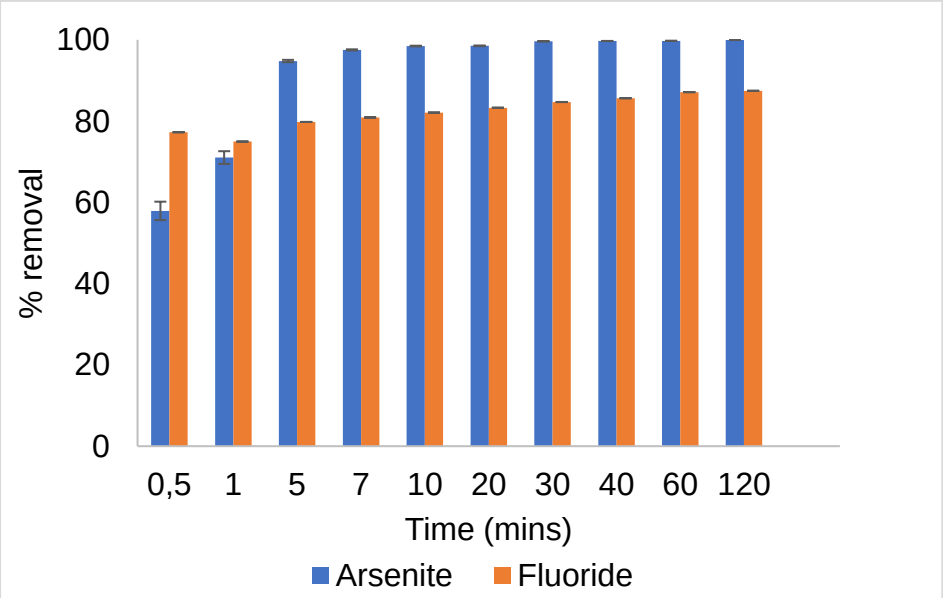

Figure 22. effect of contact time on As^{3+} and F^- removal by 5% Ce-pPD from aqueous solution. (Initial F^- and As^{3+} concentration: 5 mg/L and 10 mg/L, adsorbent dose: 0.4 g, solution volume: 50 mL, shaking speed: 250 rpm and temperature:297 K).

Fig 22. Portrays the obtained results of the effect of contact time on As^{3+} and F^- removal by 5% Ce-pPD. The attained results portrayed that as contact time increases As^{3+} and F^- removal increases. A gradual increase of As^{3+} and F^- sorption was seen from 0.5 mins to 15 mins, it then slowly increases from 15 mins to 30 mins for As^{3+} and F^-, then it reaches an equilibrium contact time. An equilibrium contact time is that at which the curve starts to appear to be asymptotic with the x-axis. The primary increase in As^{3+} and F^- sorption might be due to the presence of active binding sites on the adsorbent surface, that bonded with the metal ions in solution. As time increases an equilibrium was reached, this could be due to the reduction of these active sites, thereby, leading to the adsorbent surface saturation. The equilibrium contact time was recorded to be 30 minutes for both As^{3+} and F^-. These optimum values were further used for subsequent batch experiments.

4.4.3.2. Kinetics model.

The kinetic data models (pseudo-fist, pseudo-second orders and linearized Elovich as well as intraparticle diffusion) were determined from the obtained data of contact time and are shown in Fig 23.

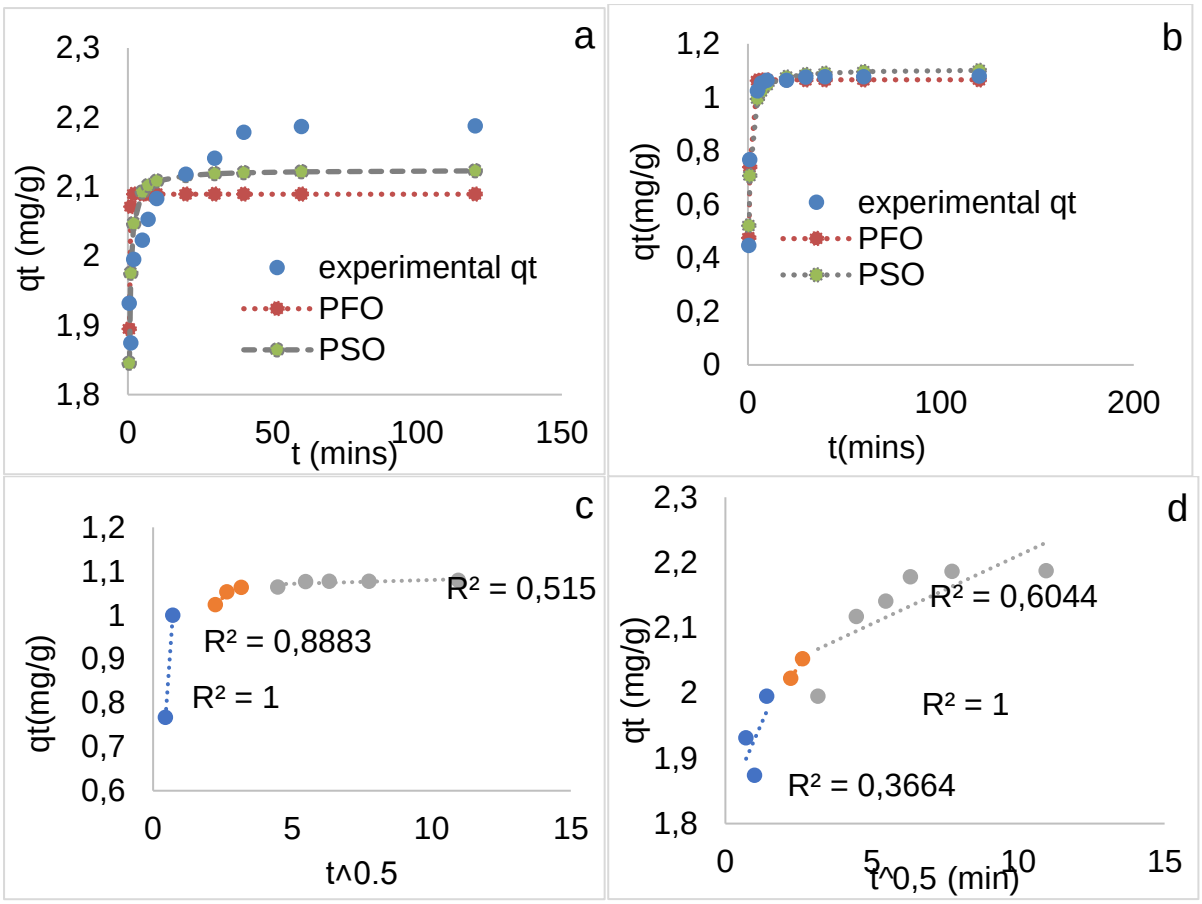

Figure 23. kinetics model of F^- and As^{3+} adsorption by 5 % Ce-pPD composite: (a) and (b) are the respective plots for pseudo-first and pseudo-second-order $As^{3+}$and F^-, (c) and (d) As^{3+} and F^- intraparticle diffusion plots.

From the attained kinetic data model, As^{3+} and F^- adsorption were better described by a pseudo-second kinetic model with R^2 of As^{3+} (0.97)> F^- (0.99). Hence the sorption performance is due to chemisorption. The low values of goodness of fit of the 5 % Ce-pPD composite (χ^2 and RMSE) shown in Table 11 for pseudo-second-order implies favourability in chemisorption reaction at the solid-liquid interface. Furthermore, the Elovich kinetic model was used to validate that chemosorption is limiting, this was confirmed by the higher correlation coefficient shown in Table 12.

Table 11.Non-linearized kinetic model parameters of F^- and As^{3+} adsorption by 5 % Ce-pPD composite.

Non-linear	Pseudo-first-order		Pseudo-second-order	
	F^-	As^{3+}	F^-	As^{3+}
K_2	4.749	6.235	1.183	1.607
q_t	2.089	2.124	1.066	1.106
R^2	0.239	0.639	0.99	0.969
χ^2	0.004	0.002	0.0004	0.001
RMSE	0.092	0.064	0.021	0.037

The intraparticle diffusion kinetic data (Fig 23 (c-d) and Table 12) shown that chemisorption is not the only limiting step. This was validated by the intraparticle plot with three distinct phases as shown in Fig 23(c-d). Thus, adsorption of As^{3+} and F^- might be attributed to: (i) external diffusion, (ii) intraparticle diffusion and (iii) diffusion of adsorbates ions into the internal surface of the solid material (adsorbent) Ruthven et al, 1984; Gupta et al, 2011).

Table 12. linearized kinetics model parameters of F^- and As^{3+} adsorption by 5 % Ce-pPD composite..

Elovich	β	α	R2
F^-	0.058	1.68*1015	0.935
As^{3+}	0.1	1.6*104	0.704
Intraparticle diffusion	Ci	Ki	R2
As^{3+}			
phase 1	0.37	0.89	1
phase 2	0.93	0.04	0.89
phase 3	1.06	0.002	0.52
F^-			
phase 1	1.83	0.10	0,37
phase 2	1.86	0.07	1
phase 3	2	0.02	0.6

Comparatively, the rate constant values for phase 1, 2 and 3 (K_1) shown in table 12, suggests that the adsorption process was very rapid on the layer and dominates the intraparticle diffusion for F^-. While for As^{3+} adsorption process was very rapid on the internal surface of the adsorbent and intraparticle diffusion. However, when comparing the correlation coefficient values of three distinctive phases have shown that the limiting factors for both As^{3+} and F^- adsorption is mainly due to external and intraparticle diffusion, which occurred at a short period of time. Based on the obtained positive values of C_i shows that intra-particle diffusion is the limiting step and external diffusion happened at some extent.

4.4.3.3. Effect of adsorbent dose.

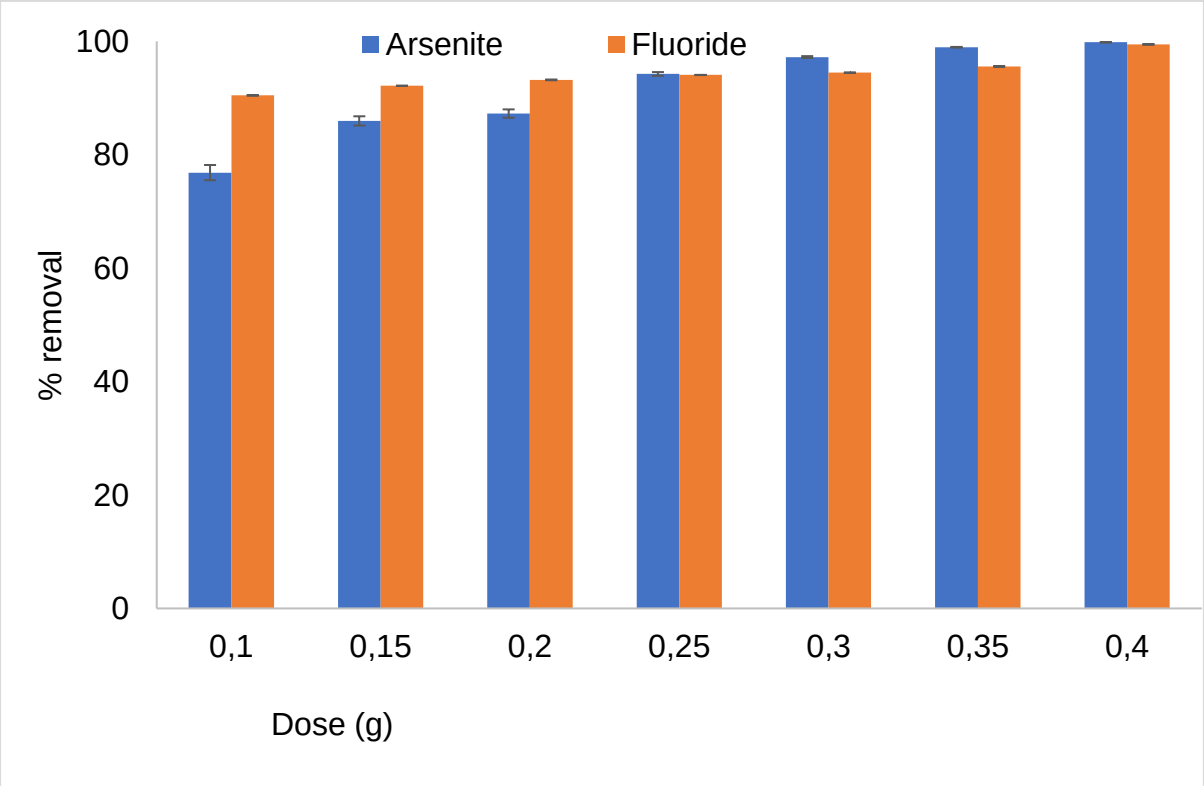

Figure 24. Effect of adsorbent dose on As^{3+} and F^- uptake by 5 %Ce-pPD composite (Initial F^- and As^{3+} concentration: 5 mg/L and 10 mg/L, adsorbent solution volume: 50 mL, contact time: 30 mins, shaking speed: 250 rpm and temperature: 297 K).

Fig 24. portrays the response of adsorbent dose on As^{3+} and F^- sorption using 5 % Ce-pPD. The obtained data showed that As^{3+} and F^- ions uptake increases with adsorbent dose increment. An increase in As^{3+} and F^- uptake with the rapid increase of the adsorbent dose is attributed to an increase in active metal ion binding sites. In conclusion, the adsorbent dose has a significant effect on As^{3+} and F^- uptake in

solution. An optimal dose of 0.35 g and 0.2 g for As^{3+} and F^- were reached, chosen as the optimal dose respectively, and was further used in the subsequent batch experiments.

4.4.3.4. Effect of Initial adsorbate concentration.

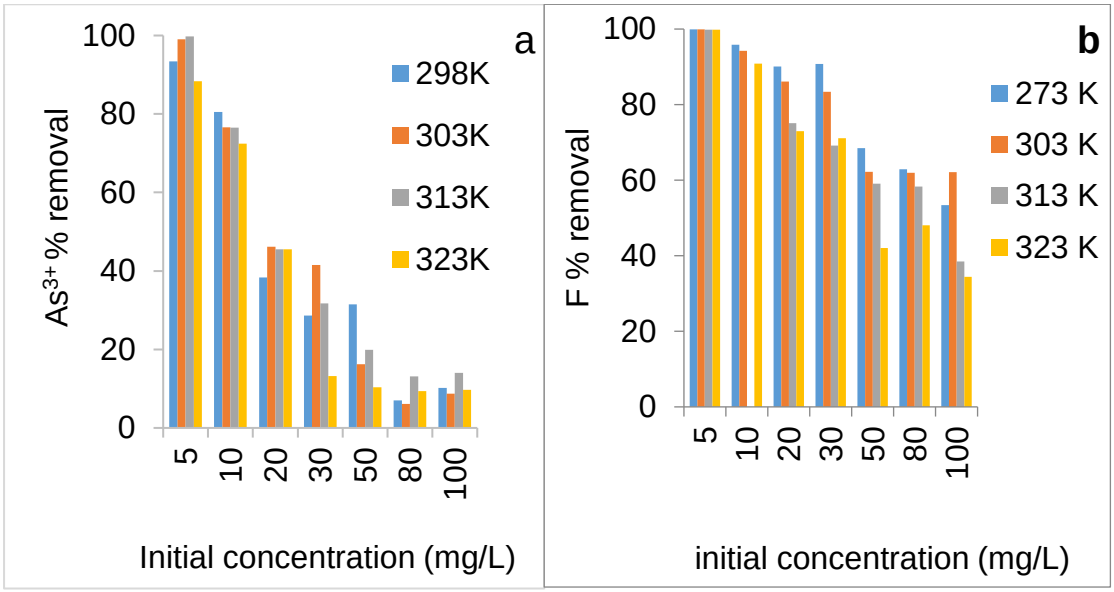

Figure 25. Effect of initial adsorbate concentration on F^- and As^{3+} removal using 5% Ce-pPD composite. (Initial F^- and As^{3+} concentration: 5 mg/L and 10 mg/L, adsorbent dose: 0.35 g and 0.2 g, solution volume: 50 mL, contact time: 24 hrs, shaking speed: 250 rpm and temperature: 298-323 K).

Figure 25. display effect of initial adsorbate concentration at different operating temperatures. It is observed that As^{3+} and F^- uptake decreases with increasing initial concentration. The reduction in As^{3+} and F^- removal with increasing initial concentration might be due to the absence of more available sorption sites on the adsorbent layered-surface resulting in the overall reduction of removal efficiency. Thus, the 5 % Ce-pPD adsorbent binding site within the composite surface area is saturated. The same pattern was observed with different working temperatures. Hence, this is due to a reduction in mass transfer movement which allowed a better reaction between both As^{3+} and F^- ions across the Ce-pPD sorbent surface.

4.4.3.5. Isotherm models.

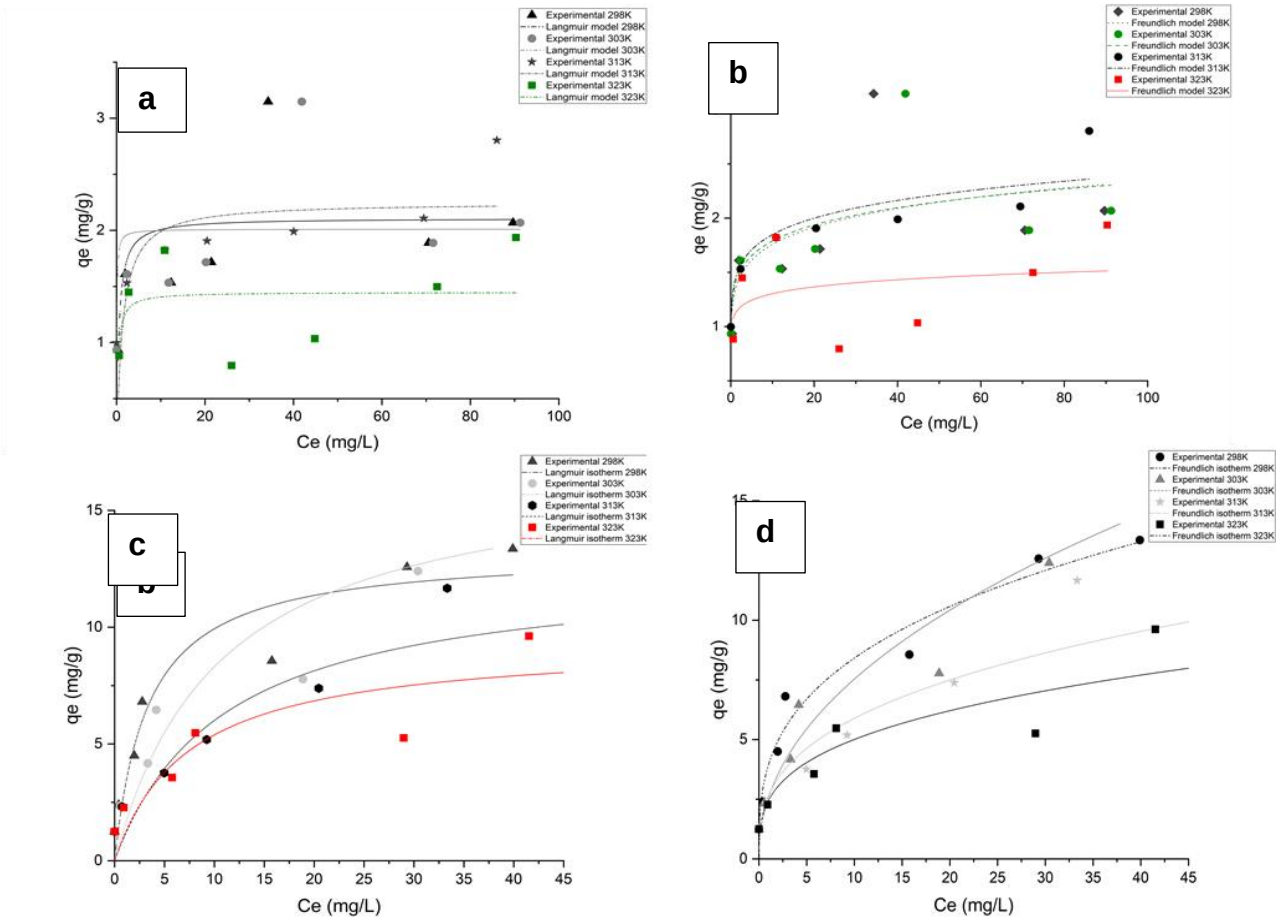

Figure 26. Adsorption isotherm plots of As^{3+} and F^- removal using 5 % Ce-pPD composite: (a) and (b) As^{3+} Langmuir and Freundlich Isotherm models plots, and (c) and (d) F^- for Langmuir and Freundlich Isotherm models

The fitting plots of Langmuir and Freundlich isotherms with their respective calculated parameters are shown in Fig 26 (a-d) and Table 13. The attained As^{3+} and F^- adsorption isotherm model data showed a better fit on both Langmuir and Freundlich Isotherm model. The feasibility of the isotherm models was further validated by R_L (0-1) and n (1-10) values respectively which are within the fitting ranges. However, based on the goodness of fit values, the As^{3+} and F^- uptake process was better described by the Freundlich isotherm model; thus, the adsorption process occurred on a multilayer surface. In Table 13, the low values of the reduced chi-squared (RCS) and residual sum of squares (RSS), implies favourability in heterogeneity in the adsorbate-adsorbent interface.

Table 13. Langmuir and Freundlich isotherm model parameters of F^- and As^{3+} removal using 5 % Ce-pPD composite.

	Langmuir			Freundlich		
	Parameters	F^-	As^{3+}	Parameters	F^-	As^{3+}
298K	Q_m	13.27	2.11	K_f	3.94	1.32
	K_i	0.3	1.99	n	3.03	8.02
	R_L	0.25	0.048	R^2	0.97	0.42
	R^2	0.92	0.43	Adj. R^2	0.96	0.31
	Adj. R^2	0.91	0.32	χ^2	0.86	0.22
	χ^2	2.12	0.31	RSS	4.31	1.5
	RSS	10.59	1.56			
303K	Q_m	17.1	2.01	K_f	2.57	1,38
	K_i	0.09	16.25	n	2.13	8.76
	R_L	0.53	0.01	R^2	0.93	0.48
	R^2	0.87	0.37	Adj. R^2	0.92	0.38
	Adj. R^2	0.85	0.24	χ^2	2.24	0.28
	χ^2	4.23	0.35	RSS	11,21	1.41
	RSS	21.15	1.74			
313K	Q_m	12,58	2.24	K_f	2.65	1.42
	K_i	0,09	0.77	n	2.88	8.8
	R_L	0,53	0.21	R^2	0.87	0,84
	R^2	0,88	0.21	Adj. R^2	0.85	0.8
	Adj. R^2	0,85	0.06	χ^2	2.24	0.06
	χ^2	2,15	0.29	RSS	11.18	0.84
	RSS	10.77	1.43			
323K	Q_m	9.38	1.45	K_f	2.45	1.11
	K_i	0.13	3.31	n	3.22	4.74
	R_L	0.43	0.06	R^2	0.86	0.13
	R^2	0.8	0.17	Adj. R^2	0.84	0.04
	Adj. R^2	0.76	0.01	χ^2	1.59	0.21
	χ^2	2.28	0.02	RSS	7.93	1.0
	RSS	11.39	1.01			

Furthermore, the linearized D-R model was also plotted to determine the effect of the porous nature of the composite as well as the mean free energy of the sorption process. The obtained calculated Q_{max} values of F^- decrease with increasing temperature confirming that adsorption infinity is high at low temperature. Whereas,

As^{3+} data revealed that adsorption infinity is high at high temperature as shown in Table 14. The obtained Polanyi potential (E) value for both F^- and As^{3+} are < 8kg/mol, thus, the adsorption process is physical in nature.

Table 14. D-R linear isotherms parameters of F^- and As^{3+} removal using 5 % Ce-pPD composite.

DR		F^-	As^{3+}
298K	β	$1x10^{-8}$	$6x10^{-8}$
	E	7.07	2.89
	q_e	$7.05x10^{-3}$	$1.96x10^{-3}$
	R^2	0.5799	0.5955
303K	β	$1x10^{-8}$	$9x10^{-9}$
	E	7.07	7.45
	q_e	$6.88x10^{-3}$	$1.7x10^{-3}$
	R^2	0.5298	0.8811
313K	β	$9x10^{-9}$	$5x10^{-9}$
	E	7.45	7.45
	q_e	$5.85x10^{-3}$	$1.97x10^{-3}$
	R^2	0.5428	0.6767
323K	β	$9x10^{-9}$	$6x10^{-8}$
	E	7.45	2,89
	q_e	$5.23x10^{-3}$	$1.37x10^{-3}$
	R^2	0.5603	0.2021

4.4.3.6. Thermodynamics.

Thermodynamic parameters such as enthalpy changes (ΔH°(kJ/mol^{-1})), entropy changes (ΔS°(kJ/mol^{-1})) and Gibbs free energy changes (ΔG°(kJ/mol^{-1})) were used to determine the spontaneity, type of reaction and the degree of randomness during the uptakes of both $As^{3+}$and F^- by the 5 % Ce-pPD composite. The obtained parameters from the plot of 1/T vs ln K_C were calculated using the following equations:

$$lnK = \frac{\Delta H^*}{R} + \frac{\Delta S^\circ}{R} \quad (16)$$

$$\Delta G = \Delta H^\circ - T\Delta S^\circ \quad (17)$$

Where K is the equilibrium constant, R is the gas constant (8.134 kJ mol^{-1} K^{-1}) and T is the solution temperature (K).

Table 15. Table showing thermodynamics parameters of F^- and As^{3+} removal using 5% Ce-pPD composite.

	F^-	As^{3+}
ΔH° (kJ/mol^{-1})	-0.5604	1.4212
ΔS° (kJ/mol^{-1})	-0.0003	0.0062
	ΔG° (kJ/mol^{-1})	
298K	-0.642	-3.2827
303K	-0.6435	-3.3139
313K	-0.6462	-3.3763
323K	-0.6490	-3.4388

	F	As3+
ΔH◦	37,08	-92,4
ΔS◦	-0,018	0,41
ΔG◦		
298K	42,444	-214,58
303K	42,534	-216,63
313K	42,714	-220,73
323K	42,894	-224,83

Table 15. Portrays the obtained thermodynamic parameters for As^{3+} and F^- sorption processes. From the attained data, ΔG° values were determined to be negative for both F^- and As^{3+} for adsorption processes. Thus, an indication that sorption reaction was

feasible and spontaneous for both As^{3+} and F^- adsorption by 5 % Ce-pPD composite. The ΔG° values were observed to decrease with an increasing temperature; hence it indicates favourability of the sorbate-sorbent mechanisms for both pollutant removal. Additionally, the As^{3+} removal process was exothermic with an increase in the degree of randomness as validated by negative values of ΔH° and ΔS° values respectively. Whereas the F^- removal process was endothermic with a decrease in the degree of randomness as confirmed by positive values of ΔH° and ΔS° individually.

4.4.3.7. Effect of pH and pH_{pzc}.

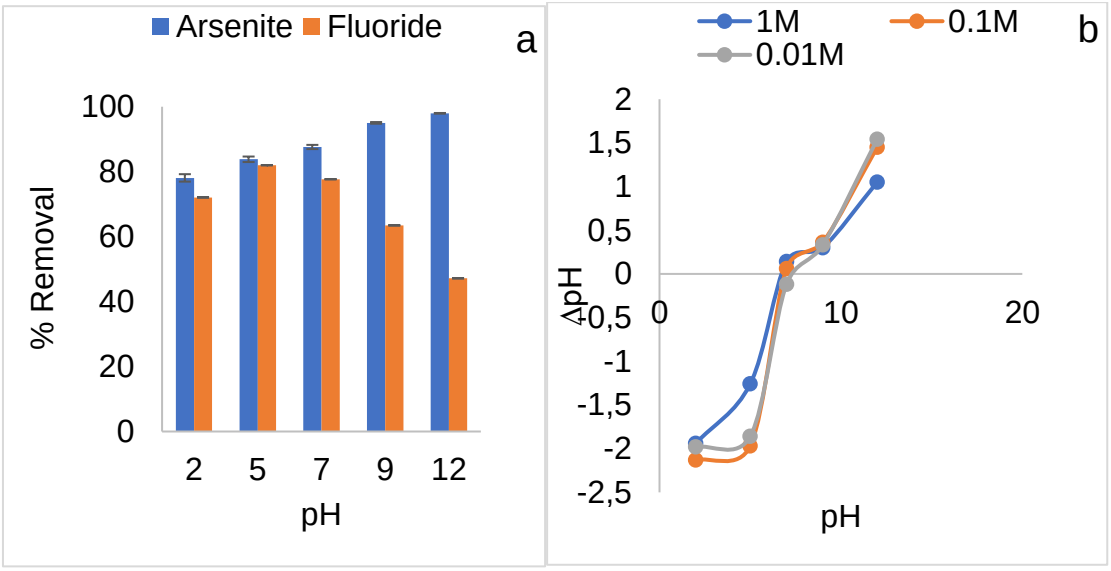

Figure 27: (a) and (b) are the plots of effect of pH on F^- and As^{3+} removal using 5 % Ce-pPD and the pH_{pzc} of 5 % Ce-pPD composite. (Initial As^{3+} and F^- concentration: 5 mg/L and 10 mg/L, adsorbent dose: 0.35 g and 0.2 g, solution volume: 50 mL, contact time: 30 mins, shaking speed: 250 rpm and temperature: 297 K).

Fig 27. Presents the results of effect of solution pH towards As^{3+} and F^- uptake by 5% Ce-pPD. The surface charges of the 5 % Ce-pPD composite were evaluated by determining the pH at the point of zero charges to determine the chemical process that is responsible for As^{3+} and F^- removal. pH_{pzc} is described as the pH at which net surface charges are equal to zero. Furthermore, the surface is negatively charged when the pH value is above pH_{pzc} and negatively charged at the pH value below the pH_{pzc}. From the data obtained (Fig 27(a)), the pH_{pzc} was found to be 7.

The relationship between As^{3+} and F^- removal and pH solution was evaluated and the results are shown in Fig 27 (b). pH is one of the most important factors controlling

arsenic speciation in aqueous solutions. Under oxidising conditions, $H_2AsO_3^-$ is dominant at low pH (less than about pH 6.9), whilst at higher pH, $HAsO_3^{2-}$ becomes dominant (Li et al, 2011). Elizalde-Gonzalez et al (2001) stated that at pH less than at pH 9.2, the uncharged arsenite species $H_3AsO_3^0$ will predominate. Thus, an increase in As^{3+} removal with increasing pH might be attributed to electrostatic attraction and ion exchange as validated by pH_{pzc}. The hypothesized removal mechanism is expressed by Eq. 18 and 19 where m represents the 5 % Ce-pPD.

$$\equiv MOH + H_3As_3 \leftrightarrow \equiv MH_2As_3 + H_2O \quad (18)$$

$$\equiv MOH + H_2As_3^- \leftrightarrow \equiv MHAs_3^- + H_2O \quad (19)$$

High F^- removal by 5 % Ce-pPD was observed near-neutral pH, the percentage removal was observed to increase from pH 2 to 5 and decrease from pH 7-12. The low F^- uptake in the low pH region (<2) could be due to reduced availability of free F^- ions due to the formation of H---F bonds(Guo et al, 2014), while the reduction at high pH (>7.0) may be due to competitive interaction with hydroxyl ions. An increase in F^- sorption is attributed to ionic exchange through solute-sorbent reaction and electrostatic attraction between adsorbent and adsorbate charges as expressed by Eq. 20 and 21 where M represents 5 % Ce-pPD.

$$\equiv MOH + H^+ + F^- \leftrightarrow \equiv MF + H_2O \quad (20)$$

$$\equiv M(OH)2 + 2F^- \leftrightarrow \equiv MF_2 + 2OH^- \quad (21)$$

4.4.3.8. Effect of co-existing ions.

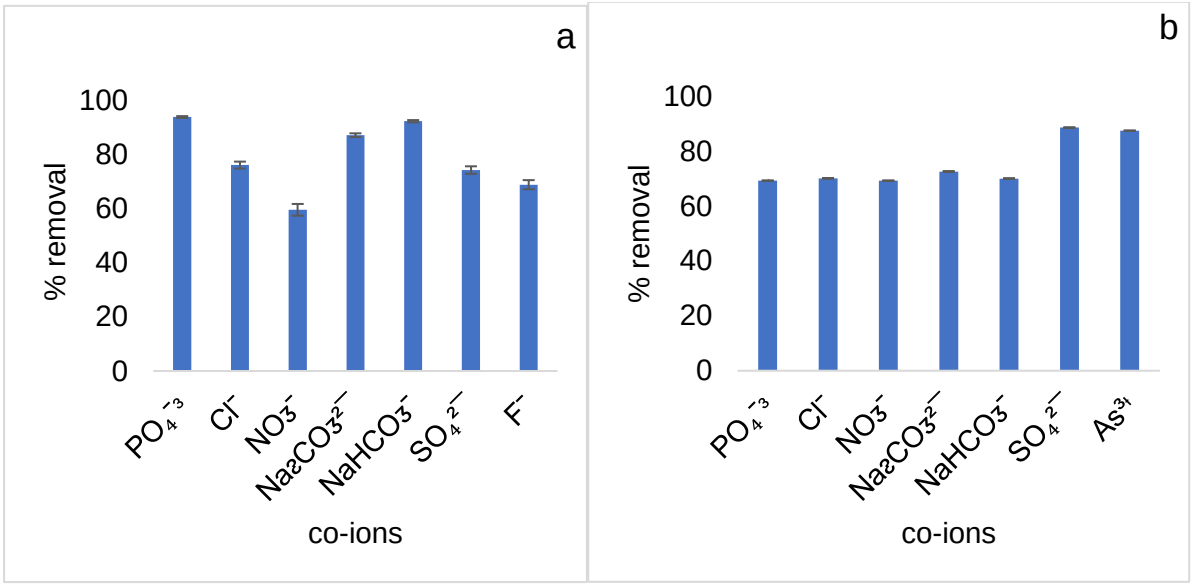

Figure 28: (a) and (b) effect of co-existing ions As^{3+} and F^- uptake using 5 % Ce-pPD composites. (Initial F^- and As^{3+} concentration: 5 mg/L and 10 mg/L, adsorbent dose: 0.35 g and 0.2 g, solution volume: 50 mL, contact time: 24 hrs, shaking speed: 250 rpm and temperature:297 K).

Fig 28. Represents results of effect of co-ions towards fluoride and arsenic removal from aqueous solution using 5 % Ce-Ppd. Simultaneous occurrence of sulphates, nitrates, carbonates, phosphates, fluoride, chloride, and arsenite in groundwater is common. However, their existence in an aqueous solution can pose a great or minimum effect in fluoride and arsenite removal using various adsorbents. Thus, this is due to their ionic states which encourage the adsorption by either physical or chemical sorption by the proposed adsorbents (Vasudevan et al, 2010). Figs 28 (a-b) depict the effect of co-existing ions on As^{3+} and F^- removal using Ce-pPD. The obtained data showed the occurrence of nitrates, fluoride, sulphates, and chloride have a great effect on As^{3+} sorption, whereas carbonates and phosphates pose minimal effect. Fluoride results portrayed that nitrates, phosphates, carbonates, and chloride exhibit great effect, whereas sulphates and arsenite pose minimal effect. The effect of co-ions can be shown in the following order: for As^{3+}: NO_3 >F^-> SO_4^{2-} > Cl^- > CO_3^{2-} > PO_4 and **F^-**: HCO_2 > NO_3> CO_3^- > PO_4^- > Cl^-> As^{3+}> SO^{-4} respectively.

4.4.3.9. Regeneration.

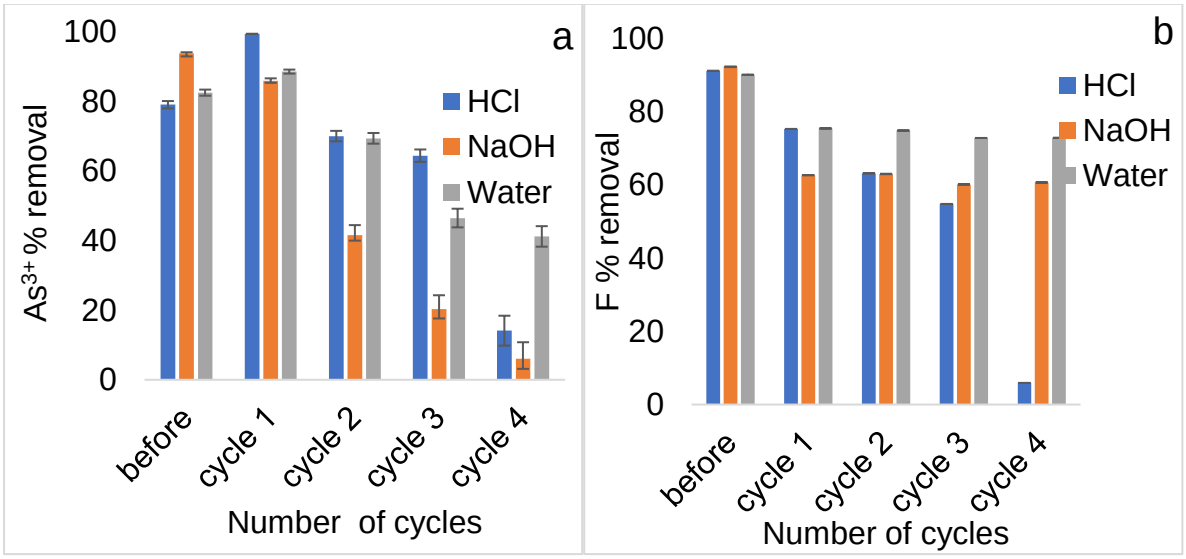

Figure 29. Regeneration results of 5 % Ce-pPD composite after As^{3+} and F^- removal in aqueous solution. Initial F^- and As^{3+} concentration: 5 mg/L and 10 mg/L, adsorbent

dose:0.25 g and 0.2 g, solution volume: 50 mL, contact time: 30 mins, shaking speed: 250 rpm and temperature:297 K).

Fig 29 (a-b). indicates the adsorption-desorption cycles of As^{3+} and F^- into 5 % Ce-pPD using HCl, H_2O, and NaOH as regenerants. It was observed that As^{3+} adsorbed on the surface of 5 % Ce-pPD initial increased at cycle 1, then decreased from cycle 2 to 4 when using HCl, H_2O, and NaOH respectively. The decrease might be attributed to the decrease of the adsorbent dose which was due to a loss during the desorption and washing process whereas the initial increase might be attributed to the presence of non-binding active sites after the desorption process through sorbent ionization (Desmarets et al, 2001). However, among the three proposed desorbing agents, water has been reported as a better desorbing agent as observed in Fig 29 (a and b). The attained reusability F^- data portrayed that as the regeneration cycles increase the usability is reduced and remained constant when using water and NaOH from cycle 2 to 4 and continually decreased when using HCl in Fig 29 (b). Nevertheless, it was observed that HCl and H_2O are good fluoride and arsenite desorbing agents on Ce-pPD.

4.4.3.10. Mechanism of As^{3+} and F^- sorption.

The mechanisms that are responsible for arsenite and fluoride adsorption by 5 % Ce-pPD were determined by various kinetics models, isotherm models, thermodynamics, and effect of pH as well as point of zero charges as discussed above. The kinetics models (pseudo-first-order, pseudo-second-order, and intraparticle diffusion) revealed that they are different mechanisms that are responsible for the sorption of the proposed adsorbates ions. The adsorption process includes physio-sorption, chemo-sorption, internal attachment of solid/liquid interface. This was validated by the isotherm models, thermodynamics, and BET analysis results. The other mechanisms that a suggested to be responsible include electrostatic attraction and ionic exchange as revealed by the point of zero charges and obtained effect of pH results.

4.4.4. Anti-microbial potency.

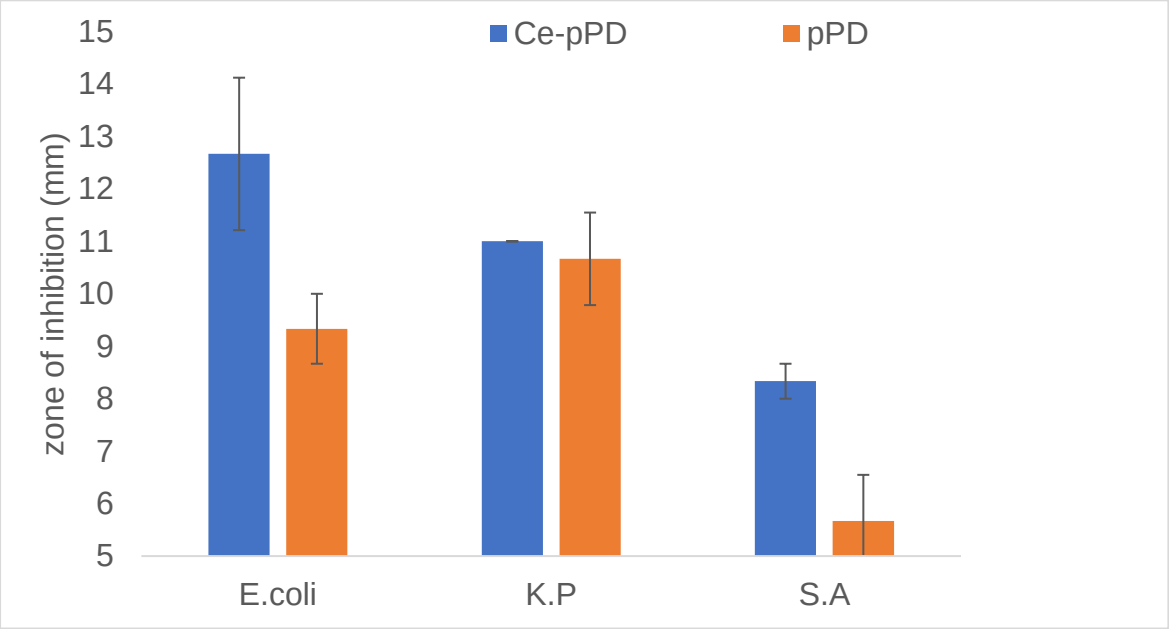

Figure 30.Antimicrobial activity of 5 % Ce-pPD and bare pPD composite.

The antimicrobial activity of 5 % Ce-pPD and raw pPD results are shown in Fig 30. In this study, the antimicrobial activity of Ce-pPD composite was studied using the zone of inhibition method. It was observed that 5 % Ce-pPD composite portrayed high zone of inhibition towards *Escherichia coli and Klebsiella pneumonia* (gram-negative) compared to *Staphylococcus aureus* (gram-positive). *Escherichia coli* and *Klebsiella pneumonia* with about 11-12 mm zone of inhibition and Staphylococcus aureus 5-8 mm. The antimicrobial potency of the proposed composite might be attributed to different factors such as chemical oxidants and the complex functional groups contained within the composite (Tao et al. 2014). Recently, Kumar et al. 2017, reported that polyaniline nanocomposites synthesized in acidic solution with strong oxidants such as ammonium persulfate; present complex structure and various functional groups as well as the oxidant chemical which bioaccumulate, denature and oxidizes the lipid membrane of the bacterial causing leakages in the membrane then burst, thus, leading to cell death

Also, Ce-composites have been reported to be potent against these concerned pathogens (Kaygusuz et al, 2017). Ce nanoparticles are reported to be more susceptible to Gram-negative compared to Gram-positive microbes (Morais et al, 2015). The greatest antimicrobial activities of Ce nanoparticles on gram-negative bacteria might be due to direct contact and the unbalanced outer membrane of the

bacteria (Masadeh et al. 2015, Farias et al. 2018). The efficiency of these nanoparticles depends on the morphology and size. However, various studies have suggested that antimicrobial activities occur due to three processes between bacterial and nanocomposites: (i) adsorption, (ii) oxi-reduction, and (iii) toxicity (Thill et al. 2006, Pelletier et al. 2010).

4.5. Comparison of Fe-pPD and Ce-pPD composites towards As^{3+} and F^- uptake from aqueous solutions

Table 16 shows the progression of sorption capacities towards fluoride and arsenite in an aqueous solution between the synthesized 2.5 % Fe-pPD and 5 % Ce-pPD in this study. Evidently, from the experimental point of view, the CepPD was observed to have high As^{3+} and F^- ions removal capacity with high affinity in fluoride removal (13.27 mg/g) compared to Fe-pPD (6.76 mg/g) as shown in Table 16. Thus, this might be due to the solubility and ionization (an increase in negative or positive charges on the surface of the adsorbent to be more reactive) of the dopant metal oxides as already explained.

Table 16. comparison of 2.5 % Fe-pPD and 5 % Ce-pPD composites towards As and F removal

	2.5%Fe-pPD		**5 % Ce-pPD**	
	As^{3+}	F^-	As^{3+}	F^-
Time (mins)	40	40	20	20
Dose (g)	0.25	2	0.3	0.2
Initial concentration (mg/L)	5-100	5-100	5-100	5-100
pH	9	7	9	5
Adsorption capacity (mg/g)	1.87	6.79	2.11	13.27

4.5. Conclusion.

It was observed that Ce metal oxide was successfully incorporated on the pPD polymer matrix using chemical oxidative polymerization. This was validated by characterization results which include FTIR, XRD, and SEM-EDS spectra. The synthesized composite has the potential to effectively remove arsenite, fluoride as well as disinfect pathogen in an aqueous solution. About, 86.6 (2.11 mg/g) and 94.6 % (13.27 mg/g) of the initial concentration of As^{3+} and F^- respectively were removed.

Batch experiment data revealed that that contact time, adsorbent dose, initial adsorbate concentration, temperature, and pH have a significant effect on arsenite and fluoride sorption using 5 % Ce-pPD composite. The adsorption kinetic process followed the pseudo-second-order. Thus, chemisorption is the limiting step. The intraparticle diffusion model predicted that As^{3+} and F sorption is not only due to intra-particle diffusion. Adsorption isotherm data was better described by the Freundlich isotherm model, indicating the heterogeneity of the adsorbate-adsorbent interface. Thermodynamically, the F^- removal process was endothermic with a decrease in the degree of randomness as confirmed by positive values of ΔH° and ΔS° individually. While, the As^{3+} removal process was exothermic with an increase in the degree of randomness as validated by negative values of ΔH° and ΔS° values respectively. The synthesized 5 % Ce-pPD composite successfully shown effective antimicrobial action towards waterborne pathogens and it can be reused just by mere washing with clean water for about four cycles.

References.

Abiye, T., Bybee, G. and Leshomo, J., 2018. Fluoride concentrations in the arid Namaqualand and the Waterberg groundwater, South Africa: Understanding the controls of mobilization through hydrogeochemical and environmental isotopic approaches. *Groundwater for Sustainable Development*, *6*, pp.112-120.

Ashbolt NJ. Microbial contamination of drinking water and disease outcomes in developing regions. Toxicology. 2004; 198:229–38.

Ashbolt, N.J., 2004. Microbial contamination of drinking water and disease outcomes in developing regions. *Toxicology*, *198*(1-3), pp.229-238.

Berg, M., Tran, H.C., Nguyen, T.C., Pham, H.V., Schertenleib, R., Giger, W., 2001. Arsenic contamination of groundwater and drinking water in Vietnam: a human health threat.

Bhowmik, A.K., Alamdar, A., Katsoyiannis, I., Shen, H., Ali, N., Ali, S.M., Bokhari, H., Schäfer, R.B. and Eqani, S.A.M.A.S., 2015. Mapping human health risks from exposure to trace metal contamination of drinking water sources in Pakistan. *Science of the Total Environment*, *538*, pp.306-316.

Chouhan, S. and Flora, S.J.S., 2010. Arsenic and fluoride: two major ground water pollutants.

D.S. Morais, S. Fernandes, P.S. Gomes, M.H. Fernandes, P. Sampaio, M.P. Ferraz, et al., Novel cerium doped glass-reinforced hydroxyapatite with antibacterial and osteoconductive properties for bone tissue regeneration, Biomed. Mater. 10 (2015) 55008

Dahaghin, Z., Kilmartin, P.A. and Mousavi, H.Z., 2020. Novel ion imprinted polymer electrochemical sensor for the selective detection of lead (II). *Food chemistry*, *303*, p.125374.

Desmarets, C., Schneider, R. and Fort, Y., 2001. Nickel-catalysed synthesis of 3-chloroanilines and chloro aminopyridines via cross-coupling reactions of aryl and heteroaryl dichlorides with amines. Tetrahedron Letters, 42(2), pp.247-250.

Desta, M.B., 2013. Batch sorption experiments: Langmuir and Freundlich isotherm studies for the adsorption of textile metal ions onto teff straw (Eragrostis tef) agricultural waste. *Journal of thermodynamics*, *2013*.

Edmunds, W.M. and Smedley, P.L., 2005. Fluoride in natural waters Essentials of Medical Geology ed BJ Alloway and O Selinus.

Elizalde-Gonzalez M.P., Mattusch J., Wennrich R., Morgenstern P. (2001) Sorption on natural solids for arsenic removal. Chemical Engineering Journal. 81, 187-195.

Farias, I.A.P., Santos, C.C.L.D. and Sampaio, F.C., 2018. Antimicrobial activity of cerium oxide nanoparticles on opportunistic microorganisms: a systematic review. *BioMed research international*, *2018*.

Fito, J., Tefera, N. and Van Hulle, S.W., 2017. Adsorption of distillery spent wash on activated bagasse fly ash: kinetics and thermodynamics. *Journal of environmental chemical engineering*, *5*(6), pp.5381-5388.

Guo, H., Yang, L. and Zhou, X., 2014. Simultaneous removal of fluoride and arsenic from aqueous solution using activated red mud. *Separation Science and Technology*, *49*(15), pp.2412-2425.

Gwaku, F., 2015. *Rice hull ash silica gel immobilized pediastrum boryanum for deflouridation of water* (Doctoral dissertation, BUSE).

He, J., Xu, Y., Xiong, Z., Lai, B., Sun, Y., Yang, Y. and Yang, L., 2020. The enhanced removal of phosphate by structural defects and competitive fluoride adsorption on cerium-based adsorbent. Chemosphere, 256, p.127056.

Jiang, J.Q., 2001. Removing arsenic from groundwater for the developing world—a review. Water Sci. Technol. 44 (6), 89– 98Environ. Sci. Technol. 35 (13), 2621–2626.

Jones, N.F., Pejchar, L. and Kiesecker, J.M., 2015. The energy footprint: how oil, natural gas, and wind energy affect land for biodiversity and the flow of ecosystem services. *BioScience*, *65*(3), pp.290-301.

Joseph T, Dubey B, McBean EA. Human health risk assessment from arsenic exposures in Bangladesh. Sci Total Environ. 2015;527–528:552–60.

Kang, D., Yu, X., Tong, S., Ge, M., Zuo, J., Cao, C. and Song, W., 2013. Performance and mechanism of Mg/Fe layered double hydroxides for fluoride and arsenate removal from aqueous solution. *Chemical Engineering Journal*, *228*, pp.731-740.

Katsoyiannis IA, Mitrakas M, Zouboulis AI. Arsenic occurrence in Europe: emphasis in Greece and description of the applied full-scale treatment plants. Desalin Water Treat. 2014;54(1–8):2100–7.

Kaygusuz, H., Torlak, E., Akın-Evingür, G., Özen, İ., Von Klitzing, R. and Erim, F.B., 2017. Antimicrobial cerium ion-chitosan crosslinked alginate biopolymer films: A novel and potential wound dressing. *International journal of biological macromolecules*, *105*, pp.1161-1165.

Kumar, J.V. and Moss, M.E., 2008. Fluorides in dental public health programs. *Dental Clinics of North America*, *52*(2), pp.387-401.

Kumar, R., Oves, M., Almeelbi, T., Al-Makishah, N.H. and Barakat, M.A., 2017. Hybrid chitosan/polyaniline-polypyrrole biomaterial for enhanced adsorption and antimicrobial activity. *Journal of colloid and interface science*, *490*, pp.488-496.

Kumar, S. and Ojha, A.K., 2015. Oxygen vacancy induced photoluminescence properties and enhanced photocatalytic activity of ferromagnetic ZrO2 nanostructures on methylene blue dye under ultra-violet radiation. *Journal of Alloys and Compounds*, *644*, pp.654-662.

Lacasa, E., Cañizares, P., Rodrigo, M.A. and Fernández, F.J., 2012. Electro-oxidation of As (III) with dimensionally-stable and conductive-diamond anodes. *Journal of hazardous materials*, *203*, pp.22-2 Mark, A., 2008. Science and technology for water purification in the coming decades. *Nature*, *452*, p.20.8.

Li, Z., Jeanc, J.S., Jiang, W.T., Chang, P., Chen, C.J., Liao, L., 2011. Removal of arsenic from water using Fe-exchanged natural zeolite. J. Hazard Mater. 187, 318–323.

Ma, Y., Niu, R., Sun, Z., Wang, J., Luo, G., Zhang, J. and Wang, J., 2012. Inflammatory responses induced by fluoride and arsenic at toxic concentration in rabbit aorta. *Archives of toxicology*, *86*(6), pp.849-856.

Magdziarz, P. Bober, M. Trchová, Z. Morávková, M. Bláha, J. Prokeš, J. Stejskal, Conducting composites prepared by the reduction of silver ions with poly(pphenylenediamine),Polym. Int. 64 (2015) 496–504**.**

Magdziarz, P., Bober, P., Trchová, M., Morávková, Z., Bláha, M., Prokeš, J. and Stejskal, J., 2015. Conducting composites prepared by the reduction of silver ions with poly (p-phenylenediamine). *Polymer International*, *64*(4), pp.496-504.

Maity JP, Kar S, Liu J-H, Jean J-S, Chen C-Y, Bundschuh J, et al. The potential for reductive mobilization of arsenic [As(V) to As(III)] by OSBH2 (*Pseudomonas stutzeri*) and OSBH5 (*Bacillus cereus*) in an oil-contaminated site. J Environ Sci Health. 2011; 46:1239–46.

Masadeh, M.M., Karasneh, G.A., Al-Akhras, M.A., Albiss, B.A., Aljarah, K.M., Al-Azzam, S.I. and Alzoubi, K.H., 2015. Cerium oxide and iron oxide nanoparticles abolish the antibacterial activity of ciprofloxacin against gram positive and gramnegative biofilm bacteria. *Cytotechnology*, *67*(3), pp.427-435.

Mo, J., Yang, Q., Zhang, N., Zhang, W., Zheng, Y. and Zhang, Z., 2018. A review on agro-industrial waste (AIW) derived adsorbents for water and wastewater treatment. *Journal of environmental management*, *227*, pp.395-405.

Mudzielwana, R., Gitari, W.M. and Ndungu, P., 2019. Evaluation of the adsorptive properties of locally available alumino-silicate clay in As (III) and As (V) remediation from groundwater. *Physics and Chemistry of the Earth, Parts A/B/C*, *112*, pp.28-35.

Narayana, K.V., Raju, B.D., Masthan, S.K., Rao, V.V., Rao, P.K. and Martin, A., 2004. Cerium fluoride supported V2O5 catalysts: physico-chemical characterization and 3-picoline ammoxidation activity. *Journal of Molecular Catalysis A: Chemical*, *223*(1-2), pp.321-328.

Nephalama, A. and Muzerengi, C., 2016. Assessment of the influence of coal mining on groundwater quality: Case of Masisi Village in the Limpopo Province of South Africa. *Proceedings of the Freiberg/Germany, Mining Meets Water—Conflicts and Solutions (IMWA 2016), Leipzig, Germany*, pp.11-15.

Nriagu, J.O., Bhattacharya, P., Mukherjee, A.B., Bundschuh, J., Zevenhoven, R. and Loeppert, R.H., 2007. Arsenic in soil and groundwater: an overview. *Trace Metals and other Contaminants in the Environment*, *9*, pp.3-60.

Pelletier, D.A., Suresh, A.K., Holton, G.A., McKeown, C.K., Wang, W., Gu, B., Mortensen, N.P., Allison, D.P., Joy, D.C., Allison, M.R. and Brown, S.D., 2010. Effects of engineered cerium oxide nanoparticles on bacterial growth and viability. *Applied and environmental microbiology*, *76*(24), pp.7981-7989.

Potgieter, N., Mudau, L.S. and Maluleke, F.R.S., 2006. Microbiological quality of groundwater sources used by rural communities in Limpopo Province, South Africa. *Water science and technology*, *54*(11-12), pp.371-377.

Rajagopalan, R., Chen, B., Zhang, Z., Wu, X.L., Du, Y., Huang, Y., Li, B., Zong, Y., Wang, J., Nam, G.H. and Sindoro, M., 2017. Improved reversibility of Fe3+/Fe4+ redox couple in sodium super ion conductor type Na3Fe2 (PO4) 3 for sodium-ion batteries. *Advanced Materials*, *29*(12), p.1605694.

Rango, T., Vengosh, A., Jeuland, M., Tekle-Haimanot, R., Weinthal, E., Kravchenko, J., Paul, C. and McCornick, P., 2014. Fluoride exposure from groundwater as reflected by urinary fluoride and children's dental fluorosis in the Main Ethiopian Rift Valley. *Science of the Total Environment*, *496*, pp.188-197.

Reed, B.E. and Matsumoto, M.R., 1993. Modeling cadmium adsorption by activated carbon using the Langmuir and Freundlich isotherm expressions. *Separation science and technology*, *28*(13-14), pp.2179-2195.

Ruthven, D.M., 1984. Flow through packed beds. Principles of Adsorption & Adsorption Processes. Wiley-Interscience Publication, New York, pp.206-219.

Sadeghi, M.M., Rad, A.S., Ardjmand, M. and Mirabi, A., 2018. Preparation of magnetic nanocomposite based on polyaniline/Fe3O4 towards removal of lead (II) ions from real samples. *Synthetic Metals*, *245*, pp.1-9.

Shannon, M.A., Bohn, P.W., Elimelech, M., Georgiadis, J.G., Marinas, B.J. and Mayes, A.M., 2010. Science and technology for water purification in the coming decades. In *Nanoscience and technology: a collection of reviews from nature Journals* (pp. 337-346).

Smedley, P. and Kinniburgh, D., 2001. Chaper 1: source and behaviour of arsenic in natural waters. *Wallingford: British Geological Survey*.

Sun, C., Qiu, J., Zhang, Z., Marhaba, T.F. and Zhang, Y., 2016. Removal of arsenite from Water by Ce-Al-Fe trimetal oxide adsorbent: kinetics, isotherms, and thermodynamics. Journal of Chemistry, 2016.

Sun, Z., Huang, H., Li, L., Liu, L. and Chen, Y., 2017. Polythioamides of high refractive index by direct polymerization of aliphatic primary diamines in the presence of elemental sulfur. *Macromolecules*, *50*(21), pp.8505-8511.

Taghipour, N., Amini, H., Mosaferi, M., Yunesian, M., Pourakbar, M. and Taghipour, H., 2016. National and sub-national drinking water fluoride concentrations and prevalence of fluorosis and of decayed, missed, and filled teeth in Iran from 1990 to 2015: a systematic review. *Environmental Science and Pollution Research*, *23*(6), pp.5077-5098.

Tao, Y., Ju, E., Ren, J. and Qu, X., 2014. Polypyrrole nanoparticles as promising enzyme mimics for sensitive hydrogen peroxide detection. *Chemical Communications*, *50*(23), pp.3030-3032.

Thill, A., Zeyons, O., Spalla, O., Chauvat, F., Rose, J., Auffan, M. and Flank, A.M., 2006. Cytotoxicity of CeO2 nanoparticles for Escherichia coli. Physico-chemical insight of the cytotoxicity mechanism. *Environmental science & technology*, *40*(19), pp.6151-6156.

Thines, R.K., Mubarak, N.M., Nizamuddin, S., Sahu, J.N., Abdullah, E.C. and Ganesan, P., 2017. Application potential of carbon nanomaterials in water and wastewater treatment: a review. *Journal of the Taiwan Institute of Chemical Engineers*, *72*, pp.116-133.

Tor, A., 2006. Removal of fluoride from an aqueous solution by using montmorillonite. *Desalination*, *201*(1-3), pp.267-276.

Vasudevan, S., Sheela, S.M., Lakshmi, J. and Sozhan, G., 2010. Optimization of the process parameters for the removal of boron from drinking water by electrocoagulation—a clean technology. *Journal of Chemical Technology & Biotechnology*, *85*(7), pp.926-933.

Vrutangkumar, V.S., Sachin, G. and Harish, J.P.M., 2015. Linking increased response time to rest tremors in Parkinson's disease: a feedback control perspective.

W.H.O, Guidelines for Drinking-water Quality, vol. 1, Recommendations, 3rd ed., Geneva, 2004

W.H.O., Guidelines for Drinking Water Quality, Geneva, 2004.

Walters, S.P., Gannon, V.P. and Field, K.G., 2007. Detection of Bacteroidales fecal indicators and the zoonotic pathogens E. coli O157: H7, Salmonella, and Campylobacter in river water. *Environmental science & technology*, *41*(6), pp.1856-1862.

Wang, X., Zhang, P., Wang, W., Lei, X., Zou, B. and Yang, H., 2015. Synthesis, structure and magnetic properties of graphite carbon encapsulated Fe 3 C nanoparticles for applications as adsorbents. *RSC Advances*, *5*(35), pp.27857-27861.

World Economic Forum, *Global Risks 2015, 10th Edition* (World Economic Forum, Geneva, Switzerland, 2015

World Health Organization, 2017. Potable reuse: Guidance for producing safe drinking-water.

World Health Organization, 2017. Potable reuse: Guidance for producing safe drinking-water.

World Health Organization. 1981. Environmental Health Criteria 8. Arsenic. World Health Organization, Geneva: 174 pages

World Health Organization. Geneva: World Health Organization; 2000. Global water supply and sanitation assessment 2000 report; p. 87.

Wu, W., He, Q., Chen, H., Tang, J. and Nie, L., 2007. Sonochemical synthesis, structure and magnetic properties of air-stable Fe3O4/Au nanoparticles. *Nanotechnology*, *18*(14), p.145609.

Wu, X., Zhang, Y., Dou, X. and Yang, M., 2007. Fluoride removal performance of a novel Fe–Al–Ce trimetal oxide adsorbent. *Chemosphere*, *69*(11), pp.1758-1764.

Yan, X.P., Kerrich, R. and Hendry, M.J., 2000. Distribution of arsenic (III), arsenic (V) and total inorganic arsenic in porewaters from a thick till and clay-rich aquitard sequence, Saskatchewan, Canada. *Geochimica et Cosmochimica Acta*, *64*(15), pp.2637-2648.

Chapter 5.

Synthesis, characterization of a sustainable Fe/Ce Doped Poly –(para-phenylenediamine) adsorbent and its potential removal for chemical pollutants and pathogens in aqueous solutions.

Munzhelele E.P, Gitari M.W, Ayinde W.B

Environmental Remediation and Nanoscience (EnviReN), Department of Ecology and Resource Management, School of Environmental Sciences. University of Venda, Private Bag X5050, Thohoyandou, 0950, Limpopo Province, South Africa.

5.1. Abstract.

Chronic contamination of water bodies by both fluoride, arsenic as well as pathogens is frequently observed around the world, where millions of people are severely affected. Thus, the study focused on synthesizing a novel conjugated polymeric adsorbent by incorporating Fe/Ce oxides onto a phenylenediamine (pPD) polymer matrix (Fe/Ce-pPD) through chemical co-polymerization method and examine its potential ability for simultaneous removal of fluoride, arsenite and pathogen disinfection in aqueous solution. The successful synthesis of 1:1 Fe/Ce-pPD was validated by FTIR, XRD, SEM-EDS, TEM, and BET morphological and structural analysis. Batch sorption experiments were carried out to determine significant factors affecting As^{3+} and F^{-} uptake by the synthesised composite. The optimized adsorption data were used to derive the adsorption kinetics and isotherm model, which aided to determine the mechanism and process that are occurring between the absorbates and adsorbent. The modified 1:1 Fe/Ce-pPD has shown high fluoride removal (96.7% (14.75 mg/g)) and arsenite (88.66% (4.71 mg/g)) respectively) in aqueous solution. F^{-} and As^{3+} sorption followed pseudo-second order; thus, chemisorption is the limiting step for pollutants uptake. The isotherm data model was better described by Freundlich isotherm model. Thermodynamics study portrayed that adsorption process was endothermic in nature. Also, the regeneration studies revealed that the adsorbent can be regenerated up to 4 cycles using 0,1 M (HCl and NaOH) and water. The 1:1 Fe/Ce-pPD composite was observed to have the potency to inactivate pathogens in

aqueous solution. Overall, the 1:1 Fe/Ce-pPD composite efficiency and performance towards these toxic pollutants is deemed to be a worthy emergent technology in water treatment.

Key words: Contaminated water, modified 1:1 Fe/Ce poly para-phenylenediamine, batch adsorption experiment, antimicrobial activity.

5.2. Introduction.

Water contamination has been recognised as one of the biggest global issues, particularly in developing countries (WHO, 2010), and is regarded as the main contributing factor of water scarcity. Consequently, water scarcity is slowly becoming a potential risk to public health and the environment (Shahin, 2015). Thus, an increase in pollution load in water sources is adversely affecting economic and ecological functions globally. Contamination of groundwater by different chemical pollutants (fluoride, arsenic, lead, mercury, chromium, etc) and pathogens (bacteria, fungi, and viruses) has affected millions of people worldwide, due to prolonged intake of contaminated water. Excessive intake of water with high fluoride, and arsenic concentrations as well as microbes can result into severe and fatal human health.

Arsenic is one of the most toxic elements at low concentrations that are abundant on the earth`s crust. Its sources in water bodies are mainly due to ore smelting in mining industries. Various studies have reported that arsenic enters drinking water mostly as inorganic trivalent (arsenite) or pentavalent (arsenate) oxidation states (Bibi, 2015; Itabashi et al, 2019). Comparably, arsenate (As^{5+}) is said to be more stable than arsenite (As^{3+}), for which it predominates under normal conditions. Hence, As^{3+} is more toxic than As^{5+}. The contamination of drinking water by arsenite is of global concern due to its toxicity and carcinogenic. Prolong exposure to arsenite is a serious concern because of its noticeable adverse effect on public health that varies from severe lethality to enduring and carcinogenic effects (Abernathy, 2003). As a result, World Health Organization (W.H.O) has set a permissible limit of 0.1 mg/L. Long-term exposure to water contaminated with an arsenic concentration greater than 0.1 mg/L may result in a disease called arsenicosis. General symptoms include skin and lung cancer, gastrointestinal infections, etc. Thus, arsenite removal from aquatic systems is more important to protect the environment and public health.

Generally, intake of fluoride is essential to prevent bone and teeth molting. Nevertheless, its excessive intake may result in dental and skeletal fluorosis. Thus, the W.H.O has set a threshold of 1.5 mg/L. However, high fluoride concentrations have been reported worldwide. Various sources of fluoride have been determined, this includes natural and anthropogenic activities (economic developments such as industrial developments). Recently, it has been predicted that about 6 million of people are being affected worldwide due to chronic exposure to high fluoride concentrations (Saikia, 2017).

The short and long-term exposure effects of these contaminants have been reported. Chronic occurrence of arsenite As^{3+} (most with reported major incidences) and fluoride (F^-) in different water resources is often observed around the world and has gained global attention of researchers over the years. The effect of As^{3+} and F^- in the environment concerning their toxicity, mobility, bioaccumulation, and biomagnification is accountable for a continuous interest to investigate their fate (de Oliveira et al, 2014). Additionally, the co-occurrence of As^{3+} and F^- has been reported around the world, however, this can lead to uncertain and complicated human health problems If they are simultaneously consumed over a long time. Thus, millions of people are at a potential risk of being affected, which calls for researchers' attention to come up with a remedy.

Also, contamination of water sources by water-borne pathogens have been known worldwide. The introduction of microbes in water sources is mainly due to poor sewage disposal as well as human and animal droppings. Thus, drinking water contaminated with human and animal faeces is the main cause of various water-borne diseases (diarrhoea, typhoid fever, hepatitis, and others) caused by various pathogenic bacteria, viruses, and parasites (Rai et al, 2012). World Health Organization has reported that about 3.5 million people die due to unsafe drinking water and lack of sanitation (Wright et al, 2006, Ashbolt, 2015).

There are various technologies designed for fluoride and arsenite removal, and microbial disinfection in water. Nevertheless, few of them are designed for the simultaneous removal of fluoride, arsenic, and pathogen in aqueous solutions. These removal technologies include ion-exchange, precipitation, membrane, and adsorption (Shannon, 2010; Mohapatra, 2009; Jadhav, 2015). Among these technologies,

adsorption has been far embraced because it eased to operate, flexible, reusable, promote environmental stability (Shakoor, 2019)

Different advanced composite materials have been recently developed for the removal of the mention pollutants, that include activated carbon, alumina, brick powder, oxide ores, Fe-Ce oxides, Fe-Al doped polymers, and other materials (Zhang, 2016; Siddiqui and Chaudhry, 2018; Guerra et al, 2018). Consequently, the cost of the adsorbents limits its feasibility for industrial utilization and environmental stability due to leaching, sludge production and cost of production. Thus, chemical modification of conjugated polymeric composites through doping process helps to improve the surface area and particle size of the sorbent which improves the adsorption capacity. Thus, the study has focused on synthesizing Fe/Ce doped poly(para-phenylenediamine) adsorbent through chemical oxidative polymerization and evaluate its potential ability for fluoride, arsenite and pathogen removal in aqueous solution.

5.3. Methods and materials.

5.3.1. Materials.

Chemicals (pPD) poly (p-phenylenediamine), Ammonium persulfate ($(NH4)_2S_2O_8$), Iron (III) chloride heptahydrate ($FeCl_3.5H_2O$), cerium (IIII) chloride heptahydrate ($CeCl_4.5H_2O$ sodium fluoride (NaF) and sodium hydroxide (NaOH), NaCl, KCl, HCl, and $NaAsO_3$ were used. All reagents were of analytical grade and were used without any purifications. The working solutions of different fluoride and arsenite concentrations were prepared in deionized water from Millipore water (18.2 MΩ/cm).

5.3.2. Adsorbent preparation.

5.3.2.1. Preparation of Poly-phenylenediamine (pPD).

Poly-pPD was synthesized by a modified method (Pham et al., 2011; Mdlalose et al., 2017). Briefly, pPD (1.62 g, 0.015 mol) was dissolved in HCl (50 mL, 0.1 M) and stirred for 3 h on an ice bath. Next, the pPD polymerization was initiated by a dropwise addition of the freshly prepared oxidant solution of ammonium persulfate (3.42 g) in HCl (25 mL, 0.1 M) for 30 min. The resulting mixture was stirred for 24hrs at room temperature to ensure complete polymerization of the pPD monomer. The pH of each poly (p-phenylenediamine) was adjusted to 9 with the addition of 2 M NaOH and shaken at 250 rpm for 30 min. The reaction was quenched by adding acetone and the

resulting crude product was washed with de-ionized water and dried under vacuum at 60 °C for 24 hrs.

5.3.2.2. Fe/Ce Doped Poly-Phenylenediamine (Fe/Ce-pPD)

0.015 M Poly-pPD (1.62 g) was dissolved in HCl (50 mL, 0.1 M) and stirred for 3hrs on an ice bath. $FeCl_3.6H_2O$ and $CeCl_3.7H_2O$ solutions with various percentage by volume ratio (1:1%, 1:2 %, and 2:1%,) was prepared in 20 mL deionized water before doping process. Each of these salt solutions was added and mixed separately with the pPD solutions. Next, the Fe/Ce-pPD polymerization was introduced by a dropwise addition of the freshly prepared oxidant solution of ammonium persulfate (3.42 g) in HCl (25 mL, 0.1 M) for 30 min. The solution was under stirring for 24 hours to allow the formation of Fe/Ce-pPD at room temperatures at 400 rpm. The pH of each Fe/Ce doped poly-phenylenediamine was adjusted to 9 with the addition of 2 M NaOH to precipitate the metal hydroxides and shaken at 250 rpm for 30 min. The product was collected by filtration and washed with deionized water, then dried in a vacuum oven at 60 ^oC for 24hrs.

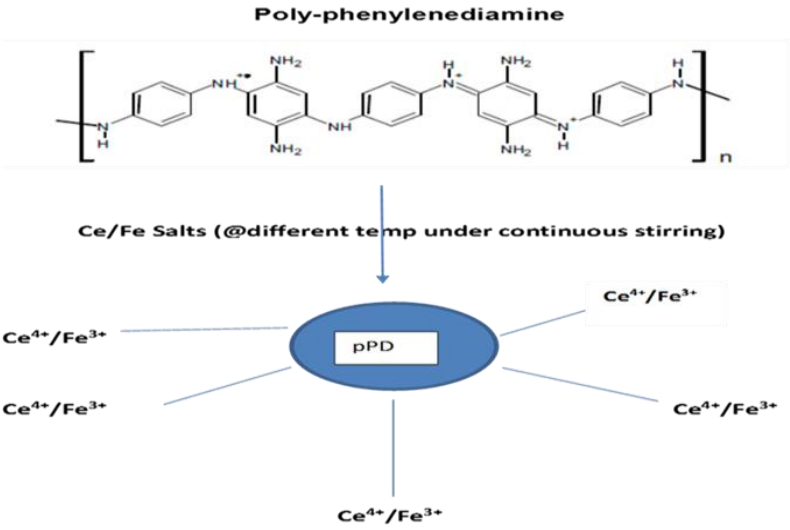

Figure 31: Diagram shows the step on how Fe/Ce-pPD was synthesized of 1:1 Fe/Ce doped poly-phenylenediamine

5.3.2.3 Adsorption capacity of pPD, and Fe/Ce-pPD composites

A mass of 0.4 g of pPD and each Fe/Ce-pPD species was contacted with 50 mL of 10 mg/L and arsenite and fluoride solution at 250 rpm for 30 min. The equilibrium pH of

each mixture was measured to evaluate the pH status of untreated and treated water. After the equilibrium pH measurement, the mixture was centrifuged, and the supernatants were analyzed for residual pollutant ions.

T*he percentage of fluoride removal was calculated by using the following formula*

$$\% \text{ of fluoride removal} = \frac{Co - Ce}{Co} * 100 \quad (1)$$

C_o is the initial fluoride concentration in mg/L, C_e equilibrium concentration in mg/L

The adsorption equilibrium capacity of the adsorbent was calculated using

$$q_e = \frac{Co - Ce}{m} * v \quad (2)$$

qe is the equilibrium capacity of the adsorbent, m is the mass of the adsorbent in g and v is the volume of fluoride in mg/L.

5.3.3. Characterizations of the synthesized materials.

The morphological and physicochemical properties of the synthesized adsorbent were evaluated using the Scanning Electron Microscope (SEM) (SEM with an FEI Nova NanoSEM 230 with the field emission gun equipped with an Oxford Xmax SDD detector operating at an accelerating voltage of 20Kv for the EDS detector (Oxford X-Max with INCA software). The infra-red spectrum of the synthesized adsorbents was obtained using the ALPHA Fourier Transform Infra-red spectrum equipped with ATR-Diamond (Bruker, Germany). Bruker-D8 Powder Diffractometer with a theta-theta goniometer X-ray diffraction (XRD) technique was employed to examine the crystalline phase identification. F^- and pH measurements of the fluoride in the supernatants were determined using a fluoride ion-selective electrode (9609 BNWP Orion, USA) coupled to an ISE/pH/EC electrode (Thermo SCIENTIFIC-ORION VERSA STAR Advanced Electrochemistry meter fluoride ion-selective electrode) calibrated with four fluoride standards containing TISAB III at the volume ratio of 1:10. Furthermore, the As^{3+} measurements in the supernatants were determined using Metrohm 850 professional ion chromatography (Switzerland). CHNS analysis was done using the Thermo Flash 2000 series CHNS/O organic Elemental analyzer. The inductively coupled plasma mass spectrometry (IC-PMS) was used to determine the trace chemical ions before and after Arsenite and fluoride uptake by the synthesizes adsorbent at different time interval (15mins-24hours). A mass of 0.2 mg of Fe/Ce-pPD composited was

agitated with 50 mL of 5 mg/L/10 mg of As^{3+} and F^- at room temperature. After agitation, the samples where filtered and 15 ml of each filtrates was added into a BOECO Germany bottles and preserved by adding 1 drop of nitric acid and sent for analysis.

5.3.4. Batch experiments.

Stock solutions containing 1000 mg/L As^{3+} and F^- were prepared by dissolving 0.1733 g of $NaAsO_3$ and 2.210 g NaF, respectively in a 1000 mL volumetric flask using Milli-Q water (18.2 MΩ/cm). The working solutions were prepared through appropriate dilutions from the stock solution. To evaluate the effect of contact time and adsorption kinetics, the contact time was varied from 0.5 to 120 min. Adsorbent dosage of 0.4 g/50 mL and adsorbate concentration of 5 and 10 mg/L of F^- and As^{3+} concentration respectively was maintained. After agitation, mixtures were centrifuged at 250 rpm for 20 min. The optimum adsorbent dosage was evaluated by varying adsorbent dosage from 0.1-0.4 g/50 mL. To evaluate the adsorbate concentration and adsorption isotherms, initial concentration of F^- and As^{3+} were varied from 5 to 100 mg/L at a temperature of 298, 323, and 343 K.

The obtained data were used to determine the adsorption thermodynamics. The effects of parameters like pH ranges (2-12) and co-existing ions (F, Cl, NO_3^-, CO_3^{2-}, SO_4^{2-}) were also evaluated. The initial pH was adjusted using 0.01 M NaOH and 0.01 M HCl. All experiments were conducted in triplicate and the mean values were reported. The pHpzc was evaluated using the solid addition method as described by Gitari et al. (2017).

5.3.5. Adsorption kinetics.

The As^{3+} and F^- adsorption kinetics were studied at an initial concentration of 5 and 100mg/L respectively. The experimental data were analyzed using the non-linear equation of pseudo-first-order and pseudo-second-order models as well as the intraparticle diffusion (Eqn. 3, 4 and 5) (Lagergren, 1898; Ho and McKay, 1998; Sharma et al, 1960):

$$qt = qe(1 - e^{-kit}) \quad (3)$$

$$qt = \frac{qe^2\, k_2 t}{1 + k_2\, q_e t} \quad (4)$$

$$qt = k_t t^{0.5} + ci \quad (5)$$

q_e and q_t (both in mg/g) are the amounts adsorbed per unit mass at a time, t (in min). K_1 (min^{-1}) and K_2 ($g.mg^{-1}min$) are first and second-order rate constant, respectively. Ki (mg /g min^{-1}) is the intra particle diffusion rate constant and is determined from the slope of $t^{0.5}$ vs qt and C_i is the constant attained from the intercept and reflects the thickness of the boundary layer. The greater the intercept, the bigger the boundary layer effect (Mudzielwana et al, 2018).

Similarly, the Elovich linear equation (Eq. 6) has general application to chemisorption kinetics. The equation was used to validates that chemisorption is the limiting step for fluoride and arsenite uptake. It is often valid for systems in which the adsorbing surface is heterogeneous. qt is the quantity of adsorbate adsorbed at time t (mg/g), α is a constant related to chemisorption rate and β is a constant which depicts the extent of surface coverage. The two constants (α and β) can be calculated from the intercept and slope of the plot from the equation.

$$qt = \beta \ln(\partial\beta) + \beta lnt \quad (6)$$

5.3.6. Adsorption isotherms.

The adsorption isotherms were modeled using the theoretical Langmuir and empirical Freundlich isotherms (Weber and Chakravorti, 1974; Bolster and Homberger, 2007). The Langmuir isotherm model assumes monolayer interaction between the adsorbate molecules attached to the surface of the adsorbent during equilibrium. Freundlich isotherm model assumes that there is a mutual interaction between the adsorbate molecules adsorbing onto the multilayer or heterogeneous surface of the adsorbent. The non-linearized forms of Langmuir and Freundlich equations are expressed as (Eq. 7 and 8):

$$qe = \frac{q_m K_L C_e}{1 + K_L C_e} \quad (7)$$

$$qe = K_f Ce^{\frac{1}{n}} \quad (8)$$

Where: C_e is the equilibrium concentration (mg/L); Q_e is the adsorption capacity (mg/g); Q_m is the theoretical maximum adsorption capacity (mg/g) and k_L is the Langmuir constant related to the enthalpy of adsorption (L/mg). K_f is the Freundlich constant related to adsorption capacity and 1/n is the adsorption intensity. When 0 <

1/n < 1, the adsorption is favourable; when 1/n=1, the adsorption is irreversible; and when 1/n > 1, the adsorption is unfavourable.

Equally, Langmuir isotherm can be expressed in terms of a dimensionless constant separation factor or equilibrium parameter R_L (Eq. 9).

$$R_L = \frac{1}{1 + k_L C_i} \quad (9)$$

Also, R_L is a dimension separation factor, C_i the initial arsenite and fluoride concentration (mg/L) (when R_L=1 irreversible, 0<R_L<1 favourable, R_L=1 linear and R_L>1 unfavourable).

Dubinin Radushkevich (D-R) model is a more general model in which assumption is not based on homogenous surface or constant adsorption potential, it gives insight into the sorbent porosity as well as the adsorption energy. The value of adsorption energy further provides information as to whether the adsorption process is physical or chemical in nature (Dubinin, 1947). D-R model is expressed mathematically as:

$$lnqe = lnqo - \beta e^2 \quad (10)$$

where qe is the amount of RhB ions adsorbed per unit weight of adsorbent (mg/g), qo is the maximum adsorption capacity, β is the activity coefficient useful in obtaining the mean sorption energy E (kJ/mol) and Ɛ is the Polanyi potential. Ɛ and E are expressed by Eqs (11) and (12).

$$\varepsilon = RT\left(1 + \frac{1}{Ce}\right) \quad (11)$$

$$\mathrm{E} = \sqrt{\frac{1}{2\beta}} \quad (12)$$

where R is the gas constant (J/mol K) and T is the temperature (K). qo and β (mol2 /kJ2) can be calculated respectively from the intercept and the slope of the plot of lnqe vs $Ɛ^2$.

5.3.7. Goodness of fit evaluation

The fitness between the experimental data and the simulated data was determined by the coefficient of determination (R^2) (Eq. (13)), root mean square error (RMSE) (Eq. (14)), and the sum of the squared errors (SSE) (Eq. (15)).

$$R^2 = 1 - \frac{\Sigma(q_{e,exp} - q_{e,calc})2}{\Sigma(q_{e,exp} - q_{e,mean})2} \quad (13)$$

$$RMSE = \sqrt{\frac{1}{n-1}\sum_{i=1}^{n}\left(q_{e,exp} - q_{e,calc}\right)^2}_{\text{i}} \quad (14)($$

$$SSE = \sum_{i=1}^{n}\left(q_{e,calc} - q_{e,exp}\right)^2 \quad (15)$$

where qe, calc is the theoretical concentration of adsorbate on the adsorbent, which has been calculated from one of the isotherm models. qe, i, means is the experimentally measured adsorbed solid-phase concentration.

5.3.4. Antimicrobial activity test.

Bacterial resistance and efficacy of the synthesized pPD and 1:1 Fe/Ce-pPD were determined from the observed zone of inhibition (mm) using the standard Agar-Well disc diffusion method (Kirby Bauer disk diffusion test). Medium 1 agar plates were divided into half; 1-5 mL pipette tips were used to punch a small circle to add the adsorbent. 50µl of the bacterial strains (*E. coli*; ATCC 25922 IN; *S. Aureus*; ATCC 259231 Tm and *K. Pneumoniae*; ATCC 700603) was inoculated into the sterile medium 1 agar. Then, 50 µl of 1mL/0,01 mg of the sorbent was deposited into the punched circles. Then incubated for 24 hrs at 37 ˚C. The minimal zone of inhibition was observed and measured.

5.4. Results and discussion.

5.4.1. Adsorbent optimization.

The percentage removal of arsenite and fluoride ions by the pPD and Fe/Ce-pPD adsorbents is shown in Fig 32. An amount of 0.4 g each of the synthesized materials was agitated with 50 mL of an initial concentration of pollutant ions (10 mg/L and 5mg/L for fluoride and arsenite respectively) at room temperature for 30 minutes at 250 rpm. The respective adsorption experiments were carried out by varying the ratio percentage volume of Fe^{3+} and Ce^{4+} metal ions (v/v%) of pPD and Fe/Ce-pPD (2.5%, 5%, and 10%) for the respective uptake.

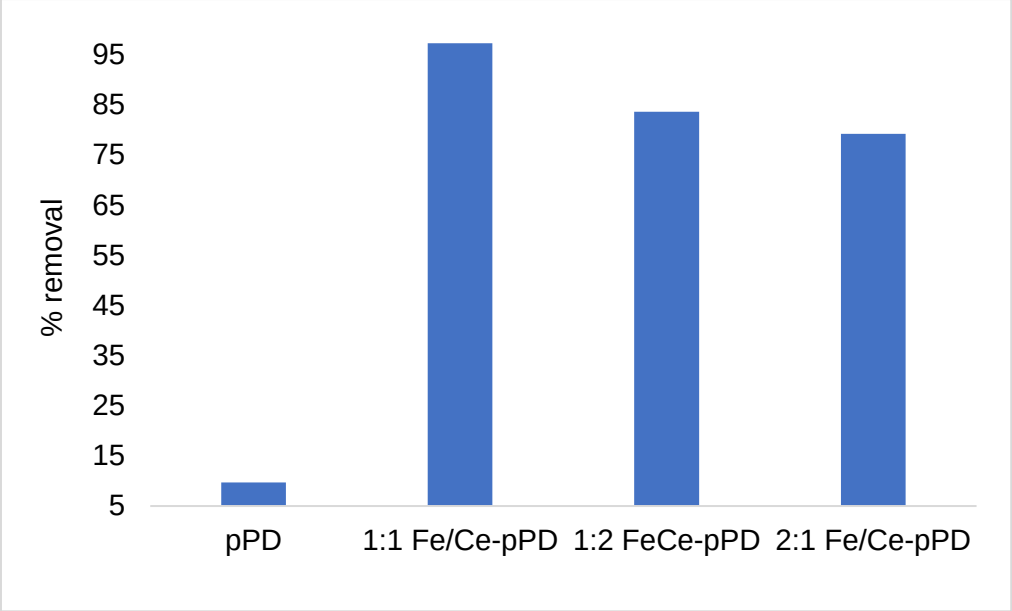

Figure 32. As^{3+} and F^- percentage removal as a function of Fe/Ce concentration into pPD polymer: (initial concentrations of As^{3+} and F^- 5 mg/L and 10, adsorbent dose: 0.4 g, contact time: 30 mins and temperature: 297 K).

Relatively, the obtained results portrayed that the doped pPD have high removal efficiency towards As^{3+} and F^- uptake compared to the raw pPD. Hence, doping pPD with Fe/Ce metal oxides have improved the sorption capacity of the polymer. The enhancement in sorption efficiency might be due to the enhanced surface of area as seen in BET analysis, chemical properties introduce during modification (solubility and ionization), and an increase of functional groups (N-Fe/Ce). Thus, doping pPD with Fe/Ce metal oxides has increased the occurrence of active adsorption sites, validating an increase in pollutants uptake. Consequently, the incorporation of these two-metal oxide-modified polymeric adsorbent was a reliable factor that have enhanced As^{3+} and F^- uptake. Hence, the 1:1 Fe/Ce-pPD composite was selected as the most efficient adsorbent and further used for arsenic, fluoride, and pathogen removal in an aqueous solution.

5.4.2. Characterization.

5.4.2.1. FTIR results.

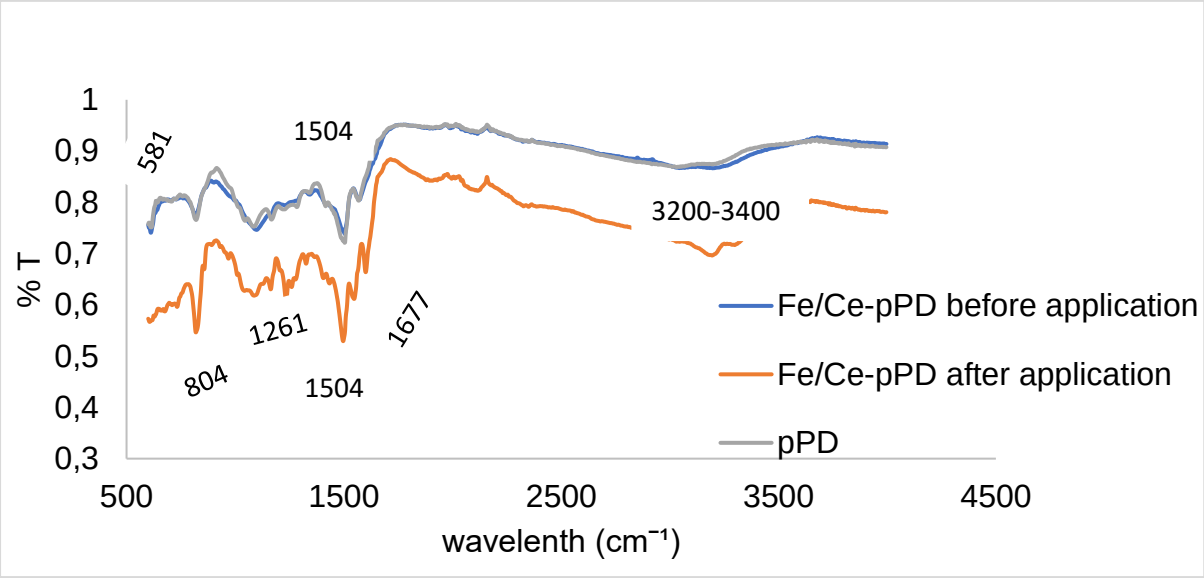

Figure 33. FTIR of pPD and 1:1 Fe/Ce-pPD before and after As^{3+} and F^- removal from aqueous solution.

Fig 33. is showing the FTIR spectrum of the synthesized pPD, and 1:1 Fe/Ce-pPD composites which determine the functional groups of the composites and any change that may have happened to the spectrum due to incorporation of Fe and Ce across the pPD network. The results portrayed that 1:1 Fe/Ce-pPD composite is dominated by pPD signal bands as validated by the same peak signals. Thus, Fe/Ce incorporation did not alter pPD functional groups. Comparatively, the transmittance of 1:1 Fe/Ce-pPD after As^{3+} and F^- uptake spectrum has reduced compared to 1:Fe/Ce-pPD before As^{3+} and F^- uptake. Thus, the reduction in transmittance may be due to the absorption energy by a new coordinated complex of Fe/Ce-pPD-F or FeCe-pPD-As. As shown in Fig. 33, the broad band between 3200-3400 cm^{-1} may be attributed to the presence of stretching vibration of N–H group and a hydroxyl group (OH) stretching from physically adsorbed H_2O (moisture) bound to the respective composite surface (Haldorai et al, 2009; Pham et al, 2011). The appearances of strong peaks at 1677 cm^{-1} and 1504 cm^{-1} relate to the C=C and C=N stretching vibrations of the phenazine ring within the composite matrix (Archana and Jaya, 2014). The C–N–C stretching vibrations of benzenoid and quinoid imine units are recognized by the peaks at 1407 cm^{-1} and 1261

cm^{-1}. Also, C–H bending vibrations of benzene bases in the phenazine skeletons are the bands at 805 cm^{-1} and 581 cm^{-1} respectively (Chen et al, 2009).

5.4.2.2. XRD results.

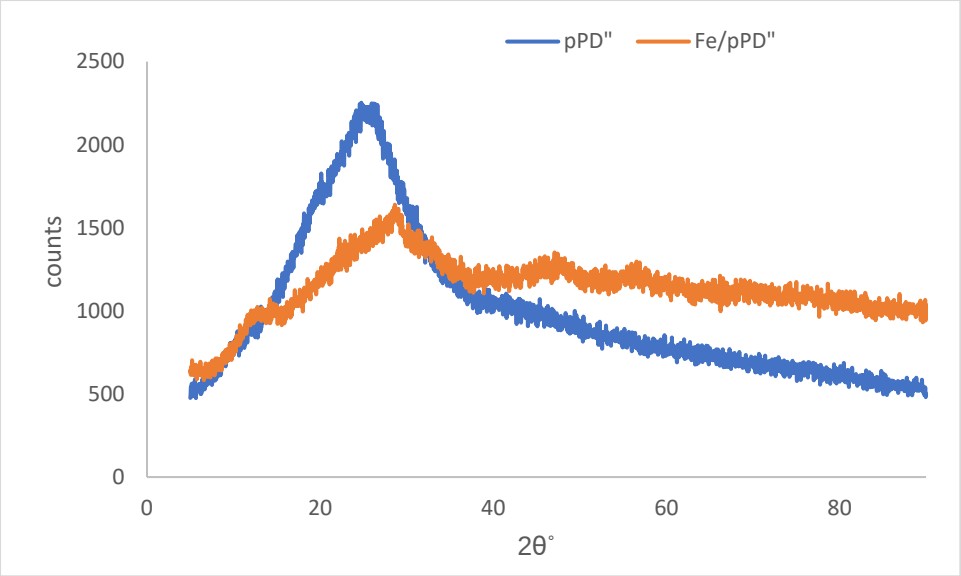

Figure 34. XRD results of pPD and 1:1 Fe/Ce-pPD

Fig 34 is showing the diffraction pattern of the degree of crystalline structural phase of poly-pPD network which was introduced by doping Fe/Ce metal ions. The X-ray diffraction spectrum of the pPD and 1:1 Fe/Ce-pPD shows a series of sharp peaks at between 5-90 2θ region (Fig 34). The pPD spectra shows a large, broad intensity peak centered at 25˚, which may be attributed to the amorphous portion of pPD synthesized by oxidative polymerization similar to XRD spectrum of pPD reported by Li et al, (2013). The diffractogram of Fe/Ce-pPD composite within the same plot (Fig. 34) has shown a significant structural phase change that may be due to the incorporation of Fe and Ce metal oxides on the pPD network, accredited to the formation of a crystal phase. The introduction of these two metal oxides has caused a formation of new peaks at 2θ (5-20º, 20-40º, 55-55º, 55-65º and 65-90º) with a shift of peaks at 25º to 30º. Thus, the chemically synthesized polymer composite has sharpness of the crystalline peaks and well long range of ordering (Wang et al, 2015), when compared to the raw pPD polymer.

5.4.2.3. SEM-EDS results.

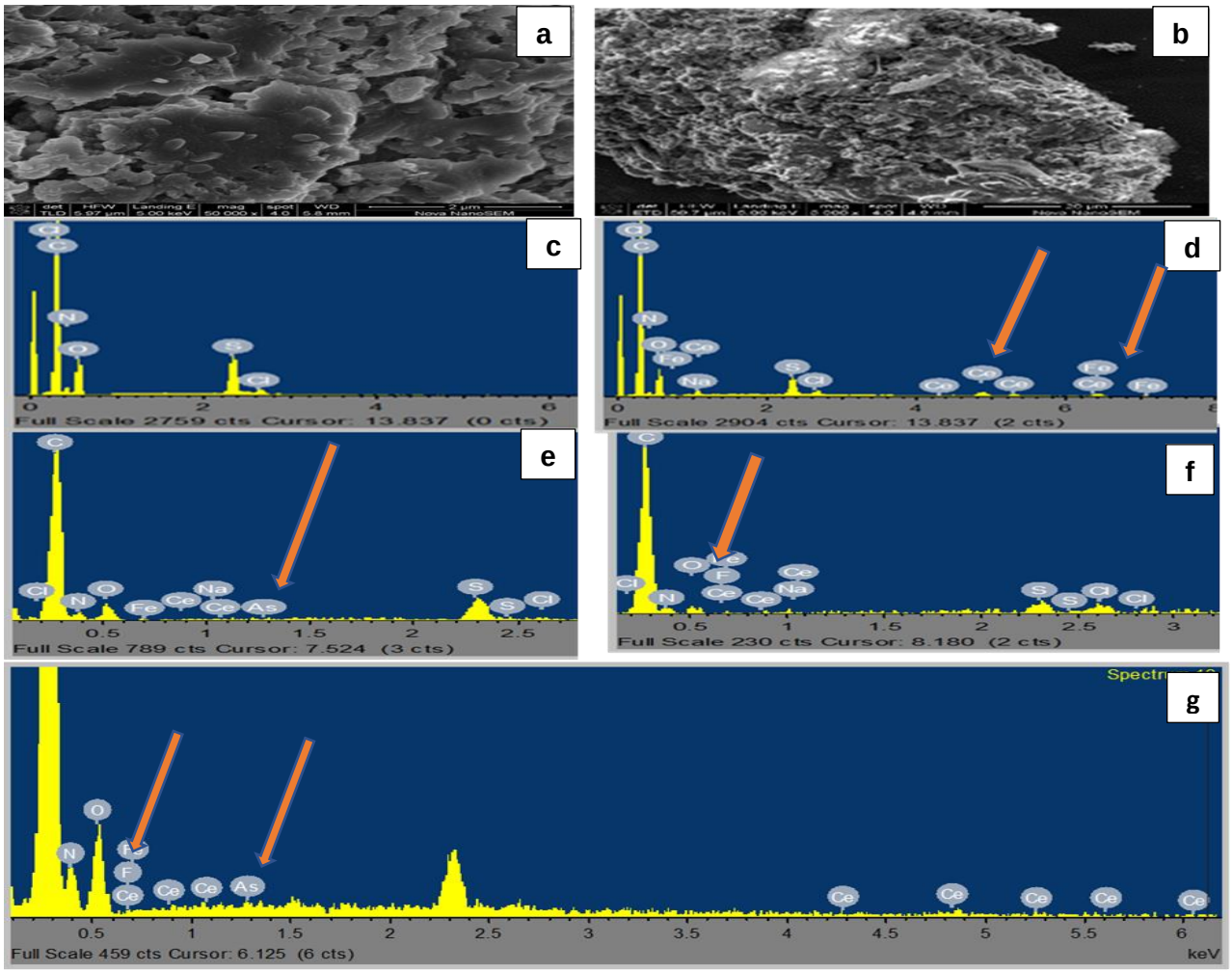

Figure 35. SEM-EDS analysis: (a) and (b) The SEM images of raw pPD and 1:1 Fe/Ce-pPD; (c) and (d) EDS spectra of raw pPD and 1:1 Fe/Ce-pPD; (e and f) EDS spectra of 1:1 Fe/Ce-pPD after application for As^{3+} and F^- sorption; (g) EDS spectrum for 1:1 Fe/Ce-pPD after simultaneous uptake of F^- and As^{3+}.

The scanning electron microscopy was done to evaluate the surface morphology of synthesized pPD and 1:1 Fe/Ce-pPD as shown in Figure 35 (a and b). The morphology of pPD was found to be a spherical like arrangement, while the morphology of 1:1 Fe/Ce-pPD shows a well-ordered combination, due to incorporation of 1:1 Fe/Ce metal oxides in the polymer matrix as portrayed in Fig 35 (a) and (b) respectively. The successful incorporation of the metal oxides within the polymer media was confirmed by the EDS spectrum (Fig 35 (d)), where Fe /Ce elements in the spectrum after the doping process occurred compared to the raw pPD (Fig 35(c)). Generally, the surface morphology of the doped poly-pPD composites depends on the type of polymers of

the phenylenediamines as well as the oxidant used during the synthesis (Stejskal, 2015). Additionally, the potential ability of the synthesized adsorbent for F^- and As^{3+} sorption is validated by the EDS plotting analysis as shown in Fig 35 (e-f). The EDS spectrum after the adsorption process displayed the potential ability for simultaneous removal of F^- and As^{3+} as validated by the EDS spectrum in Fig 35 (g).

5.4.1.4. TEM results.

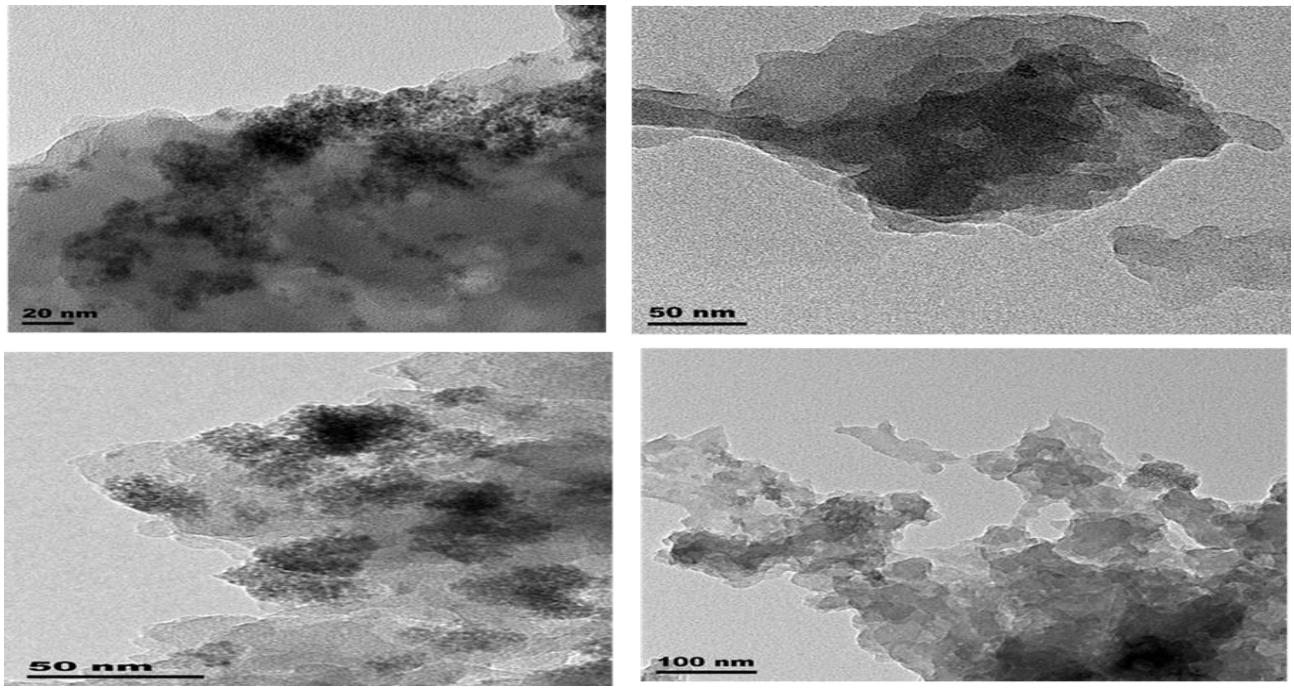

Figure 36. TEM analysis of 1:1 Fe/Ce-pPD.

The structural characteristics and shapes of the composites are shown by the TEM results in Fig 36. The average particle sizes range between 20-100 nm clustering of irregular fragmental particle morphology was observed in the synthesized 1:1 Fe/Ce-pPD composites.

5.4.2.5. BET analysis.

Table 17. depict the attained BET results, the obtained data revealed the incorporation of 1:1 Fe/Ce on pPD matrix have improved the surface area of pPD. An increase in the surface area was observed, which increase from 8.6832 m^2/g to 29.73 m^2/g. Thus, validates that the 1:1 Fe/Ce modified pPD have a high surface area aiding to the possibility of adding to enhanced adsorption capacity. Additionally, a decrease in average particle size has aided to an increase in pore volume, which ultimately

increases the pore diameter and subsequently allows multiple adsorptions of concerned pollutants.

Table 17. BET analysis.

	pPD	1:1 Fe/Ce-pPD
Surface area (m^2/g)	8.6832	29.7333
Pore volume (cm^2/g)	0.016918	0.074760
Pore diameter (µm)	7.79	10.06
Average particle size (µm)	60.9	20.8

Chemically stability of the adsorbent.

5.4.2.6. IC-PMS results of 1:1 Fe/Ce-pPD

Table 18. shows the leaching results of metal ions in the filtrates. The aim of of this experiment was to examine the leaching capabilities of pPD, Fe, and Ce. The obtained results portrayed that the concentrations of the metal ions fluctuations as time increases. Additionally, results have demonstrated that As^{3+} was removed as validated by its decrease as time increases. The fluctuations in metal ions concentrations might be due to decomposition of pPD polymer at low temperature, leading to degradation of the doping ions (Yao et al, 2014). Thus, the doping ions (Ce, Fe, Na, e.t.c) are released into the filtrates with increase in the pPD concentration. This may be due to the dissolution of the metal ions which is controlled by the mass transport of the ions during the sorption process.

Table 18. IC-PMS results of 1:1 Fe/Ce-pPD after fluoride and arsenite uptake from aqueous solution.

	Ce	As	Ca	Fe	Na	P
Contact time						
0.5 M pPD						
15 min	13.15	4.78	9.04	5.19	81	*BDL
30 min	26.5	4.21	16.23	1.99	180	
1 hr	29.32	4.85	10.87	0.49	194	*BDL
6 hrs	31.91	2.49	17	9.04	122	*BDL
12 hrs	44.08	3.55	10.93	0.98	249	*BDL
24 hrs	19.23	1.12	11.88	0.6	155	*BDL
1 M pPD						
15 min	17.43	4.89	31.52	5.21	178	*BDL
30 min	26.55	5.01	11.49	9.61	174	*BDL
1 hr	45.88	4.53	21.48	0.89	254	*BDL
6 hrs	30.43	3	20.94	1.98	225	*BDL
12 hrs	27.52	1.49	15.35	5.83	108	*BDL
24 hrs	22.71	5.04	9.7	7.14	107	*BDL

5.4.2.7. CHNS analysis results of Fe/Ce-pPD composite before and after As^{3+} and F^- uptake.

The Fe/Ce-pPD composite before and after the application was weighed and analyzed for CHNS contents, as shown in Table 19. An increase in N, C, and H was observed after application with no trace sulphur in the adsorbent. The increase in N, C, and H might be due to formation of a larger polymer chain of 1:1 Fe/Ce-pPD after reaction with the As^{3+} and F^- solutions leading to enriched polymer chain (Peng et al 2011). However, the radical cations of aniline formed in this polymerization process either initiate the growth of a new chain or can participate in the propagation of the already

growing chain through condensation polymerization (Amer and Brandt, 2018). Additionally, the occurrence of S in 1:1 Fe/Ce-pPD composite before the application is due to use of $(NH_4)_2SO_4$ as an oxidant. While the absence of S after the application is because $(NH_4)_2SO_4$ easily dissolves in water (U.S Coast Guard. 1999).

Table 19. CHNS results of 1:1 Fe/Ce-pPD before and after fluoride and arsenite adsorption from aqueous solution.

	Weight (mg)	N [%]	C [%]	H [%]	S [%]
Before application	6,73	12,81	47	4,15	3,15
after application	5,472	23,46	63,75	5,43	BDL

5.4.3. Batch experiments.

5.4.3.1. Effect of contact time

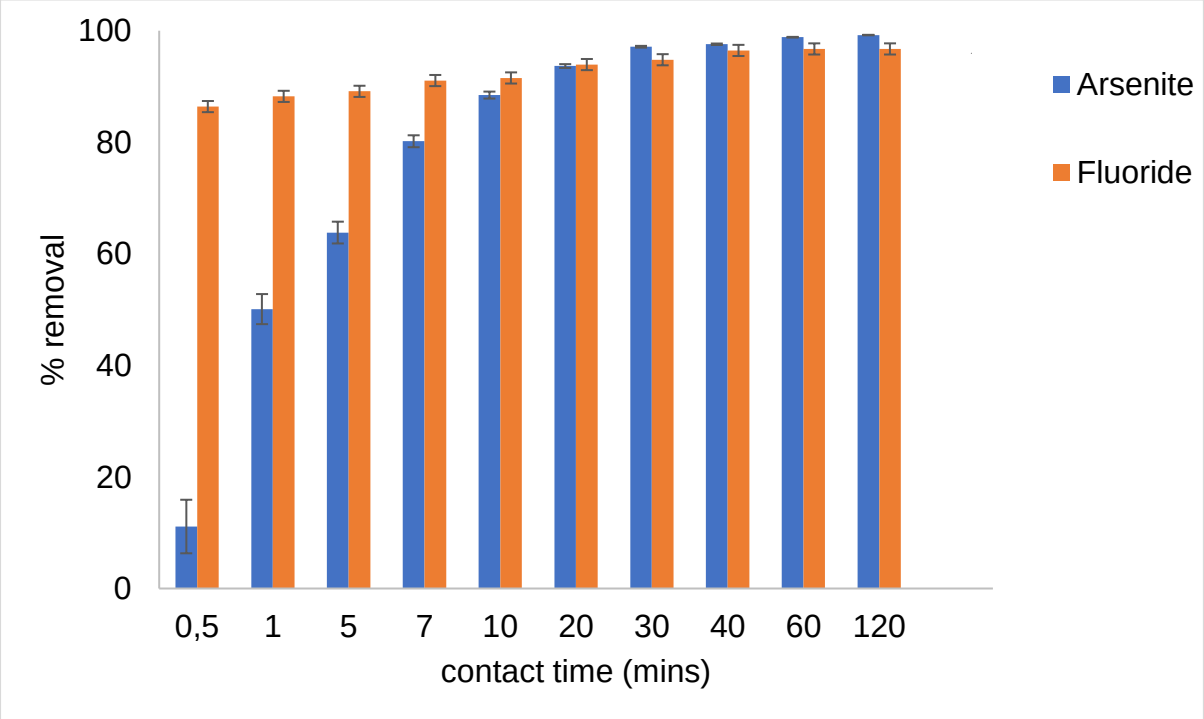

Figure 37. Effect of contact time on F^- and As^{3+} removal using 1:1 Fe/Ce-pPD composite (Initial concentration: 5 mg/L and 10 mg/L respectively, adsorbent dose: 0.4 g, solution volume: 50 mL, shaking speed: 250 rpm and temperature: 297 K).

Fig. 38 is showing the effect of contact time towards As^{3+} and F^- uptake from aqueous solution. The effect of contact time in $As^{3+}$and F^- uptake by 1:1 Fe/Ce-pPD was evaluated between 0.5-120 minutes. The attained results portrayed that As^{3+} and F^- sorption increase with increasing contact time. The sorption performance was faster within the first 30 mins, it then reduces indicating that the equilibrium time was reached. Thus, 30 mins was selected as an optimal contact time for consecutive experiments. The rapid metal ion uptake is due to available active adsorption sites in the surface of the 1:1 Fe/Ce-pPD composite. The obtained optimal of 30 mins was further used for subsequent experiments.

5.4.3.2. Kinetics models.

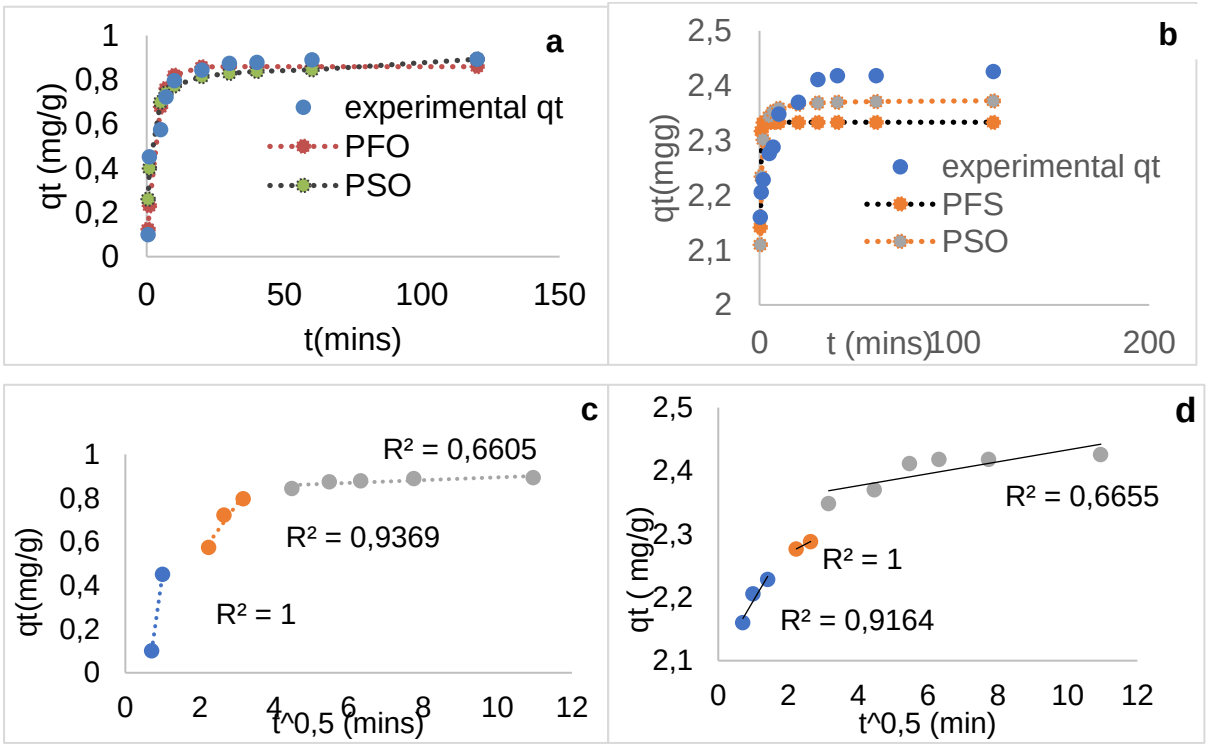

Figure 38. Kinetics model of As^{3+} and F^- adsorption by 1:1 Fe/Ce-pPD: (a) and (b) are the pseudo-first and pseudo-second-order plots for As^{3+} and F^-, (c) and (d) are intra-particle plot for As^{3+} and F^-.

Fig 38(a-d) is showing the respective plots kinetic models of As^{3+} and F^- uptake from aqueous solution. The kinetic data models (non-linear pseudo-first and pseudo-second orders, linearized Elovich, and intraparticle diffusion) were determined from the obtained experimental data of contact time. The pseudo-second-order (Fig. 38 (a) and (b)) with significantly higher value of 0.92 and 0.71 R^2 when compared with

pseudo-first-order, showed a better fit in As^{3+} and F^- uptake. Thus, validating that the initial As^{3+} and F^- uptake occurred through chemisorption. The feasibility of the kinetic model was further validated by lower values of reduced chi-square (χ^2) and root mean square error (RMSE) of the goodness of fit, thus implying favourability in chemisorption adsorption process in contrast to physisorption due to weak van de Waal forces. Furthermore, a linear plot of Elovich parameters validates that chemisorption is the limiting step due to its high correlation coefficient value shown in Table 20. Thus, implying the rate of metal ions uptakes by the synthesized composite favourability at the solid-liquid boundary occurred via the chemisorption process.

Table 20. Kinetics models parameters of fluoride and arsenite adsorption by 1:1 Fe/Ce-pPD from aqueous solution.

Non-linear				
	Fluoride		Arsenite	
	PFO	PSO	PFO	PSO
K_2	4.996	6.742	0.311	0.533
q_t	2.333	2.3745	0.859	1.615
R^2	0.371	0.709	0.892	0.915
χ^2	0.999	0.999	0.991	0.990
RMSE	0.071	0.052	0.186	0.075
Linear				
Elovich	β	0.061	0.093	
	α	$3*10^{16}$	$4.7*10^3$	
	R^2	0.96	0.935	
Intra-particle diffusion	K_1	0,094	1.198	
	R^2	0.916	1	
	K_2	0.029	0.235	
	R^2	1	0.936	
	K_3	0.009	0.006	
	R^2	0.666	0,661	

The obtained intra-particle diffusion plot produced three distinctive phases, indicating that the intraparticle diffusion mechanism is not the only limiting step as shown in Fig 38 (c) and (d). The first phase for both As^{3+} and F^- occurred between 1-3 and 1-2 , which might be due to external diffusion; second phase 2-5 and 2-, might be attributed

intra-particle diffusion; and third phase after 5 and 5 min could be due to attachment of adsorbate molecules to the internal surface of the sorbent (Mudzielwani, 2019). The rate constant for phase 1, phase 2 and phase 3 (K_1, K_2 and K_3 respectively) (Table 20), suggests that the adsorption process was very rapid on the layer and dominates the intraparticle diffusion for F^-. whereas on As^{3+} it was external diffusion due to the difference in the rate of mass transfer in the initial and final phase of adsorption based on the higher correlation coefficient value of phase 2 for F^- when compared to phases 1 and 3 and phase 1 for As^{3+} when compared to phase 2 and 3.

5.4.3.3. Effect of adsorbent dose

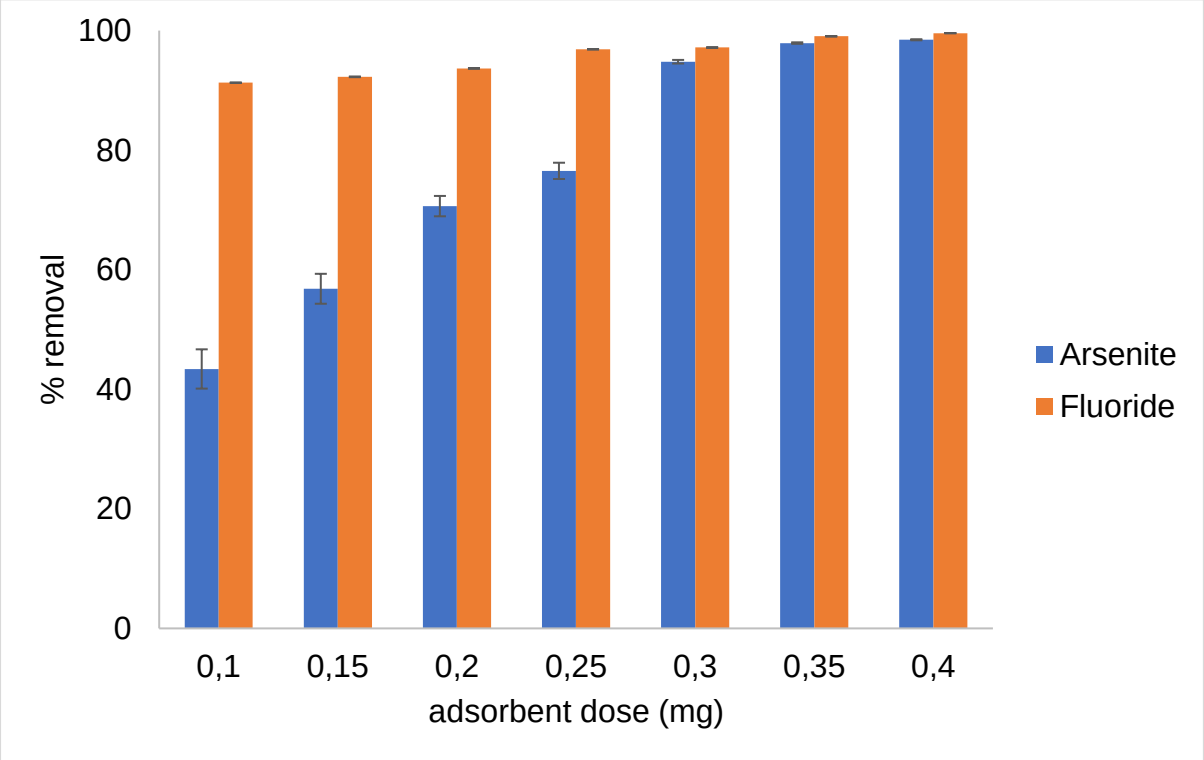

Figure 39. Effect of adsorbent dose on $As^{3+}$and F^- uptake by 1:1 Fe/Ce-pPD composite. (Initial concentration: 5 mg/L and 10 mg/L, solution volume: 50 mL, shaking speed: 250 rpm and temperature: 297 K).

The response of adsorbent dose on As^{3+} and F^- removal is presented in Fig 39. An increase in As^{3+} and F^- sorption with increasing adsorbent dose was observed. A gradual increase in sorption capacity with a rapid increase of adsorbent load is due to an increase in surface area, where more active sites are available for As^{3+} and F^- removal. Thus, 1:1 Fe/Ce-pPD, can efficiently remove As^{3+} and F^- ions with adsorbent dose increment. Consequently, the adsorbent dose has a significant effect on As^{3+}

and F^- sorption. An adsorbent dose of 0.3 g and 0.25 g for As^{3+} and F^- respectively was reported to be the optimal dose. Hence, they were chosen for further batch adsorption experiments.

5.4.3.4. Effect of pH

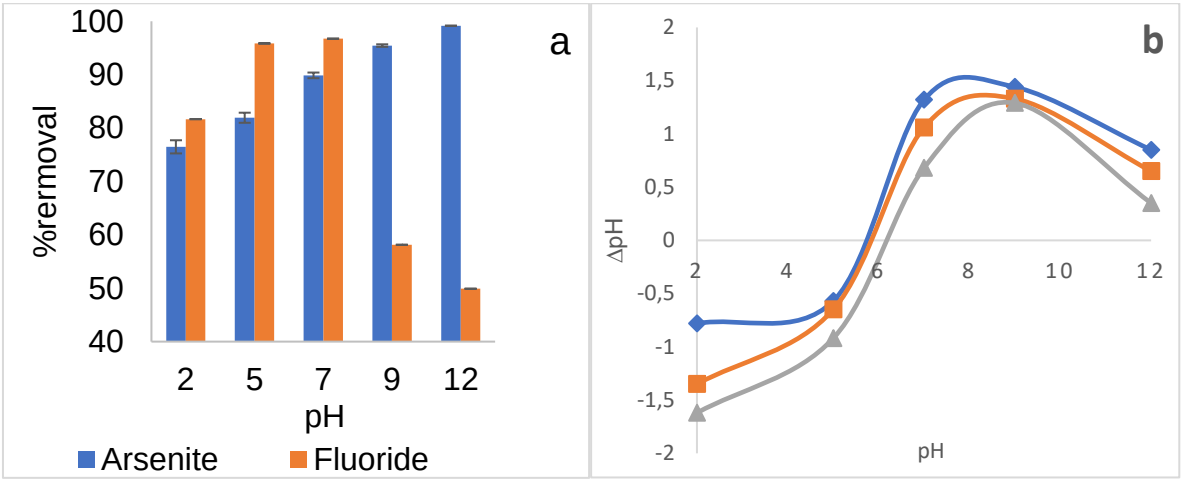

Figure 40. (a) and (b) are the plots of effect of pH on As^{3+} and F^- adsorption by 1:1 Fe/Ce-pPD composite and point of zero charge. (Initial concentration: 5mg/L and 10mg/L, adsorbent dose: 0.3 g and 0.2 g, solution volume: 50 mL, contact time: 40 mins, shaking speed: 250 rpm and temperature: 297 K).

Fig 40 (a-b) is showing results of effect of solution pH and point of zero charge. The sorption efficiency of As^{3+} and F^- by the adsorbent was influenced by solution pH. Point of zero charge is one of the imported phenomena which determines the surface charges of the materials, where, it is generally described as the pH at which the net charge of total particle surface is equal to zero. The obtained pH_{pzc} was reported to be 5.5-6.

Fluoride sorption by Fe/Ce-pPD was pH dependent. The F^- sorption increase with the rise in pH, reaching a maximum of 96.74% at pH 7, then further decrease with increasing pH. Thus, an increase in fluoride removal with increasing pH to neutral might be attributed to electrostatic attraction and ion exchange between the adsorbent surface charges and fluoride ion. However, reduction in fluoride removal might be due to competition between OH^- ions and F^- ion. The hypothesized fluoride removal mechanism is summarized by Eq. 18 and 19 (Mudzielwana et al, 2019):

$$\equiv MOH + H^{+} + F^{-} \leftrightarrow \equiv MF + H_2O \quad (18)$$

$\equiv M(OH)2 + 2F^- \leftrightarrow \equiv MF_2 + 2OH^-$ (19)

Additionally, this study shows that As^{3+} removal efficiency by 1:1 Fe/Ce-pPD significantly depends on the pH solution. It was observed that As^{3+} uptake increase with increasing pH. Due to the speciation of arsenite in solution; at pH >9, As^{3+} occurs as neutral charged and negatively charged at pH <9(Addo Ntim, 2011) as expressed in Eq 20 and 21. Hence, arsenite is not stable aiding to low chances of sensing repulsion force during removal by the composites. However, high arsenite removal at pH above the point of zero charge is might be due to several process, namely, electrostatic attraction and ion exchange.

$\equiv MOH + H_3As_3 \leftrightarrow \equiv MH_2As_3 + H_2O$ (20)

$\equiv MOH + H_2As_3^- \leftrightarrow \equiv MHAs_3^- + H_2O$ (21)

5.4.3.3. Effect of initial concentration of the adsorbate.

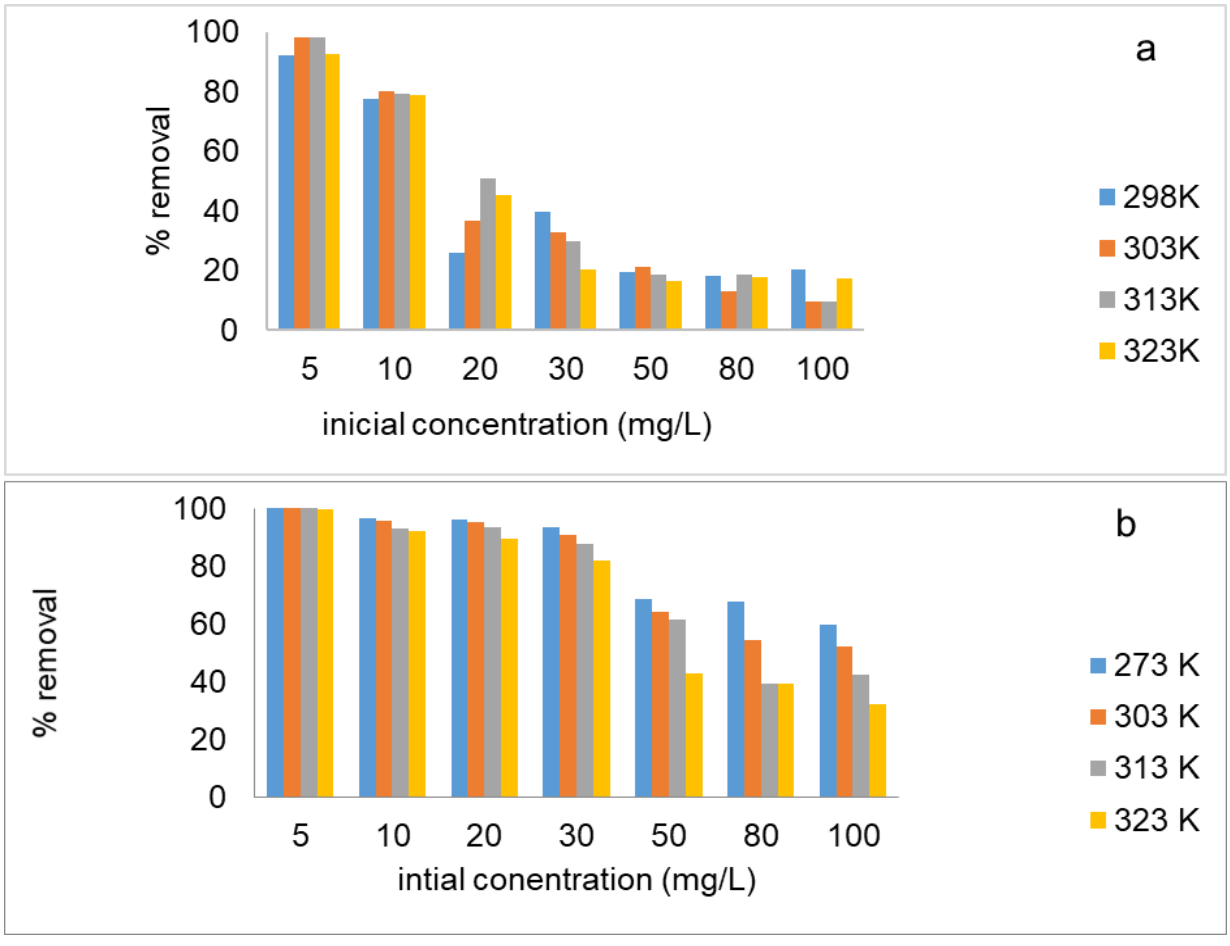

Figure 41. (a) and (b) effect of initial concentration on As^{3+} and F^- uptake using 1:1 Fe/Ce-pPD composite (Initial concentration: 5 mg/L and 10 mg/L, adsorbent dose: 0.3

g and 0.2 g, solution volume: 50mL, contact time: 24 hrs, shaking speed: 250 rpm and temperature: 298-323 K).

The results of effect of the initial concentration of the adsorbate ions on As^{3+} and F^- sorption at different working temperatures is shown in Fig. 41 (a-b). It was observed that As^{3+} and F^- sorption decreased with an increasing initial concentration of the adsorbate ions. Initially, high As^{3+} and F^- removal were observed at an initial concentration of 5 mg/L owing to the excessive active site that is present in the aqueous solution. As the initial concentration increase from 10-100 mg/L, a sudden decrease was observed due to the absence of binding sites on the surface of the adsorbent. Thus, the surface area of the 1:1 Fe/Ce-pPD composite was saturated. A similar trend was observed with different working temperatures, which could be attributed to mass transfer influencing better chemical interaction. An optimum initial concentration was concluded to be 5 mg/L for As^{3+} whereas for F^- is 10 mg/L were further used for subsequent experiments.

5.4.3.6. Adsorption isotherms.

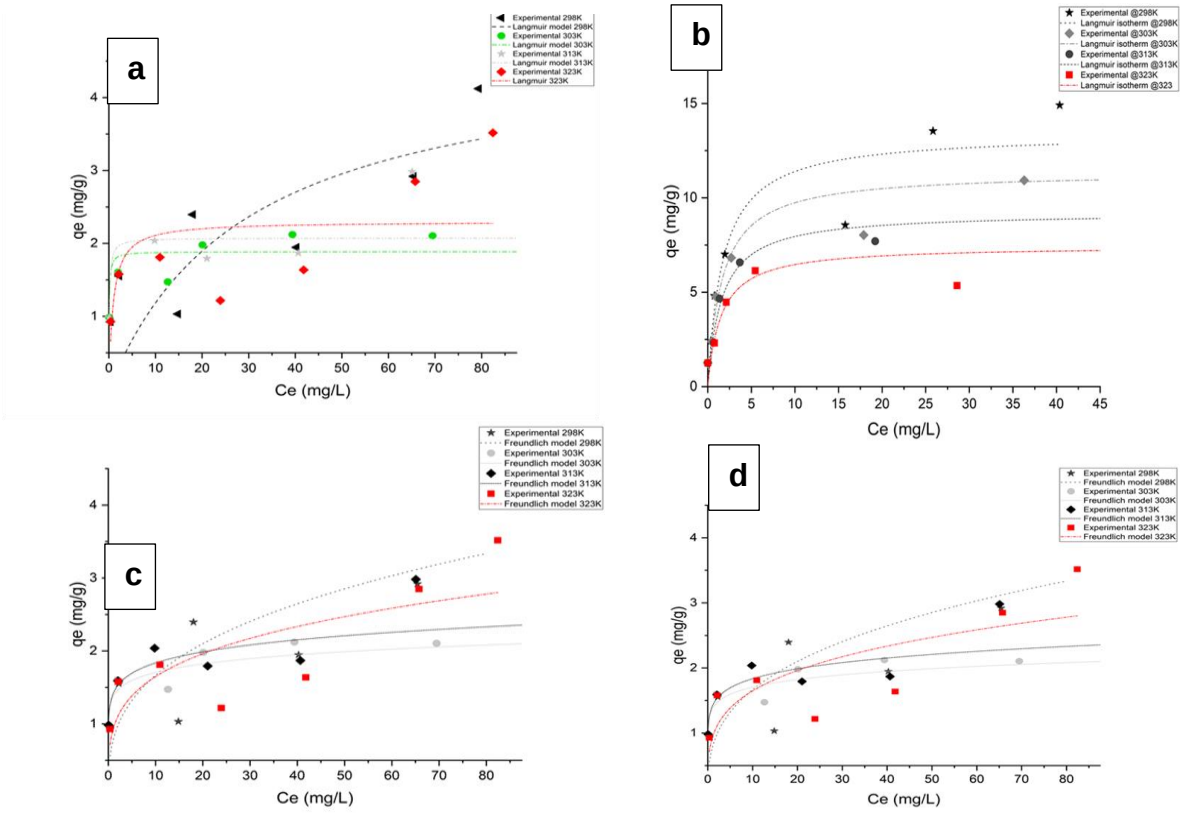

Figure 42. Adsorption isotherms models of F^- and As^{3+} adsorption by 1:1 Fe/Ce-pPD composite: (a) and (c) are the respective plots of Langmuir and Freundlich modes for As^{3+} and (b) and (d) for F^-.

The Langmuir and Freundlich isotherm models fitting plots and their respective calculated parameters are displayed in Fig. 42 and table 21. The obtained adsorption isotherm data for As^{3+} and F^- both were better described by both Langmuir and Freundlich isotherm model. This was validated by the RL and n values which are within the fitting ranges.

Table 21. Table for adsorption model parameters of fluoride and arsenite adsorption.

	Langmuir			Freundlich		
		F^-	As^{3+}		F^-	As^{3+}
298k	Q_m	13.4	4.71	K_f	4.68	0.77
	K_i	0.57	0.03	n	3.28	2.99
	R^2	0.88	0.47	R^2	0.94	0.69
	Adj. R^2	0.86	0.36	Adj.R^2	0.93	0.61
	χ^2	3.93	0.81	χ^2	1.85	0.5
	RSS	19.63	4.08	RSS	9.26	2.48
	RL	0.15	0.87			
303K	Q_m	11.35	1,89	K_f	4.31	1.37
	K_i	0.6	13,13	n	3.74	10.42
	R^2	0.89	0,68	R^2	0.95	0.81
	Adj. R^2	0.87	0.62	Adj. R^2	0.94	0.77
	χ^2	2.36	0.07	χ^2	1.11	0.04
	RSS	11.79	0.32	RSS	5.55	0.19
	RL	0.14	0.07			
313K	Q_m	9.22	2.07	K_f	4.01	1.41
	K_i	0.62	8.67	n	4.61	8.7
	R^2	0.91	0.49	R^2	0.9	0.61
	Adj. R^2	0.89	0.38	Adj. R^2	0.88	0.53
	χ^2	1.24	0.22	χ^2	1.28	0.17
	RSS	6.2	1.1	RSS	6.42	0.84
	RL	0.14	0.02			
323K	Q_m	7.45	2.3	K_f	3.45	0.92
	K_i	0.65	1.11	n	5.05	3.98
	R^2	0.86	0.33	R^2	0.89	0.6
	Adj. R^2	0.83	0.19	Adj. R^2	0.85	0.52
	χ^2	1.12	0.68	χ^2	0.98	0.41
	RSS	5.58	3.43	RSS	4.91	2.05
	RL	0.13	0.15			

However, based on the goodness of fit values, the As^{3+} and F^- uptake process was better described by the Freundlich isotherm model. Thus, the adsorption process was occurring on a multilayer surface of the synthesized adsorbent. The low values of the Reduced chi-squared (χ^2) and residual sum of squares (RSS) in Table 21, implies favourability in heterogeneity in the adsorbate-adsorbent interface.

Furthermore, the linearized D-R model was plotted to determine the effect of the porous nature of the composite as well as the mean free energy of the sorption process. It was observed that the Q_{max} value of F^- decrease with increasing

Table 22. Linearized D-R calculated parameters of fluoride and arsenite adsorption.

D-R model	Parameters	F^-	$As^{3\cdot}$
298K	R^2	0.58	0.36
	β	$9*10^{-9}$	$9*10^{-8}$
	E	7.45	2.36
	qe	7.48	2.15
303K	R^2	0.6	0.76
	β	$1*10^{-8}$	$1*10^{-8}$
	E	7.07	7.07
	qe	6.88	1.86
313K	R^2	0.62	0.67
	β	$9*10^{-9}$	$2*10^{-8}$
	E	7.45	5
	qe	6.09	2.004
323K	R^2	0.65	0.4
	β	$9*10^{-9}$	$6*10^{-}8$
	E	7.45	2.89
	qe	5.35	1.99

temperature confirming that adsorption affinity is high at low temperature. Whereas As^{3+} data revealed that adsorption affinity is high at high temperatures as shown in Table 22. The obtained Polanyi potential (E) value is < 8 kg/mol, thus, the adsorption process is physical nature.

5.4.3.8. Thermodynamics.

Thermodynamic parameters such as enthalpy changes (ΔH°(kJ/mol^{-1})), entropy changes (ΔS°(kJ/mol^{-1})), and Gibbs free energy changes (ΔG°(kJ/mol^{-1})) were used to determine the spontaneity, type of reaction, and the degree of randomness during the uptakes of both $As^{3+}$and F^- by the 1:1 Fe/Ce-pPD. These parameters from the plot of 1/T vs ln K_C were calculated using the following equations:

$$lnK = \frac{\Delta H^*}{R} + \frac{\Delta S^\circ}{R} \quad (15)$$

$$\Delta G = \Delta H^\circ - T\Delta S^\circ \quad (17)$$

Where K is the equilibrium constant, R is the gas constant (8.134 kJ mol^{-1} K^{-1}) and T is the solution temperature (K).

Table 23. Thermodynamic parameters of fluoride and arsenite adsorption.

	As	F
ΔH	17,63	53,25
ΔS	0,056	0,076
ΔG		
298	0,942	75,898
303	0,662	76,278
313	0,102	77,038
323	-0,458	77,798

The obtained thermodynamic values for As^{3+} and F^- adsorption are displayed in Table 23. From the presented thermodynamic parameters, ΔG° were calculated to be positive for both As^{3+} and F sorption process. Thus, the reaction was not feasible and validating that the reaction was not spontaneous for both metal ions adsorption. It was observed that the ΔG° values decreased with an increasing temperature, which indicates the favourability of the sorbate-sorbent mechanisms. Thermodynamically, As^{3+} and F^- sorption process were endothermic in nature with an increase in the degree of randomness as validated by positive values of ΔH° and ΔS° distinctly.

5.4.3.9. Effect of co-existing ions.

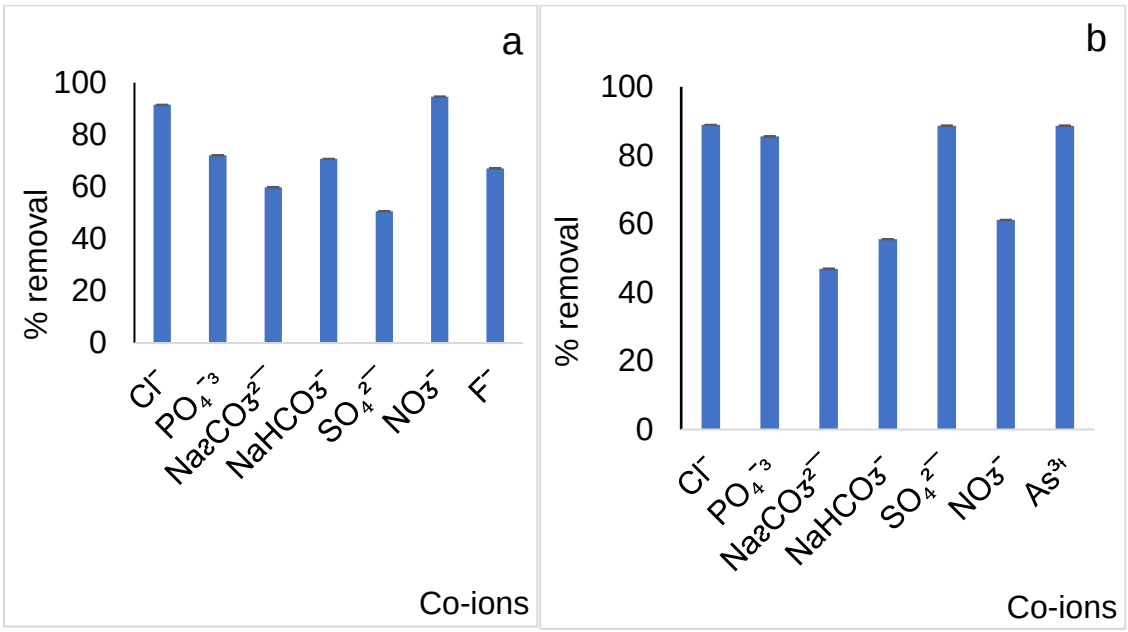

Figure 43. Effect of co-existing ions on F^- and As^{3+}uptake using 1:1 Fe/Ce-pPD composite. (initial concentration: 5 mg/L and 10 mg/L, adsorbent dose:0.3 g and 0.2 g, solution volume: 50 mL, contact time: 24 hrs, shaking speed: 250 rpm and temperature: 297 K).

Fig 43 is showing the effect of co-ions toward As^{3+} and F^- uptake from aqueous solution. The co-existence of ions such as phosphates, carbonates, chloride, arsenic, fluoride, and nitrates can pose a significant effect on fluoride and arsenite removal in aqueous solution. From the obtained results, it was observed that the co-occurrence of co-ions in aqueous solution can pose a significant effect on both arsenite and fluoride ions. The, co-occurrence of existing ions seem to reduce the movement of the adsorbate with the active binding sites; hence, causing high coulombic repulsion forces (Ayinde et al, 2018). The obtained results demonstrated that carbonates, fluoride, and phosphates pose excessive effect on As^{3+} sorption while chloride and nitrates pose minimum effect on arsenite sorption (Fig 43 (a)). Whereas carbonates and nitrates pose a great effect on F^- removal and phosphates, arsenite, and chlorine posing less effect (Fig 43 (b)). The effect order for As^{3+} and F^- can be summarized in the following way: As^{3+}: NO_3^- > F^- > CO_3^{2-}> PO_4^- >Cl^-> and F^-: CO_3^- > NO_3^-> PO_4^- Cl^- > As^{3+} respectively. Thus, the co-occurrence of existing ion has reduced the interaction of the concerned pollutants with the active adsorption sites by occupying the vacant sites causing competition among the present ions.

5.4.3.10. Regeneration.

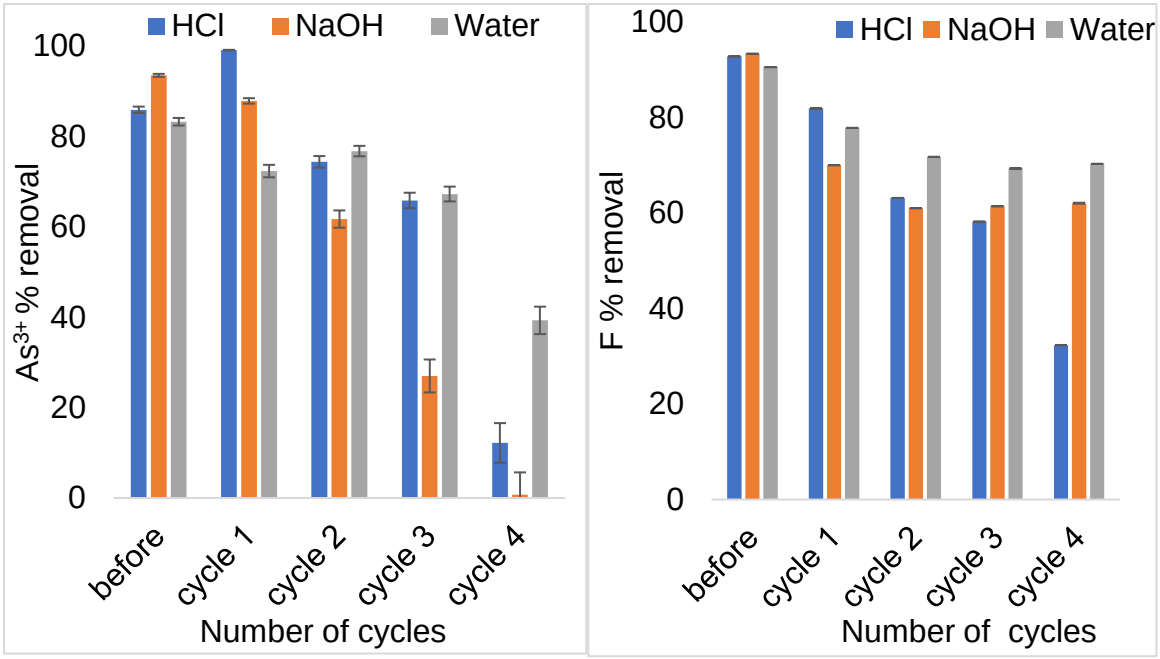

Figure 44. Regeneration results of 1:1 Fe/Ce-pPD (Initial F^- and As^{3+} concentration: 5 mg/L and 10 mg/L, adsorbent dose: 0.3 g and 0.2 g, solution volume: 50 mL, contact time: 20 mins, shaking speed: 250 rpm and temperature: 297 K).

Fig 44 is showing the regeneration results of of Fe/Ce-pPD. The re-usability of 1:1 Fe/Ce-pPD As^{3+} and F^- loaded was evaluated, and the obtained results are shown in Fig 44. As^{3+} and F^- adsorption by the 1:1 Fe/Ce-pPD composites decrease with an increasing number of regeneration cycles. The reduction in adsorption capacity might be due to occupation of the adsorption sites by the adsorbate ions and reduction in adsorbent amount due to dissolution of the pPD network (Desmarets et al, 2001; Mdlalose et al, 2018). Comparatively, it was observed that deionized water seems to be a better regenerant compared to HCl and NaOH.

5.6 Antimicrobial.

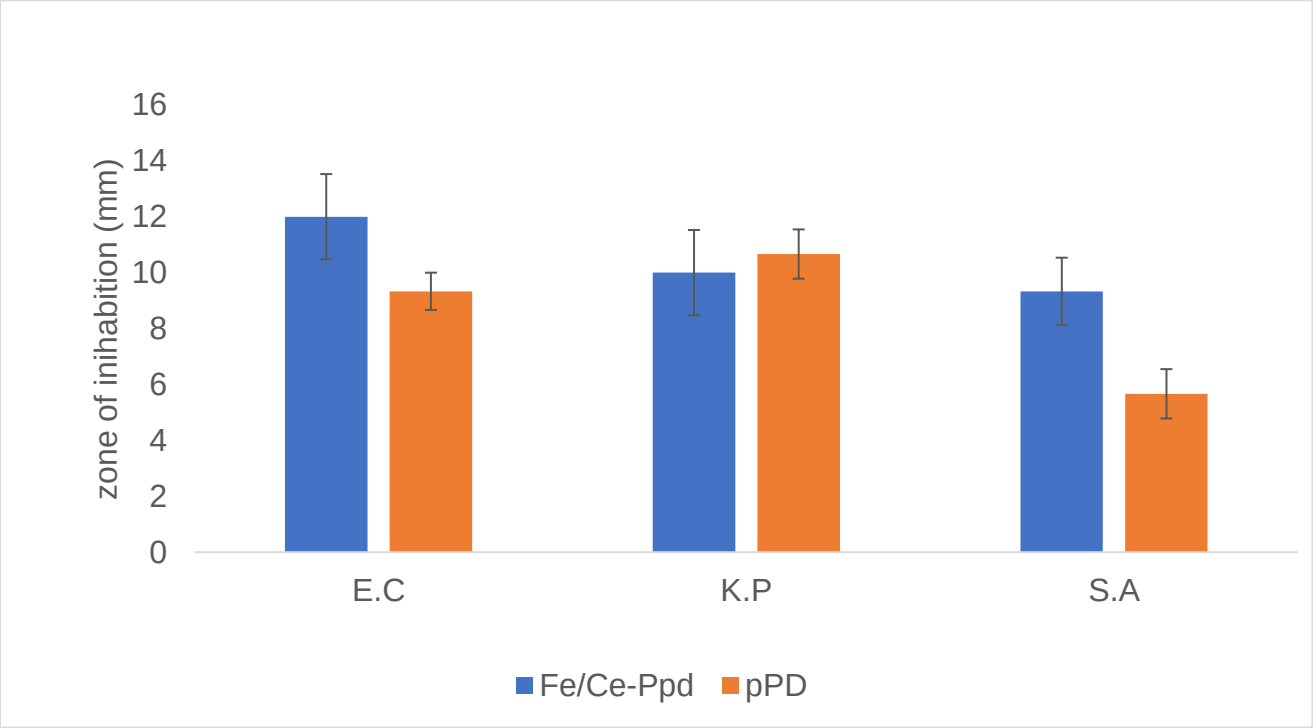

Figure 45. The results of zone of inhibition for raw pPD and 1:1 Fe/Ce-pPD towards *Escherichia coli, Klebsiella pneumonia* and *staphylococcus aureus*.

Fig 45 is showing the antimicrobial ported of pPD and 1:1 Fe/Ce-pPD. In this study, the antimicrobial activity of pPD and Fe/Ce-pPD hybrid composite was evaluated using the zone of inhibition method while comparing with raw pPD polymer. Comparatively, the zone of inhibition against the concerned pathogens *Escherichia coli, Klebsiella pneumonia* and *staphylococcus aureus* using 1:1 Fe/Ce-pPD is 12, 10 and 9,3mm respectively whereas for bare pPD is 9, 10 and 5,7mm. Thus, 1:1 Fe/Ce-PD has antimicrobial potency. The potency of the synthesized composite against these waterborne pathogens is associated with a series of compositions within the sorbent. Firstly, the complex functional groups within the polyaniline polymers might have the ability to bioaccumulate the lipid membranes of the cell wall and causes cell denaturation. Thus, causing cell bursting leading to bacterial death. Secondly, the synthesis of the polyaniline composite in an acidic condition in the present of ammonium persulfate has a role in the antimicrobial activity due to the present of the chemical oxidant which oxidizes the bacterial lipid membrane leading to bacterial cell burst (Kucekova, 2014). Additionally, the antibacterial action of the 1:1 Fe/Ce-pPD composite may be due to the existence of co-coordinatively unsaturated Fe metal of the adsorbent which generates reactive oxidative species which distraction cell wall

(Inbaraj et al, 2012). Therefore, 1:1 Fe/Ce-pPD can be an efficient antibacterial agent for both Gram-positive and negative bacterium cells.

5.5. Comparison of the synthesized materials towards As^{3+} and F^- removal

Table 24. Comparison of the synthesized materials on fluoride and arsenite adsorption.

	2.5 % Fe-pPD		5 % Ce-pPD		1:1 Fe/Ce-pPD	
	As^{3+}	F^-	As^{3+}	F^-	As^{3+}	F^-
Time (mins)	40	40	20	20	20	20
Dose (g)	0.25	2	0.3	0.2	0.3	0.2
initial concentration (mg/L)	5-100	5-100	5-100	5-100	5-100	5-100
pH	9	7	9	5	9	7
adsorption capacity (mg/g)	1.87	6.79	2.11	13.27	4.71	14.75

Table 24 is comparing removal efficiency and conditions of **As^{3+} and F^-** uptake by Fe-pPD, 5 % Ce-pPD, and 1:1 Fe/Ce-pPD. From this study, the modification of pPD with Fe and Ce metal oxides have significantly improved the adsorption performance of the pPD composite. An improvement in adsorption capacity of the synthesized composites was observed in the following order 2.5 % Fe-pPD>5 % Ce-pPD>1:1 Fe/CepPD. Thus, the introduction of Fe and Ce metal oxides on the pPD matric has played a significant role in improving the chemical properties of the polymer (solubility, ionization, and surface area) enhancing the sorption efficiency of the composites. Comparatively, the combined doped polymeric (1:1 Fe/Ce-pPD) adsorbent have high adsorption capacity (14.75 mg/g and 4.71 mg/g) in both fluoride and arsenite removal from aqueous solution with high infinity towards fluoride removal compared to the other composites as shown in Table 24. Although, the Fe-pPD and Ce-pPD have low adsorption capacity than Fe/Ce-pPD, they have shown better performance.

5.5. Conclusion.

Fe/Ce metal oxides were successfully incorporated into the pPD matrix through chemical oxidative polymerization. Successful polymerization of 1:1 Fe/Ce-pPD was confirmed by different morphological characterizations including FTIR, BET, SEM-EDS, and XRD. The synthesized composite has the potential ability for As^{3+} and F^- sorption. However, 1:1 Fe/Ce incorporation has chemically improved the adsorption

capacity of the pPD polymer because of the change from amorphous to crystalline as validated by XRD analysis. Sorption capacity of the adsorbent towards arsenite and fluoride depends on various factors such as contact time, adsorbent dose, initial concentration of the adsorbates, temperature, and solution pH. Adsorption kinetics studies have shown that the process mechanism better fits pseudo-second-order as validated by kinetic plots and parameters obtained. Thus, chemisorption is the limiting step. The adsorption mechanism between the adsorbates and the adsorbent was evaluated using the non-linear isotherms (Langmuir and Freundlich models). Attained data revealed that the adsorption process better fit the Freundlich isotherm model as validated by the obtained model parameters. Additionally, the synthesized adsorbent has shown potency towards an antimicrobial activity. Thermodynamically, As3+ and F^- sorption process were endothermic with increase in the degree of randomness as validated by positive values of ΔH° and ΔS° respectively. The, study proved that the synthesized adsorbent can be economically viable and help to eradicate water pollution.

3.4.9. References.

Abernathy, C.O., Thomas, D.J. and Calderon, R.L., 2003. Health effects and risk assessment of arsenic. *The Journal of nutrition*, *133*(5), pp.1536S-1538S.

Addo Ntim, S. and Mitra, S., 2011. Removal of trace arsenic to meet drinking water standards using iron oxide coated multiwall carbon nanotubes. *Journal of Chemical & Engineering Data*, *56*(5), pp.2077-2083.

Amer, I. and Brandt, S., 2018. Synthesis and characterization of Poly (p-phenylenediamine) and its derivatives using aluminium triflate as a co-catalyst. *Cogent Engineering*, *5*(1), p.1499701.

Archana, S. and Jaya Shanthi, R., 2014. Synthesis and characterization of poly (p-phenylenediamine) in the presence of sodium dodecyl sulfate. *Research Journal of Chemical Sciences.*

Ashbolt, N.J., 2015. Microbial contamination of drinking water and human health from community water systems. *Current environmental health reports*, *2*(1), pp.95-106.

Ayinde, W.B., Gitari, M.W., Muchindu, M. and Samie, A., 2018. Biosynthesis of ultrasonically modified Ag-MgO nanocomposite and its potential for antimicrobial activity. *Journal of Nanotechnology*, *2018*.

Bibi, S., Farooqi, A., Hussain, K. and Haider, N., 2015. Evaluation of industrial based adsorbents for simultaneous removal of arsenic and fluoride from drinking water. *Journal of Cleaner Production*, *87*, pp.882-896.

Chen, X., Zhang, Q., Qian, C., Hao, N., Xu, L. and Yao, C., 2015. Electrochemical aptasensor for mucin 1 based on dual signal amplification of poly (o-phenylenediamine) carrier and functionalized carbon nanotubes tracing tag. *Biosensors and Bioelectronics*, *64*, pp.485-492.

de Oliveira, L.M., Ma, L.Q., Santos, J.A., Guilherme, L.R. and Lessl, J.T., 2014. Effects of arsenate, chromate, and sulfate on arsenic and chromium uptake and translocation by arsenic hyperaccumulator Pteris vittata L. *Environmental pollution*, *184*, pp.187-192.

Desmarets, C., Schneider, R. and Fort, Y., 2001. Nickel-catalysed synthesis of 3-chloroanilines and chloro aminopyridines via cross-coupling reactions of aryl and heteroaryl dichlorides with amines. *Tetrahedron Letters*, *42*(2), pp.247-250.

Gitari, M.W., Masindi, V., Tutu, H. and DeBeer, M., 2017. Synthesis of cryptocrystalline magnesite–bentonite clay composite and its application for neutralization and attenuation of inorganic contaminants in acidic and metalliferous mine drainage. *Journal of Water Process Engineering*, *15*, pp.2-17.

Guerra, F.D., Attia, M.F., Whitehead, D.C. and Alexis, F., 2018. Nanotechnology for environmental remediation: materials and applications. *Molecules*, *23*(7), p.1760.

Haldorai, Y., Lyoo, W.S. and Shim, J.J., 2009. Poly (aniline-co-p-phenylenediamine)/MWCNT nanocomposites via in situ microemulsion: synthesis and characterization. *Colloid and Polymer Science*, *287*(11), pp.1273-1280.

Ho, Y.S. and McKay, G., 1998. Sorption of dye from aqueous solution by peat. *Chemical engineering journal*, *70*(2), pp.115-124.

Inbaraj, B.S., Tsai, T.Y. and Chen, B.H., 2012. *Synthesis, characterization, and antibacterial activity of superparamagnetic nanoparticles modified with glycol chitosan.* Science and Technology of Advanced Materials.

Itabashi, T., Li, J., Hashimoto, Y., Ueshima, M., Sakanakura, H., Yasutaka, T., Imoto, Y. and Hosomi, M., 2019. Speciation and Fractionation of Soil Arsenic from Natural and Anthropogenic Sources: Chemical Extraction, Scanning Electron Microscopy, and Micro-XRF/XAFS Investigation. *Environmental science & technology*, *53*(24), pp.14186-14193.

Jadhav, S.V., Bringas, E., Yadav, G.D., Rathod, V.K., Ortiz, I. and Marathe, K.V., 2015. Arsenic and fluoride contaminated groundwaters: a review of current technologies for contaminants removal. *Journal of Environmental Management*, *162*, pp.306-325.

Kucekova, Z., Humpolicek, P., Kasparkova, V., Perecko, T., Lehocký, M., Hauerlandova, I., Saha, P. and Stejskal, J., 2014. Colloidal polyaniline dispersions: antibacterial activity, cytotoxicity and neutrophil oxidative burst. *Colloids and Surfaces B: Biointerfaces*, *116*, pp.411-417.

Lagergren, S.K., 1898. About the theory of so-called adsorption of soluble substances. *Sven. Vetenskapsakad. Handingarl*, *24*, pp.1-39.

Li, Y., Li, G., Peng, H., Qin, Y. and Chen, K., 2013. Facile synthesis of high-quality ultralong poly (aniline-co-p-phenylenediamine) nanofibers. *Synthetic Metals*, *164*, pp.42-46.

Mdlalose, L.M., 2018. *The synthesis, characterization and performance evaluation of polyphelenediamine-and polypyrrole-clay composites for removal of oxo-anionic wastewater contaminants* (Doctoral dissertation).

Mohapatra, M., Anand, S., Mishra, B.K., Giles, D.E. and Singh, P., 2009. Review of fluoride removal from drinking water. *Journal of environmental management*, *91*(1), pp.67-77.

Mudzielwana, R., Gitari, M.W., Akinyemi, S.A. and Msagati, T.A., 2018. Performance of Mn 2+-modified bentonite clay for the removal of fluoride from aqueous solution. *South African Journal of Chemistry*, *71*, pp.15-23.

Mudzielwana, R., Gitari, M.W. and Ndungu, P., 2019. Performance evaluation of surfactant modified kaolin clay in As (III) and As (V) adsorption from groundwater: adsorption kinetics, isotherms and thermodynamics. *Heliyon*, *5*(11), p.e02756.

Peng, C.W., Hsu, C.H., Lin, K.H., Li, P.L., Hsieh, M.F., Wei, Y., Yeh, J.M. and Yu, Y.H., 2011. Electrochemical corrosion protection studies of aniline-capped aniline trimer-based electroactive polyurethane coatings. *Electrochimica acta*, *58*, pp.614-620.

Pham, Q.L., Haldorai, Y., VAN HOA, N.G.U.Y.E.N., Tuma, D. and Shim, J.J., 2011. Facile synthesis of poly (p-phenylenediamine)/MWCNT nanocomposites and characterization for investigation of structural effects of carbon nanotubes. *Bulletin of Materials Science*, *34*(1), pp.37-43.

Rai, B.K., Vidyarthi, S.N., Amit, R.S., Bhardwaj, N. and Ojha, A., 2012. Spectral, magnetic and antimicrobial studies of Co (II), Ni (II) and Cu (II) complexes with bidentate Schiff base ligands. *Oriental Journal of Chemistry*, *28*(3), pp.1403-1409.

Saikia, P.P., Kotoky, P. and Goswami, U., 2017. Distribution of fluoride and arsenic contents in the ground water system, Jorhat District, Assam, India. *Int. J. Sci. Res*, *6*, pp.844-847.

Shahin, S.M. and Salem, M.A., 2015. The challenges of water scarcity and the future of food security in the United Arab Emirates (UAE). *Natural Resources and Conservation*, *3*(1), pp.1-6.

Shakoor, M.B., Niazi, N.K., Bibi, I., Rahman, M.M., Naidu, R., Dong, Z., Shahid, M. and Arshad, M., 2015. Unraveling health risk and speciation of arsenic from groundwater in rural areas of Punjab, Pakistan. *International journal of environmental research and public health*, *12*(10), pp.12371-12390.

Shakoor, M.B., Niazi, N.K., Bibi, I., Shahid, M., Saqib, Z.A., Nawaz, M.F., Shaheen, S.M., Wang, H., Tsang, D.C., Bundschuh, J. and Ok, Y.S., 2019. Exploring the arsenic removal potential of various bio-sorbents from water. *Environment international*, *123*, pp.567-579.

Shannon, M.A., Bohn, P.W., Elimelech, M., Georgiadis, J.G., Marinas, B.J. and Mayes, A.M., 2010. Science and technology for water purification in the coming

decades. *Nanoscience and technology: a collection of reviews from nature Journals*, pp.337-346.

Sharma, S.K. and Le Maguer, M., 1996. Kinetics of lycopene degradation in tomato pulp solids under different processing and storage conditions. *Food Research International*, *29*(3-4), pp.309-315.

Siddiqui, S.I. and Chaudhry, S.A., 2018. A review on graphene oxide and its composites preparation and their use for the removal of As3+ and As5+ from water under the effect of various parameters: application of isotherm, kinetic and thermodynamics. *Process Safety and Environmental Protection*, *119*, pp.138-163.

Wang, T., Zhang, L., Li, C., Yang, W., Song, T., Tang, C., Meng, Y., Dai, S., Wang, H., Chai, L. and Luo, J., 2015. Synthesis of core–shell magnetic Fe3O4@ poly (m-phenylenediamine) particles for chromium reduction and adsorption. *Environmental science & technology*, *49*(9), pp.5654-5662.

World Health Organization, 2010. *World health statistics 2010*. World Health Organization.

Water.org. http://water.org/learn-about-the-water-crisis/billion/. Accessed August 2018.

Wright, M.S., Peltier, G.L., Stepanauskas, R. and McArthur, J.V., 2006. Bacterial tolerances to metals and antibiotics in metal-contaminated and reference streams. *FEMS microbiology ecology*, *58*(2), pp.293-302.

Yao, J. and Wang, H., 2014. Zeolitic imidazolate framework composite membranes and thin films: synthesis and applications. *Chemical Society Reviews*, *43*(13), pp.4470-4493.

Zhang, L., Zeng, Y. and Cheng, Z., 2016. Removal of heavy metal ions using chitosan and modified chitosan: A review. *Journal of Molecular Liquids*, *214*, pp.175-191.

Chapter 6.

6.1. General conclusions.

The study reported that Fe and Ce were successfully incorporated into the bare pPD network through chemical oxidative polymerization. Successfully synthesis of pPD, 5 % Ce-pPD, 2.5 % Fe-pPD, and 1:1 Fe/Ce-pPD was validated by various morphological analysis such as FTIR, BET, SEM-EDS, TEM, and XRD analysis. The synthesized composites have displayed the potential ability towards fluoride and arsenite removal in an aqueous solution. The obtained batch experimental results revealed that contact time, adsorbent dose, initial concentration, pH, and temperature have a significant effect on fluoride and arsenite sorption. The non-linear and linear kinetic model plots revealed that chemisorption is not the only limiting step for both fluoride and arsenite uptake by the synthesized adsorbents. However, intraparticle plots revealed that chemisorption is not the only limiting step as validated by three distinctive phases in the solution interphase. Fluoride and arsenite isotherm model data was better described by the Freundlich isotherm model. Thus, implying heterogeneity between adsorbate-adsorbent interphase for the synthesized adsorbents predominate. The regeneration results revealed that the synthesized adsorbents can be economically viable. The synthesized adsorbents have portrayed antimicrobial activity towards *Escherichia coli*, *Staphylococcus aureus* and *Klebsiella pneumonia*. The application of these produced adsorbents in different water applications has shown and widened the scope of remediating these pollutants in the environment and overall wellbeing of human health.

6.2. Recommendation.

This study focus on synthesis, characterization, and evaluation of the synthesized iron/cerium-based polymeric adsorbents for fluoride and arsenite as well as microbial disinfection in aqueous solution. However, further strategies can be explored to enhance the removal potency for a wide application. Also, there is a need to do an extensive study on

- Chemically stability of the proposed adsorbents
- Antimicrobial activity of the synthesized adsorbents

- Column study
- Application in field water
- A method technique to design and develop the materials for household and industrial use.